THE CITY UNIVERSITY

MECHANICAL ENGINEERING DEPARTMENT

DYNAMIC RESPONSE OF GEARED SYSTEM

WITH BACKLASH

by

FATHI BASMAJI, BSc, MSc, M.Eng.

A thesis submitted to the City University

as part of the requirements for the

degree of Doctor of Philosophy

OCTOBER 1983

LIST OF CONTENTS

LIST OF FIGURES

LIST OF PLATES

ABSTRACT

Dynamic Response of Geared System
with Backlash
1983

F. BASMAJI

Supervised by: Dr.H.R.HARRISON

The impact phenomenon associated with the loss of contact of a pair of spur gears driven under load has been investigated. A specially designed test rig with its measuring instruments has been used to measure and record the dynamic response of the loaded gear system with a variety of parameter changes.

An advanced Fourier Analyser has also been utilized to analyse and plot the frequency spectrum of the strain in the output shaft. In addition a simplified digital simulation model is developed to reproduce the experimental results. Numerical tooth shifting has been introduced to involve the idea of internal input rather than external input to simulate gear tooth meshing.

The geared system when running free or loaded is found to oscillate at frequencies equal to gear speed and its integral multiples for speeds lower than 1100 rev/min. When running at speeds starting from 1100 rev/min and over the geared torsional system is found to oscillate at frequencies equal to half the gear shaft corresponding running frequency and its integral multiples. The subharmonic oscillation is observed with and without load for this test setup, except when running at speeds of 1700 rev/min and over, and loading of 4 lbf.ft (5.424 N m).

NOMENCLATURE

Subharmonic	Integer ratio frequency, measured below the running speed corresponding frequency.
Rev/s	Unit of the running speed frequency and its integral multiples.
Hz	Unit of the system natural frequencies.
Rev/min	Running speed.
A	Ampere.
PCD	Pitch circle diameter.
m	Module.
2B	Total angular backlash (Radians).
$2B_1$	Total circular backlash (mm).
C	Centre distance.
ΔC	Centre distance change.
K_1, K_2, K_3	Stiffness of the input, intermediate, and the final shafts respectively.
J_1, J_2, J_3, J_4	Inertia of the motor rotor, gears and first flywheel, second flywheel, and the brake respectively.
ω_{nf}	Fundamental natural frequency of the total system.
ω_{n2}, ω_{n3}	Second and third natural frequency of the total system.
ω_{nm}	Natural frequency of the separated motor side.
ω_{nb}	Natural frequency of the separated brake side.
R_1, R_2, R_3, R_4	Strain gauge resistances.
N	Number of samples in the Fourier Analyser.
T	Total time in the Fourier Analyser.
F_{max}	Maximum frequency of the Fourier Analyser.
RMS value	Root mean square value.

I. INTRODUCTION

1.1 General

Toothed gears have found wide application in various branches of mechanical engineering. In many machines such as metal cutting machine tools, automobiles, marine engines, etc., toothed gears form vital elements of main and ancillary mechanisms.

Toothed gears are distinguished from other mechanisms by high efficiency, compact layout, reliable service and simple operation. On the other hand:

1- Their manufacturing requires special equipment and tools.

2- Errors in teeth machining may cause vibration and noise during operation.

The vibration and noise in gears is one of main problems which some times limits the use of gears. The aspect of noise was commonly recognized by many companies and they found it most important to keep the noise level within allowable limits. For gears in mesh the energy loss which goes into vibration is dissipated as heat and impact between mating gears, which causes shock forces and loads, and the vibration resulting from impact causes noise. As an example of noise Fig 1.1 shows the noise level in the present test rig. This noise was measured by precision sound level meter, type 2204 made by B & K, and using $\frac{1}{2}$" condenser microphone, the output was then taken to Fourier Analyser and plotted. The distance between the microphone and the noise source was 30cm.

To study a geared torsional system a basic model may consist of spur gears, driving motor, and flexible shafts. A system such as this can experience dynamic torques and tooth loads many times greater than the mean transmitted torque. These dynamic loads can be caused by induced external excitations. It is also possible for the system to have internal excitations caused mainly by tooth profile and pitch errors, stiffness variation of the gear teeth, and loss of contact between the gear teeth in backlash.

One of the main parameters which causes vibration and some excessive dynamic stresses is the backlash. Although it is

tooth meshing frequency

gear wheel ringing frequencies
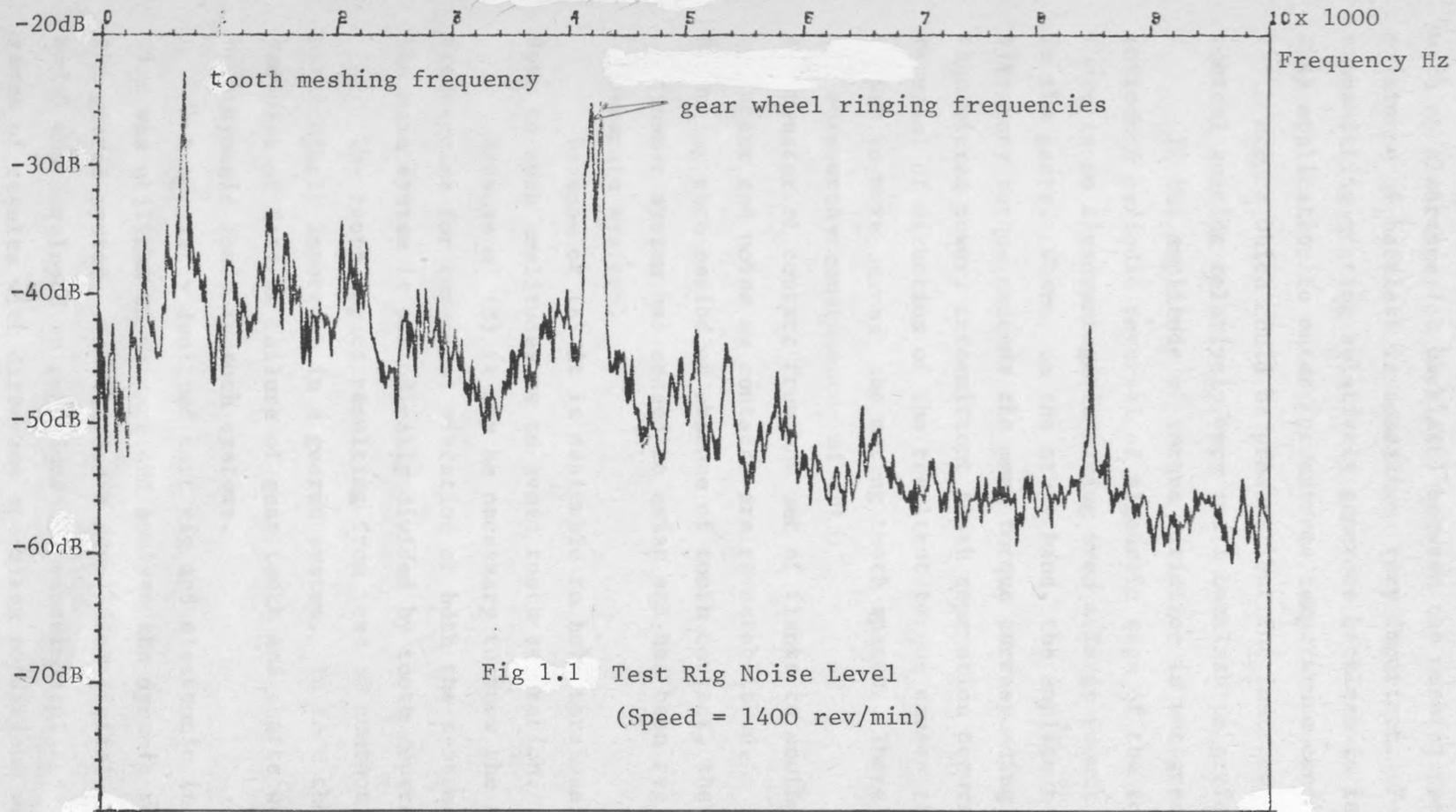
Fig 1.1   Test Rig Noise Level
(Speed = 1400 rev/min)

possible in certain circumstances to make and run a pair of gears
with no clearance (or backlash) between the meshing teeth, but the
existence of backlash is sometimes very important. For power
transmitting gearing relatively generous backlash is indicated in
this application to cater for extreme temperature conditions and
tooth errors which could be present, but for instrument and
control gearing relatively very small backlash is preferable.

If the amplitude of torque variation is not great enough to
introduce periodic reversal of algebraic sign of the total torque
there is no disadvantage in having even a large amount of backlash
in the gears. Where, on the other hand, the amplitude of the
vibratory torque exceeds the mean torque corresponding to the
transmitted power, intermittent tooth separation occurs because
reversal of direction of the resultant torque causes the teeth of
a gear to move across the mating tooth spaces. There are at least
two noteworthy consequences of this:

A- Transfer of contact from one set of flanks to another produces
   impact and noise as contacts are re-established.

B- During each period of absence of tooth contact, the nominal
   dynamic system has ceased to exist and has been replaced by two
   separate systems.

Because of (A) it is desirable to hold torsional vibration
down to such amplitudes as to avoid tooth separation.

Because of (B) it may be necessary to know the natural
frequencies for torsional vibration of both the systems into which
the main system is periodically divided by tooth separation.

The tooth impact resulting from loss of contact is
particularly important in a geared system. In fact there are many
examples of fatigue failure of gear teeth and shafts caused by
high dynamic loads in such systems.

A specially designed test rig and electronic instrumenta-
tion was utilized to measure and analyse the dynamic response of
the geared system. In addition a simplified digital simulation
model was developed to reproduce the experimental results. A wide
range of results with different operating conditions were analysed
and plotted as a frequency spectrum to identify the sources of
vibrations.

When running at speeds ranging from 250 rev/min to 1000
rev/min, the output shaft was found to oscillate at frequencies
corresponding to the running speed and its integral multiples.

When running at speeds ranging from 1100 rev/min to 2000
rev/min, the output shaft was found to oscillate at frequencies
corresponding to half the running speed and _its_ integral multiples.
This oscillation at half the running speed (or subharmonic
frequency)could results in premature failure of the geared system.

1.2 Literature Survey

1.2.1 Related Studies of Gear Dynamics:

Most of the research considering the dynamics of gears since
1900 has been experimental. A large programme was started in 1925
by special committee of the ASME, and their results were published
in 1931. Many empirical expressions for calculating dynamic loads
and dynamic factors of gear teeth were developed. These expressions,
which indicated that dynamic loads increased with speed, were not
very accurate.

Extensive tests were made by Harris (1), using an optical
system to obtain dynamic photo-elastic stress patterns of the test
gears. These results gave the indication that tooth stiffness is a
function of contact ratio and mean load with stiffness variation
decreasing as mean load increased. He found that for a single
error the tooth following the error tooth will take the greatest
force. He also determined that random errors tend to stimulate
vibration with a period close to the natural frequency of the gear
pair and at high speeds this leads to peak loads on every second or
third tooth. In addition he used a special differential analyser
to model a one-degree of freedom system for several different
combinations of tooth error and stiffness variation.

Attia (2) used strain gauges to investigate the instantaneous
static and dynamic tooth load. These gauges were used to record the
deflections of the gear teeth and to measure the maximum
instantaneous load on the tooth as it traverses the zone of contact
at different speeds and under different loads. The magnitude and

shape of the tooth loading were found to depend greatly on speed and mean load.

Gregory, Harris and Munro (3) conducted an experimental study on a test rig originally used by Harris (1). They studied the dynamics of heavily-loaded, high speed spur gears with very small manufacturing errors. Their results confirm earlier conclusions which indicated that tooth stiffness variation in the presence of light damping below (0.07) of critical damping, could cause large vibrations at the fundamental tooth engaging resonance speed, or at harmonics and subharmonics of the fundamental. These subharmonics correspond to contact between every second tooth, third tooth, and so on.

The same authors in (3) have made an analytical study (4) to explain the non-linear behaviour of gears. They assumed a one-degree of freedom torsional model consisting of a gear pair connected by gear teeth with time-varying stiffness and profile errors, and a harmonic stiffness variation was assumed. However, damping was completely ignored and as a result the authors admit that their theoretical analysis is inadequate. When viscous damping was added it was found necessary to resort to an analogue computer. Analogue results indicate that loss of contact will occur only if damping is less than (0.07) of critical which confirms earlier experimental results obtained by Harris (1).

Houser and Seireg (5,6) used a direct drive test to study dynamic tooth loads in both spur and helical gears. They investigated the influence of large manufacturing pitch errors and face width variations. Strain gauges were used to measure dynamic tooth loads and dynamic shaft torque. While the effects due to face width variations were not significant the tests involving pitch errors showed significant dynamic tooth strain effects which were speed dependent and independent of load.

These tests, however, were conducted at speeds away from system resonance and did not consider backlash effects.

Baronet and Tordion (7) have made some theoretical calculations based on two-dimensional theory of elasticity and transform functions to obtain the stress distribution in a gear tooth acted on by a concentrated load. Computations were carried

out for 20° and 25° pressure angles , standard full depth system, for a number of teeth ranging from 20-150. They found the results are in reasonably good agreement with a suggested formula for tip loading but differ appreciably when the loading is applied at lower positions along the tooth profile.

Brickner and Olerich (8) have developed a comprehensive model for backlash in gear drive systems. The friction in the support bearings is also included in the analyses. This friction was taken as coulomb friction and not as viscous damping as was suggested by the literature. The dynamics of the gear train were represented in an open loop to display the effects of changing the values of mass, friction, and backlash angle, then they included the system in a closed loop simulation to investigate limit cycle conditions. They derived the conditions for separation and contact and were programmed for digital and analogue computations. They found the results of the simulation in the open loop mode are in agreement with the behaviour of real gear drive systems.

Chabert, Dang Tran, and Mathis (9) carried out an evaluation of the stresses induced by a static load applied to gear teeth for spur gears of different ratios with 20° pressure angle and standard addendum proportions. The stresses and deflections were computed by using the finite element method. They produced a special formula by which they could find the elastic deflection coefficient of the tooth with a high degree of accuracy.

Ichimaru and Hirano (10) have conducted theoretical and experimental studies to find the dynamic characteristics of heavy-loaded spur gears by considering a vibrating system composed of an effective mass of gear blanks and stiffness of meshing teeth with manufacturing errors under given operating conditions. They found that under heavy load conditions the plastic flow produced in the subsurface layers of gear teeth affects the variation of the dynamic load considerably owing to a local change of the tooth profile. They also found that there is some reasonable evidence that the profile change under heavy load plays a role to minimize the dynamic load factor under the corresponding operating condition.

Azar and Crossley (11) have studied the impact phenomenon resulting from the loss of contact of a pair of spur gears driven

under light load. They used data-reduction techniques to automatically plot the frequency spectra of the torsional oscillations of the output shaft. When loaded, the output shaft is found to oscillate at frequencies equal to gear tooth speed and its integral multiples. They found that loss of contact of gear teeth causes a large increase in the second harmonic component of the shaft oscillation particularly when gear tooth speed (teeth/sec) equals one-half the natural frequency of the output shaft (Hz). The magnitude of the shaft oscillations increases with backlash up to a backlash value of "0.91"mm for their test setup. They also found that when the shaft is run loaded the fundamental harmonic component of the shaft oscillation is greater than the second harmonic component while when it is run unloaded the second harmonic component dominates. The amount of backlash was found to have a strong influence on the torsional oscillation of the unloaded shaft and little effect on the torsional oscillation of the loaded shaft. They also suggested that in no instance was the output shaft found to oscillate at a frequency less than the shaft speed measured in teeth/sec; i.e. No subharmonic oscillations were observed.

Seireg, Shah, and Khazekhan (12) have conducted an experimental investigation of dynamic gear tooth load and shaft torques in gear system conditions. They used an electro-dynamic shaker to apply controlled torsional excitations on the high speed shaft of a single reduction helical gear unit.

They found that the impulsive loads rise sharply with increasing amplitudes of vibration, and there appears to be a linear relationship between the vibratory amplitude and the peak load until all the backlash is consumed, as a result back tooth impact will occur which will attenuate the peak impulsive loads.

Tobe and Sato (13) have made an approximate analysis using statistical linearization and the mean and the variance of dynamic loads were calculated numerically. They first assumed that the transmission error curve of a pair of gears measured by a single flank meshing tester can be separated into harmonic components and random ones. They found that the mean of the dynamic loads

remains at similar level as in deterministic process where the random components of error are not considered for any gear speed, but the variance of them increases rapidly with an increase in speed over resonance frequency. They also suggested for a gear system which is excited by random error as a non-linear non-stationary random process that the problem of dynamic load is analysed approximately based on the Fokker-Planck equation using statistical linearization method.

Tobe, Sato, and Takatsu (14) have worked on a relation, experimentally, between transmission errors and dynamic loads of spur gears.

Two pairs of gears were used, one pair accurate and the other rough; their dependence on gear speed and tooth load was investigated. Also they produced an analogue computer simulation and compared it with a previous work (13) of the statistical theory on the estimation of dynamic loads.

For the accurate pair of gears they found, at 65.7 kg/cm tooth loading that there was a good agreement with the analogue simulation and the dynamic load shows recurrent time variation per revolution over a wide range of gear speeds. While for the rough pair of gears they found that the recurrent time variation of dynamic load per revolution begins to miss due to a random component contained in the transmission error with an increasing gear speed, and the time variation becomes very random which is caused by a notable loss of mesh.

Johnson (15) developed a method of finding modes, together with their corresponding frequencies, of shafts coupled by straight spur gears is described and illustrated by a numerical example. This method is based on the use of receptances at the meshing point of each of a pair of geared shafts which is found separately and the frequencies are then calculated from the receptance equation. He suggested that this treatment is restricted to straight spur gears.

Wang and Morse (16) used transfer matrix techniques to give static and dynamic torsional response of a general gear system. The effects which they included in the formulation are

the geartooth stiffnesses, gear web stiffness,non-uniform cross
section of shafts, external torques, special types of joints,
general boundary conditions and multi geared branched systems.
They used an electro-hydraulic exciter and an automatic mechanical
impedance transfer function analyser. They suggested that this
analytical and experimental technique could form a base for
evaluation of torsional response of a gear train system. They
also suggested that this method may be used as an aid in
optimizing the design of gear train systems, especially where
torsional vibration problems are considered. Finally they
suggested that the present techniques can be used for long shaft
systems too.

A computer based technique was developed by Wallace and
Seireg (17) for evaluation and graphic display of stress,
deformation, and fracture patterns in gear teeth when subjected
to dynamic loading. This technique is used for conditions of
impulsive loads applied at different points on the tooth surface
and moving loads normal to the tooth profile. The technique
incorporates a viscoelastic model for the material properties and
prespecified failure criteria. They investigated the accuracy of
the simulation by applying a Hertzian impact on a cantilever beam.
This simulation treats the gear as a continuum rather than a
discrete parameter system. The mass distribution of the
continuum was taken into consideration. They suggested that this
technique automatically produces the stress and deformation
patterns resulting from a dynamic excitation without prior
idealization of the geometric boundaries or preconception of the
primary mode of system response expected in a particular case.
It also has an ability to simulate failure and fracture under
dynamic loading. They also suggested that this procedure is
applied for two-dimensional analysis and it can be extended to
three-dimensional analysis. Finally they suggested that dynamic
tooth stiffness information can be readily obtained from the
simulation procedure for different material properties and gear
wheel configurations.

Conry and Seireg (18) have found a generalized technique
for evaluation of load distribution in gear systems and automated
the selection of optimal modification for the best possible
distribution based on any prespecified type of modification. The
procedure utilizes a simplex-type algorithm and provides an
efficient and effective means for the design of gears with uniform
load distribution. They suggested that the procedure can be
applied to spur and helical gears and can easily be extended to
other types of gears. Also it could take into consideration
manufacturing and assembling errors as well as housing deflections
under load.

Wilcox and Coleman (19) considered the application of the
analytical method of finite elements to the analysis of gear tooth
stresses. A simulation of two-dimensional tooth shape with
finite elements is outlined. They gave special attention to the
asymmetric profiles (used in Hypoid gears). They found that the
developed formula tends to underpredict the stress in most cases
by an amount ranging from a fraction of a per cent up to twenty
percent.

Wang (20) has extended the dynamic torsional analysis of a
gear train to the linear and nonlinear transient analysis of
complex torsional gear train systems. He considered in the
formulation time-varying gear tooth stiffness, gear web rigidity,
gear tooth backlash, shafts of nonuniform cross section, linear
and non-linear damping elements, multishock loading, and complex-
geared branched systems. He suggested that this modelling
technique provides an effective tool in predicting both linear and
non-linear transient response characteristics inherent to gear
train systems. He also suggested that this method may be used as
a means to analyse gear train start-stop operational problems as
well as constant speed response subject to internal and external
disturbances.

Randall (21) has applied cepstrum techniques for detection
and evaluation of the side bands usually present in gear box
vibration spectra since these give valuable information about the
existence of effects (often undesirable) which cause modulation of

the basic tooth meshing pattern. The cepstrum is obtained by further Fourier transformation of the logarithmic (dB) spectrum. Peaks in the cepstrum indicate the side band spacings, and thereby the modulating frequencies, and thus often point to their source. He found that care must be taken to exclude or allow for the presence of low harmonics, which also give peaks in the cepstrum. Use of high-and-low pass filters to select out the frequency range from $\frac{1}{2}$ to $3\frac{1}{2}$ times a particular tooth meshing frequency will sometimes achieve this.

Mitchell (22) has used multi rotored transfer matrices. The rotors are coupled by a modified Hibner-type transfer matrix at each gear mesh. The method he used automatically includes the detailed book keeping within the matrix operations. He presented numerical results for the case of machining errors in the gear teeth.

Lees and Pandy (23) have analysed a complete shaft/bearing system as a set of segments, each segment terminated at a gear mesh. Equations of constraint are applied which impose on the system an amplitude controlled vibration (flexural and torsional). They used a finite element model of a gear box to determine the response of gear forces and bearing vibrations to gear profile errors, thus establishing a direct link between vibrations and gear forces. Bearing vibrations are recorded, averaged over a large number of shaft revolutions and then frequency analysed. The gear errors and the resulting excess forces are then estimated from the calculated response. They suggested that tooth pitch errors give rise to components in the vibrational spectrum at frequencies other than synchronous.

Taylor (24) has found procedures for identifying gear defects and gear meshing problems. He analysed time signal, spectrum frequencies, shape, amplitude and sum and difference frequencies to reveal which gears have defective tooth, the number of defective teeth on each gear, the number of gears that have defective tooth and the location of the defective teeth with respect to some reference point. He pointed out that defects can be indentified early enough to permit six months lead time before repair is required. This lead time facilitates planning and prevents catastrophic failures.

Randall (25) made a number of practical points in the
calculation and interpretation of the cepstrum. He pointed out
an idea about separation of harmonics and sidebands. The side-
bands often coincide with harmonic frequencies, but physically
the harmonics around and above the tooth meshing frequency are
most likely sidebands related to tooth condition. The low
harmonics may be due to entirely different reason such as:
Unbalance, misalignment and mechanical looseness. He recommended
cutting off the low harmonics at approximately half the tooth
meshing frequency.

1.2.2 Studies of Impacting of Mechanical Systems with Clearances:

A number of investigations have studied the effects of
clearances on the dynamic behaviour of mechanical systems.

Kobrinskii (26) formulated a model of a one-dimensional
system consisting of two masses with a clearance between them. A
piece wise linear solution is developed using the coefficient of
restitution to account for the energy loss due to the repetitive
impacts.

Both two-sided and one - sided collisions are studied and
stability diagrams are plotted.

Sikarskie and Paul (27) have investigated the dynamics of
hammer impact machines on the basis of a two-degree of freedom
idealization. They found some difficulty about the repetitive
impact which introduces a nonlinearity into the system. To ease
the problem from a parametric point of view, they converted to a
boundary value problem. They also made an assumption in the
analysis that the steady state response of the system has a period
equal to the forcing period, this is to verify one set of
parameters through the use of high-speed photography of an actual
machine.

Dubowsky and Freudenstein (28,29) have shown in their work
that a simplified assumption (the coefficient of restitution would
adequately describe the impact phenomenon) does not always result
in a unique solution. Since surface compliance is not considered,

-25-

this analysis does not include dynamic coupling or contact stresses while the contact duration is assumed to be zero. In fact for systems with small clearances the magnitude of the contact duration may be of the same order as that for non contact.

Dubowsky and Freudenstein introduced a refinement of an earlier model to study torsional oscillations in the gear drive of a cam pump. This model which is called an impact pair includes surface compliance and allows for one-sided as well as two-sided impacts.

Using the contact compliance for a pin joint and ball connection based on classical Hertz theory the dynamic response of the impact pair is found for the case of free vibration. This exact solution is compared with that obtained using a linearized compliance model. It is concluded that the Hertzian nonlinear representation can be linearized so that the resultant error is less than two per cent.

In addition to the free vibration case, the dynamic response of the impact pair is found for the case of constant load operation and under displacement-forced excitation. Other results that are obtained include displacements, force amplification and vibrational characterstics of the impact pair.

Veluswami and Crossley (30) have made a series of physical experiments with a steel sphere vibrating while trapped between and impinging against two end plates,(as in an impact damping device) while the plates are shaken by an electromagnetic shaker. Three different materials were used for the end plates. They found that, for the range of frequencies (0-60 Hz) and amplitudes (0-5 mm), the ball generally hits several times on one boundary before passing over to strike the other, per cycle of the shaker. They also presented data about the modes of vibration and the duration of the contacts. A record of the effects of varying the frequency and amplitude of the drive were taken for a range of clearances, for balls with different masses and for three distinctly different materials. For impact of spheres of mild steel to mild steel , it was observed that at steady state impact the phase of the ball's motion was slightly ahead of the

plate motion: The position of the impacts on the time
displacement curve preceded the maximum excursion point of the
plates by a time interval close to $\frac{1}{20}$ of the period. Also
the impacts occurred uniformly with each half cycle of the drive
motion. Two more materials were taken for the end plates; i.e. a
mild steel ball hitting nylon or rubber. They concluded that
the coefficient of restitution diminishes approximately linearly
with velocity to the point where the stress incurred approaches
the yield stress. This reduction in coefficient of restitution
means that the energy loss to internal damping increases with
velocity of impact.

        Veluswami, Crossley, and Horvay (31) obtained a mathematical
model based on an earlier experimental observation (30).   This
model was developed to portray the vibroimpacts of a steel sphere
which is trapped between two flat steel plates with clearance,
while the plates are oscillated by an electromagnetic shaker.
During each impact the motion of the ball is taken to be a brief
half wave, due to the highly nonlinear forces of surface compliance
and surface damping. Modelling is done by analogue simulation.
It was found first that linearization of the surface stiffness
does not reproduce the observed phenomena. The mathematical
model formulated is that the motion of the ball during contact is
governed by the equation :

$$M\ddot{X} + CX^{1.5}\ \dot{X} + KX^{1.5} = 0$$

Where X is the penetration, C is the damping constant, and $KX^{1.5}$
is the Hertzian force .

        For the simulation results, the recorded runs were all
steady state; a sufficient delay was allowed in each case to
ensure that the transient has dissipated. Attention in taking the
records was centered on reproducing the patterns of the multiple
impact motions. They recommended that much more work is still to
be done to study phase shifts, maximum penetration, and maximum
stresses.

1.3 Objective of this Study

As mentioned earlier there is ample evidence that the dynamic behaviour of a geared system can cause excessive wear and fatigue failure of the gear teeth along with high dynamic shaft loads. This is particularly true when the speed of the gear teeth coincides with a natural frequency of the system and tooth separation occurs. This investigation of the resonant behaviour of geared system should include the effects of the connected inertias and shafts. With the notable exception of the work done by Houser and Seireg (5), most experimental investigations have involved the use of back-to-back test apparatus which excludes such effects. However their studies were run at speeds away from system resonances.

The test rig built for this investigation uses a direct drive configuration and is specifically designed to operate over a speed range that includes the system resonance. It also included a means of varying the magnitude of the gear backlash when needed.

The torsional system consisting of a drive unit, driving gear and fixed inertia, driven gear, adjustable inertia, and load is shown in Fig (1.2a). The gear teeth are assumed to be in contact and the system oscillates as a five degrees of freedom system.

When the gear teeth separate, as shown in Fig (1.2b), the input and output sides oscillate separately. Each inertia system has its own characteristic natural frequency.

Tooth separation occurs when the mean driving torque is exceeded by torque variations in the drive unit, the load or the gear pair. Two such sources of torque variation in the gear pair are tooth stiffness variations and tooth form errors.

During separation the driven gear speeds up while the driving gear slows down because of the mean load. After separation the gear teeth may or may not impact on their rear faces depending on the size of the backlash and the magnitude of the mean load. It should be noted that the mean load tends to prevent separation and it also tends to prevent reverse impacting of the gear teeth when separation occurs.

The main objective of this investigation is to study the impact phenomenon in the system described above. This investigation is to be both experimental and analytical.

(a)

(b)
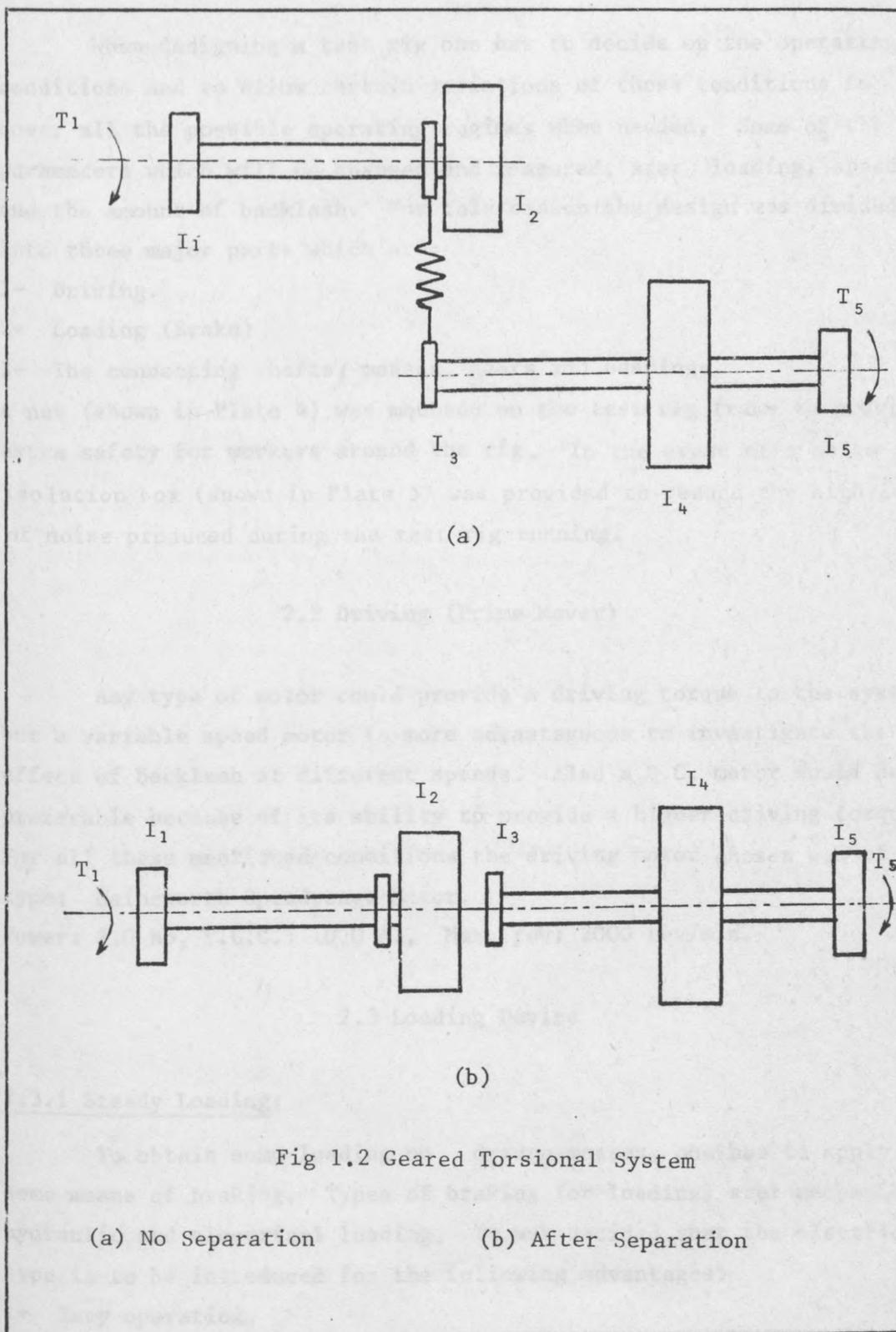
Fig 1.2 Geared Torsional System

(a) No Separation   (b) After Separation

II. TEST RIG AND ITS DESIGN

2.1 Introduction

When designing a test rig one has to decide on the operating conditions and to allow certain variations of those conditions to cover all the possible operating regimes when needed. Some of the parameters which will be changed and measured, are: loading, speed and the amount of backlash. For this reason the design was divided into three major parts which are:

1- Driving.

2- Loading (Brake)

3- The connecting shafts, masses, gears and bearings.

A net (shown in Plate 4) was mounted on the test rig frame to provide extra safety for workers around the rig. In the event of a noise an isolation box (shown in Plate 5) was provided to reduce the high level of noise produced during the test rig running.

2.2 Driving (Prime Mover)

Any type of motor could provide a driving torque to the system, but a variable speed motor is more advantageous to investigate the effect of backlash at different speeds. Also a D.C. motor would be preferable because of its ability to provide a higher driving torque. For all these mentioned conditions the driving motor chosen was of the type: Hainsworth Speedrange Motor.

Power: 2.0 hp, F.L.C.: 10.0 A., Max. rev: 2000 rev/min.

2.3 Loading Device

2.3.1 Steady Loading:

To obtain some loading on driven masses, one has to apply some means of braking. Types of braking (or loading) are: mechanical, hydraulic and electrical loading. It was decided that the electrical type is to be introduced for the following advantages:

1- Easy operation.

2- Easy control.

II. TEST RIG AND ITS DESIGN

2.1 Introduction

When designing a test rig one has to decide on the operating conditions and to allow certain variations of those conditions to cover all the possible operating regimes when needed. Some of the parameters which will be changed and measured, are: loading, speed and the amount of backlash. For this reason the design was divided into three major parts which are: 1- Driving.

2- Loading (Brake).

3- The connecting shafts, masses, gears and bearings. A net (shown in Plate 4) was mounted on the test rig frame to provide extra safety for workers around the rig in the event of a sudden failure. In addition a noise isolation box (shown in Plate 5) was provided to reduce the high level noise produced during test rig running.

2.2 Driving (Prime Mover)

Any type of motor could provide a driving torque to the system, but a variable speed motor is more advantageous to investigate the effect of backlash at different speeds. Also a D.C. motor would be preferable because of its ability to provide a higher driving torque. For all these mentioned conditions the driving motor chosen was of the type: Hainsworth Speedrange Motor. Power: 2.0 hp, F.L.C.: 10.0 A.

Max. rev: 2000 rev/min.

2.3 Loading Device

2.3.1 Steady Loading:

To obtain some loading on a driven masses, one has to apply some means of braking. Types of braking (or loading) are: mechanical, hydraulic and electrical loading. It was decided that the electrical type is to be introduced for the following advantages;

1- Easy operation.

2- Easy control.

3- Accurate and prompt control.

4- Easy to measure.

The device which was used for loading is of the type made by
JAY JAY and it is called:

Eddy Current Dynamometer

Type No: DM3/50

2.3.2 Oscillatory Loading:

When using Eddy Current Brake, with its circuit all inside
the casing, it was very difficult to add any circuit to implement
the oscillating load. Because of this, one way to implement this
type of loading is to control the input current to the braking
coils which produce the magnetic flux required to load the rotor
of the brake. These points are connected to a block under a small
cover which was easy to take out.

Because the only way to apply an oscillating load is to
change the input current to the coils, this means that the
oscillating load is operated by superimposing an AC signal with a
known frequency to the DC level of the braking current. A full
description of the circuit design is in App.A.

2.4 Shafts, Bearings and Load Inertias

2.4.1 shafts:

There was no limitation on the use of any material for the
shafts, except for the load it was going to take. The diameter of
the shaft was kept to a minimum, but at the same time the shaft
should not be too flexible specially where the gears are connected
to it, because a line of contact is required. A full description
of the shafts and their sizes are shown in App.B.

2.4.2 Bearings:

The bearings used were of standard type and self lubricated.
All the bearings were of the same shape and dimensions, type:
SKF 6004-27, single row deep groove ball bearings. The bore
diameter was: 20mm.

2.4.3 Load Inertias:

Two load inertias were selected to keep the natural frequency around 15 Hz, the reason for this frequency will be discussed in section 2.7. The sizes and weights of these inertias are shown in App.B.

2.5 Test Gears

The pair of gears which was used for this research was relatively accurate in dimensions and was specially produced for this test; i.e.with as little machining errors as possible. The gears manufactured by E.G.BAXTER & Co were of the same size . The general specifications of these gears are as follows:

Material	Mild Steel
P C D	150 mm.
Face width	20 mm.
Module m	5 mm.
Bore dia	20 mm.
Boss dia	40 mm.
Boss length	40 mm.

2.6 Method of Changing Backlash

To change the backlash it was enough to change the centre distance by moving the driving gear in or out. Looking at Fig 2.1, there are seven steps to be followed to change the backlash and they are:

1- Release the screw on the coupling D and slide D to the left until it clears the shaft where the driving gear is fixed.

2- Release the two screws B on the moving plate G.

3- Turn the handle A to the required centre distance.

4- Release the bolts C and E on the driving motor F.

5- Re-align the motor shaft to the shaft where the driving gear is fixed.

6- Slide back the coupling D to the right and tighten the screw
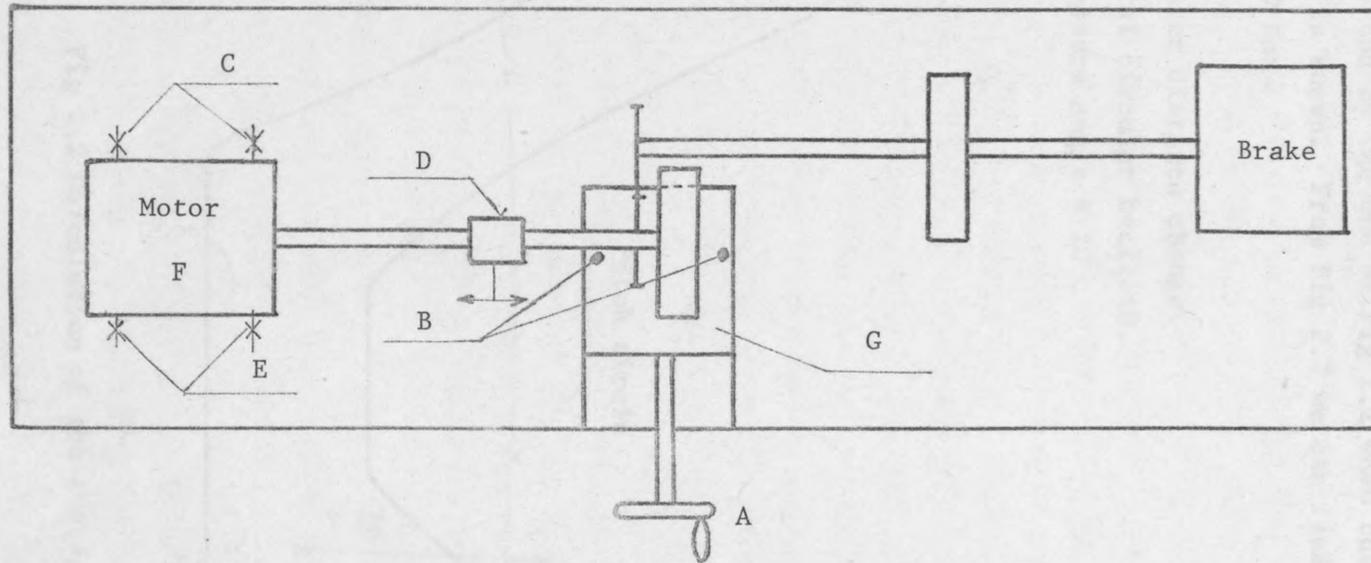
Fig 2.1 Schematic Drawing of Backlash

Changing Sequence

on the shaft to insure that there is no extra play between the
coupling and the shaft.

7- Tighten the screws B.

A special dial gauge is placed at the center of the shaft to
measure the change in center distance, which as a result will
produce a change in backlash. The average value of the backlash can
be calculated by the use of Fig 2.2 when the change of center
distance is known. From Fig 2.2 we can find that;

$2B_1 = 2\Delta C \tan\alpha$

Where:

ΔC.. center distance change.

$2B_1$. total circular backlash.

α.. pressure angle = 20^0.
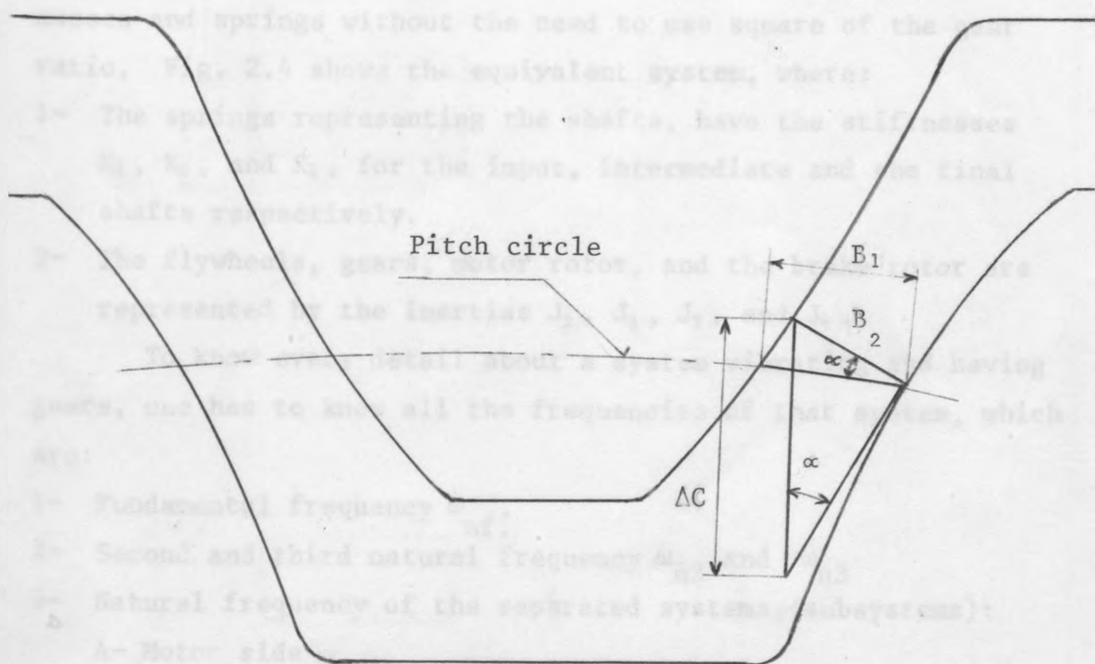
Fig 2.2 Calculation of the Average Backlash

-34-

2.7 Natural Frequencies of the System

To study the effect of backlash on the dynamic behaviour of a mechanically vibrating system with the best possible results, and to analyse the system accurately, one has to know the natural frequencies of this system. Also to magnify the effect of backlash on the dynamics of this system, it has to run in and around one of its natural frequencies.

Because the loading device was only able to operate at a frequency around 15 Hz, according to a specification by the manufacturer, the natural frequency of that system was designed to be in the range of 12-18 Hz, as a result the inertias and the shafts sizes are as it was suggested in App.B.

Fig 2.3 is a schematic drawing of the system showing the position of gears and masses on the shafts. Because the gears were of the same size, the ratio of transmission is 1:1, and from that the equivalent system is a straight forward transformation of masses and springs without the need to use square of the gear ratio. Fig. 2.4 shows the equivalent system, where:

1- The springs representing the shafts, have the stiffnesses K_1, K_2, and K_3, for the input, intermediate and the final shafts respectively.

2- The flywheels, gears, motor rotor, and the brake rotor are represented by the inertias J_1, J_2, J_3, and J_4.

To know every detail about a system vibrating and having gears, one has to know all the frequencies of that system, which are:

1- Fundamental frequency ω_{nf}.
2- Second and third natural frequency ω_{n2} and ω_{n3}
3- Natural frequency of the separated systems (subsystems):
    A- Motor side ω_{nm}.
    B- Brake side ω_{nb}.

All these systems (main system and subsystems) and their corresponding natural frequencies are shown and calculated in App.C. Fig 2.5 shows a table of the calculated total system and subsystems natural frequencies.
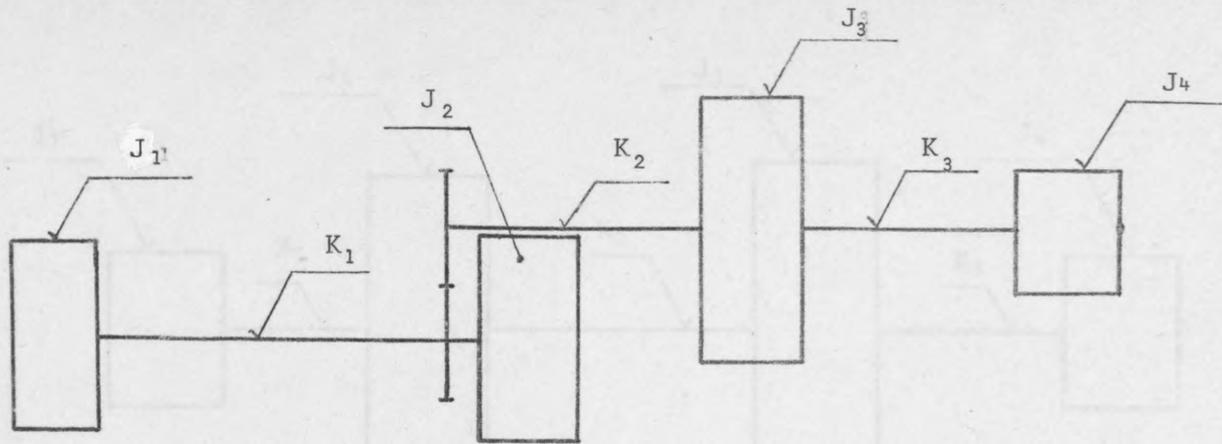
Fig 2.3 Model of Inertia and Stiffness System
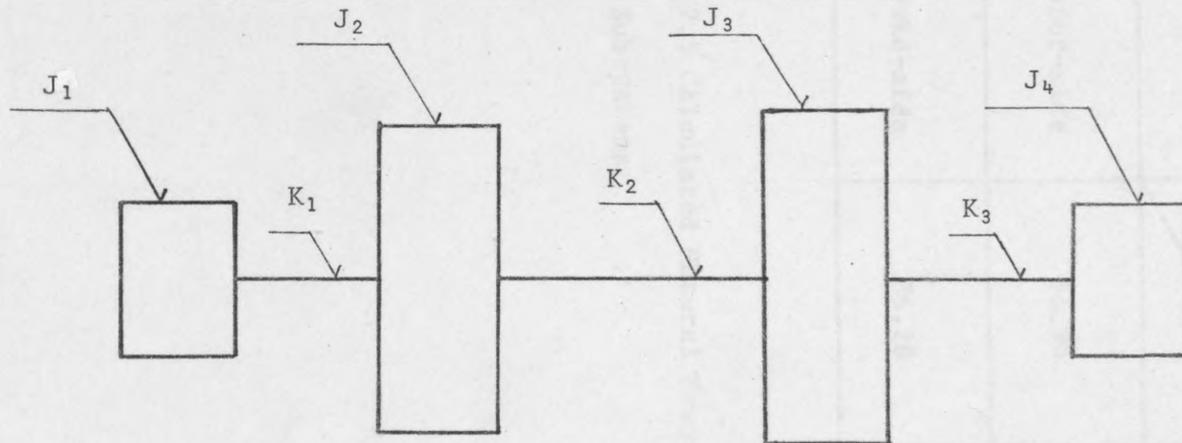
Fig 2.4 Equivalent System

Natural frequency / System	f_1 (Hz)	f_2 (Hz)	f_3 (Hz)
Total	Experimental (13.33) / 17.84	86.95	91.95
Motor-side	91.90	—	—
Brake-side	86.28	88.67	—

Fig 2.5 Calculated Natural Frequencies of the Total System and Subsystems
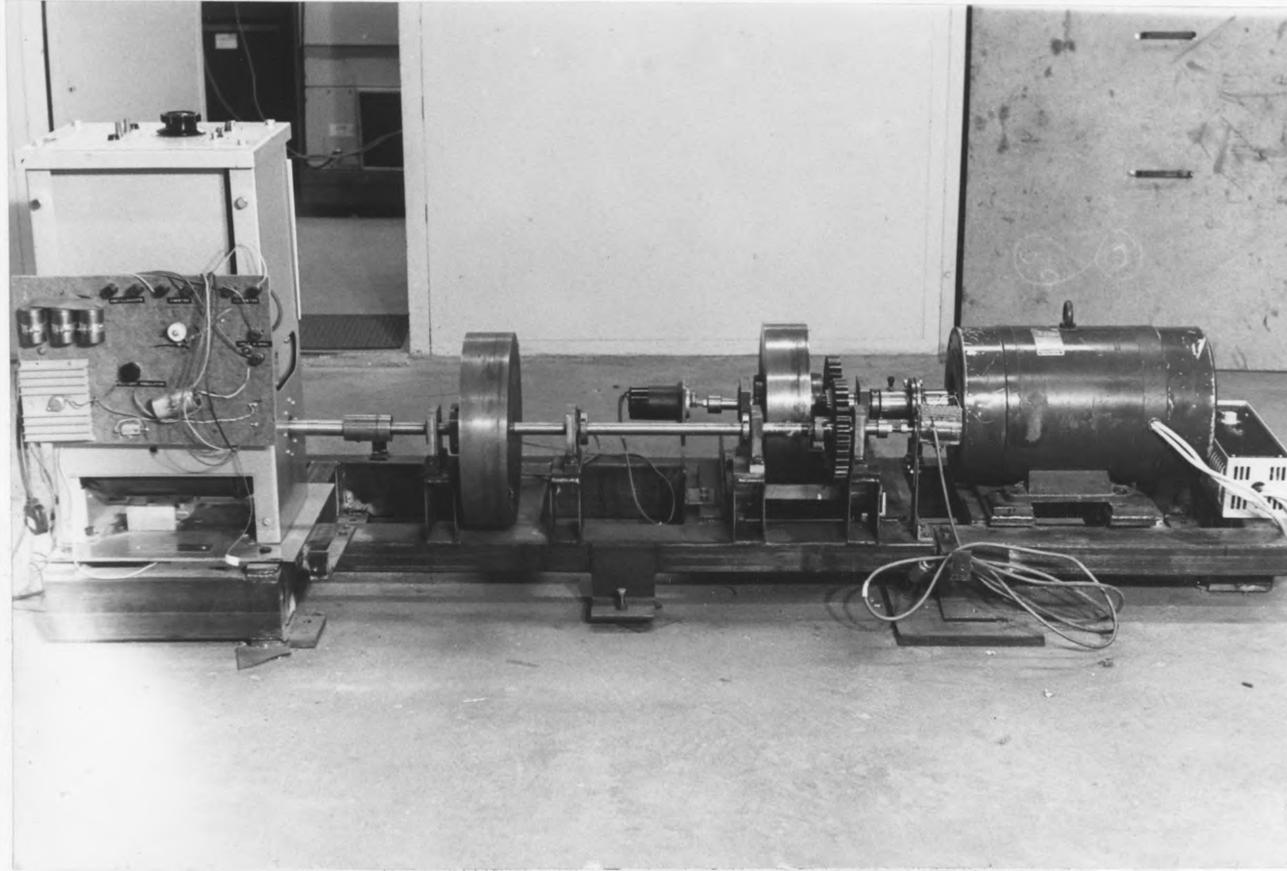
Plate 1 General View of the Test Rig
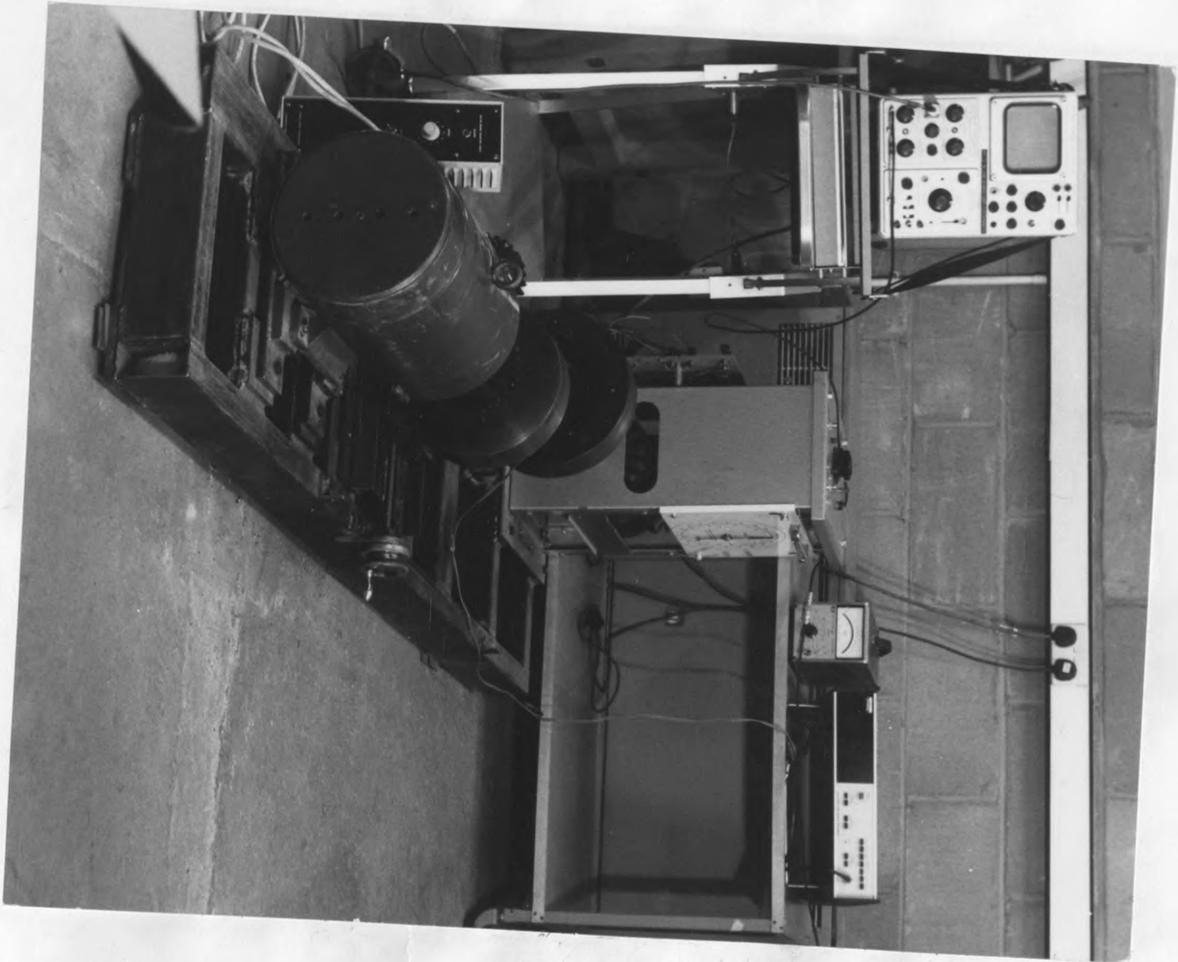
Plates 2 Test Rig with some of its Measuring Instruments
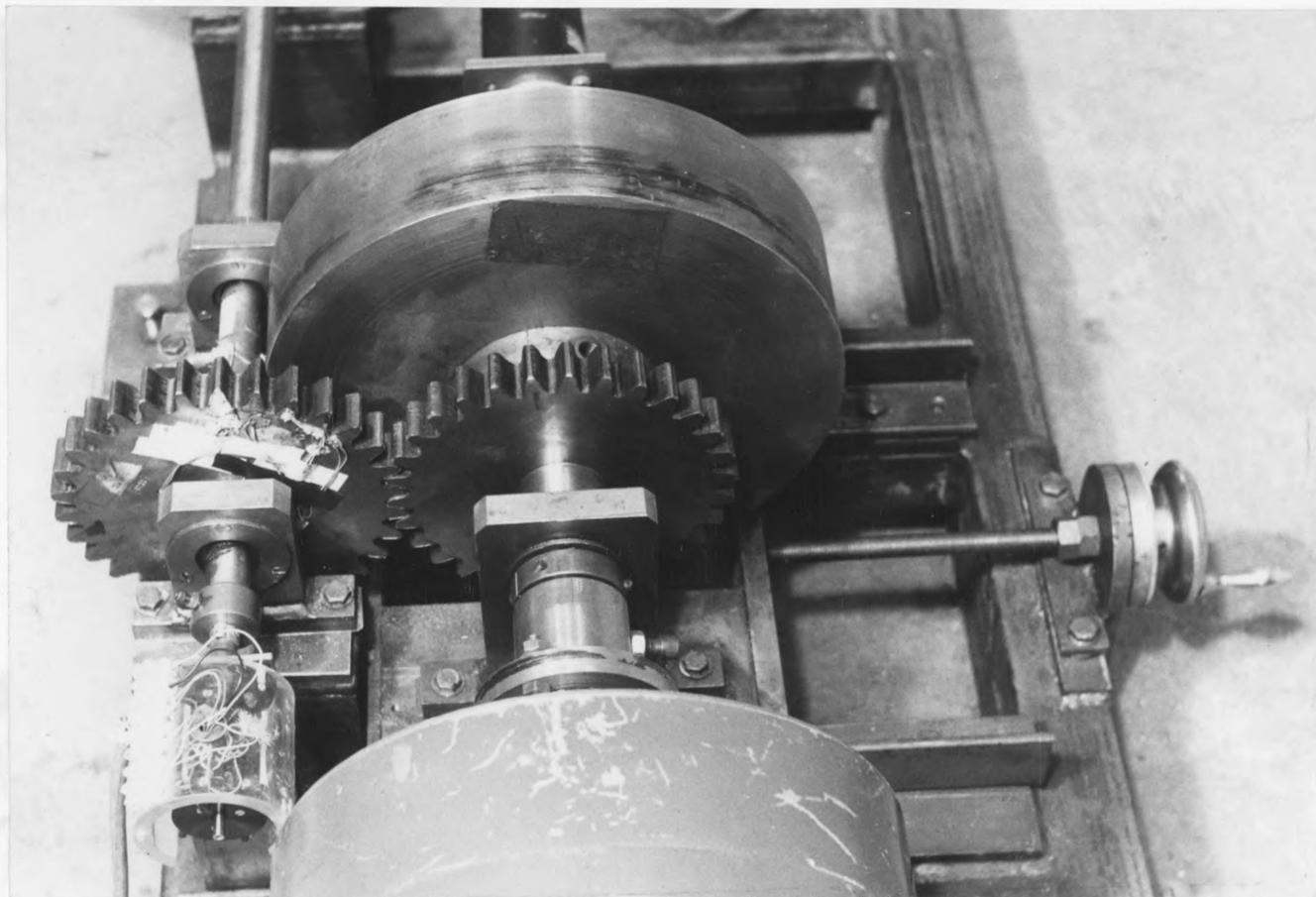
Plates 3 Test Gears with Backlash Changing Mechanisms
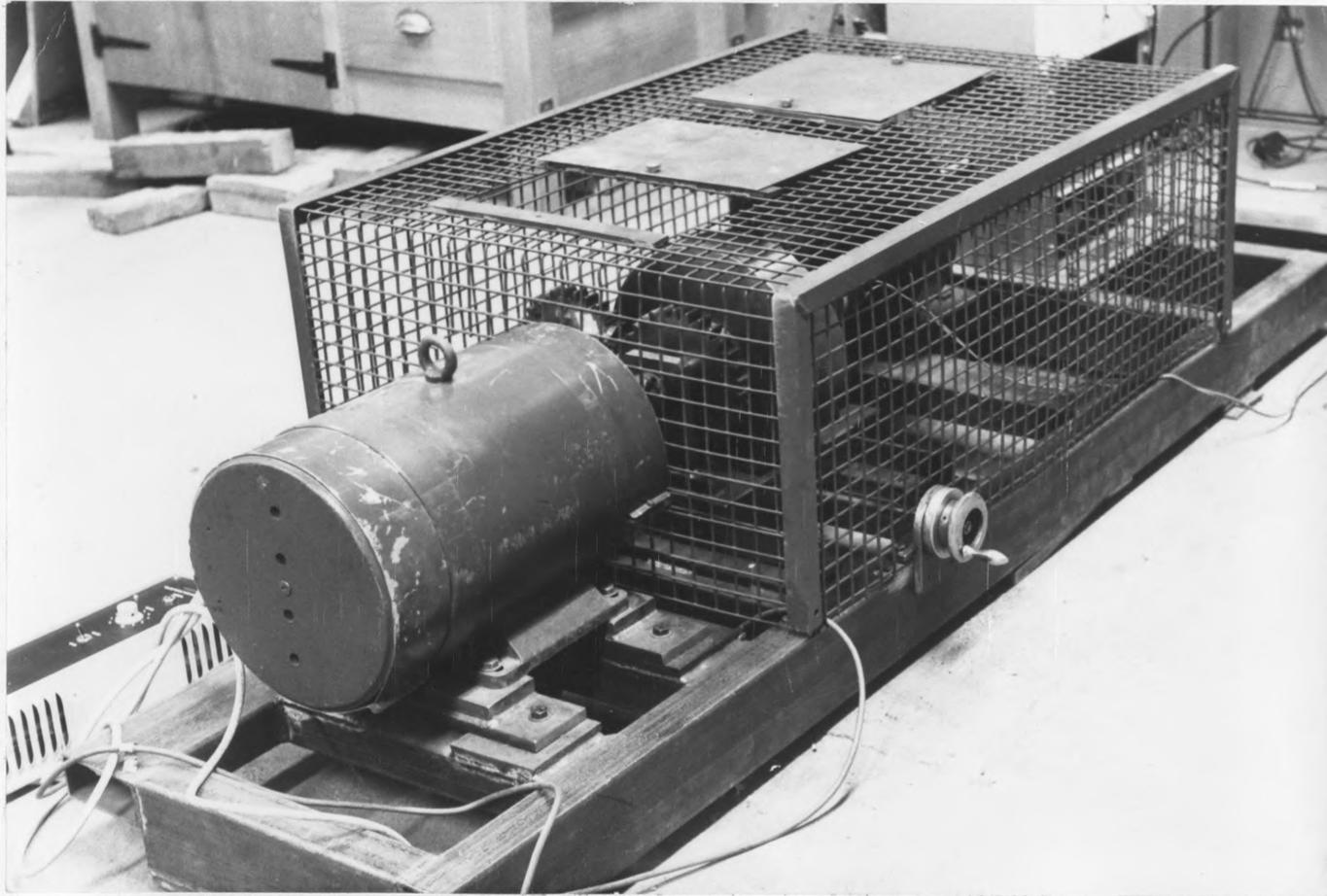
Plates 4 Test Rig with the Safety Net
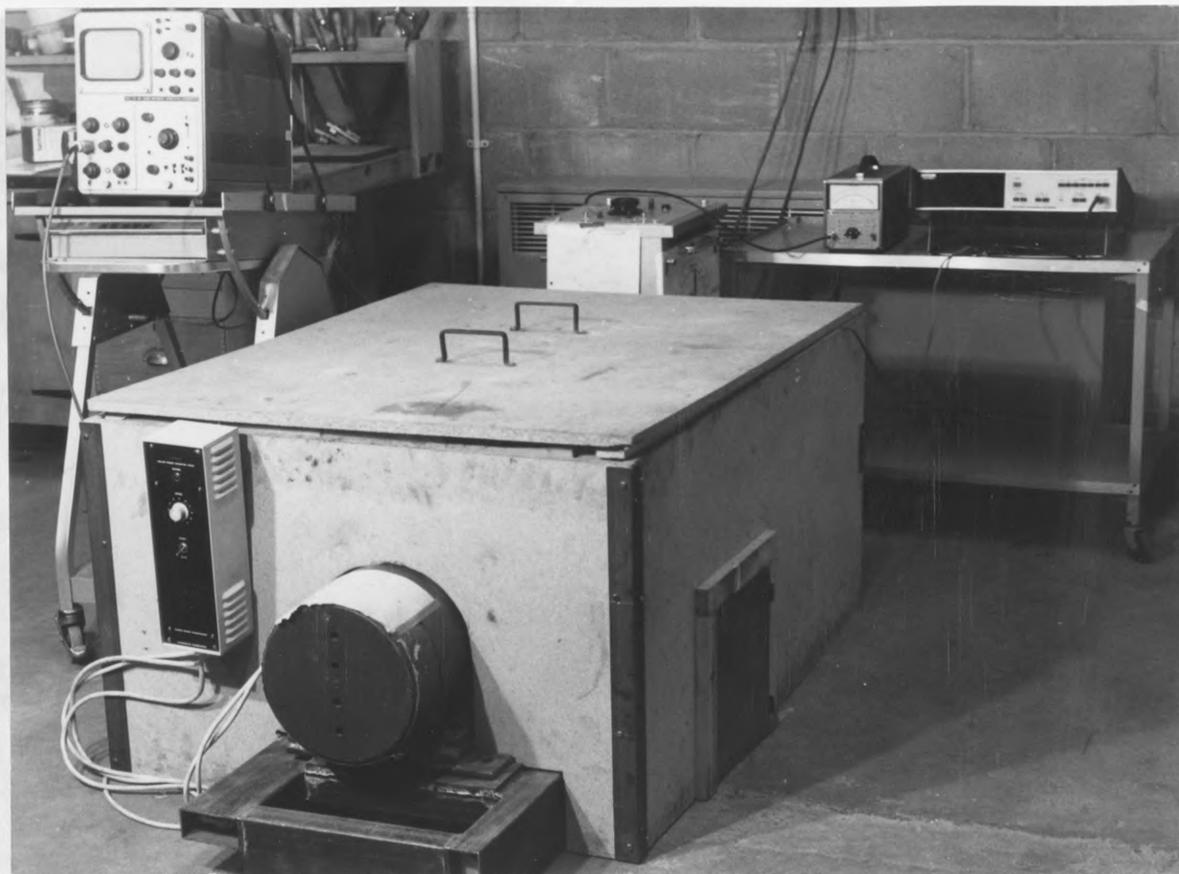
Plate 5 Noise Isolation Box
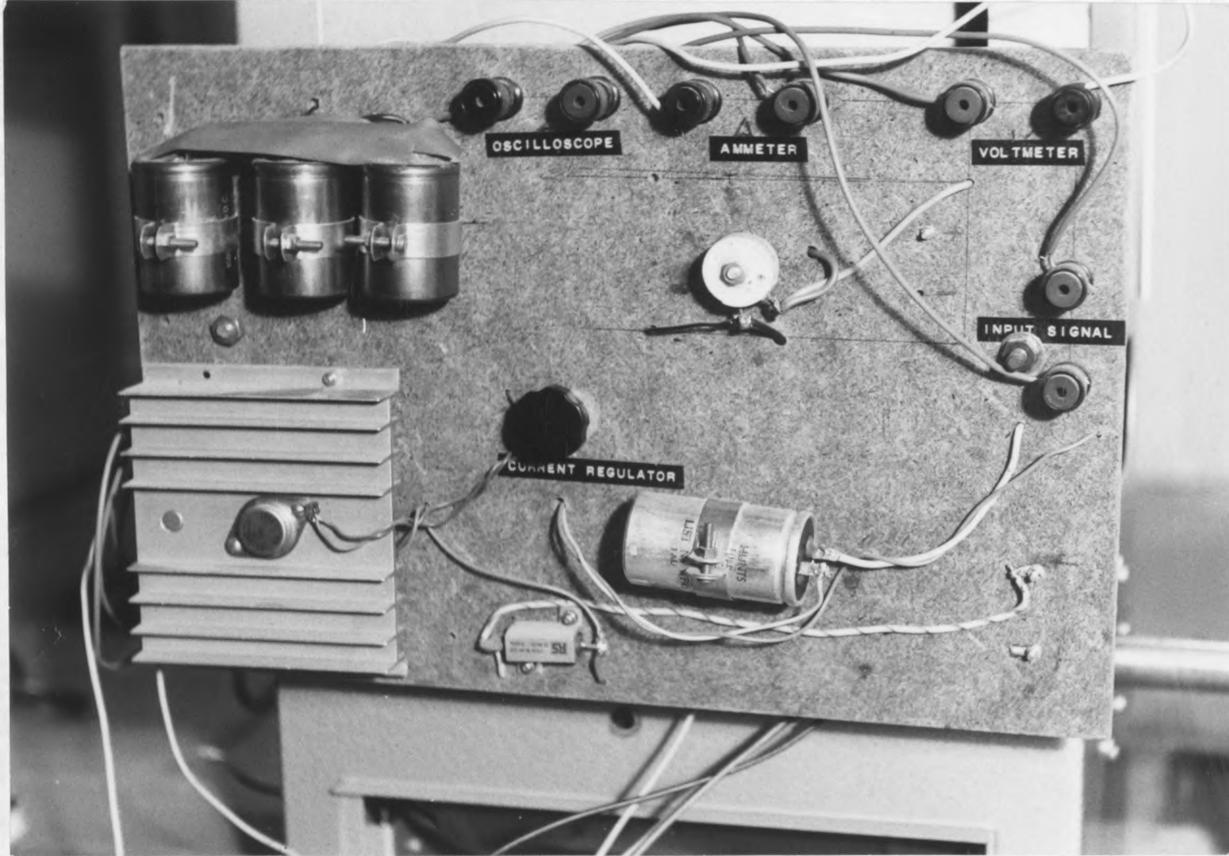
Plate 6 Oscillating Load Generation Circuit

3.1 Introduction

Numerous investigations have successfully measured dynamic loads on rotating gear wheels and the connecting shafts. Harris (1) used an optical system to obtain the dynamic photo-electric stress patterns on his test gears. However, the use of strain gauges for these measurements has been much more popular. Some research work (2,5,10,11) have coupled strain gauges with slip rings, and others, strain gauges with telemetry to measure and transmit the test information.

Particular care was required in designing the instrumentation for this study. This was necessary since the instrumented shaft and gear were run under light load. Strain gauges were selected as the transducers but the electrical signal was expected to be small.

Special signal conditioning equipment was used with the oscilloscope to amplify the strain signals after they passed through the slip rings. Since the slip rings are the major source of noise in this type of system, the strain gauges on the teeth were not used so successfully. The complete measurement system and its various components are described in the following sections.

3.2 Strain Gauges

A standard set of four SHOWA N22-FA2 were mounted on the shaft, and a set of two SHOWA N11-FA2-120-11, were mounted on the gear tooth. Fig 3.1a and 3.1b shows the position of the strain gauges on both the output shaft and the gear tooth. The strain gauges on the output shaft were fixed as close as possible to the gear boss to eliminate the effect of shaft flexibility and the strain gauges on the gear tooth were fixed as close as possible to the tooth root.

The strain gauges on the shaft were arranged as a bridge with four active gauges, this arrangement was designed to measure and transmit the dynamic response of a rotating system; i.e.to measure torsion only, and the strain due to bending will have no
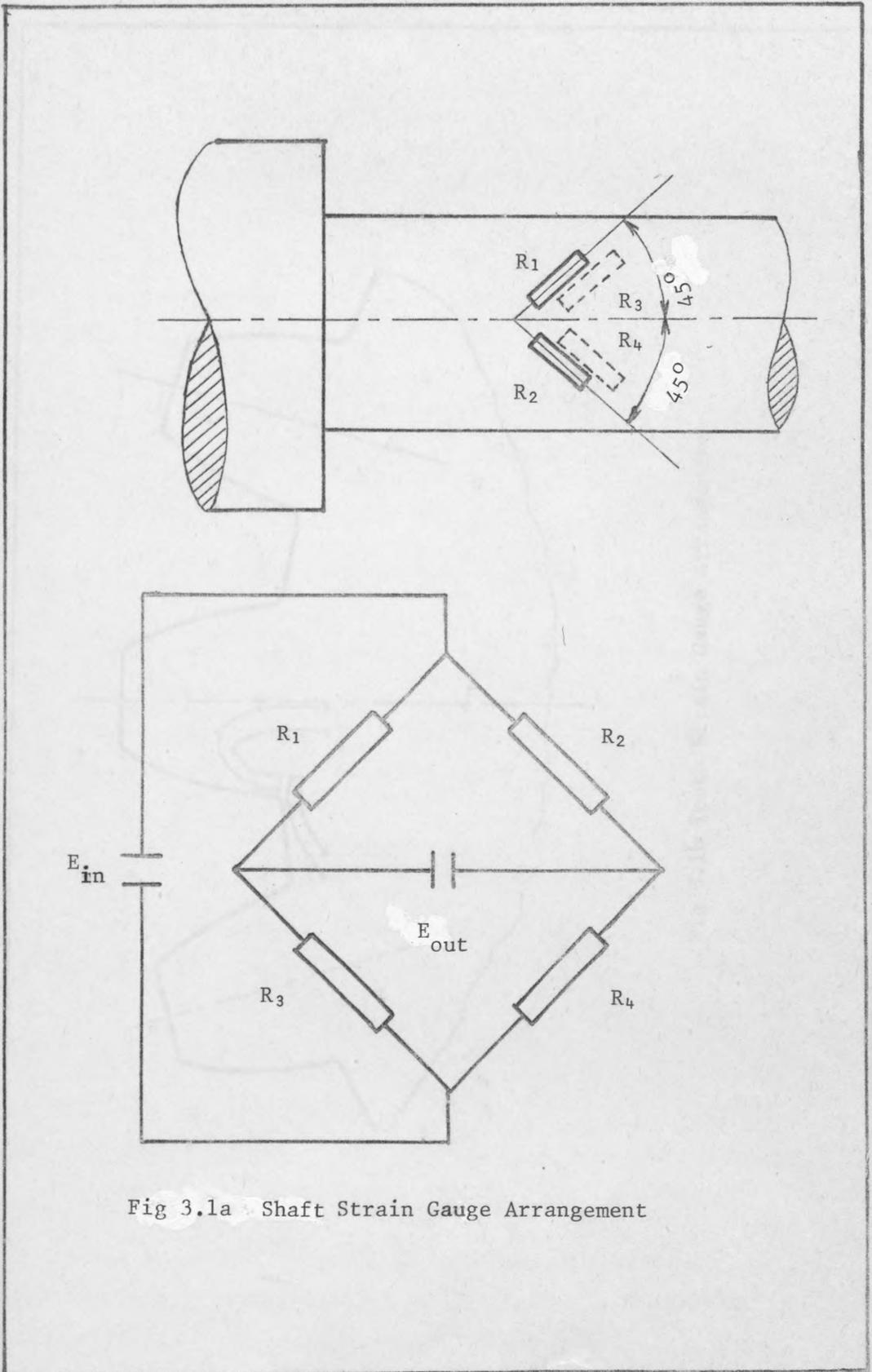
Fig 3.1a Shaft Strain Gauge Arrangement
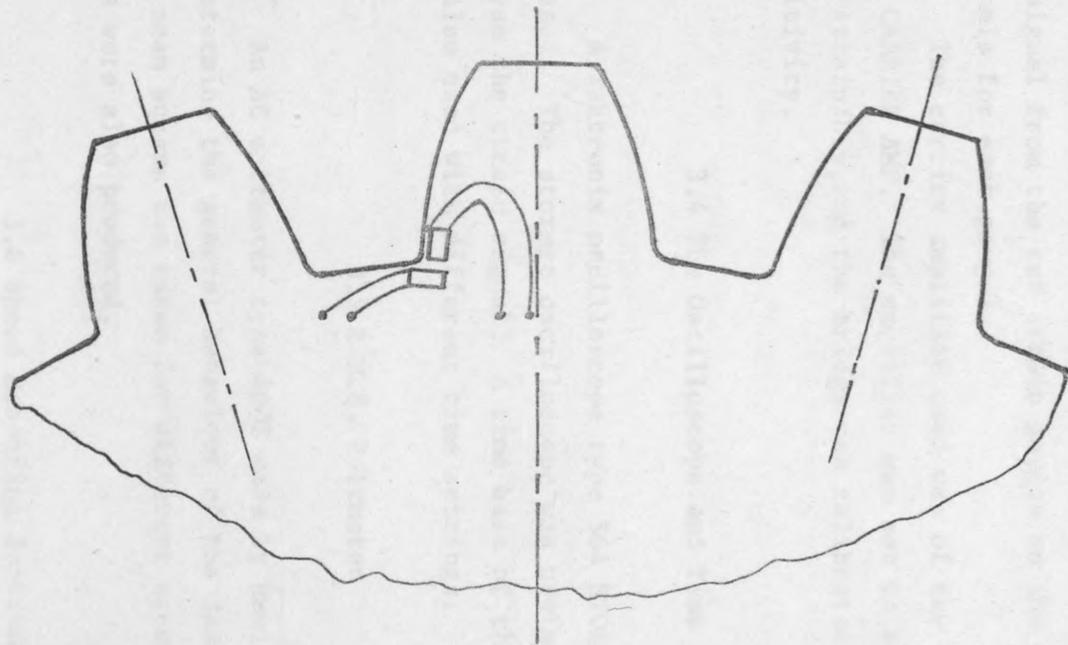
Fig 3.1b Tooth Strain Gauge Arrangement

effect on the output signal. The bridge arrangement and calculations are shown in App.D.

3.3 Slip Rings and Carrier Amplifier

A slip ring assembly of the type PL-OT made by IDM Electronics, with eight channels, was used. Four channels were taken for the bridge arrangement and the rest for transmitting the signal from the two strain gauges on the gear tooth (two channels for each gauge).

The carrier amplifier used was of the type: Tektronix 3C66 CARRIER AMP. The amplifier was set to a position of 200μ strain/Div, and the bridge was calibrated for the maximum sensitivity.

3.4 The Oscilloscope and Time Base

A Tektronix oscilloscope type 564 STORAGE OSCILLOSCOPE was used. The storage oscilloscope was useful to observe and analyse the strain signal. A time base of the type 2B67 TIME BASE was also used with different time settings.

3.5 R.M.S. Voltmeter

An AC voltmeter type 400E made by Hewlett Packard was used to determine the general behaviour of the designed system. The root mean square was taken for different speeds and loads and plots were also produced.

3.6 Speed Measuring Instruments

3.6.1 Tachometer:

For speed measurement, an AC Tacho-generator made by Crompton Parkinson was used. The generator was calibrated to produce (40) volts for each (1000) rev/min.

-48-

3.6.2 Digital Voltmeter:

To read the voltage produced by the tacho-generator a
digital voltmeter made by Schlumberger of the type A200 was also
used. The digital read-out has an important advantage of easier
and quicker reading.

3.7 Oscillating Load Generation

3.7.1 Introduction:

These instruments were used very little because the
results obtained had no significance on the overall analysis of
the designed system. For this reason there will be a little
description on these instruments. A special circuit was designed
to produce and measure this oscillating load.

3.7.2 The Oscilloscope:

A simple Philips portable oscilloscope of the type PM3200
was used for displaying the input oscillating current going into
the Eddy Current Brake circuit.

3.7.3 Function Generator:

A Feed-Back wave form generator of the type: TWG 300, was
used to produce the AC voltage needed to superimpose an AC signal
on the DC level of Eddy Current Brake with the help of the electrical
circuit designed and shown in App.A.

3.7.4 Voltmeter and Ammeter:

A separate voltmeter and ammeter were used to read out the
values of the current going through and the voltage across the
Eddy Current Brake coils.

3.8 Variable Filter

The variable filter was needed to eliminate the effect of
aliasing which will be described in section (3.9.4).

The filter used was of the type EF2 made by Barr and Stroud Limited.

3.9 Fourier Analyser

3.9.1 Introduction:

When a mechanical system starts to work and analysis of the dynamic response of that system is required, a special instrument should be used to break down the output of the system into frequencies and amplitudes. In this study the instrument used was a Fourier Analyser of the type 5451C, manufactured by Hewlett Packard. This instrument works and analyses the signal digitally which means it is more accurate and flexible, and also faster than many types of spectrum analyser.

3.9.2 Analog to Digital Converter:

One of the main functions of the ADC is to sample the input, which varies with time, into small sample intervals After sampling, each sample becomes a digital word which is stored for further processing (e.g. conversion into Fourier Transform). Looking at Fig 3.2 the sampling parameters used in the time domain are as follows:

Δt- The time between samples and it is called the sample interval.

N - The number of samples taken, and on the analyser it represents the Block Size.

T - The total time of the sample record, also called: Total Record Length.

From the definition the following can be obtained:

$$T = N \times \Delta t$$

In frequency domain, and after the Fourier transform being performed, there is a similar set of parameters. These parameters are: (from Fig 3.3)

Δf - The number of Hz between frequency points (or frequency resolution).

N/2 - The number of frequency points (equal to half of the block size). One half for real (or amplitude) and the other

Amp.

Original
Analogue Input

Time

Amp.

Sampled Analogue Input

Time

Δt = Time Between Samples

N Samples $\cdot \Delta T$ Apart = T
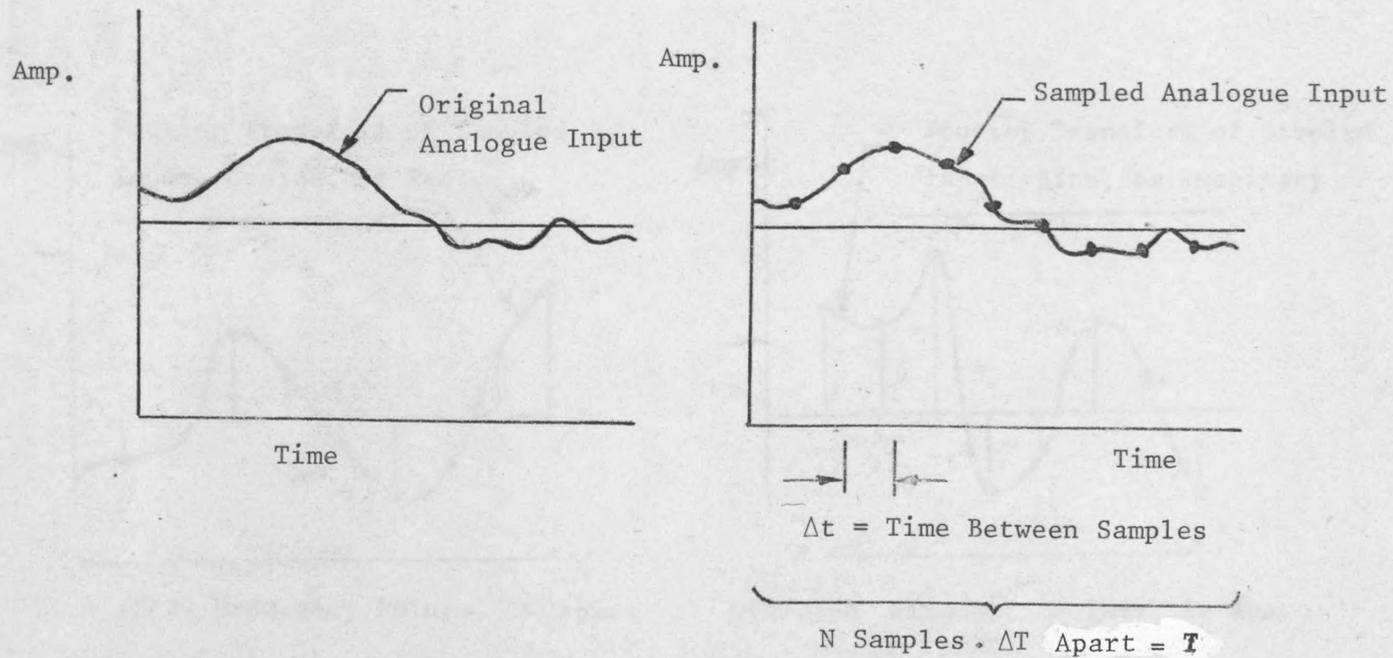
Fig 3.2 Time Signal
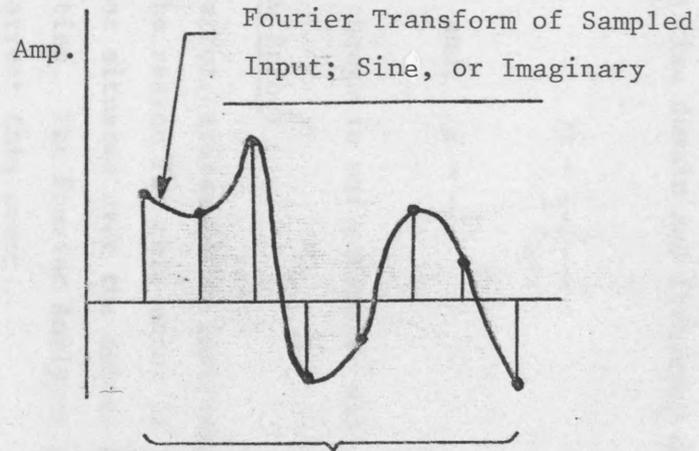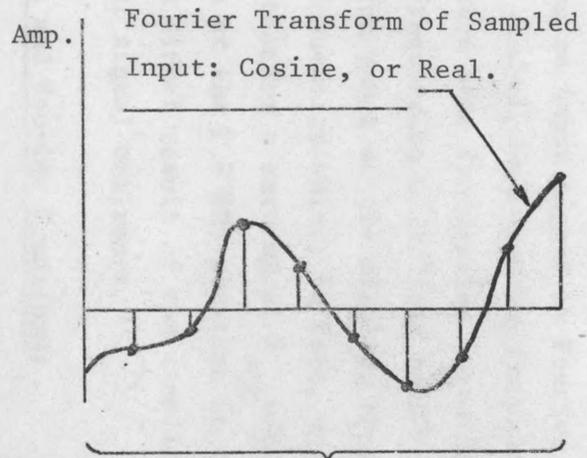
Fig 3.3 Fourier Transform

for imaginary (or phase) depending on the MODE setting.
F_{max} - The maximum frequency of the display (or the band width).
From the above definition the following can be obtained:

$$F_{max} = N/2 \times \Delta f$$

The relation between time domain and frequency domain, as shown in Fig 3.4, is:

$$\Delta t = \frac{1}{2 \ F_{max}}$$

$$\text{and,} \quad \Delta f = \frac{1}{T}$$

This means that any change in one parameter will change the others.

3.9.3 Sampling Window Error:

This type of error arises in an instrument such as the Fourier Analyser. The reason for this error is the sample window, if this window was not situated over the actual begining and end of the periodic function. The Fourier Analyser provides a function, called Hanning, to correct this error.

3.9.4 Aliasing:

When analysing an input signal by Fourier Analyser, one has to set the analyser control to a maximum frequency F_{max} if this frequency is lower than some frequencies contained in the input signal, the higher frequencies will "fold back" appearing as lower frequencies within the range of the display, thus the input will appear to contain frequencies which, in fact, are not there at all. Fig 3.5 illustrates that for a setting of $F_{max} = 2kHz$, a frequency of 2.2 kHz will show up at the 1.8 kHz position in the display.

Aliasing is a direct result of the sampling theorem and is common to all digital signal analysers.

3.9.5 Fourier Series and Fourier Transform:

Any functions that vary with time can easily be interpreted by the analysis of its frequency content. J.B. Fourier, a French mathematician, discovered that a periodic time-varying function
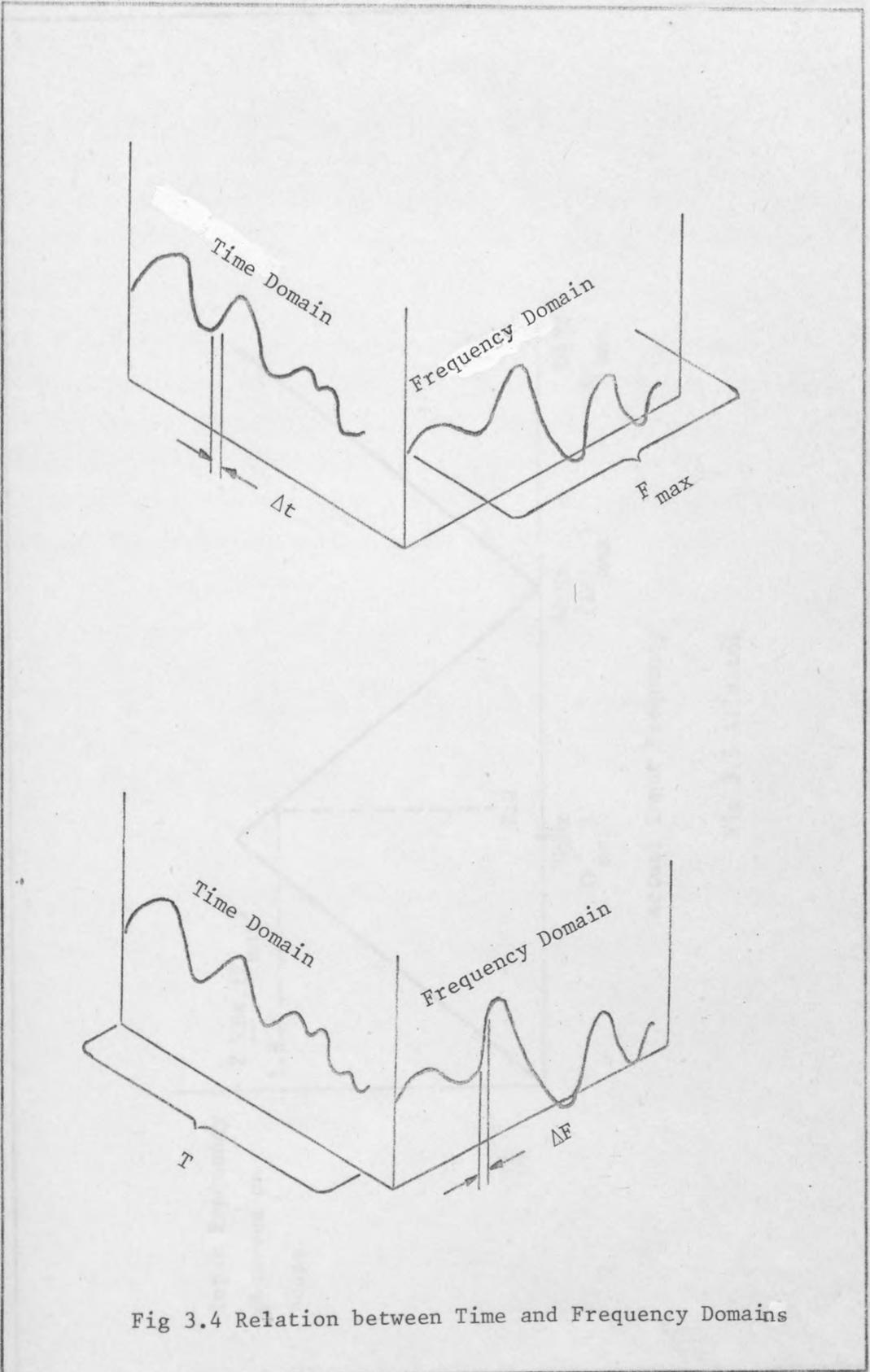
Fig 3.4 Relation between Time and Frequency Domains

Input Frequency
Observed on
Scope

2 kHz (F_{max})

1.8

2.2

2k Hz
(F_{max})

4k Hz
($2F_{max}$)

6k Hz
($3F_{max}$)
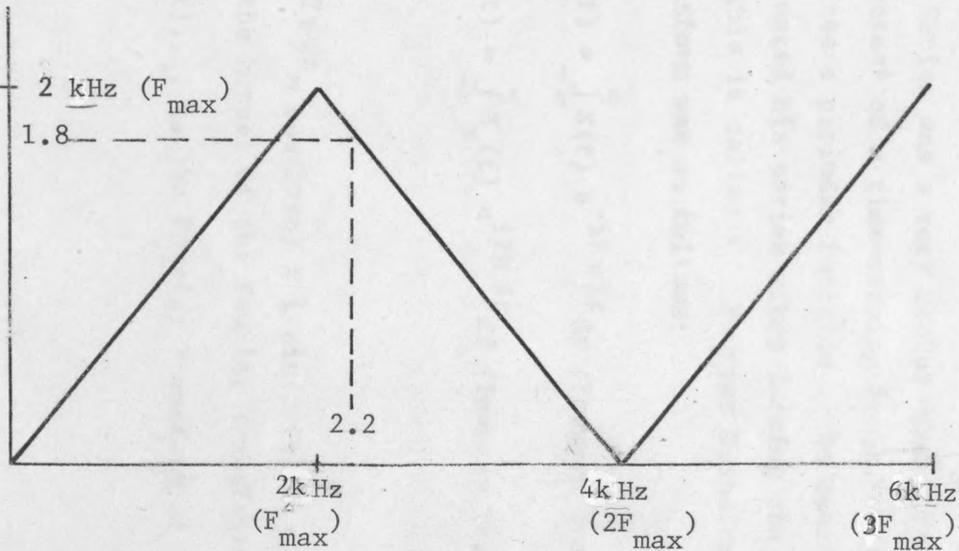
Actual Input Frequency

Fig 3.5 Aliasing

can be broken down into an infinite sum of properly weighted
sine and cosine functions of the proper frequencies. The equation
describing this statement is:

$$X(t) = a_o + \sum_{n=1}^{\infty} \left[a_n \cos\left(\frac{2\pi nt}{T}\right) + b_n \sin\left(\frac{2\pi nt}{T}\right) \right]$$

From the above equation, the amplitude and phase of each frequency
can be determined. If the frequency is $f_n = \frac{n}{T}$, the amplitude of
that frequency will be $\sqrt{a_n^2 + b_n^2}$ and the phase $\tan^{-1}(b_n/a_n)$.

The Fourier Series was a very useful tool for determining the
frequency content of a time-varying input. But the Fourier Series
always requires a periodic function . To overcome this problem
Fourier evaluated his series after letting the period approaching
infinity. This is called a Fourier Transform. The pair of
Fourier Transform was as follows:

$$S_x(f) = \int_{-\infty}^{\infty} X(t) \, e^{-i2\pi ft} dt \quad \text{(Forward Transform)}$$

$$X(t) = \int_{-\infty}^{\infty} S_x(f) \, e^{i2\pi ft} df \quad \text{(Inverse Transform)}$$

Where:

$e^{\pm i2\pi ft} = \cos(2\pi ft) \pm i \sin(2\pi ft)$, is known
as the kernel of the Fourier Transform.

$S_x(f)$.... is the Fourier Transform of X(t).

IV. EXPERIMENTAL RESULTS

4.1 Introduction

In this chapter all the results obtained by experimental work, such as time response and frequency response will be discussed, taking into account the effect of speed, backlash and load. Most of the results obtained were of the frequency response; some of the important results will be shown and analysed.

4.2 Preliminary Tests

These tests were made to give some information for subsequent analyses. Fig 4.1 shows the effect of backlash on the dynamic response for the system: a) When loaded. b) When running free. This was done for speeds ranging from 200-1800 rev/min. The block diagram showing the instrumentation used will be given in Fig 4.2, where:

SBR- The strain gauges used as a bridge on the output shaft.

SRA- The slip rings assembly.

OSC- The oscilloscope and amplifier.

FIL- The filter used to cut-off high frequencies and noise (low pass).

RMS- The root mean square voltmeter.

However, a few more results were obtained to show the RMS value changing with the load at certain speeds. The strain in the intermediate shaft under static loading is compared with the RMS value of the strain when the system is running. This static loading was produced by using a metallic arm fixed on the output inertia. Masses with different weights were suspended at the end of the arm and the value of strain was recorded for each static load setting. The area above the static line and below the total dynamic curve (the marked area),which is shown in Fig 4.3 through 4.15, is caused by dynamics and vibrations of the system through backlash and some machining errors of the rig components. For speeds lower than the first natural frequency corresponding speed the effect of backlash reduces for a

Fig 4.1a Effect of Backlash with Loading = 3.0 N m (4.068 lbf.ft)

$2B_1$ = 0.47mm (25.5 thou)

$2B_1$ = 0.2mm (11 thou)

RMS(v)

x 100 rev/min

Fig 4.1b Effect of Backlash without Loading
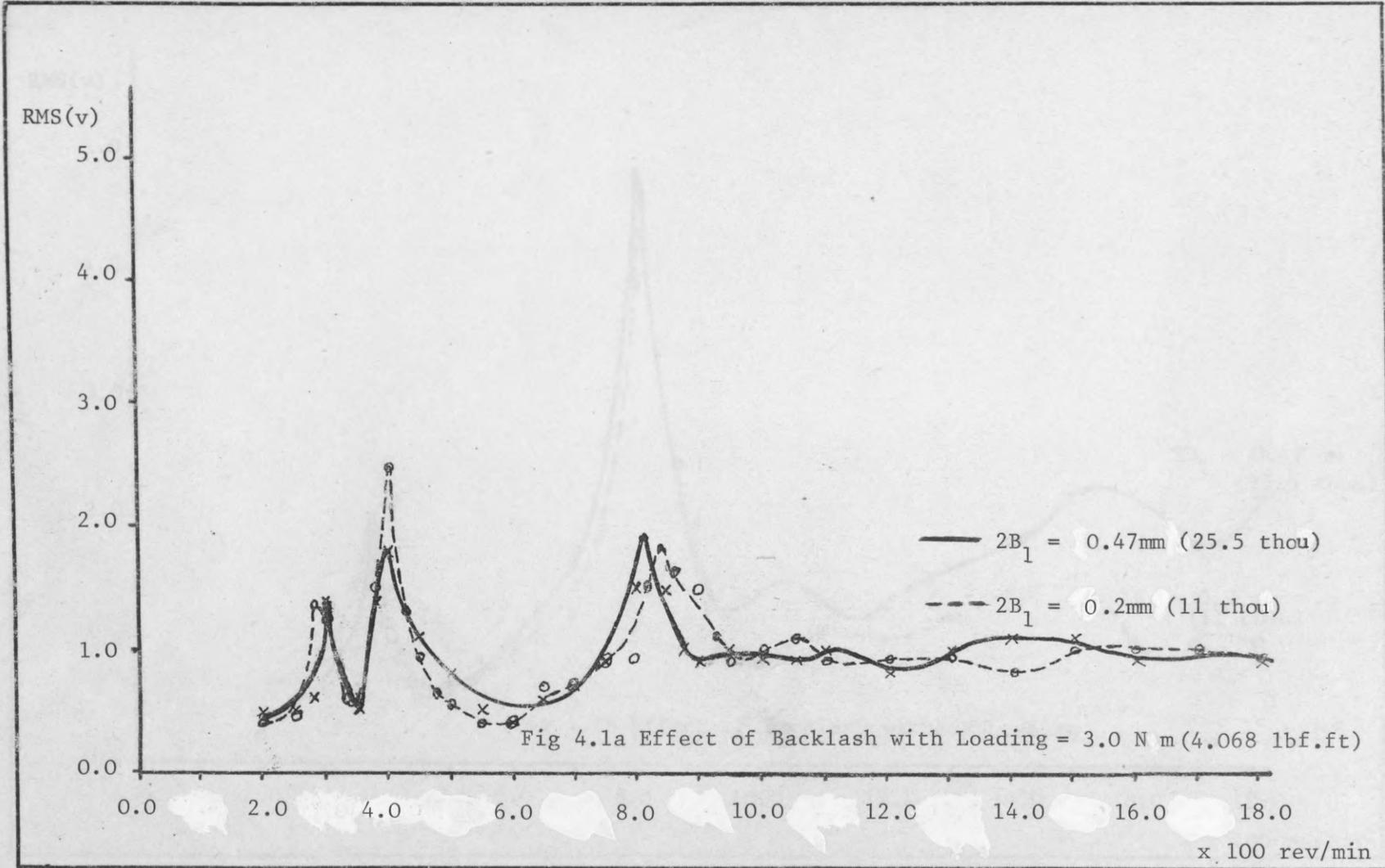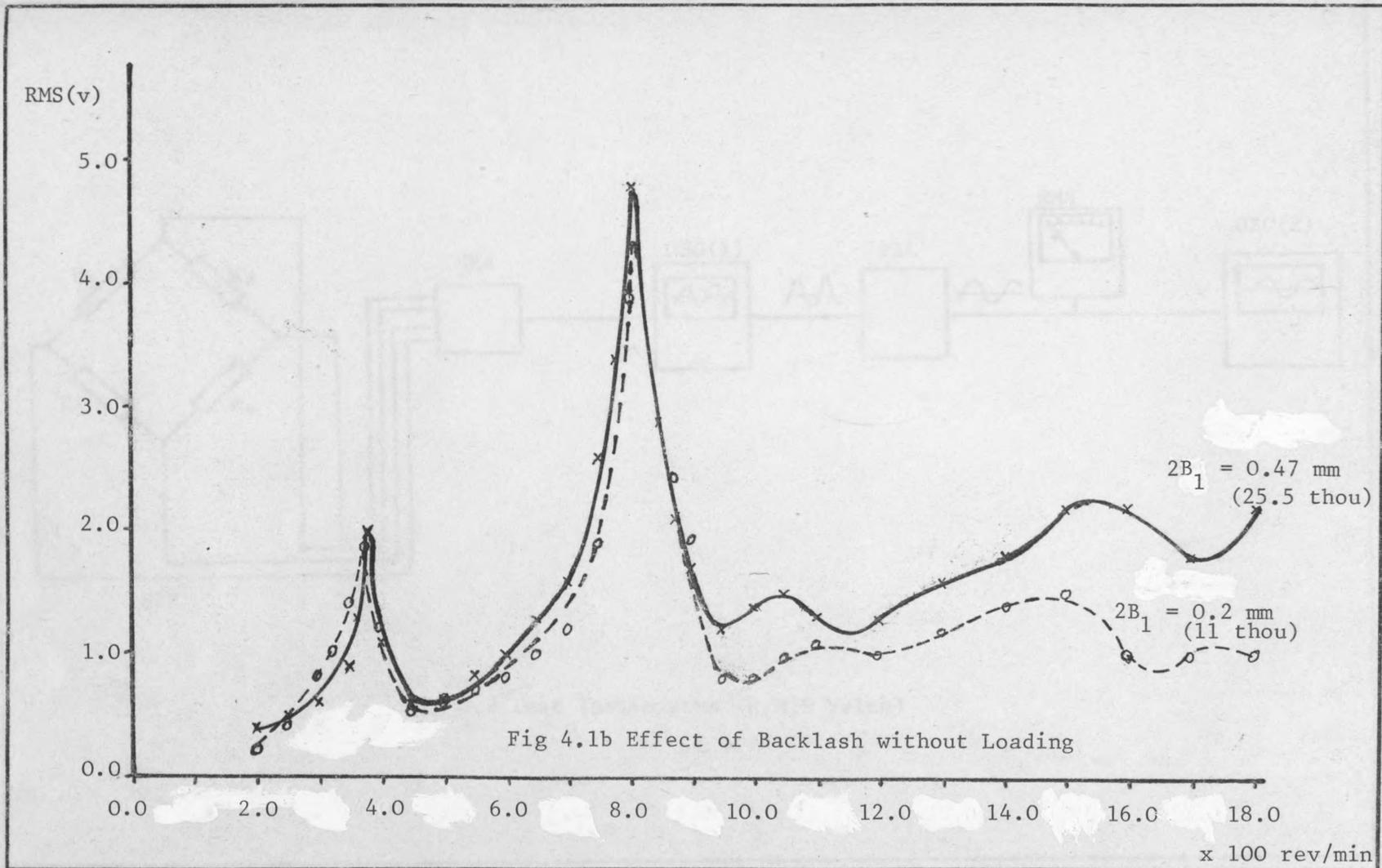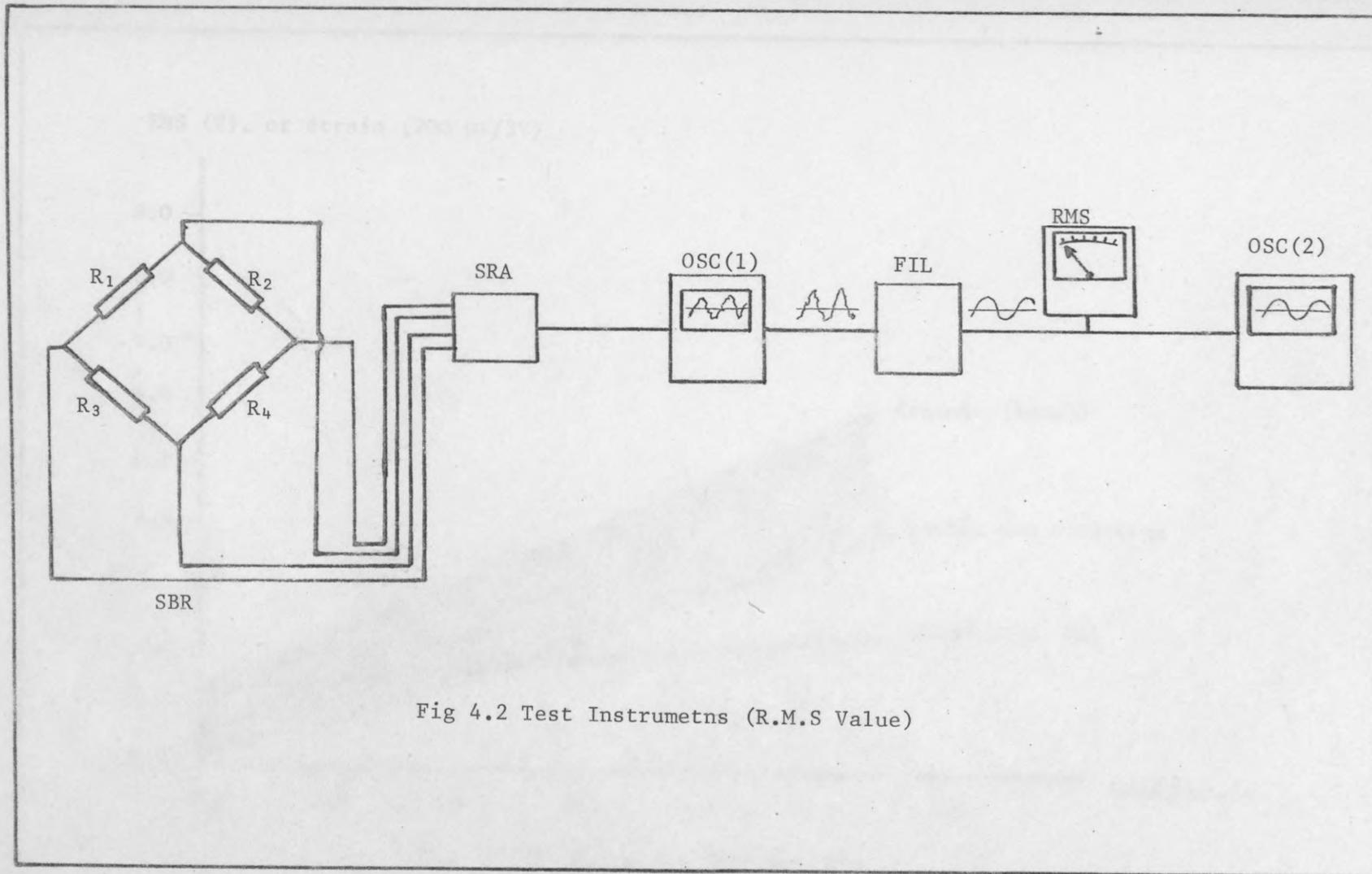
Fig 4.2 Test Instrumetns (R.M.S Value)
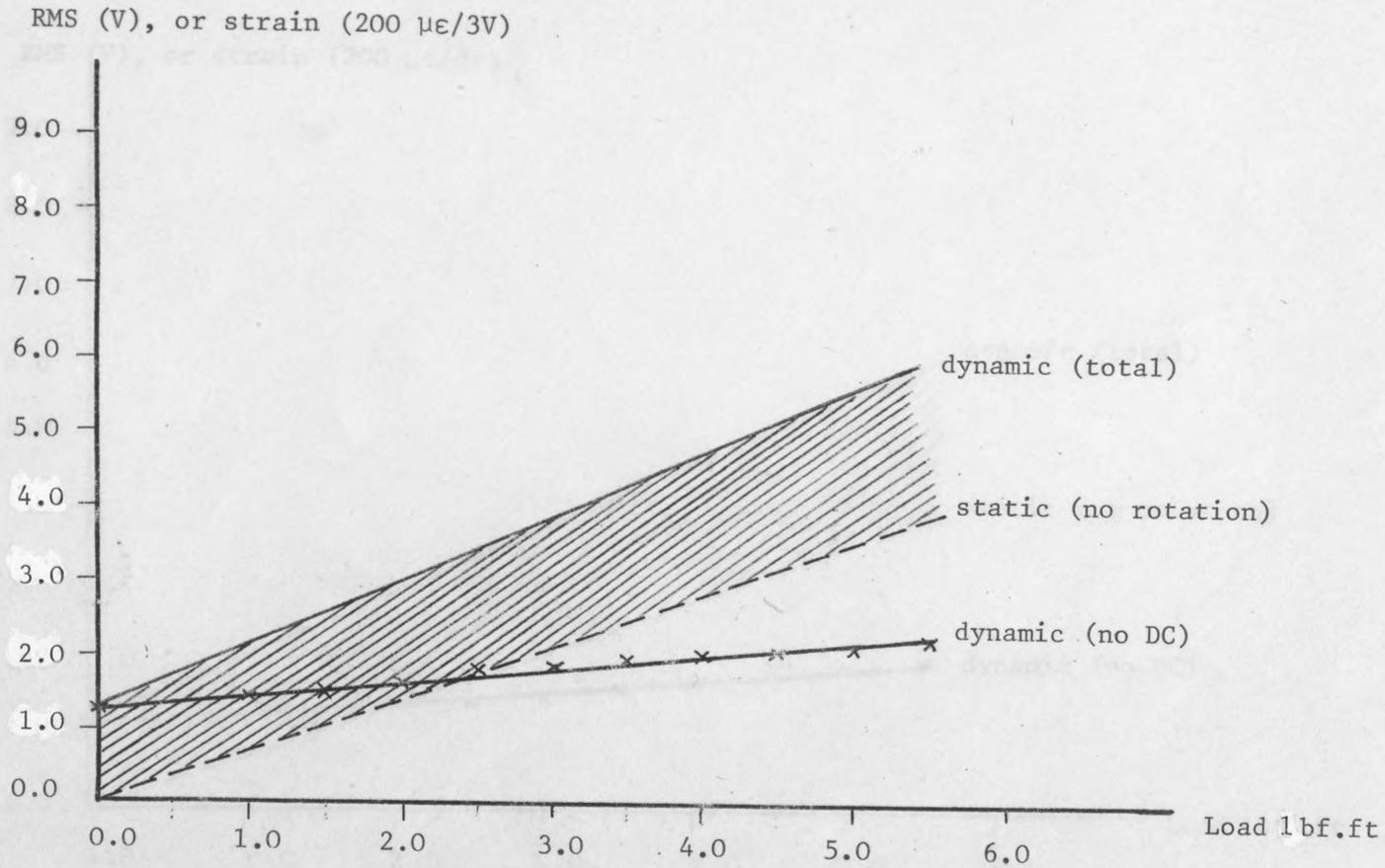
Fig 4.3 RMS Value for 2000 rev/min
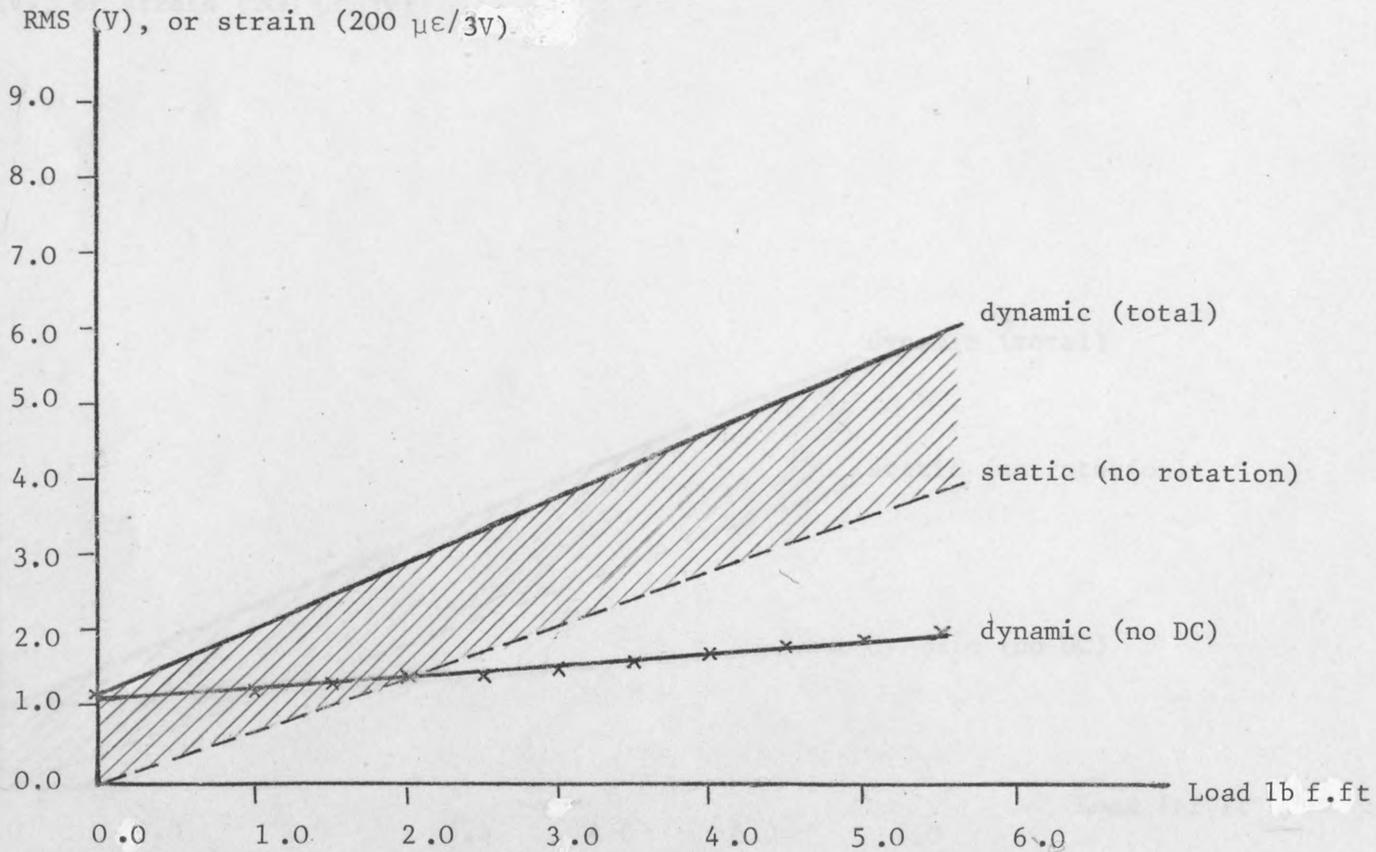
Fig 4.4 RMS Value for 1800 rev/min

RMS (V), or strain (200 µε/3V)

dynamic (total)

static (no rotation)

dynamic (no DC)

Load lbf.ft
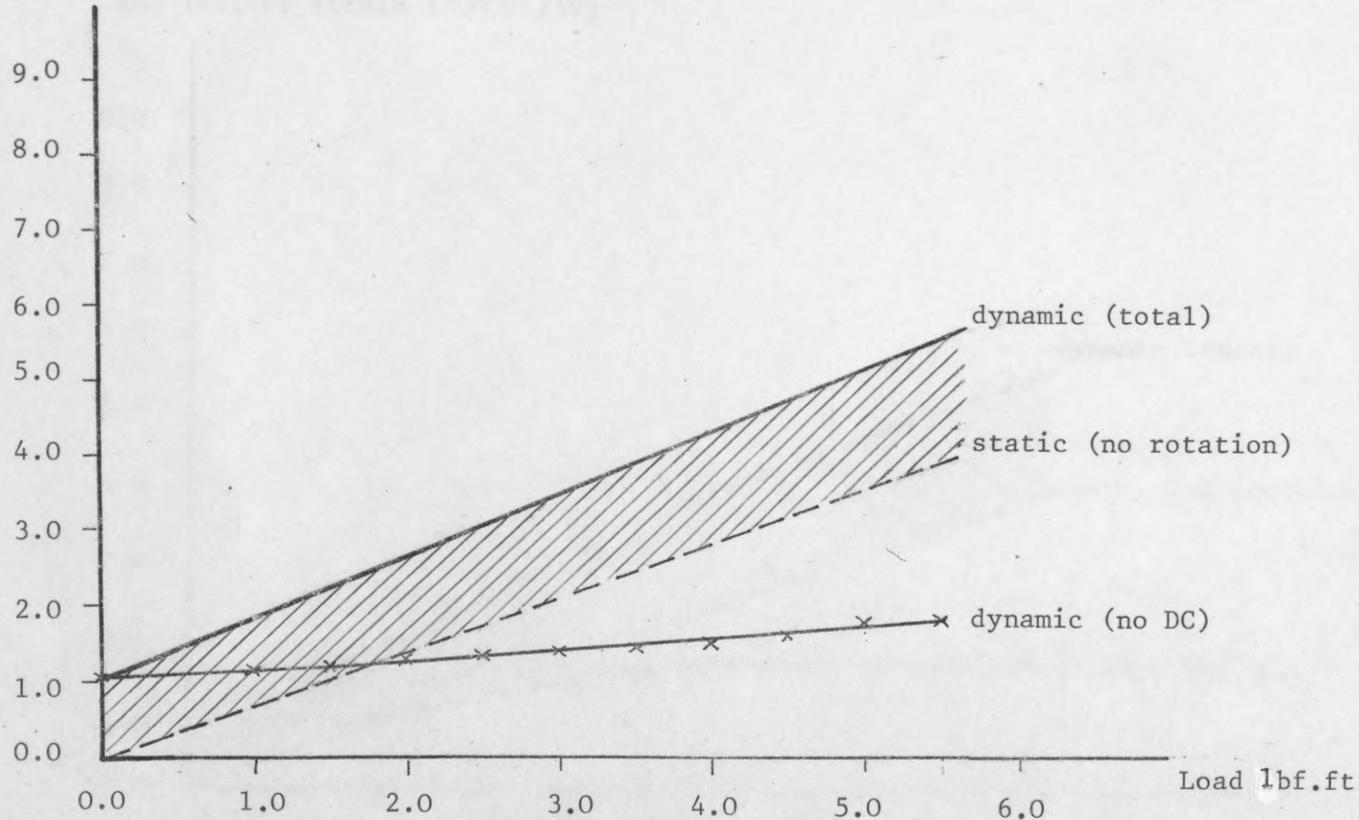
Fig 4.5 RMS Value for 1700 rev/min
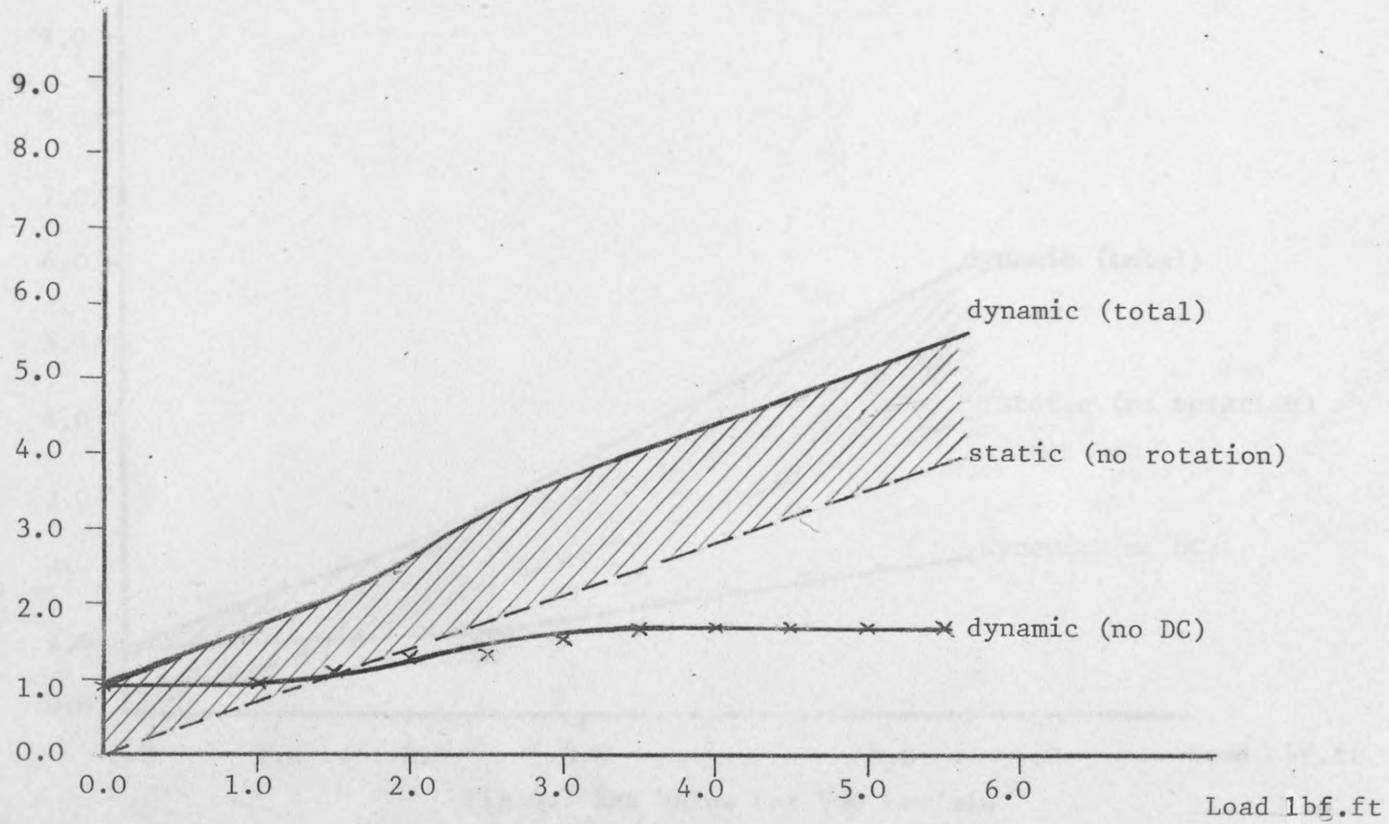
Fig 4.6 RMS Value for 1200 rev/min
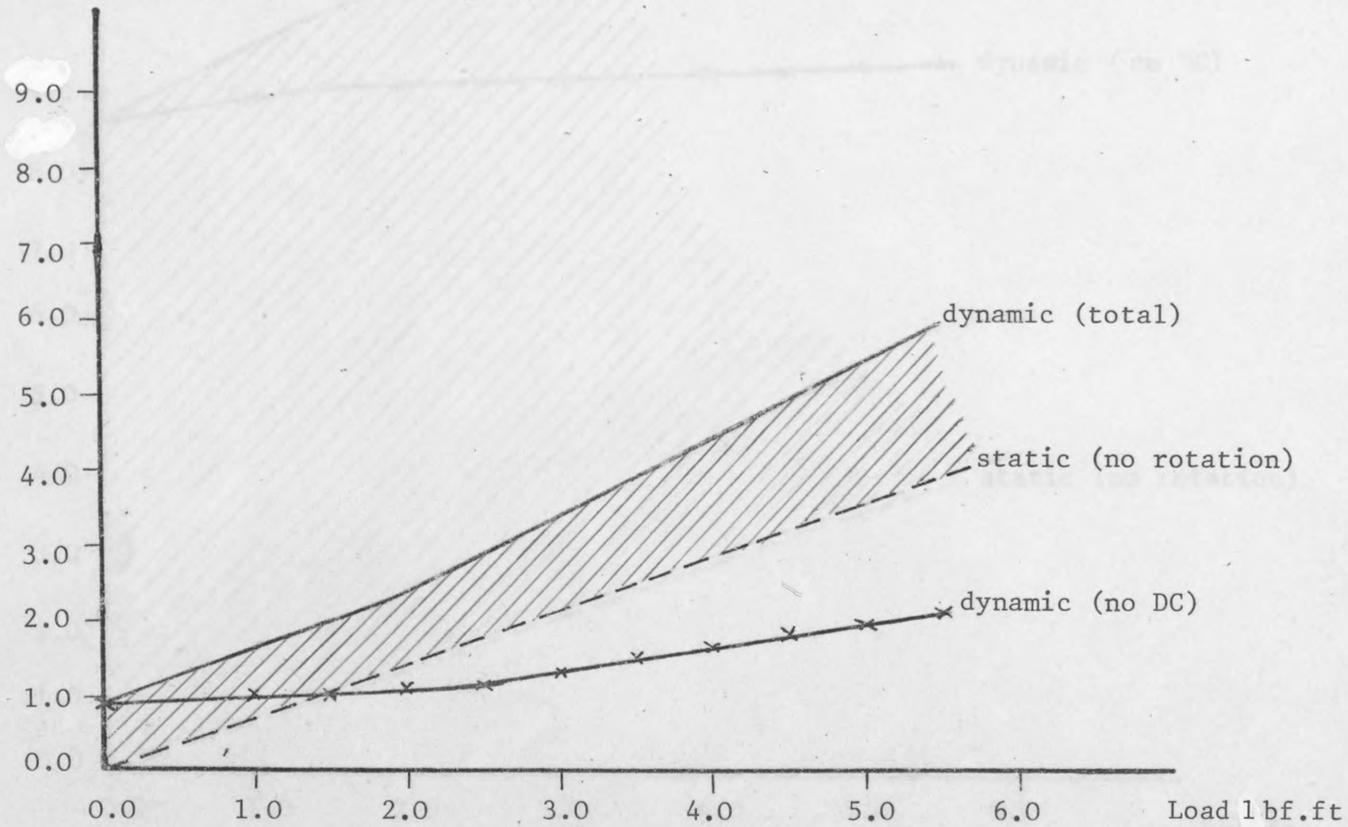
Fig 4.7 RMS Value for 900 rev/min
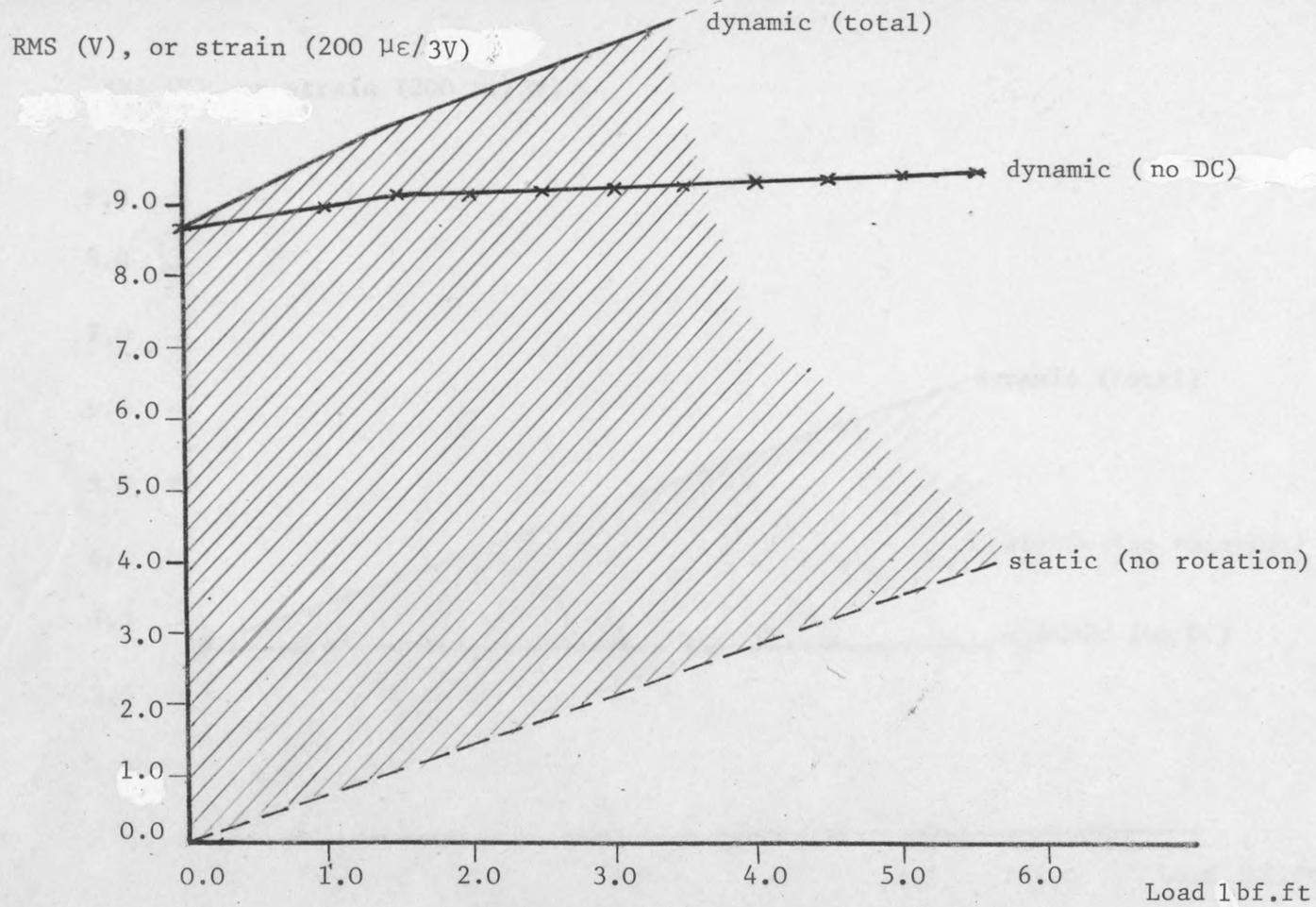
Fig 4.8 RMS Value for 780 rev/min
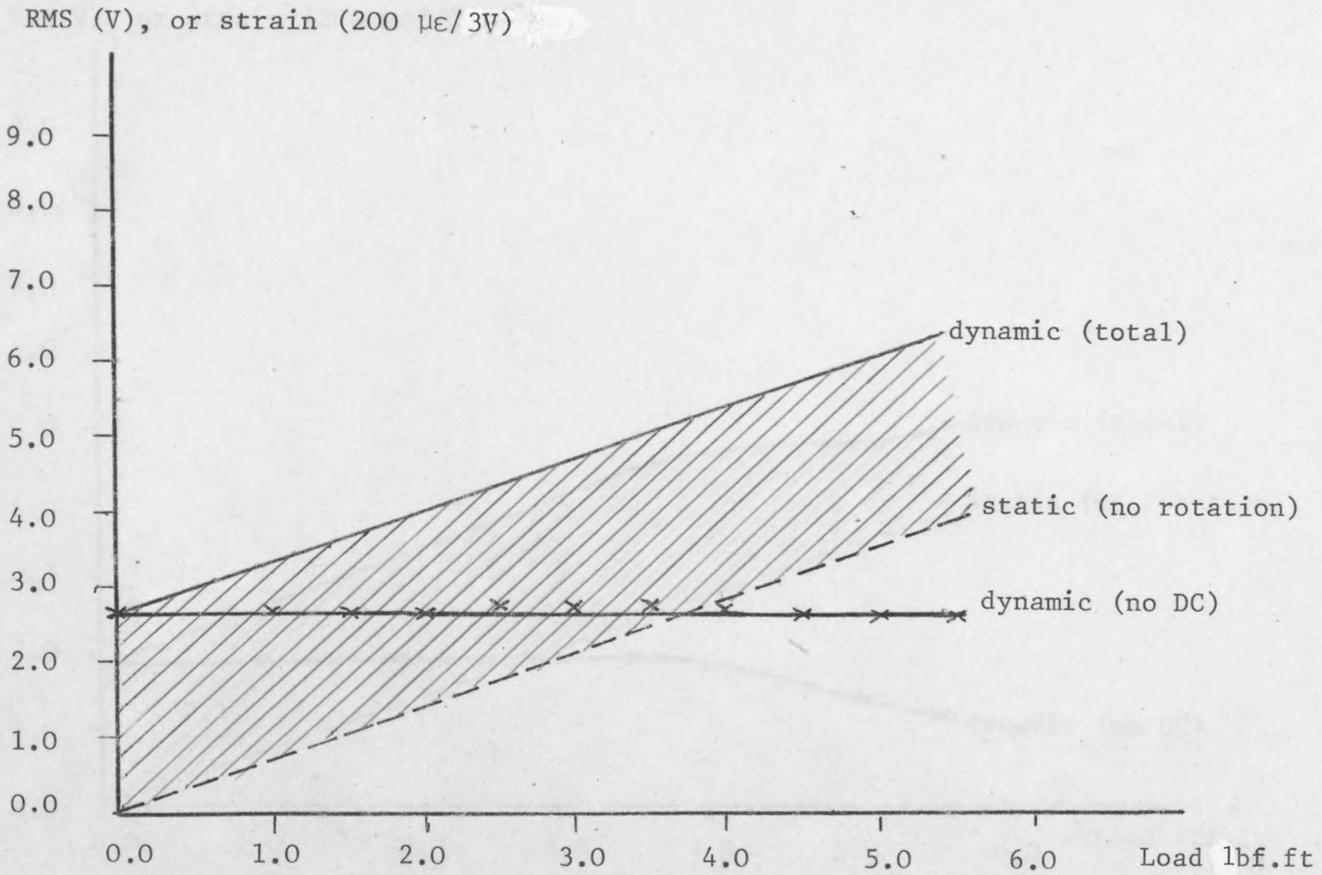
Fig 4.9 RMS Value for 600 rev/min

RMS(V), or strain (200 με/3V)

9.0

8.0

7.0

6.0

5.0 — dynamic (total)

4.0 — static (no rotation)

3.0

2.0

1.0 — dynamic (no DC)

0.0

0.0   1.0   2.0   3.0   4.0   5.0   6.0   Load lbf.ft
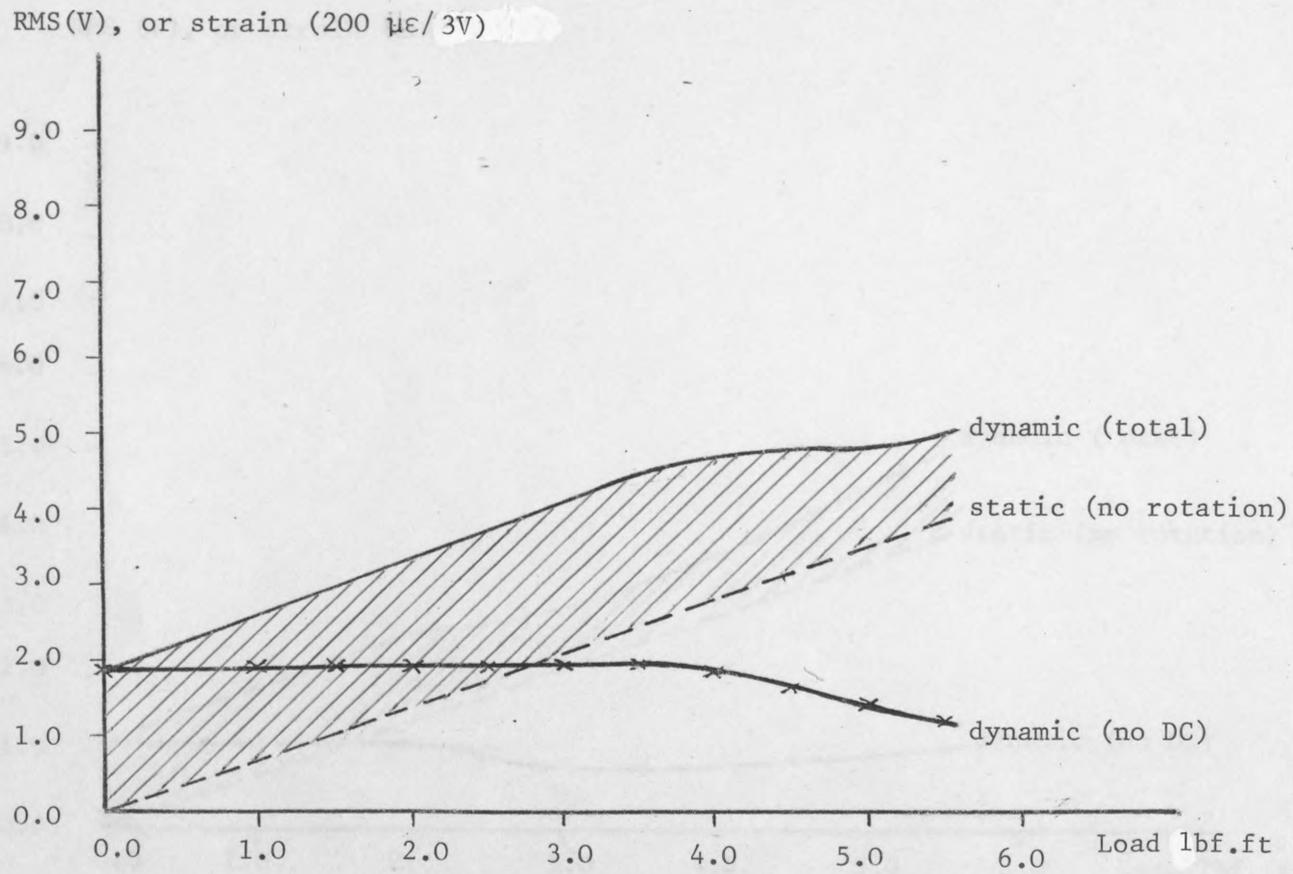
Fig 4.10 RMS Value for 550 rev/min

RMS (V), or strain (200 μɛ/ 3V)
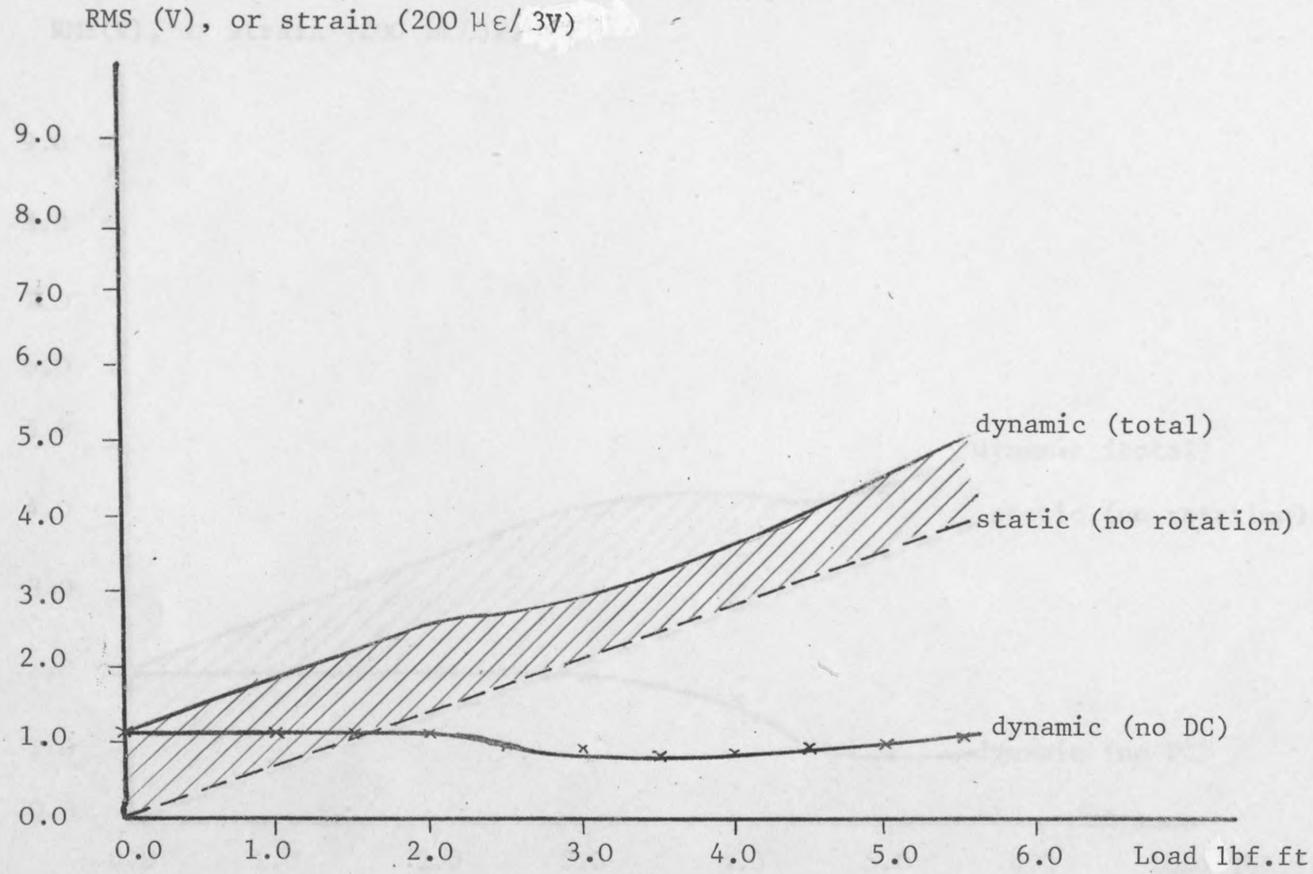
Fig 4.11 RMS Value for 450 rev/min

-69-

RMS(V), or strain (200 με/3V)

9.0

8.0

7.0

6.0

5.0

dynamic (total)

4.0

static (no rotation)

3.0

2.0

dynamic (no DC)

1.0

0.0

0.0   1.0   2.0   3.0   4.0   5.0   6.0   Load lbf.ft
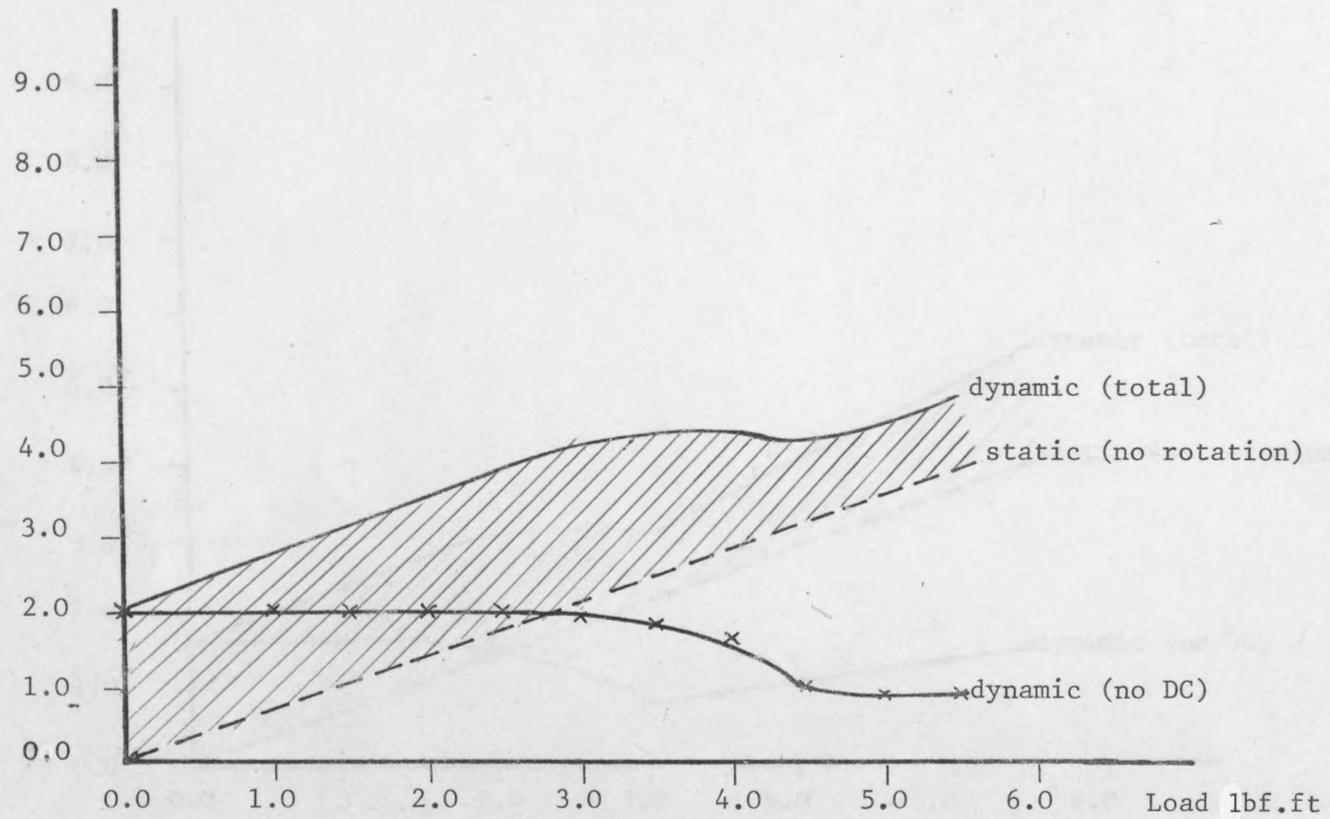
Fig 4.12 RMS Value for 325 rev/min
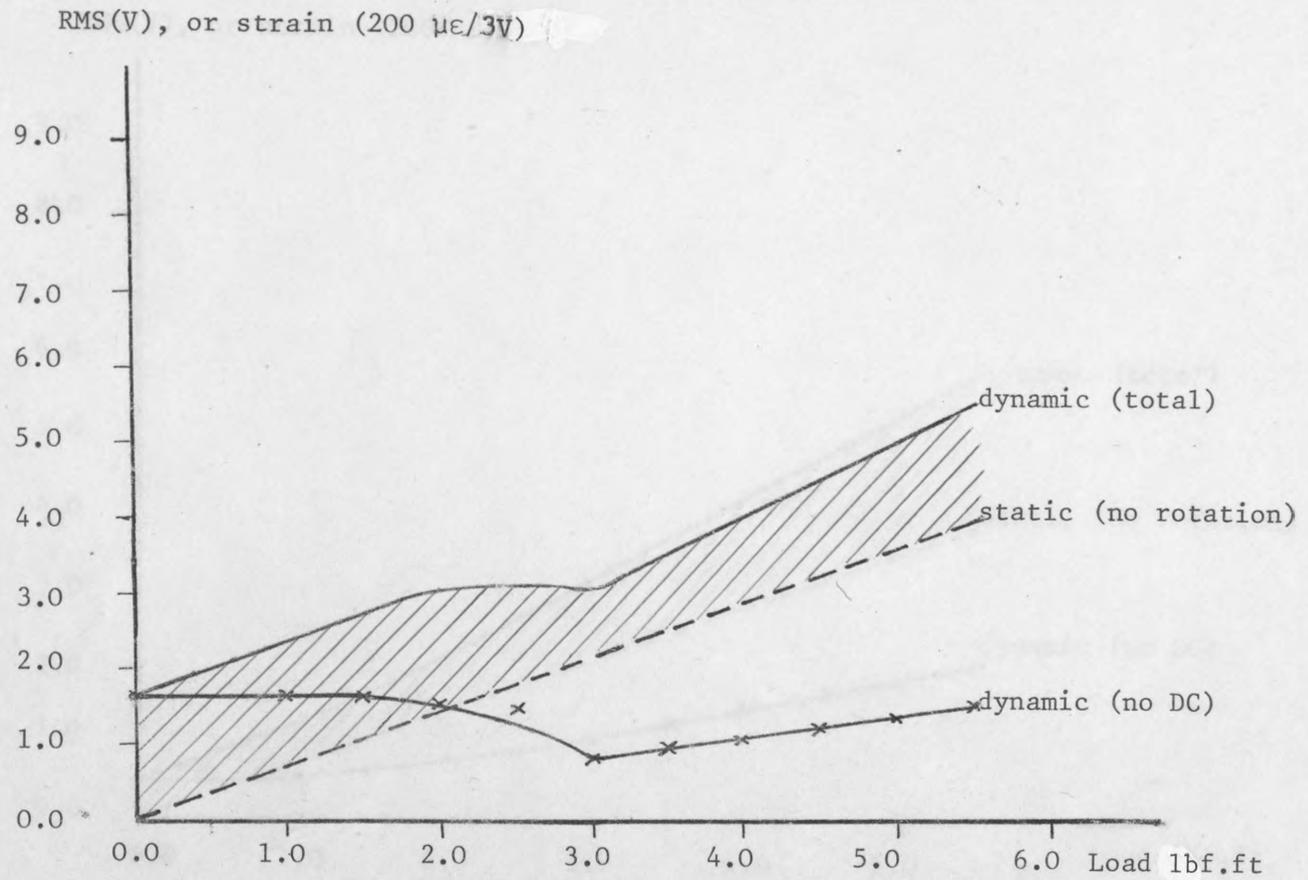
Fig 4.13 RMS Value for 300 rev/min
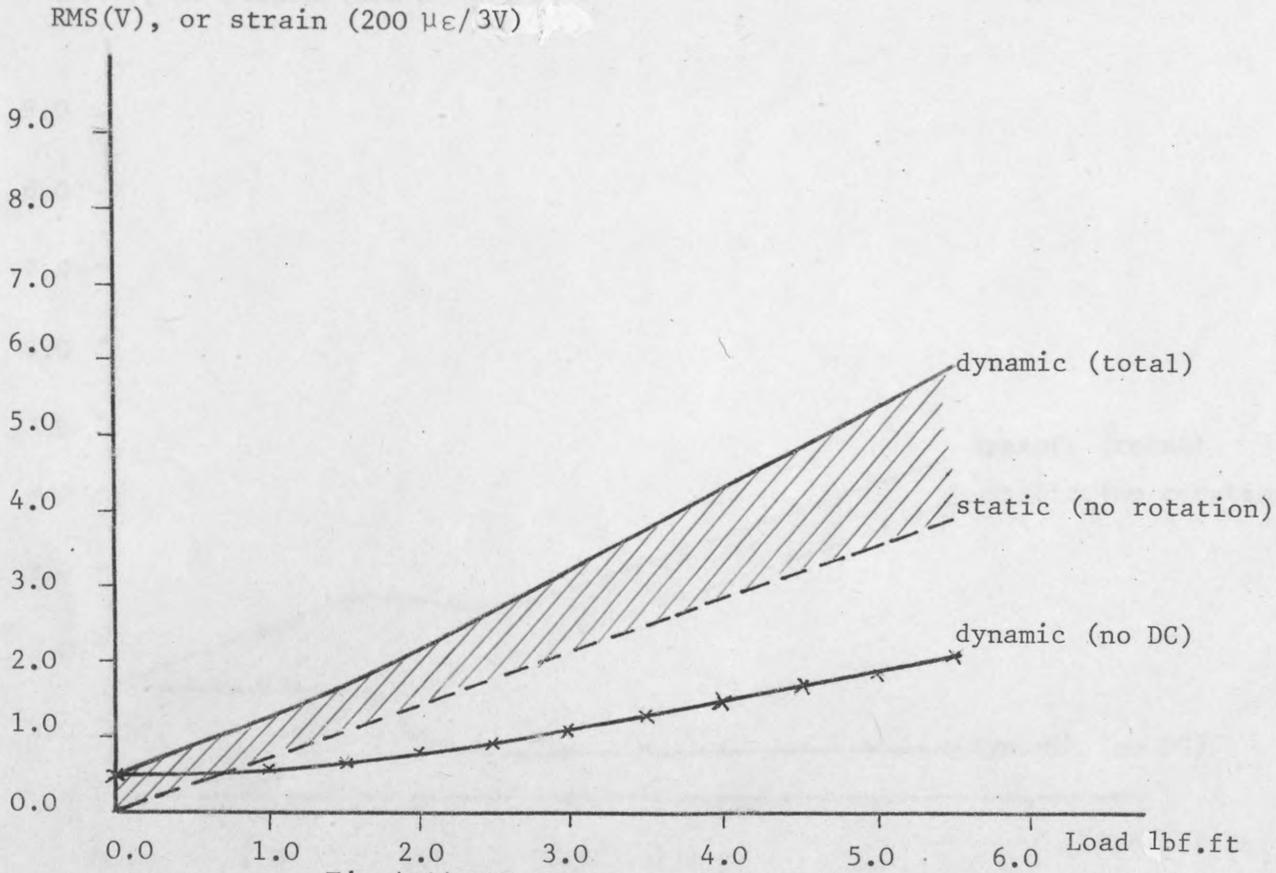
Fig 4.14 RMS Value for 250 rev/min

RMS(V), or strain (200 με/3V)

9.0
8.0
7.0
6.0
5.0
4.0
3.0
2.0
1.0
0.0

dynamic (total)
static (no rotation)
dynamic (no DC)

0.0   1.0   2.0   3.0   4.0   5.0   6.0   Load 1bf.ft
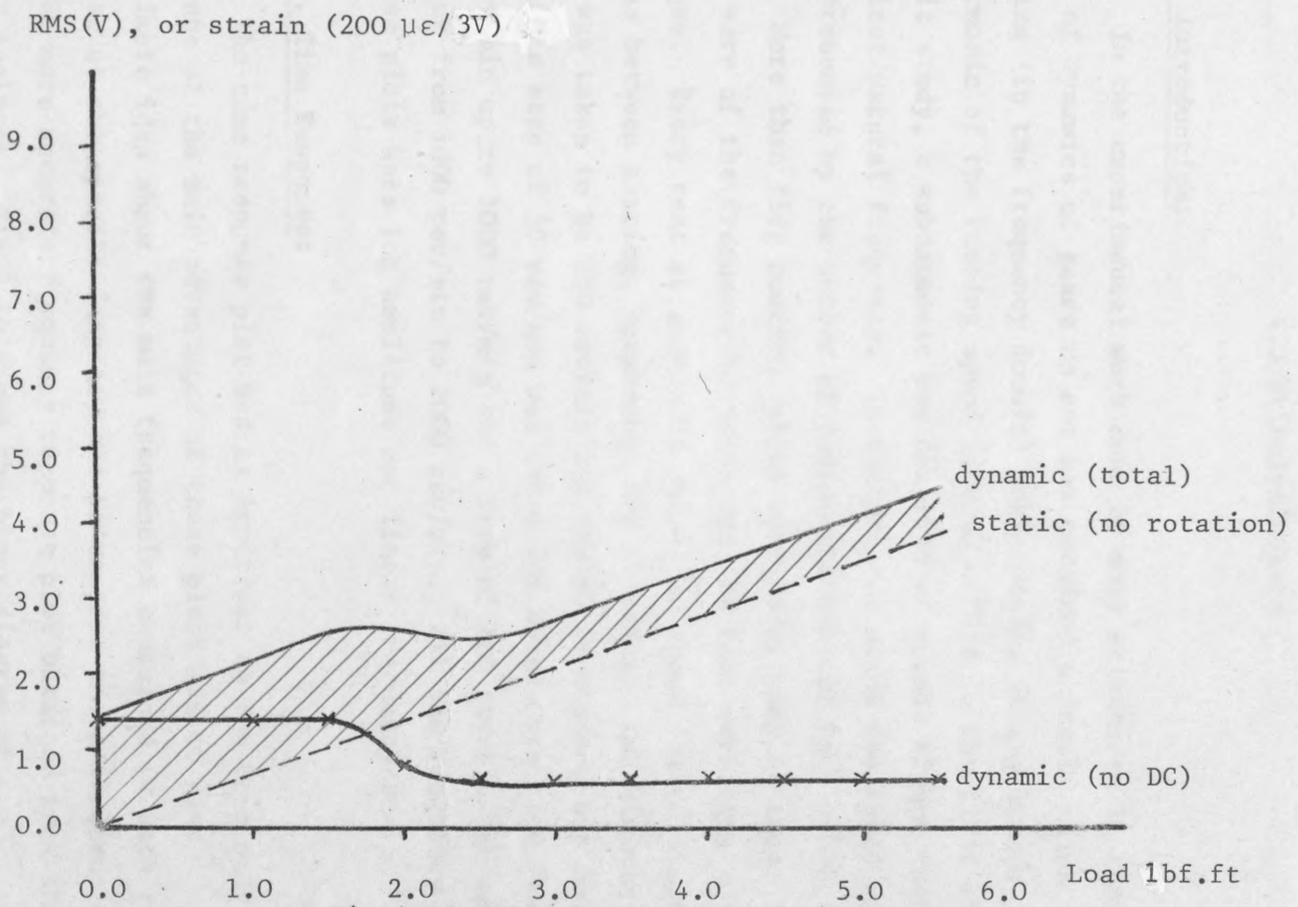
Fig 4.15 RMS Value for 200 rev/min

loading around 3.39 N m (2.5 lbf.ft), while at higher speeds the effect of backlash is significant for any loading. But for the speed equal to the speed corresponding to fundamental natural frequency the effect of backlash and imperfections is very clear and critical.

4.3 Principal Tests

4.3.1 Introduction:

In the experimental work done by many scientists in the field of dynamics of gears no one has obtained a result which contains (in the frequency domain) subharmonics at any speed; i.e. subharmonic of the running speed (rev/s). This is the first time, in this study, a subharmonic was observed at speeds higher than the first natural frequency. In the present study the speed will be represented by the number of rev/s, the nominal backlash=0.73mm.

More than five hundred plots were made, many of these plots were of the frequency response and the rest were time response. Every test at a certain specified speed lasted about 15 minutes between setting, measuring, and plotting. The minimum speed was taken to be 250 rev/min and the maximum speed was 2000 rev/min, a step of 50 rev/min was taken for speeds starting from 250 rev/min up to 1000 rev/min and a step of 100 rev/min for speeds starting from 1000 rev/min to 2000 rev/min. All the frequency response plots were log amplitude and linear frequency scale.

4.3.2. Time Response:

The time response plot was as important as the frequency plot, one of the main advantages of these plots was to give approximate idea about the main frequencies contained in each time response at the specified speed, and to compare these frequencies with the more accurate frequency response plot obtained from the Fourier Analyser. Fig 4.16 shows the block diagram of the instruments used, bearing in mind that the Fourier Analyser was used as second oscilloscope and plotter. The filter was used for cutting-off the high frequencies from the main time signal.

A sample of time response is shown in Fig 4.17 to give an idea about the values of frequencies and amplitudes contained in the time signal. In this sample the number of revolutions is (750) rev/min which corresponds to a period of (80) ms, and can easily be shown in Fig 4.17, taking into account that each 3 volts corresponds to 500 $\mu\epsilon$. The other main frequency in this sample corresponds to either the second natural frequency ω_{n_2} or the brake side frequency ω_{nb} depending on the load value.

4.3.3 Frequency Response:

For correct and accurate evaluation of the test results, a determination of the frequency content was needed. The dominant frequencies of the spectrum plot are compared with the frequencies of the test components to identify the possible sources of excitation. A block diagram showing the system used to measure, transmit, and analyse the continuous time signal will be shown in Fig 4.18. The filter was used to stop aliasing as it is described in section 3.9.4.

Fig 4.19 shows a sample of the frequency response as an introduction into the test "results analysis", which will be discussed in section 4.3.4. In this sample, the rotational speed was (600) rev/min which corresponds to (10) rev/s. Note that the scale was linear for the frequency and log for the amplitude. First frequency amplitude represents the rotational speed of 10 (rev/s), and the rest corresponds to the multiple harmonics.

4.3.4 Test Results Analysis:

A set of spectrum plots in Fig 4.20 through 4.33 shows the effect of loading on separation and impact of teeth. These results were taken for speed of (200) rev/min which corresponds to a period of (300) ms and frequency of (3.333) rev/s, with an averaging of (5) times (on the Fourier Analyser).

For loading of 0.0 - 2.712 N m (0.0-2.0 lbf.ft), the brake-side subsystem will oscillate at its own natural frequency ω_{nb}, the fundamental natural frequency of the total system ω_{nf}, and the rotational speed corresponding frequency and its integral muultiples (Fig 4.23).

From SBR

SRA

OSC

FIL

FA

PL

FA Fourier Analyser
PL Plotter
FIL Filter
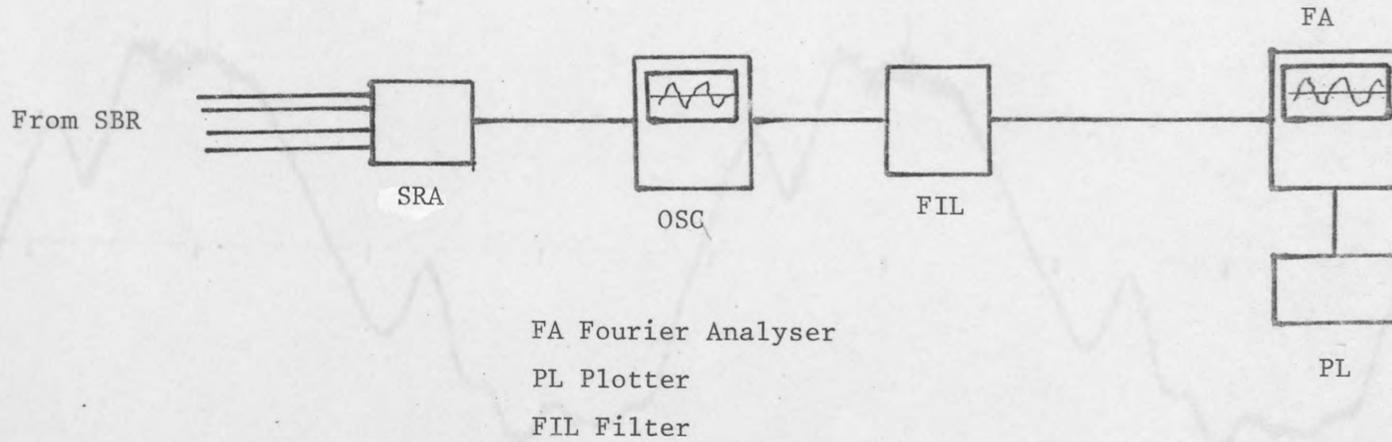
Fig 4.16 Time Response Test Instruments

Fig 4.17 Time Response for 750 rev/min (12.5 rev/s)

No Loading

Cut-off Frequency 2 KHz

1 rev ≡ 80 ms

10 ^{1} V

10^{-4} SEC
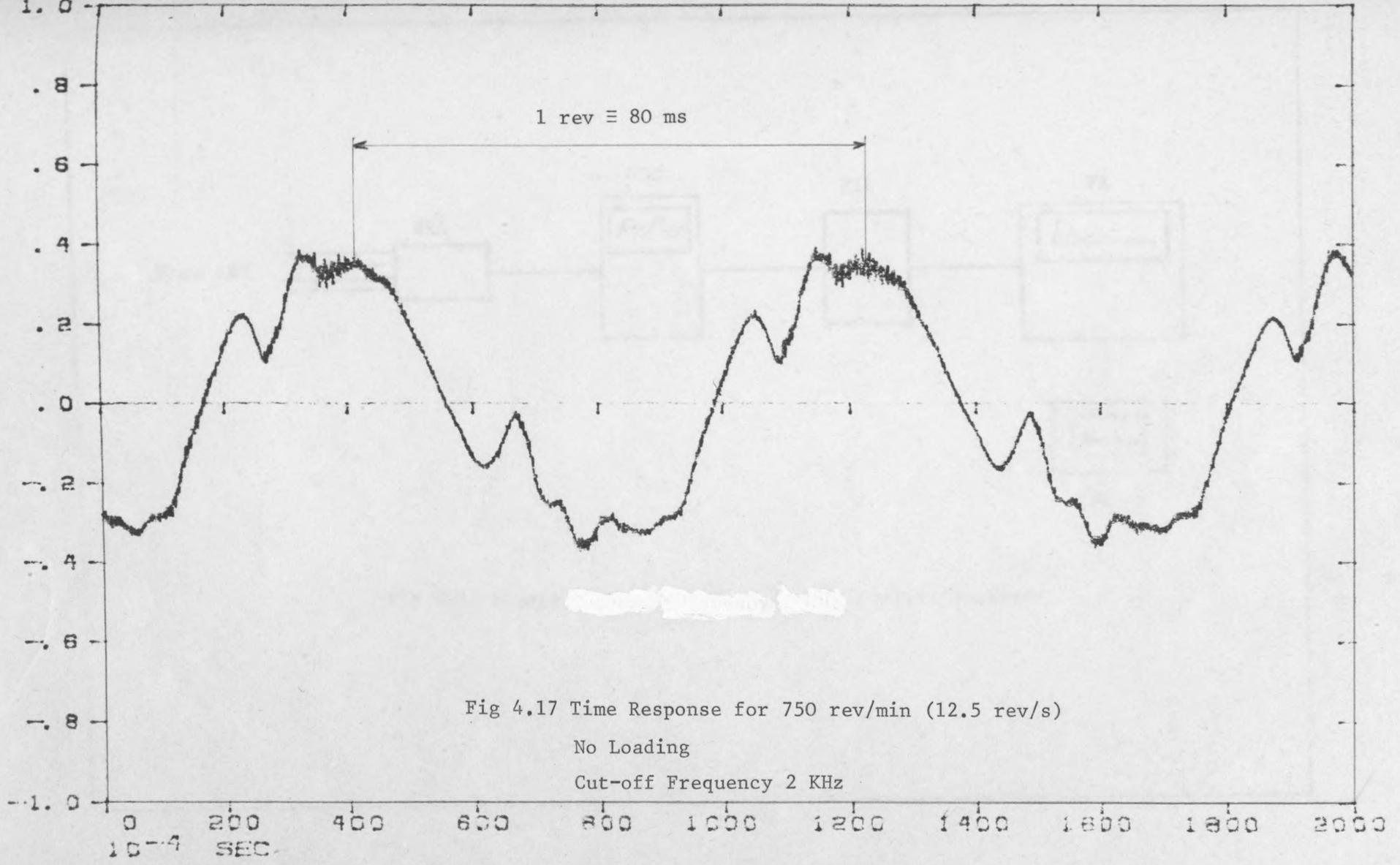
-77-
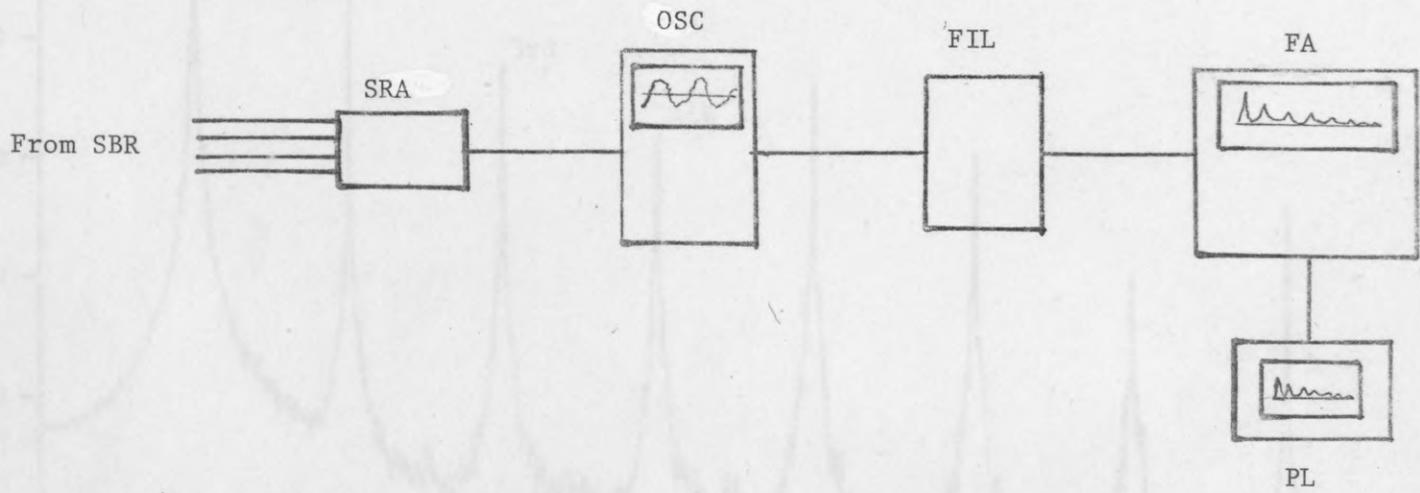
Fig 4.18 Measuring Instruments with the Fourier Analyser
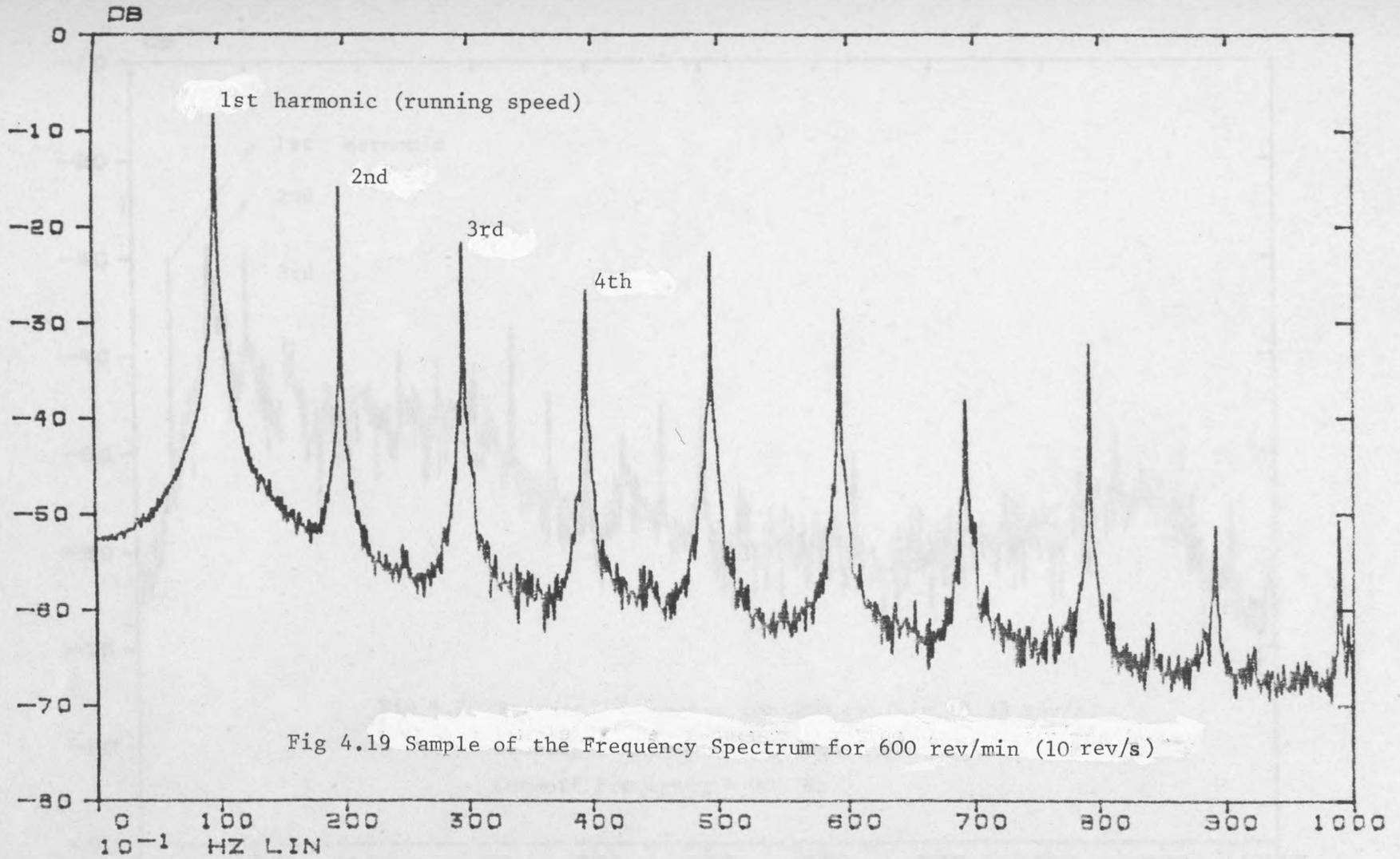
Fig 4.19 Sample of the Frequency Spectrum for 600 rev/min (10 rev/s)

DB

-10

-20

1st harmonic

2nd

-30

3rd

-40

-50

-80-

-60

-70

Fig 4.20 Frequency Response for 200 rev/min (3.33 rev/s)

Loading = 0.0 N m (0.0 lbf.ft)

-80

Cut-off Frequency = 80 Hz

-90

0   100   200   300   400   500   600   700   800   900   1000

10⁻¹   HZ LIN

Fig 4.21 Time Response for 200 rev/min (3.33 rev/s)

Loading = 0.0 N m (0.0 lbf.ft)

Cut-off Frequency = 1800 Hz

first harmonic (running speed)

Fig 4.22 Frequency Response for 200 rev/min (3.33 rev/s)

Loading = 1.356 N m (1.0 lbf.ft)

Cut-off Frequency = 80 Hz

DB

-10
-20
-30
-40
-50
-60
-70
-80
-90

0   100   200   300   400   500   600   700   800   900   1000

10^{-1} HZ LIN

-182-

Fig 4.23 Frequency Response for 200 rev/min (3.33 rev/s)

Loading = 1.356 N m (1.0 lbf.ft)

Cut-off Frequency = 180 Hz

Fig 4.24 Time Response for 200 rev/min (3.33 rev/s)

Loading = 1.356 N.m.(1.0 lbf.ft)

Cut-off Frequency = 1800 Hz

1 rev ≡ 300 ms

Fig 4.25 Frequency Response for 200 rev/min (3.33 rev/s)

Loading = 2.712 N m (2.0 1bf.ft)

Cut-off Frequency = 80 Hz

Fig 4.26 Time Response for 200 rev/min (3.33 rev/s)

Loading = 2.712 N m (2.0 lbf.ft)

Cut-off Frequency = 1800 Hz

Fig 4.27 Frequency Response for 200 rev/min (3.33 rev/s)
Loading = 4·068 N·m (3.0 lbf.ft)
Cut-off Frequency = 80 Hz

Fig 4.28 Time Response for 200 rev/min (3.33 rev/s)

Loading = 4.068 N m (3.0 lbf.ft)

Cut-off Frequency = 1800 Hz

1 rev ≡ 300 ms

Fig 4.29 Frequency Response for 200 rev/min (3.33 rev/s)

Loading = 5.424 N m (4.0 lbf.ft)

Cut-off Frequency = 80 Hz

Fig 4.30 Time Response for 200 rev/min (3.33 rev/s)

Loading = 5.424 N.m (4.0 lbf.ft)

Cut-off Frequency = 1800 Hz

1 rev ≡ 300 ms

10⁻⁴ SEC

Fig 4.31 Frequency Response for 200 rev/min (3.33 ms).
Loading = 6.78 N m (5.0 lbf.ft), Cut-off Frequency = 80 Hz
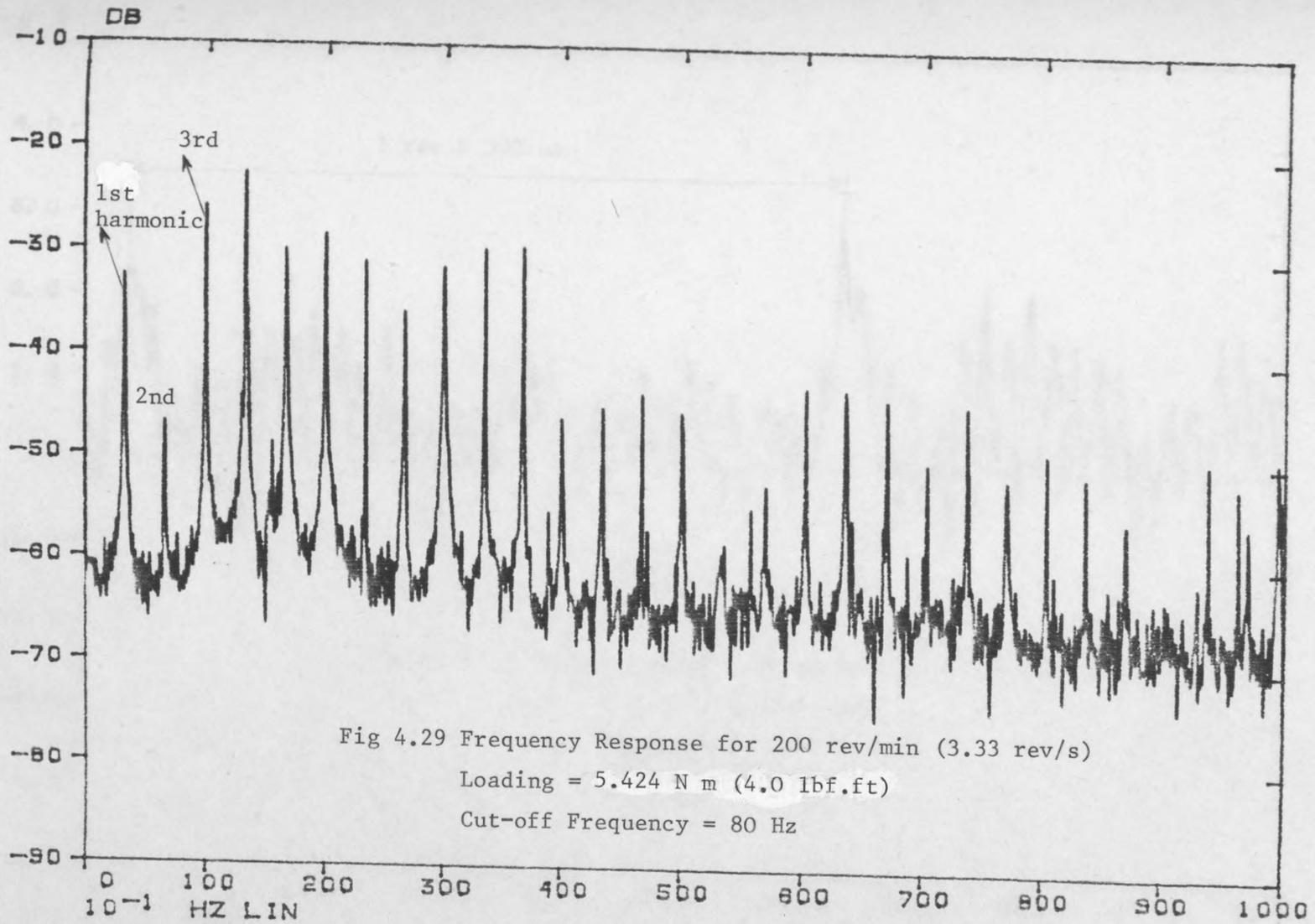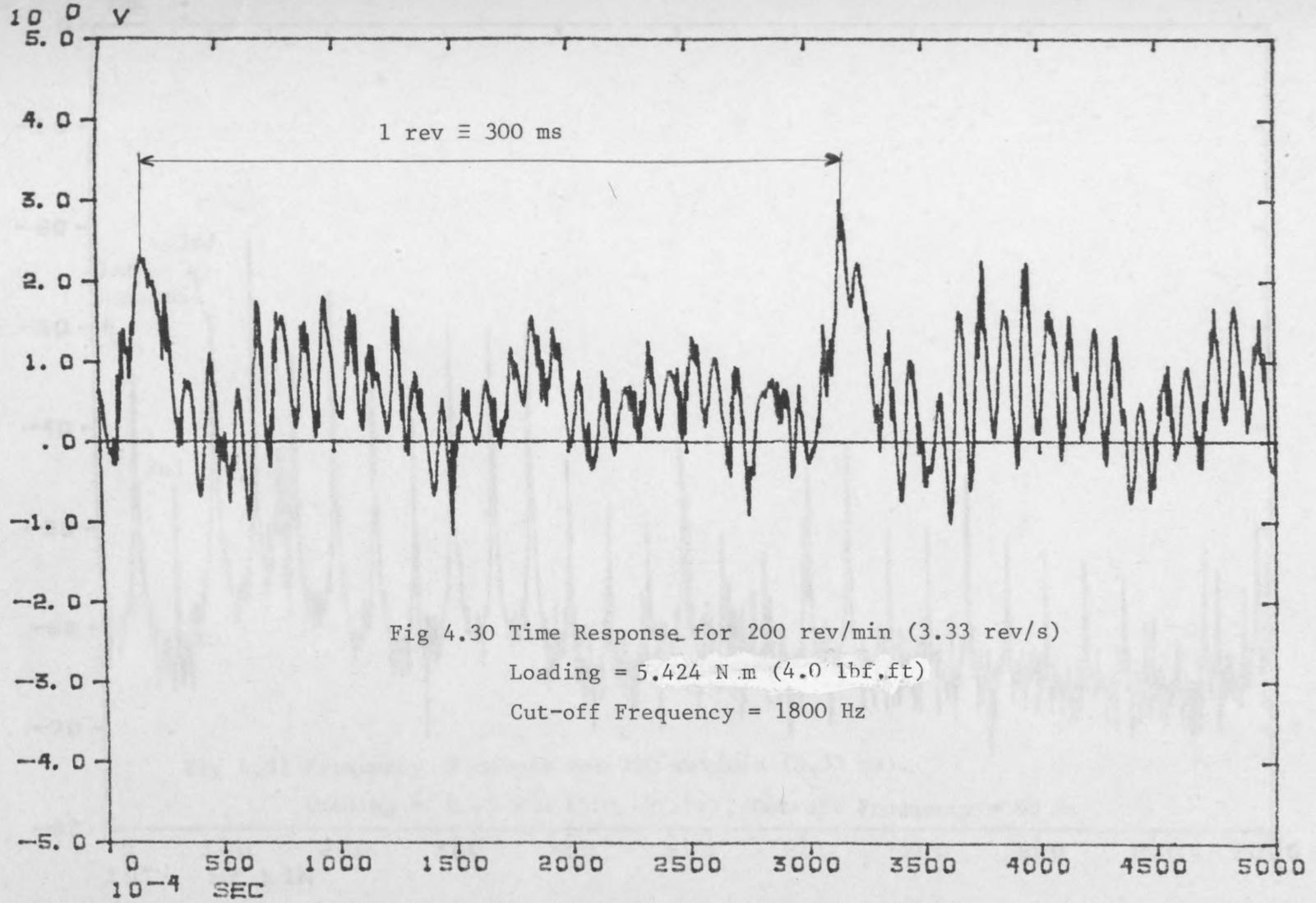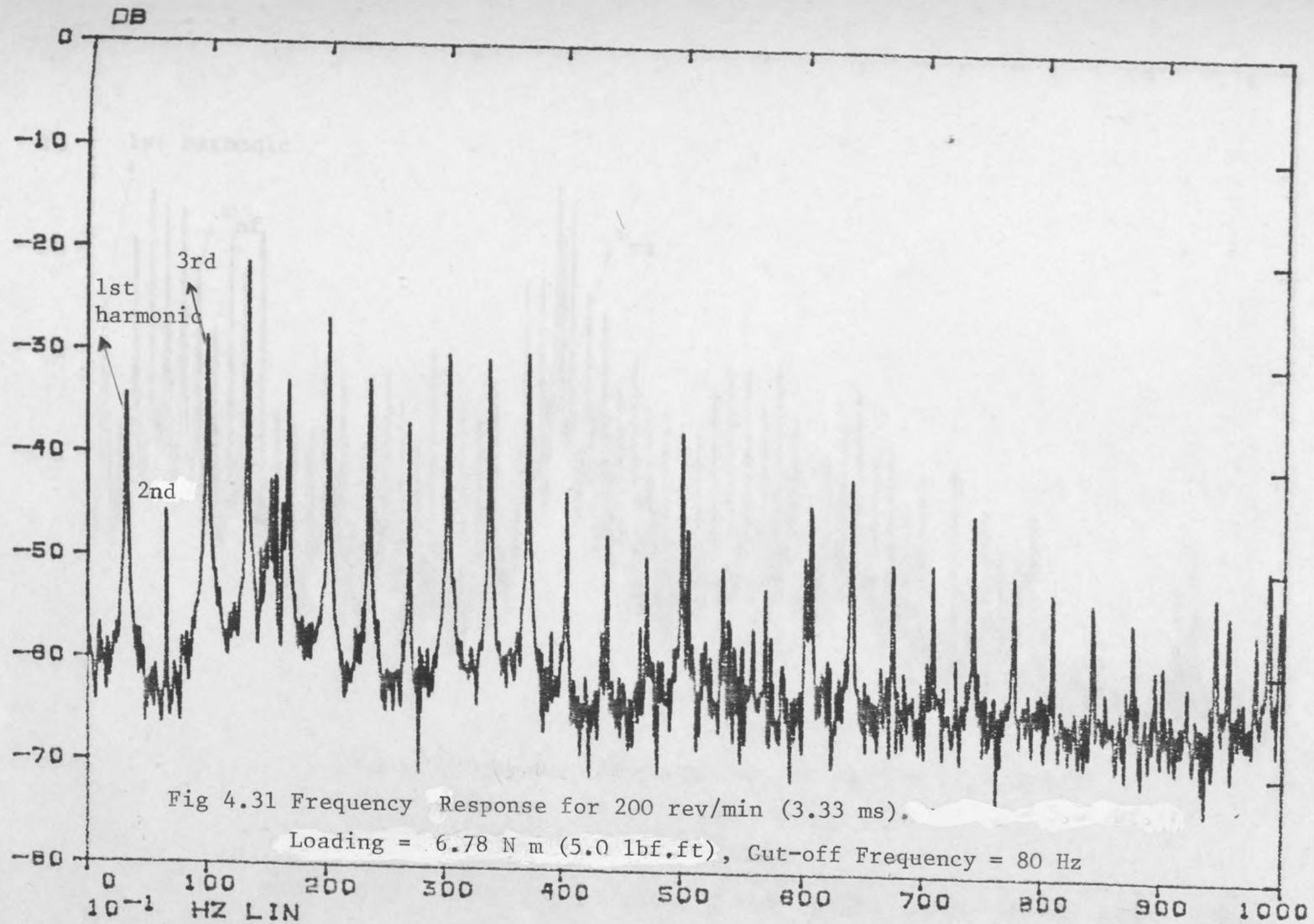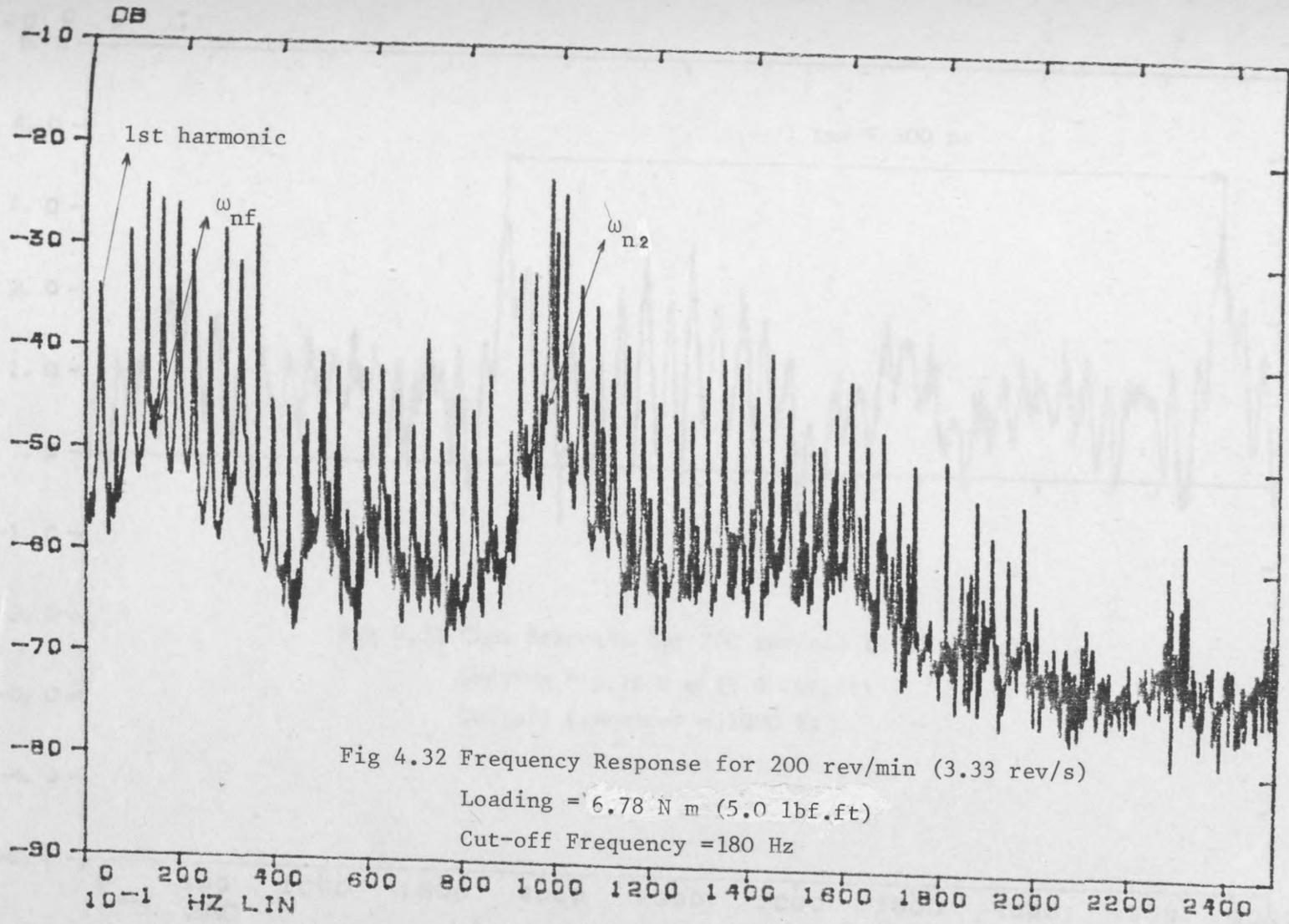
Fig 4.32 Frequency Response for 200 rev/min (3.33 rev/s)

Loading = 6.78 N m (5.0 lbf.ft)

Cut-off Frequency = 180 Hz
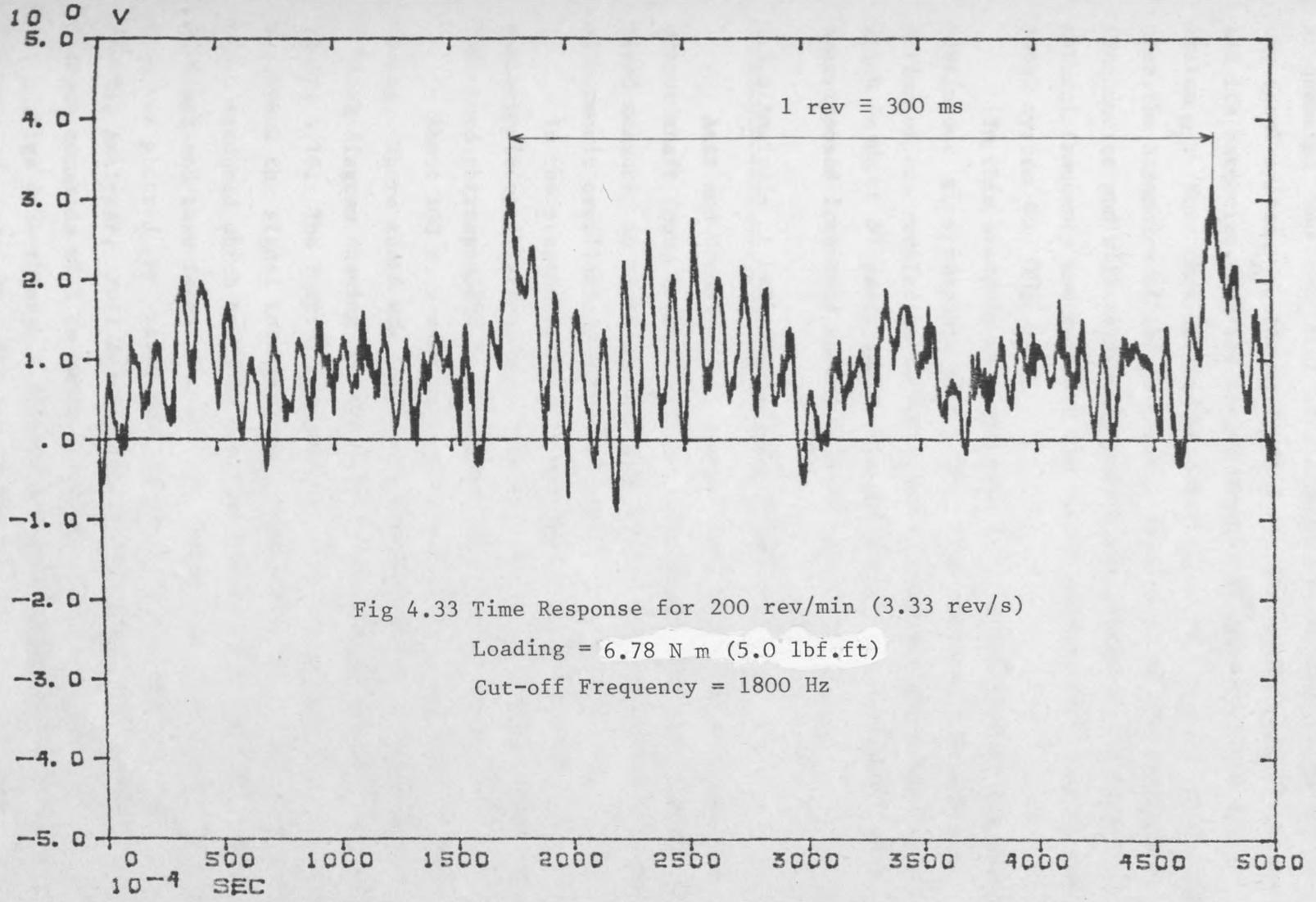
Fig 4.33 Time Response for 200 rev/min (3.33 rev/s)

Loading = 6.78 N m (5.0 lbf.ft)

Cut-off Frequency = 1800 Hz

For loading of 3.389-6.78 N m (2.5-5.0 lbf.ft) the main frequencies contained are: the fundamental natural frequency of the total system ω_{nf}, the rotational speed corresponding frequency and its harmonics, and the second natural frequency of the total system ω_2. Note that in loading range of 3.389 N m (2.5 lbf.ft) and over, the harmonics of the rotational speed will be the dominant frequencies and will relatively reduce the effect of the first natural frequency and resonate the second natural frequency of the total system ω_2 (Fig 4.32).

In this analysis each spectrum will be followed by its own continuous time response plot. This time response plot shows a period of one revolution (300 ms) and a super-imposed frequency which is about 30 peaks inside the period of one revolution; this superimposed frequency corresponds to either ω_{n2} or ω_{nb}.

4.3.5 Analysis of Subharmonic Test Results:

Azar and Crossley (11) stated that, in no instance was the output shaft found to oscillate at a frequency less than the shaft speed measured in teeth/sec (or any other measuring unit); i.e. no subharmonic oscillations were observed.

In the present study this was not the case and the subharmonic oscillations were observed always at speeds higher than the speed corresponding to the first natural frequency.

About 400 runs were made and the best possible results were chosen. Where there was some doubt the test would be repeated. A block diagram showing how the results were taken and analysed is in Fig 4.18. The Fourier Analyser was used to analyse the time signal and break the signal into frequency components. A simple programme was introduced which helps to digitize and analyse the time signal 10 times and then takes the average at the end. The resulting spectrum was plotted by using special plotting commands on the Fourier Analyser. Full description of this programme and the various commands will be shown in App.E.

Figs 4.34 through 4.71 show a sample of the results for a loading of 0.0 N m (0.0 lbf.ft), 2.712 N m (2.0 lbf.ft) and 5.424 N m (4.0 lbf.ft).

For each loading, the speed of the driving motor was varied and the results were plotted, Figs 4.34 through 4.41 show the spectrum plot and corresponding time response for a loading = 0.0 N m (0.0 lbf.ft) Figs 4.42 through 4.55 show the spectrum plot and corresponding time response for different speeds and constant loading of 2.712 N m (2.0 lbf.ft) and finally Figs 4.56 through 4.71 show the spectrum plot and corresponding time response for loading of 5.424 N m (4.0 lbf.ft).

For loading of 0.0 N m (0.0 lbf.ft) in Fig 4.34 the speed was 600 rev/min (which is lower than the speed corresponding to the natural frequency of 780 rev/min) and the number of rev/s is 10. From this figure it can be seen that the first frequency is 10 Hz; i.e. there are no subharmonics at this speed, the integral multiples of the first frequency can also be seen in this figure. Fig. 4.35 which represents the time response of the same speed verify this explanation and a period of 100 ms corresponding to speed of 600 rev/min is also shown.

Looking at Fig 4.38 which represent the speed of 1100 rev/min (which is higher than the speed corresponding to the natural frequency). This figure shows the first subharmonic at 9.166 Hz which is half the number of rev/s for that speed of 18.33 Hz. As confirmation Fig 4.39 shows a period of 109.08 ms which is twice the period corresponding to a speed of 1100 rev/min (54.54 ms).

All the speeds higher than 1000 rev/min contain a subharmonic at half the speed measured in rev/s. Figs 4.40 and 4.41 show spectrum plot and time plot respectively, for speed of 1300 rev/min for the same condition of loading = 0.0 N m (0.0 lbf.ft).

For loading of 2.712 N m (2.0 lbf.ft) Figs 4.42 and 4.43 represent the spectrum plot and time plot for a speed of 250 rev/min (4.166 rev/s), one can easily see that the first frequency is the rotational speed of 4.166 rev/s. The same applies for Figs 4.44 and 4.45 for speed of 350 rev/min, and Figs 4.46 and 4.47 for speed of 600 rev/min, and Figs 4.48 and 4.49 for speed of 900 rev/min.

Fig 4.34 Frequency Response for 600 rev/min (10 rev/s)
Loading = 0.0 N m (0.0 lbf.ft)
Cut-off Frequency = 80 Hz
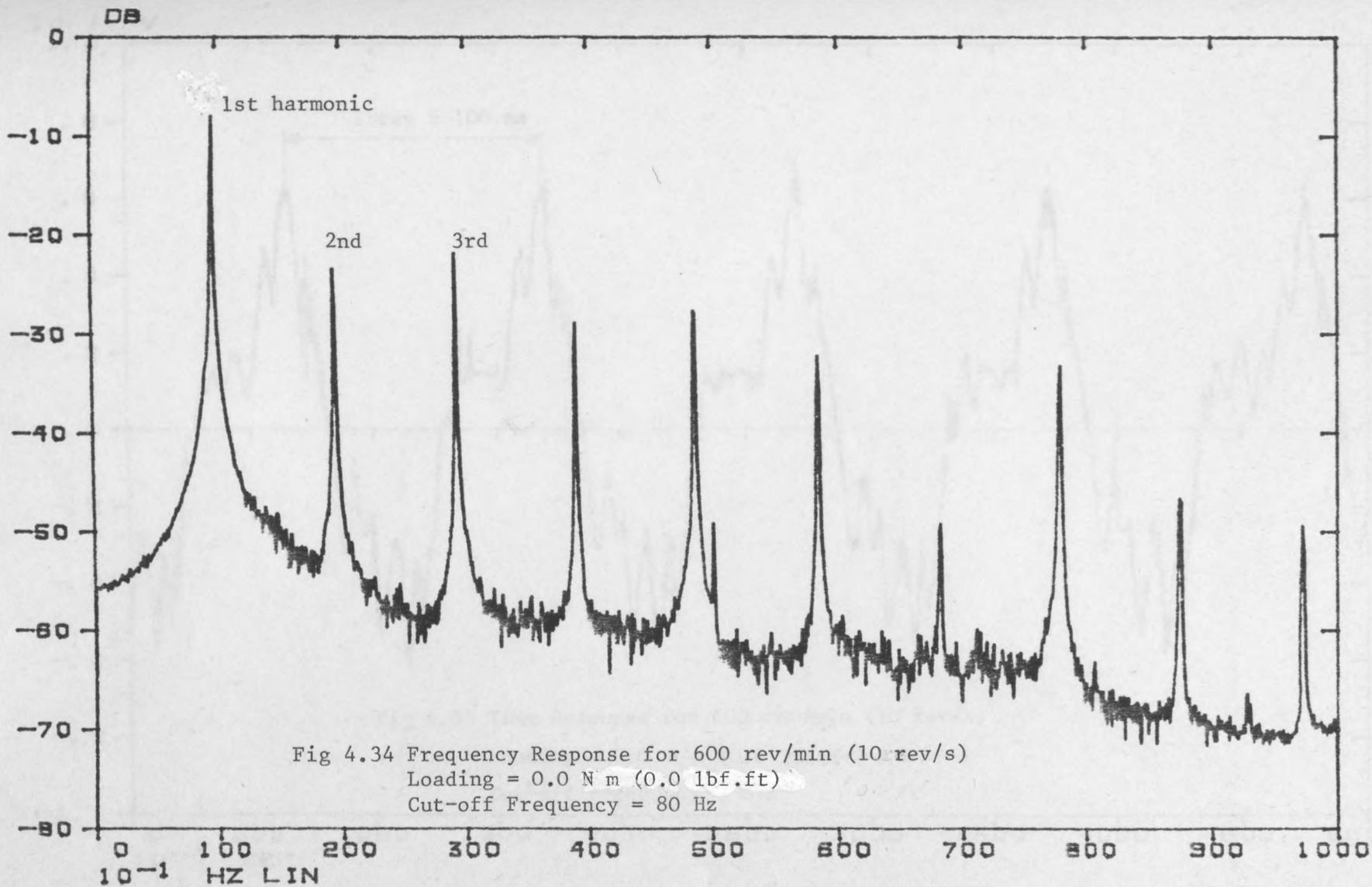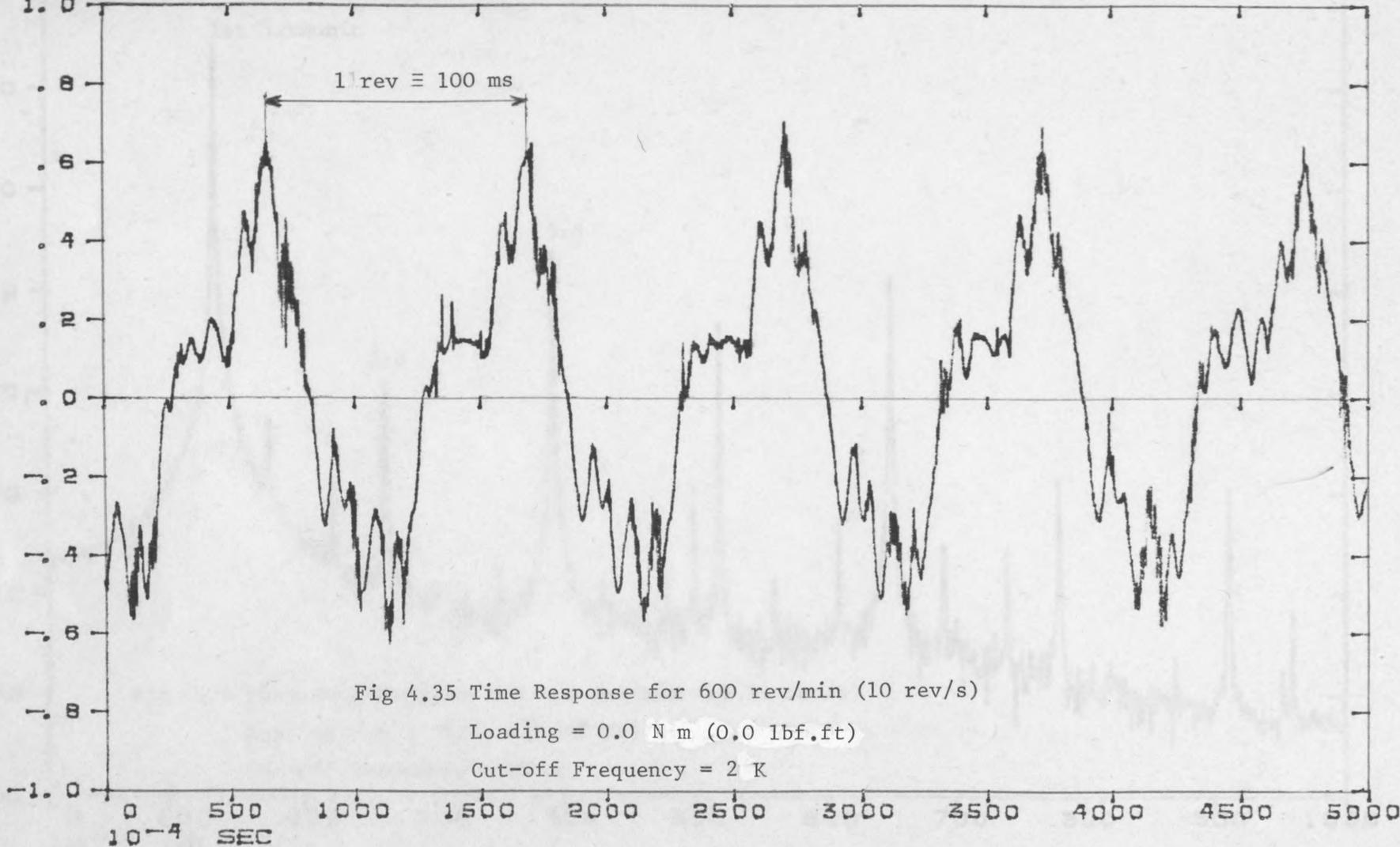
Fig 4.35 Time Response for 600 rev/min (10 rev/s)

Loading = 0.0 N m (0.0 lbf.ft)

Cut-off Frequency = 2 K

Fig 4.36 Frequency Response for 800 rev/min (13.33 rev/s)

Loading = 0.0 N m (0.0 lbf.ft)

Cut-off Frequency = 80 Hz

Fig 4.37 Time Response for 800 rev/min.   Loading = 0.0 N m (0.0 lbf.ft)
         Cut-off Frequency = 2 K

1 rev ≡ 75 ms

Fig 4.38 Frequency Response for 1100 rev/min (18.33 rev/s)

Loading = 0.0 N m (0.0 lbf.ft)

Cut-off Frequency = 80 Hz

2 rev ≡ 109.08 ms
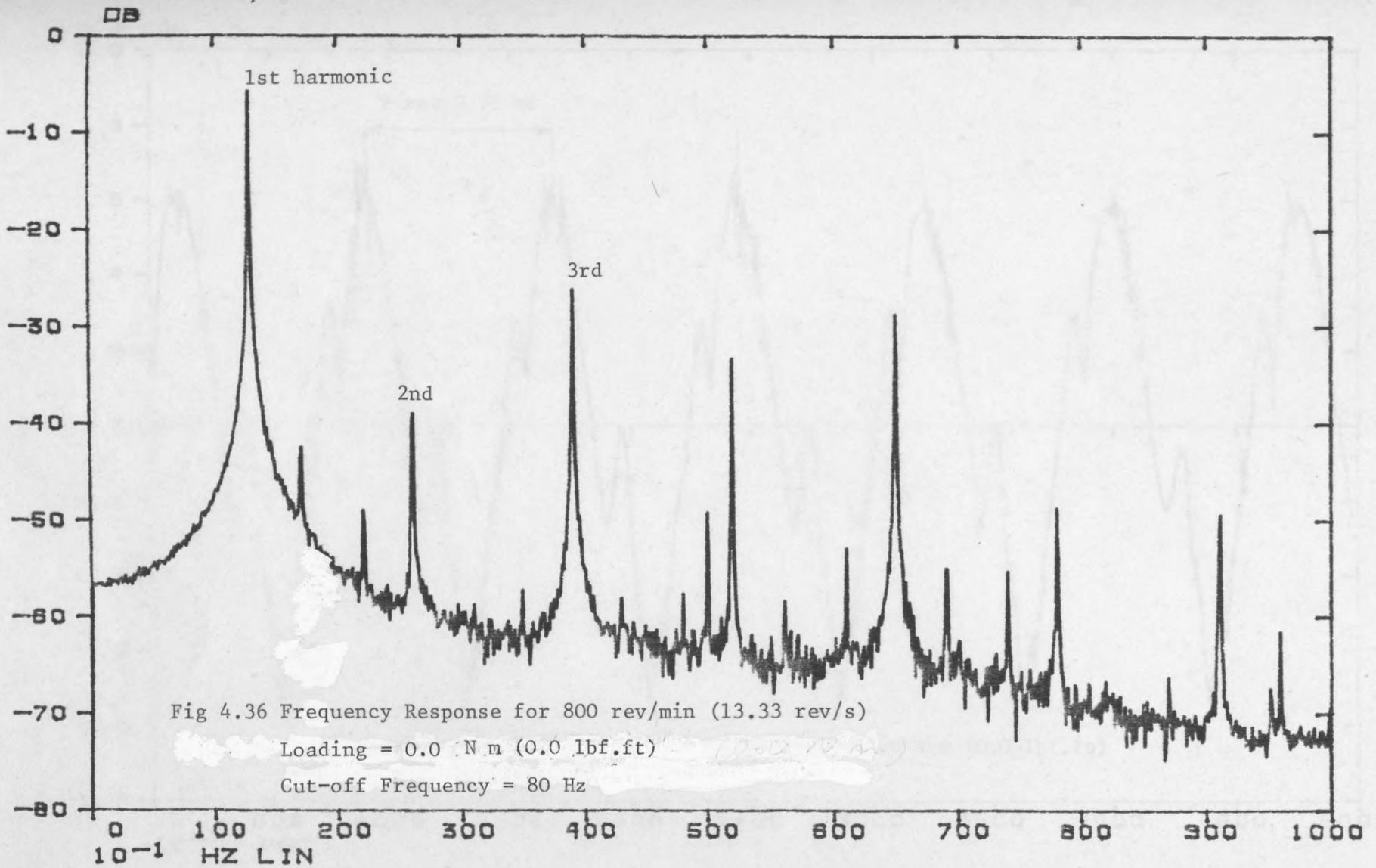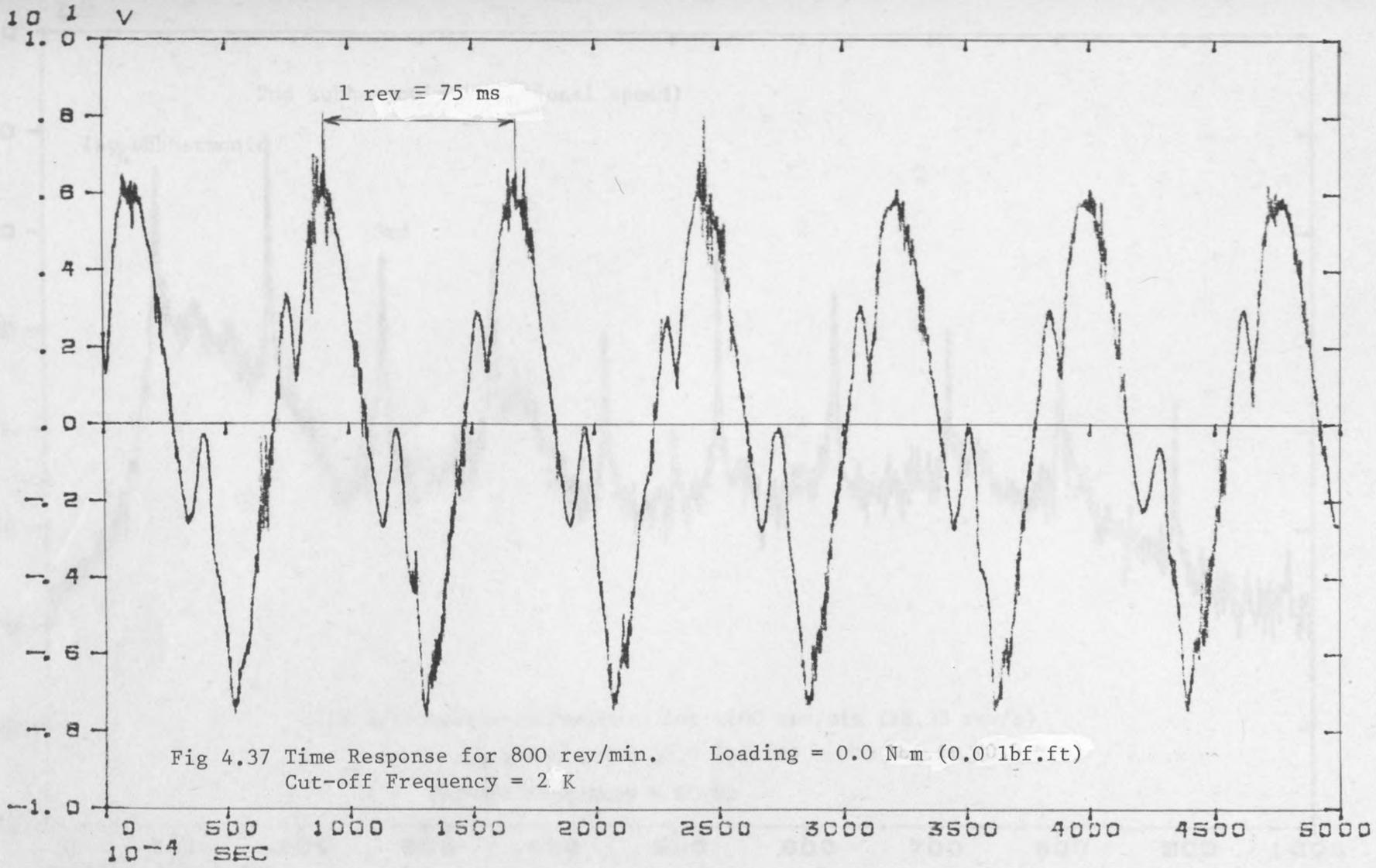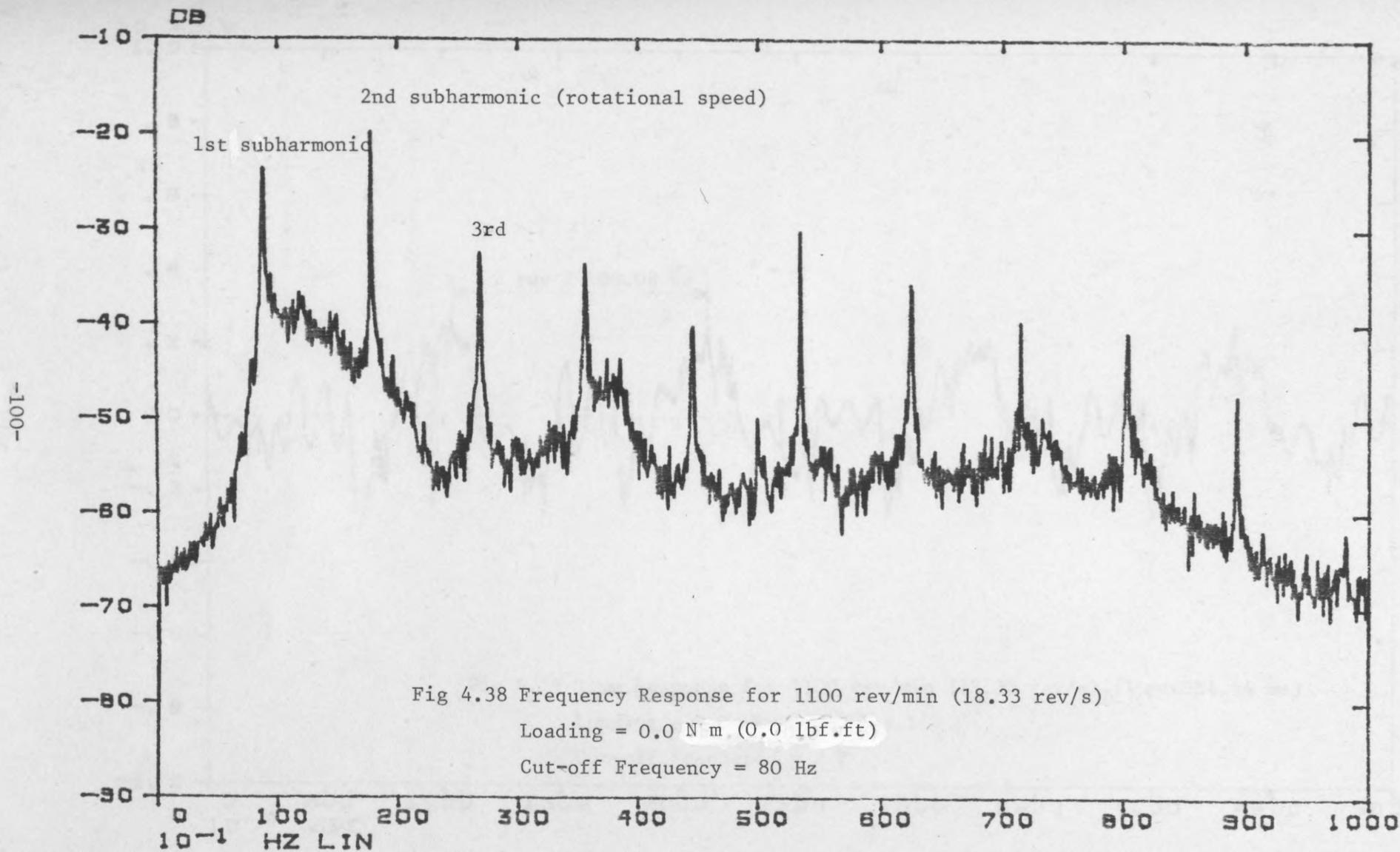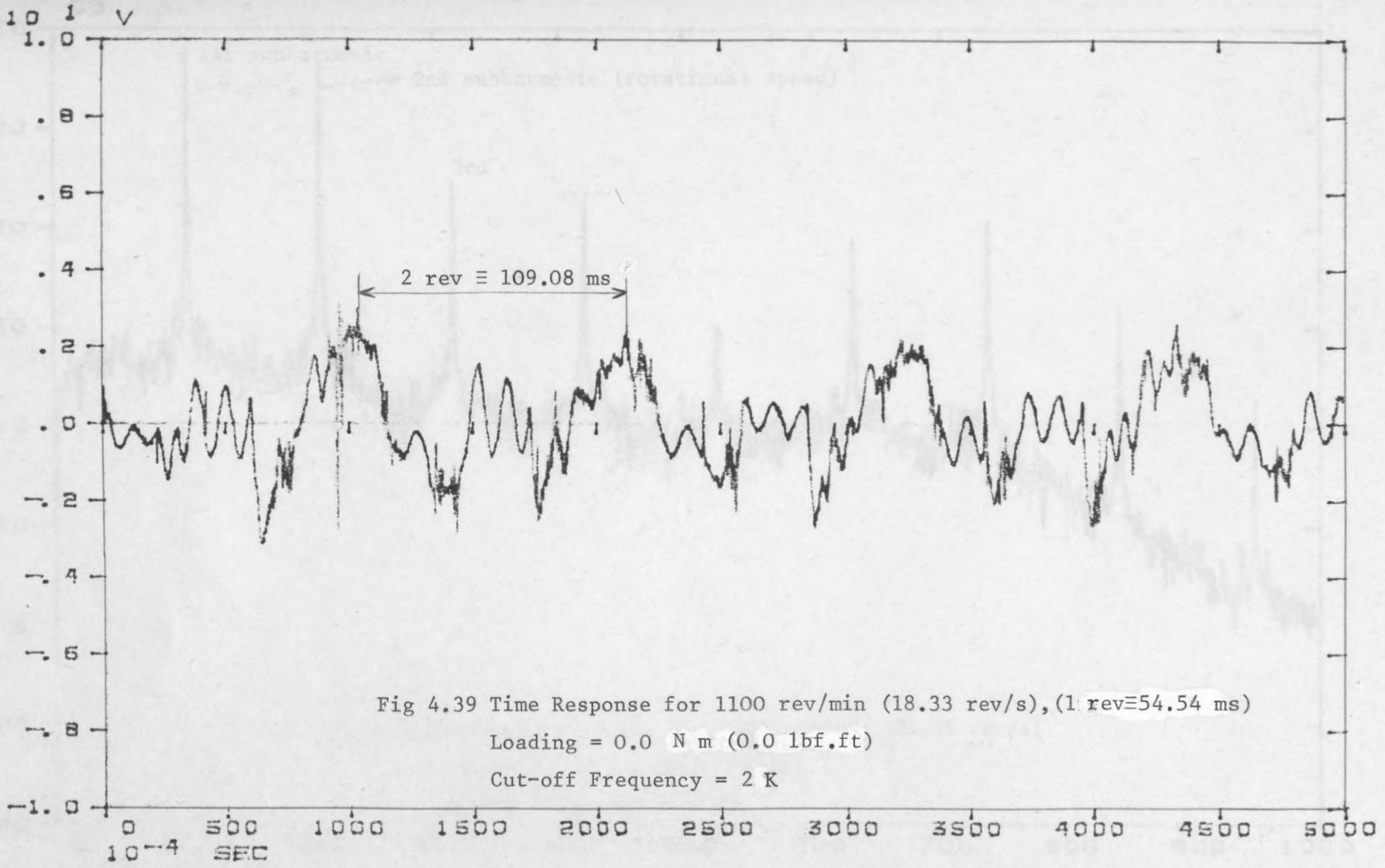
Fig 4.39 Time Response for 1100 rev/min (18.33 rev/s),(1 rev≡54.54 ms)

Loading = 0.0 N m (0.0 1bf.ft)

Cut-off Frequency = 2 K

Fig 4.40 Frequency Response for 1300 rev/min (21.66 rev/s)

Loading = 0.0 N m (0.0 lbf.ft)

Cut-off Frequency = 80 Hz
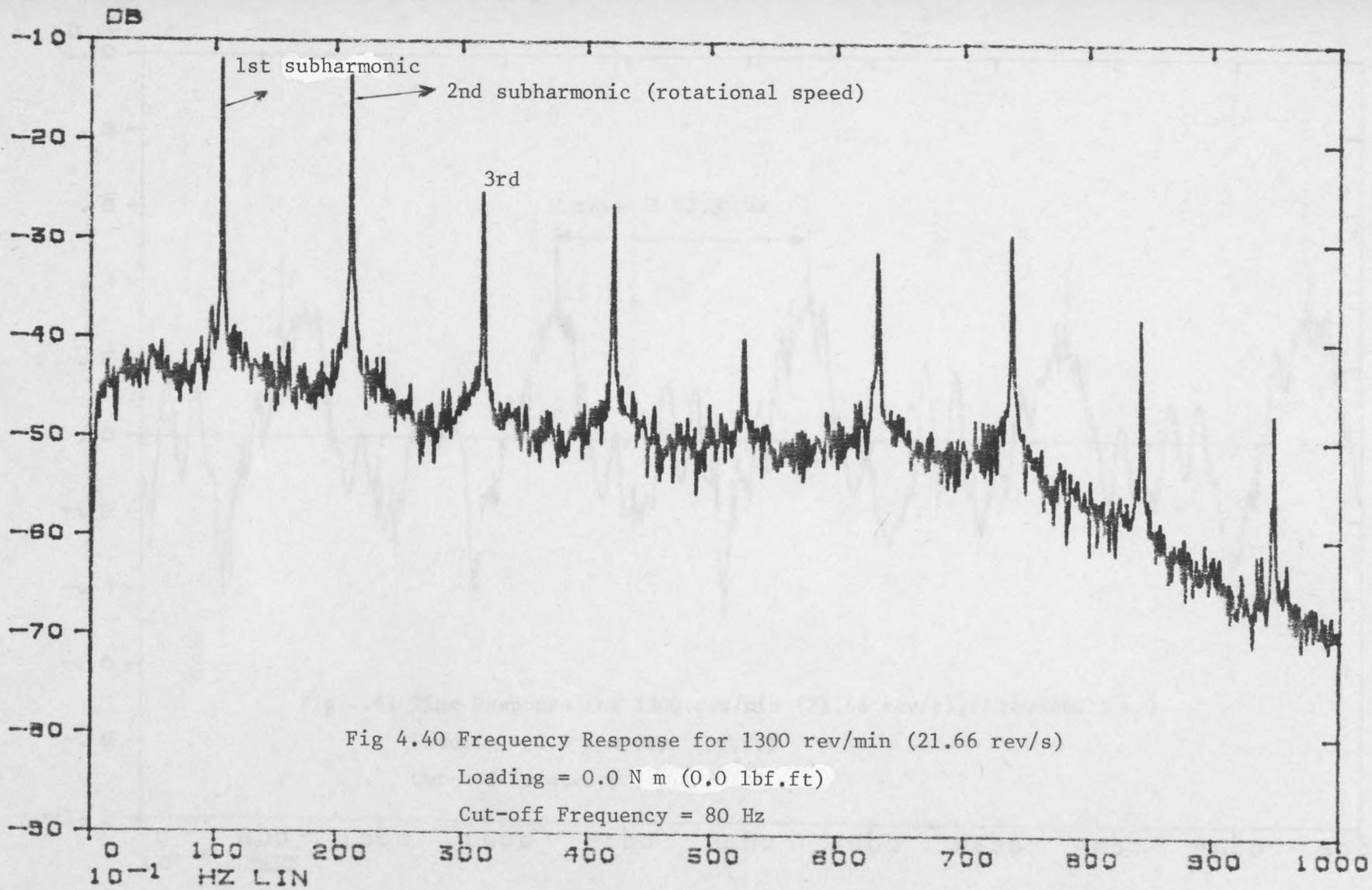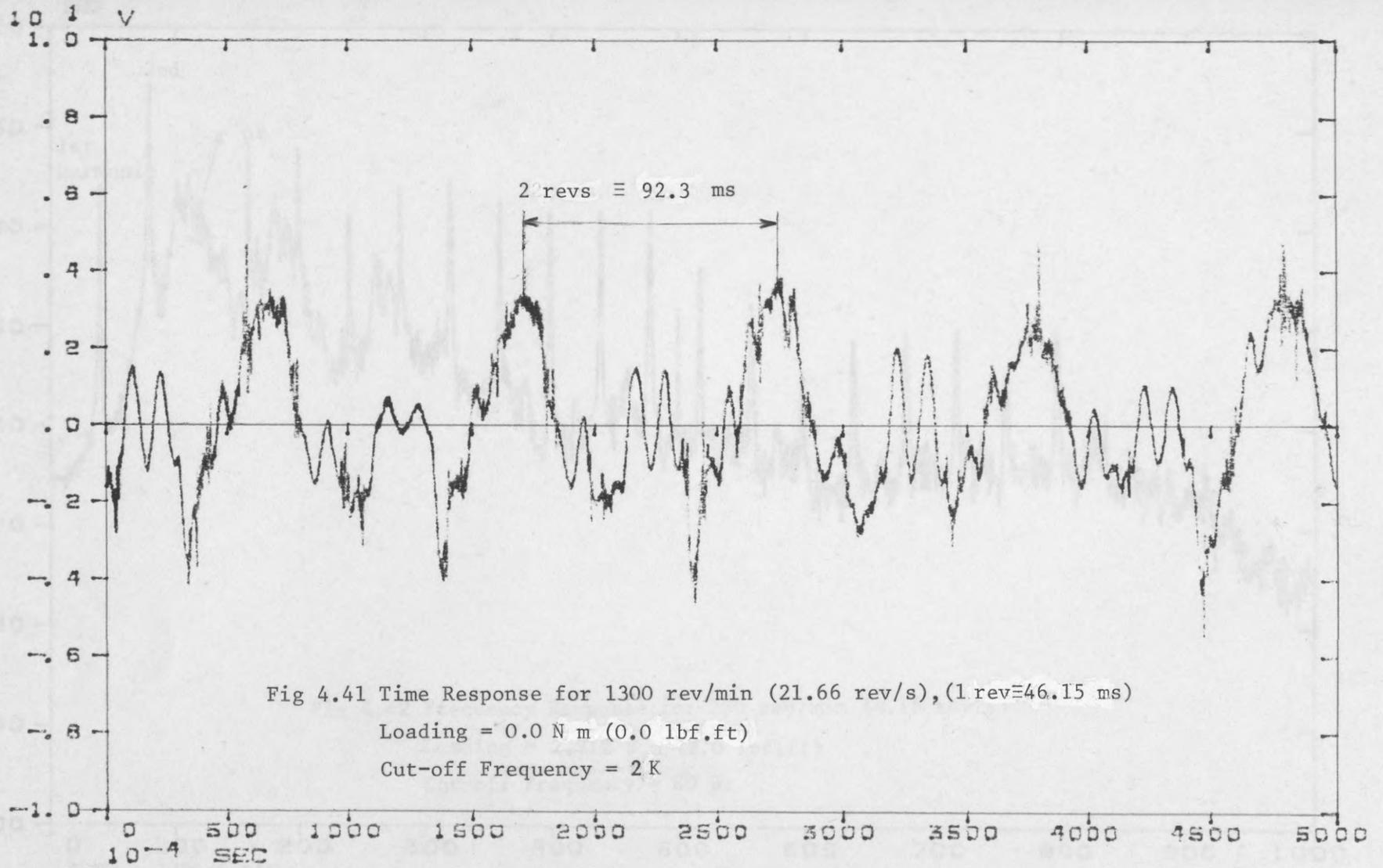
Fig 4.41 Time Response for 1300 rev/min (21.66 rev/s),(1 rev≡46.15 ms)
Loading = 0.0 N m (0.0 lbf.ft)
Cut-off Frequency = 2 K
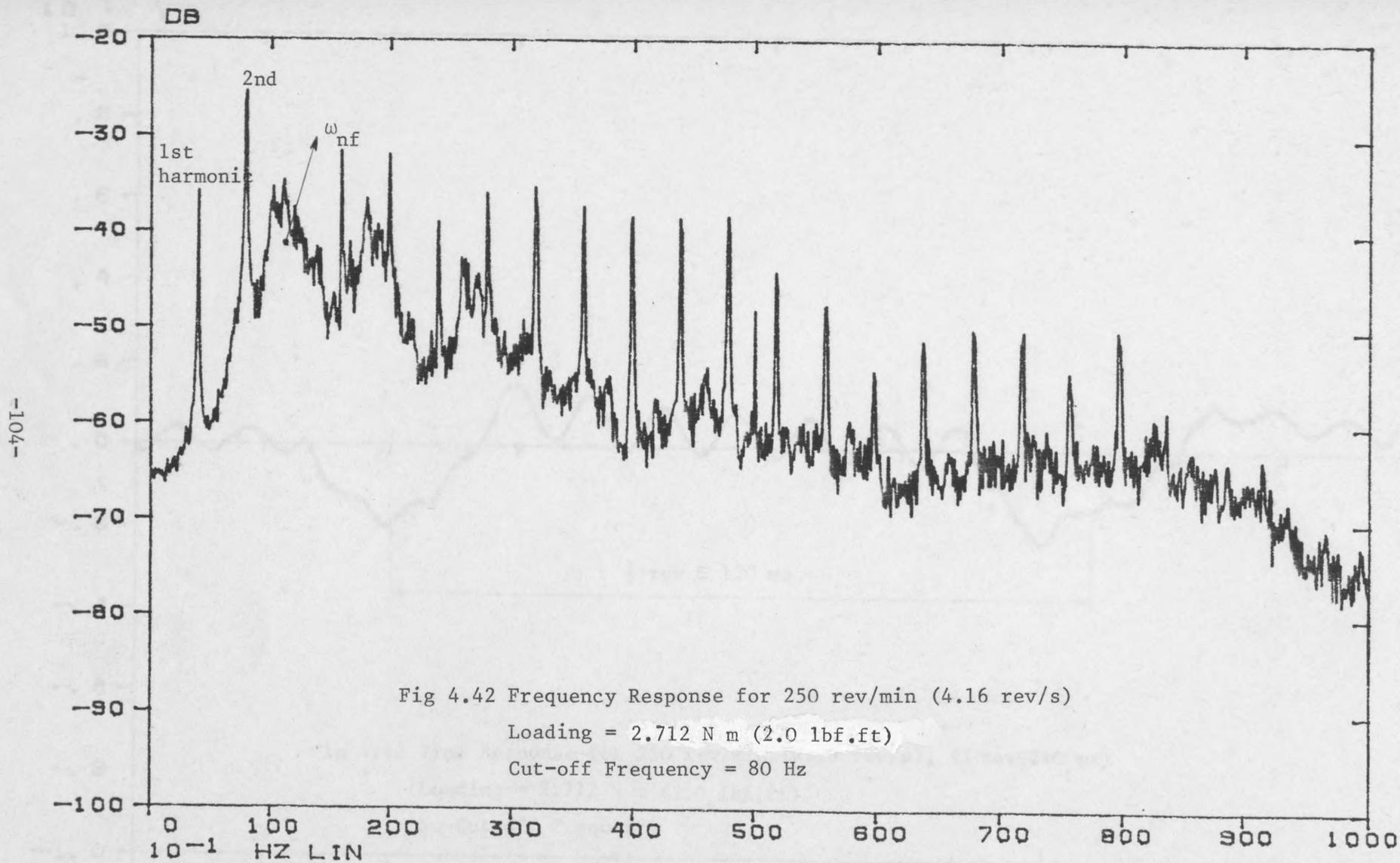
Fig 4.42 Frequency Response for 250 rev/min (4.16 rev/s)

Loading = 2.712 N m (2.0 lbf.ft)

Cut-off Frequency = 80 Hz
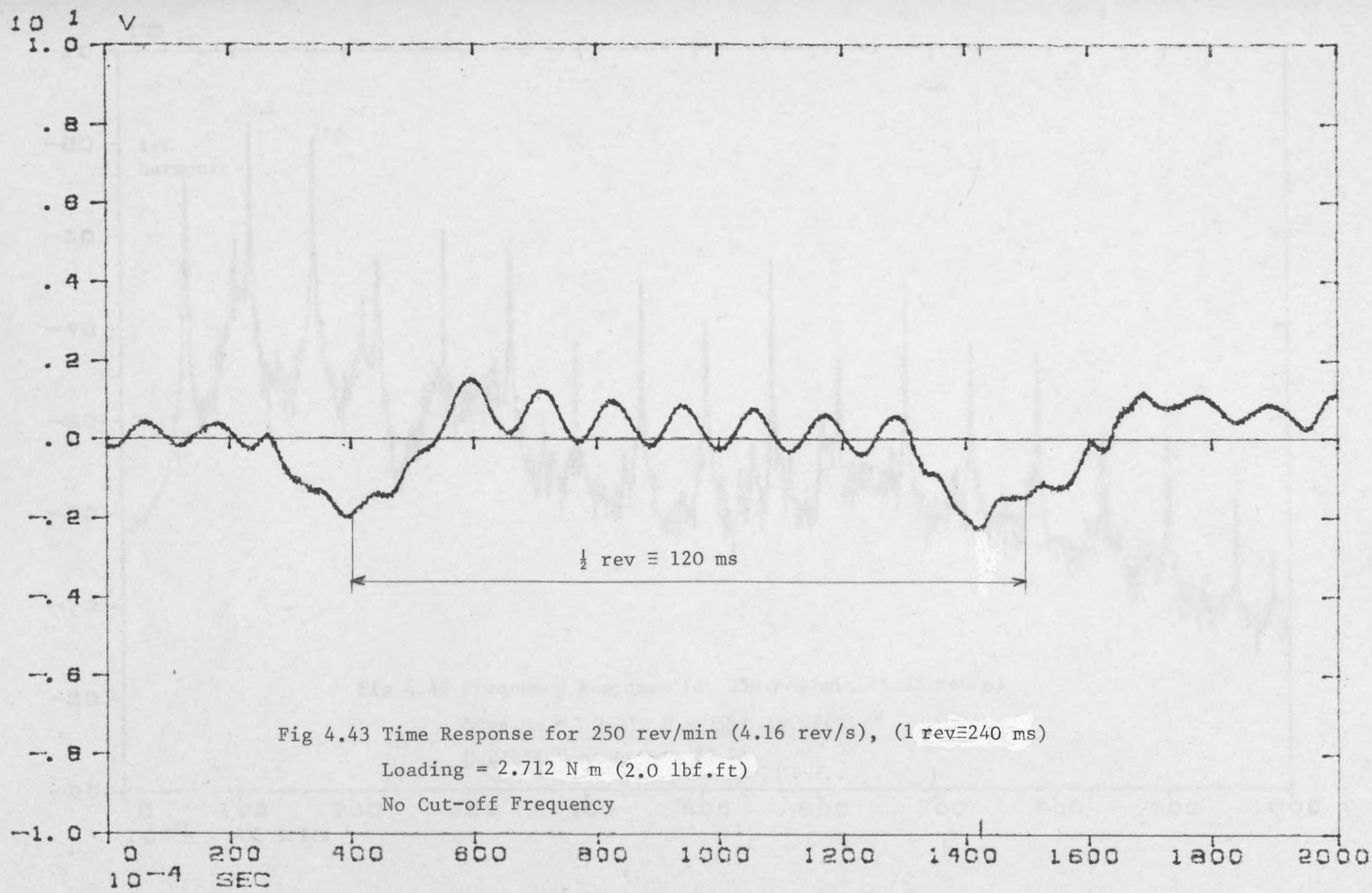
Fig 4.43 Time Response for 250 rev/min (4.16 rev/s), (1 rev≡240 ms)

Loading = 2.712 N m (2.0 lbf.ft)

No Cut-off Frequency

DB
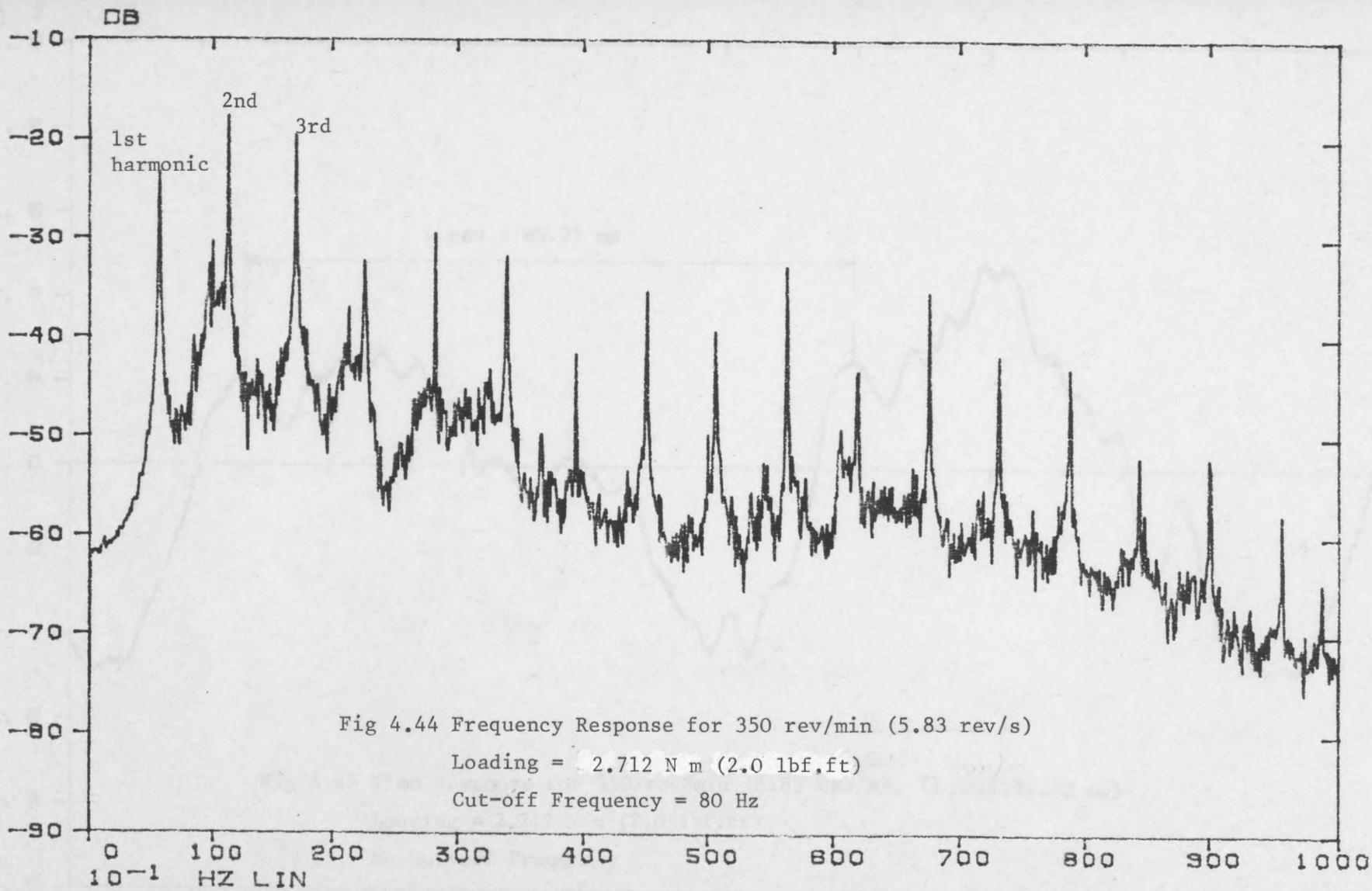
Fig 4.44 Frequency Response for 350 rev/min (5.83 rev/s)

Loading = 2.712 N m (2.0 lbf.ft)

Cut-off Frequency = 80 Hz
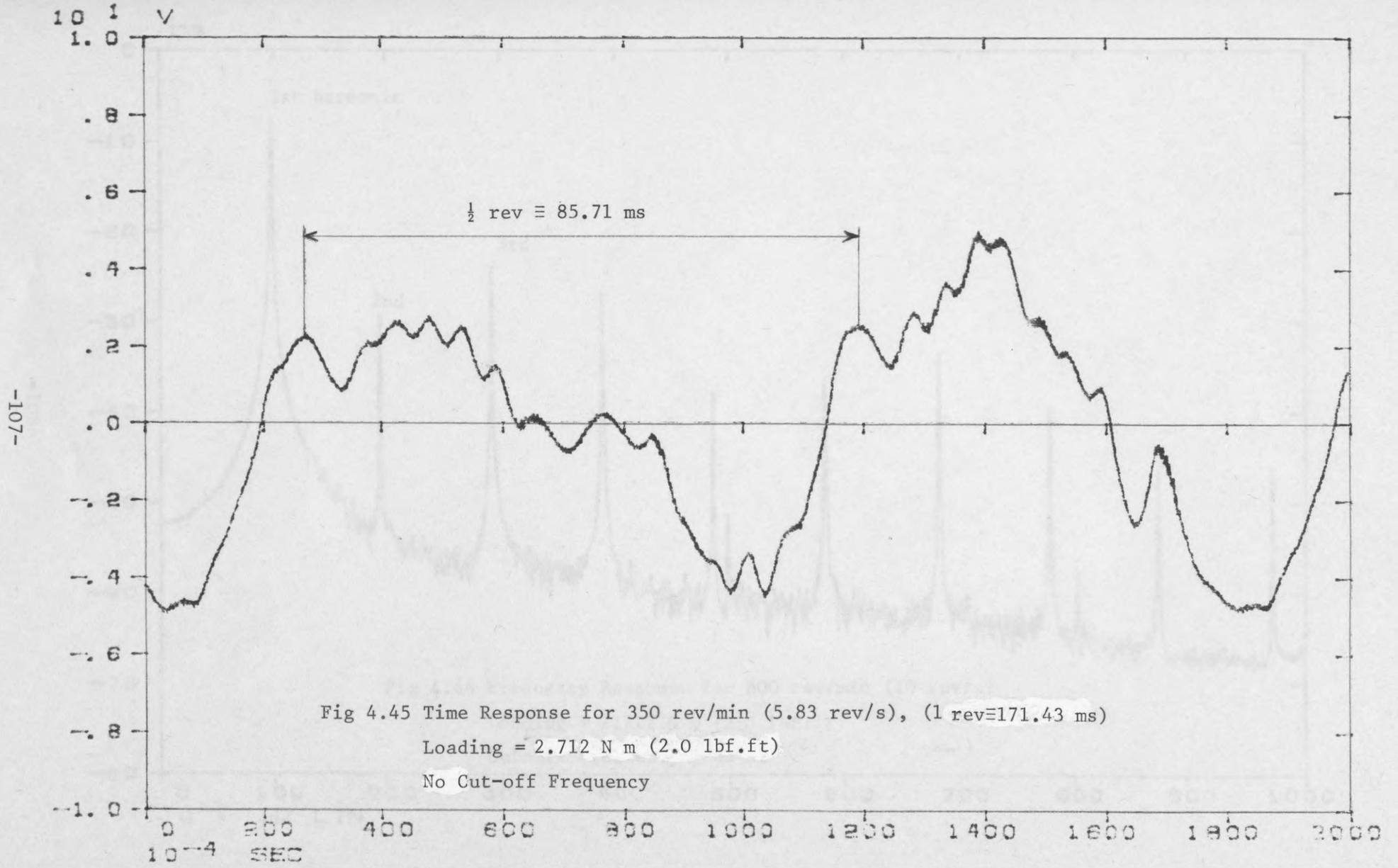
Fig 4.45 Time Response for 350 rev/min (5.83 rev/s), (1 rev≡171.43 ms)

Loading = 2.712 N m (2.0 lbf.ft)
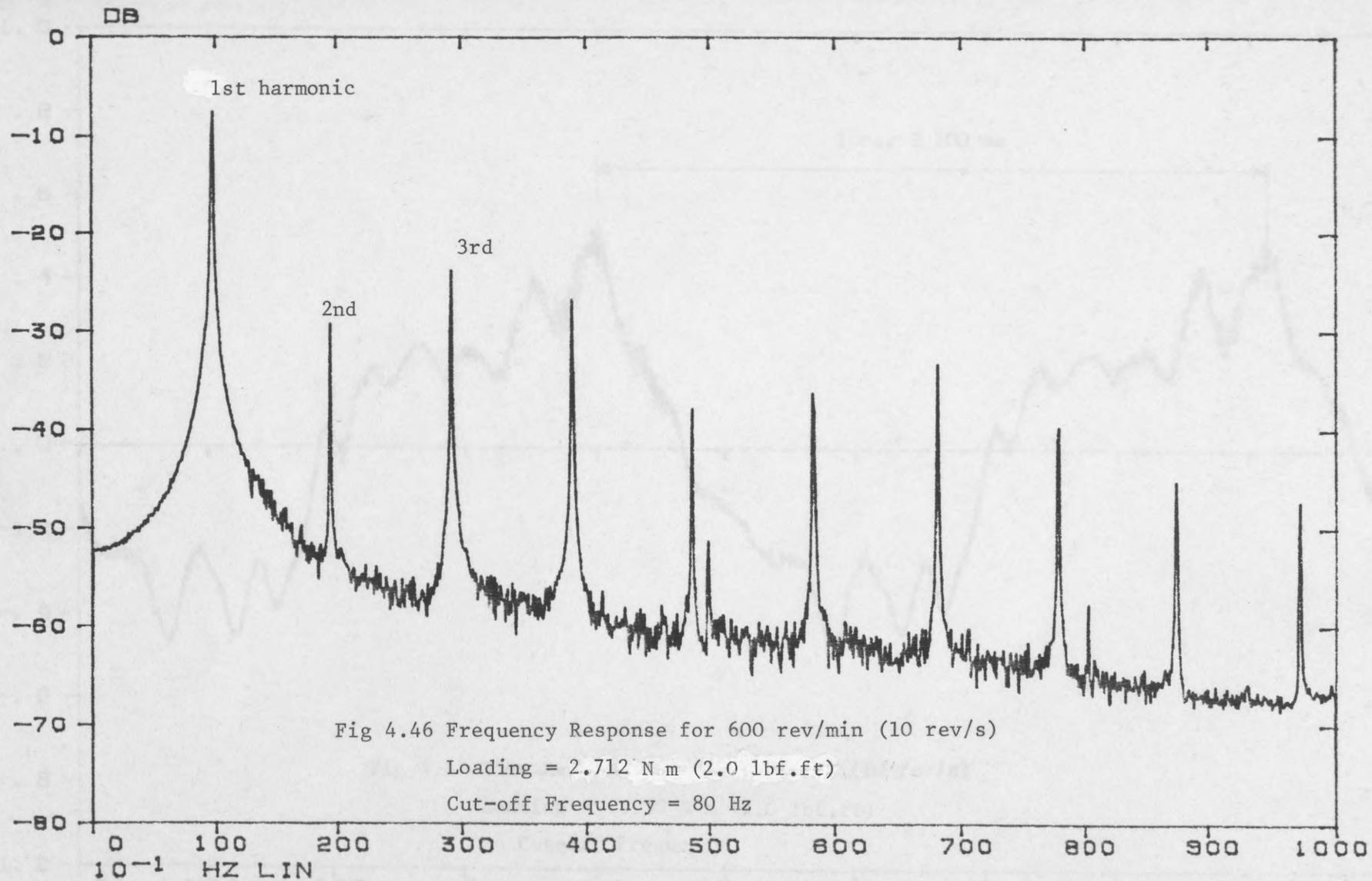
No Cut-off Frequency

-107-

Fig 4.46 Frequency Response for 600 rev/min (10 rev/s)

Loading = 2.712 N m (2.0 lbf.ft)

Cut-off Frequency = 80 Hz

Fig 4.47 Time Response for 600 rev/min (10 rev/s)

Loading = 2.712 N m (2.0 lbf.ft)

No Cut-off Frequency

Fig 4.48 Frequency Response for 900 rev/min (15 rev/s)

Loading = 2.712 N m (2.0 lbf.ft)

Cut-off Frequency = 80 Hz

Fig 4.49 Time Response for 900 rev/min (15 rev/s)

Loading = 2.712 N m (2.0 lbf.ft)

No Cut-off Frequency

Fig 4.50 Frequency Response for 1100 rev/min (18.33 rev/s)

Loading = 2.712 N m (2.0 lbf.ft)

Cut-off Frequency = 80 Hz

Fig 4.51 Frequency Response for 1200 rev/min (20.0 rev/s)

Loading = 2.712 N m (2.0 lbf.ft)

Cut-off Frequency = 80 Hz

Fig 4.52 Time Response for 1200 rev/min (20.0 rev/s), (1 rev≡50 ms)

Loading = 2.712 N m (2.0 lbf.ft)

No cut-off Frequency

Fig 4.53 Frequency Response for 1400 rev/min (23.33 rev/s)

Loading = 2.712 N m (2.0 lbf.ft)

Cut-off Frequency = 80 Hz
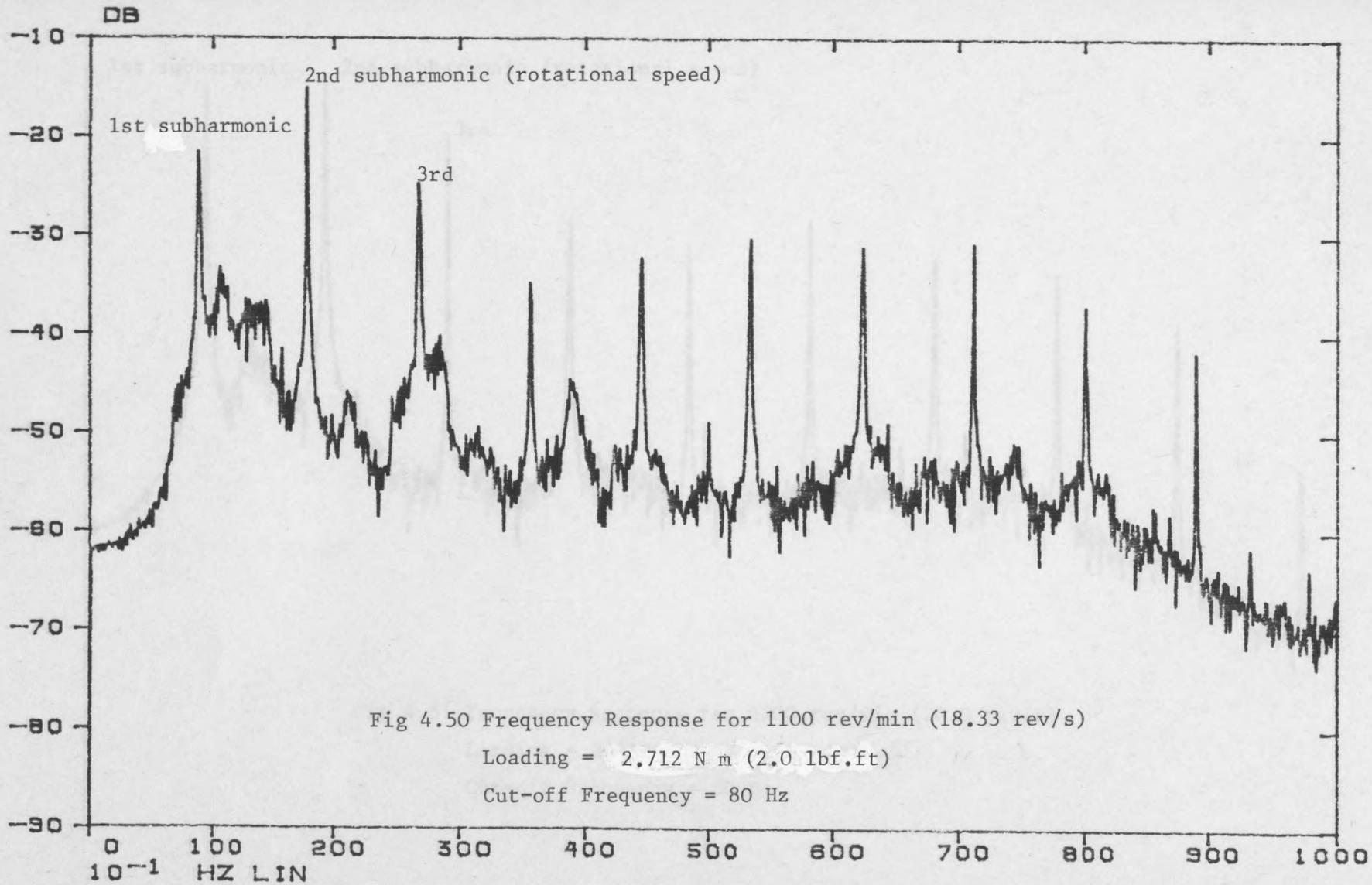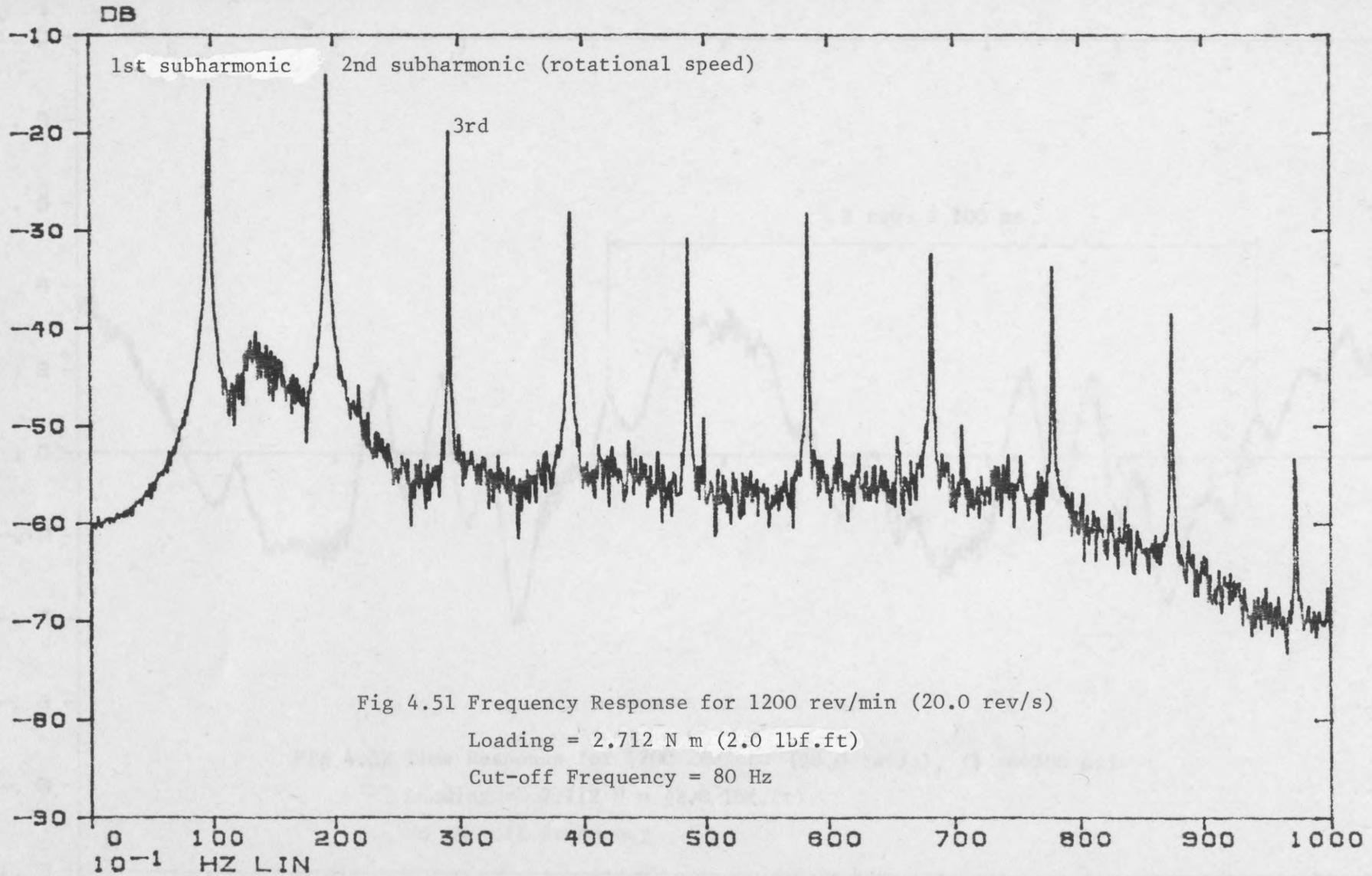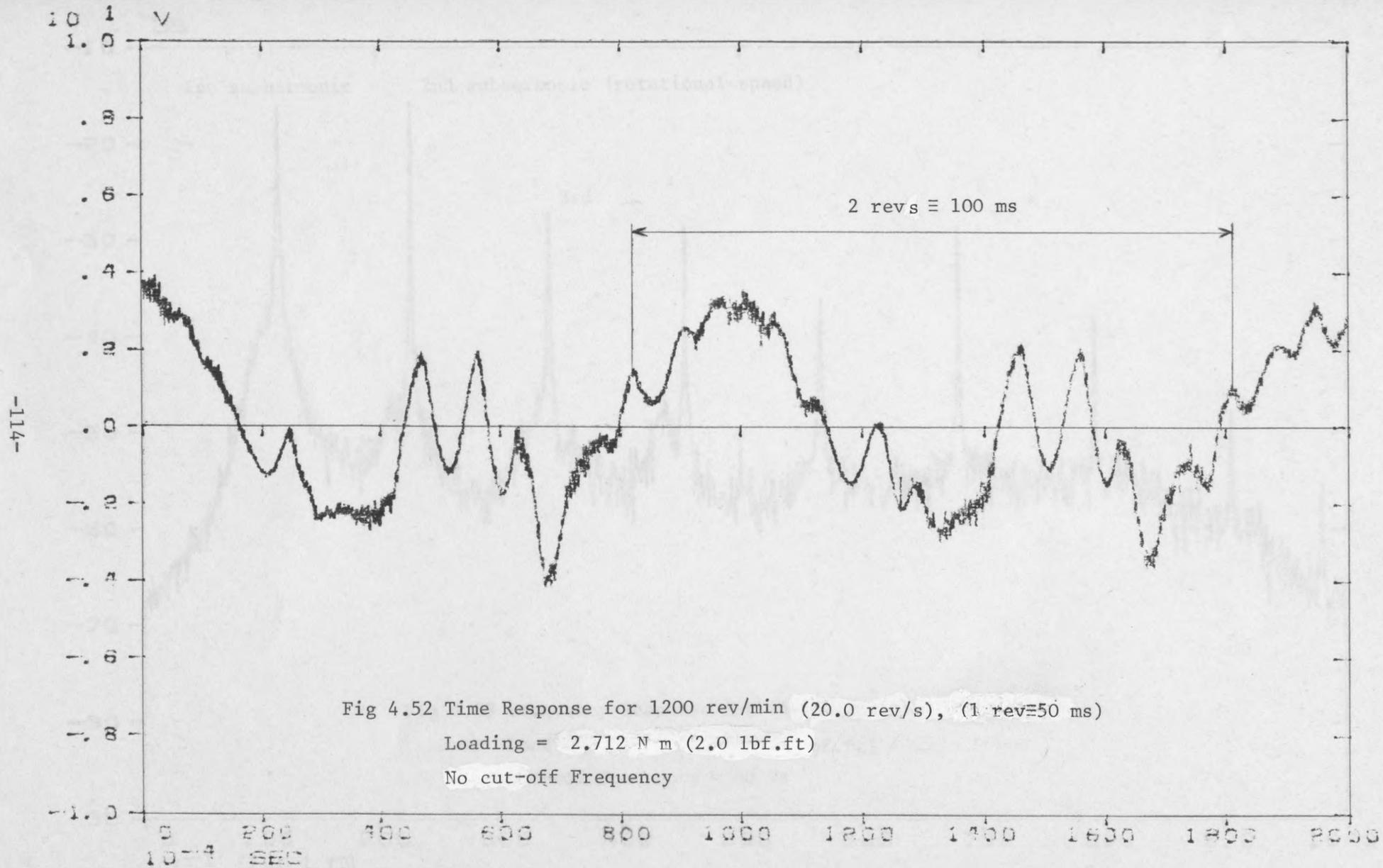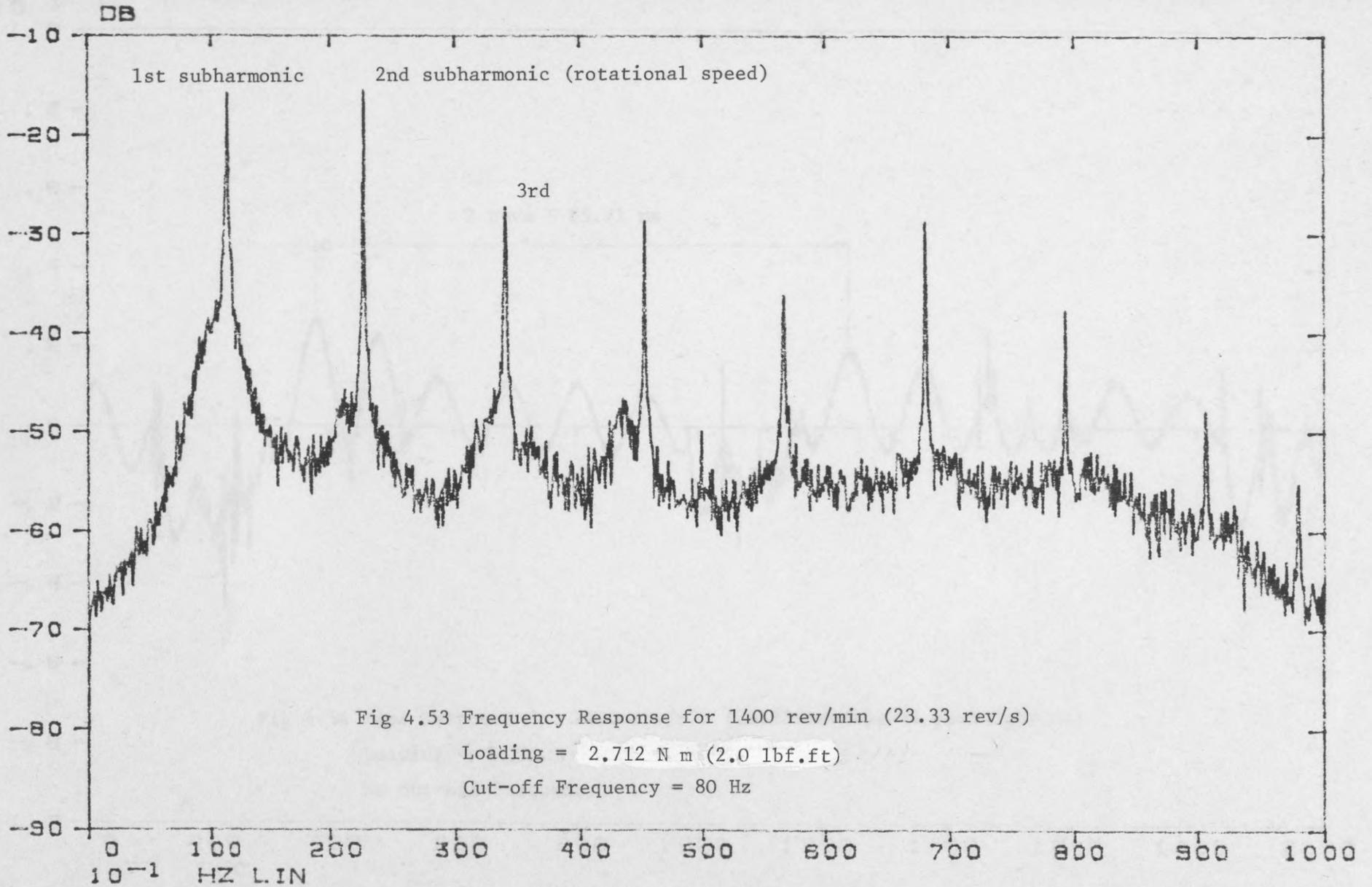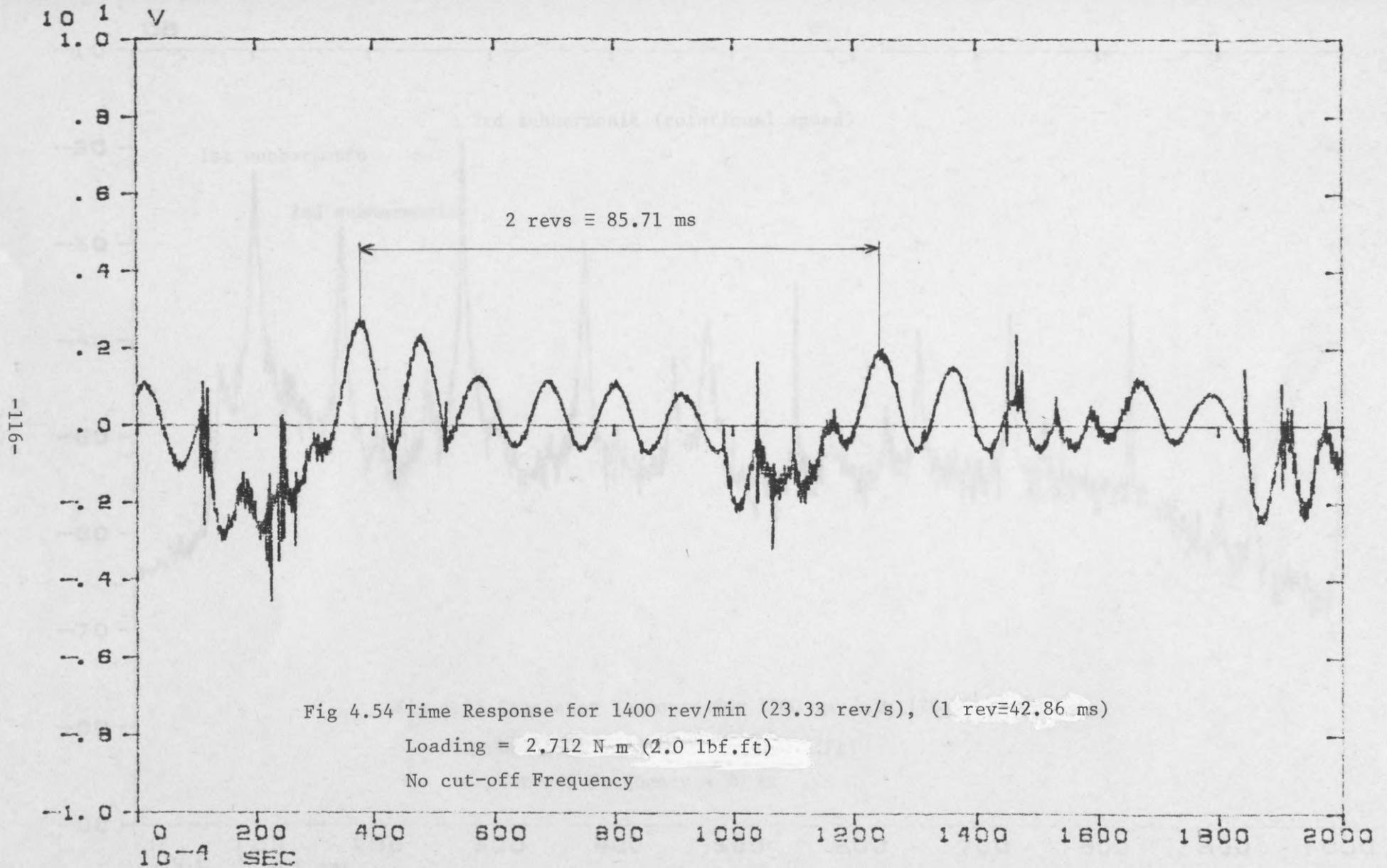
Fig 4.54 Time Response for 1400 rev/min (23.33 rev/s), (1 rev≡42.86 ms)

Loading = 2.712 N m (2.0 lbf.ft)

No cut-off Frequency
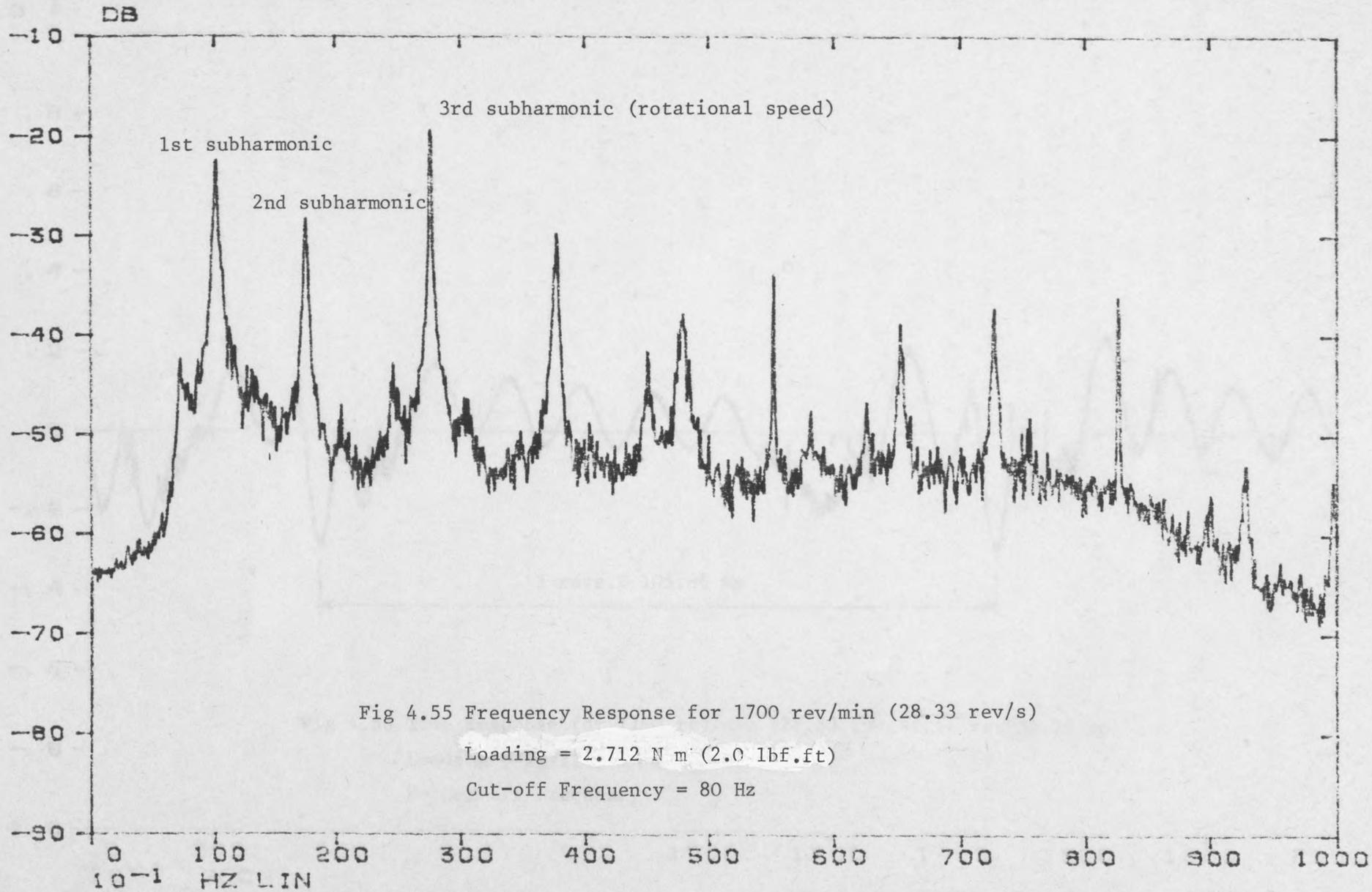
Fig 4.55 Frequency Response for 1700 rev/min (28.33 rev/s)

Loading = 2.712 N m (2.0 1bf.ft)

Cut-off Frequency = 80 Hz
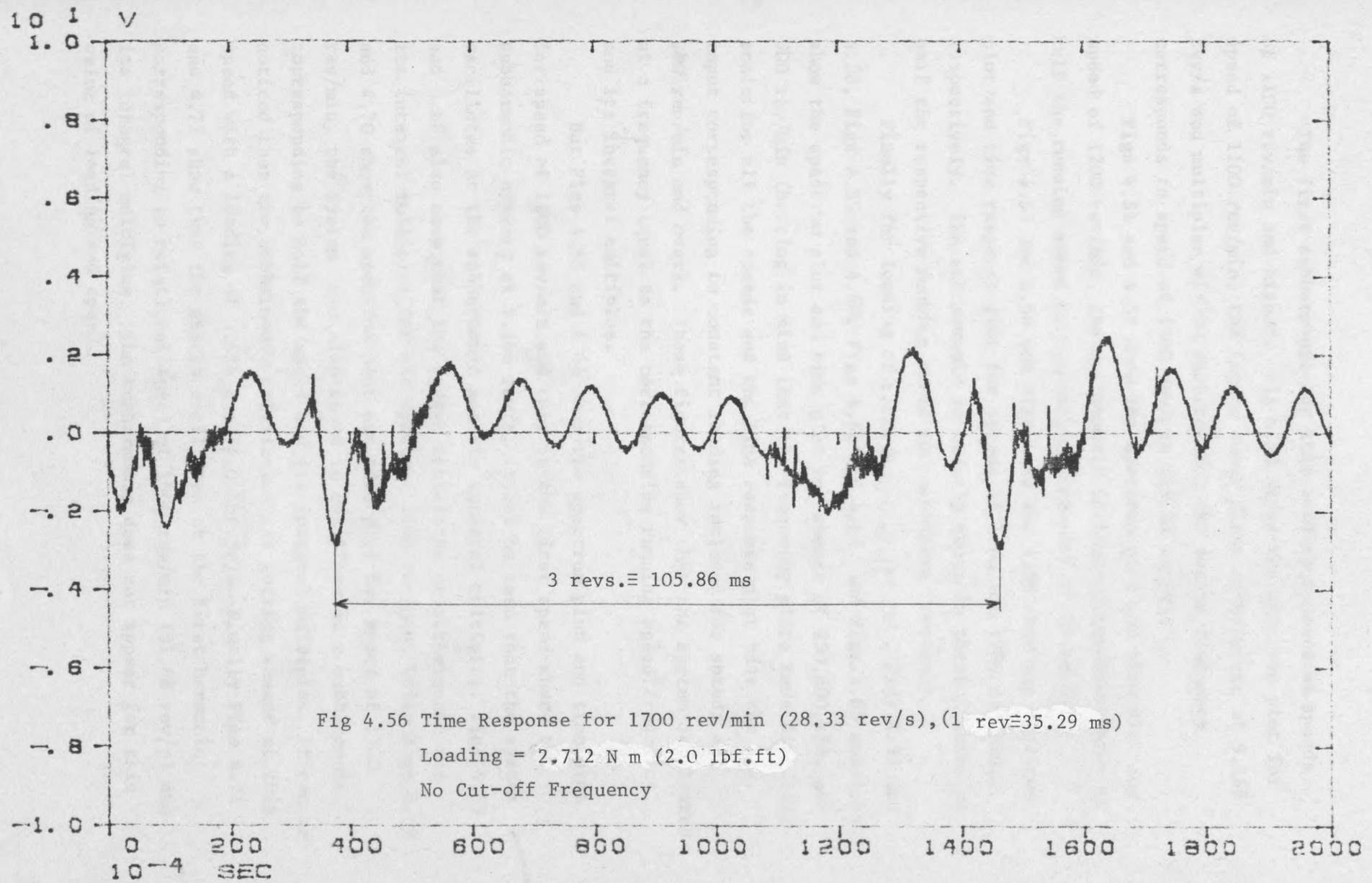
Fig 4.56 Time Response for 1700 rev/min (28.33 rev/s),(1 rev≡35.29 ms)

Loading = 2.712 N m (2.0 lbf.ft)

No Cut-off Frequency

The first subharmonic for this loading appears at speeds of 1100 rev/min and higher. Fig 4.50 shows the spectrum plot for speed of 1100 rev/min, the figure shows first subharmonic at 9.166 rev/s and multiples of that subharmonic, the second frequency corresponds to speed of 1100 rev/min (18.33 rev/s).

Figs 4.51 and 4.52 show the spectrum plot and time plot for speed of 1200 rev/min, the subharmonic in these figures is shown at half the running speed corresponding frequency of 20 rev/s.

Figs 4.53 and 4.54 and Figs 4.55 and 4.56 show the spectrum plot and time response plot for speeds of 1400 and 1700 rev/min, respectively. The subharmonic is clearly shown in these figures at half the respective running speed corresponding frequency.

Finally for loading of 5.424 N m (4.0 lbf.ft), Figs 4.57 and 4.58, Figs 4.59 and 4.60, Figs 4.61 and 4.62 and Figs 4.63 and 4.64 show the spectrum plot and time plot for speeds of 250,600,850, and 900 rev/min (bearing in mind that the frequency plots have different scales for all the speeds and the time response plot have the D.C. input corresponding to constant loading included for speeds of 900 rev/min and over). These figures show that the system oscillates at a frequency equal to the corresponding running speed frequency and its integral multiples.

But Figs 4.65 and 4.66 show the spectrum plot and time plot for speed of 1100 rev/min and this is the first speed where the subharmonic appears at 9.166 rev/s, it can be seen that the system oscillates at the subharmonic and its integral multiples. Figs 4.67 and 4.68 also show that the system oscillates at subharmonic and its integral multiples,for the speed of 1400 rev/min. While Figs 4.69 and 4.70 show the spectrum plot and time plot for speed of 1700 rev/min, the system was also found to oscillate at a subharmonic corresponding to half the speed and its integral multiples. It can be noticed that the subharmonic oscillation is getting weaker at this speed with a loading of 5.424 N m (4.0 lbf.ft). Finally Figs 4.71 and 4.72 show that the system oscillates at the first harmonic corresponding to rotational speed of 1900 rev/min (31.66 rev/s) and its integral multiples. The subharmonic does not appear for this value of loading and speed.

Fig 4.57 Frequency Response for 250 rev/min (4.16 rev/s)

Loading = 5.424 N m (4.0 1bf.ft)

Cut-off Frequency = 180 Hz

Fig 4.58 Time Response for 250 rev/min (4.16 rev/s)

Loading = 5.424 N m (4.0 lbf.ft)

Cut-off Frequency = 2 K

Fig 4.59 Frequency Response for 600 rev/min (10 rev/s)
        Loading = 5.424 N m (4.0 lbf.ft)
        Cut-off Frequency = 180 Hz

Fig 4.60 Time Response for 600 rev/min (10 rev/s)

Loading = 5.424 N m (4.0 lbf.ft)

Cut-off Frequency = 1 K

Fig 4.61 Frequency Response for 850 rev/min (14.16 rev/s)

Loading = 5.424 N m (4.0 lbf.ft)

Cut-off Frequency = 180 Hz

Fig 4.62 Time Response for 850 rev/min (14.16 rev/s),(1 rev≡70.6 ms)

Loading = 5.424 N m (4.0 lbf.ft)

Cut-off Frequency = 1 K

Fig 4.63 Frequency Response for 900 rev/min (15 rev/s)

Loading = 5.424 N m (4.0 1bf.ft)

Cut-off Frequency = 180 Hz

Fig 4.64 Time Response for 900 rev/min (15 rev/s), (1 rev≡66.66 ms)

Loading = 5.424 N m (4.0 lbf.ft)
Cut-off Frequency = 1 K

Fig 4.65 Frequency Response for 1100 rev/min (18.33 rev/s)

Loading = 5.424 N m (4.0 lbf.ft)

Cut-off Frequency = 180 Hz

Fig 4.66 Time Response for 1100 rev/min (18.33 rev/s),(1 rev=54.54 ms)
Loading = 5.424 N m (4.0 lbf.ft)
Cut-off Frequency = 1 K

Fig 4.67 Frequency Response for 1400 rev/min (23.33 rev/s)
Loading = 5.424 N m (4.0 lbf.ft)
Cut-off Frequency = 180 Hz

Fig 4.68 Time Response for 1400 rev/min (23.33 rev/s),(1 rev≡42.8 ms)
        Loading = 5.424 N m (4.0 lbf.ft)
        Cut-off Frequency = 1 K

2 revs ≡ 85.6 ms

10⁻⁴ SEC

-131-

Fig 4.69 Frequency Response for 1700 rev/min (28.33 rev/s)

Loading = 5.424 N m (4.0 1bf.ft)

Cut-off Frequency = 180 Hz

10 ^{1} V

1 rev ≡ 35.3 ms

Fig 4.70 Time Response for 1700 rev/min (28.33 rev/s),(1 rev≡35.3 ms)

Loading = 5.424 N m (4.0 lbf.ft)

Cut-off Frequency = 1 K

10 $^{-4}$ SEC

Fig 4.71 Frequency Response for 1900 rev/min (31.66 rev/s)

Loading = 5.424 N m (4.0 lbf.ft)

Cut-off Frequency = 180 Hz

-134-

Fig 4.72 Time Response for 1900 rev/min (31.66 rev/s), (1 rev≡31.58 ms)

Loading = 5.424 N m (4.0 lbf.ft)

Cut-off Frequency = 1 K
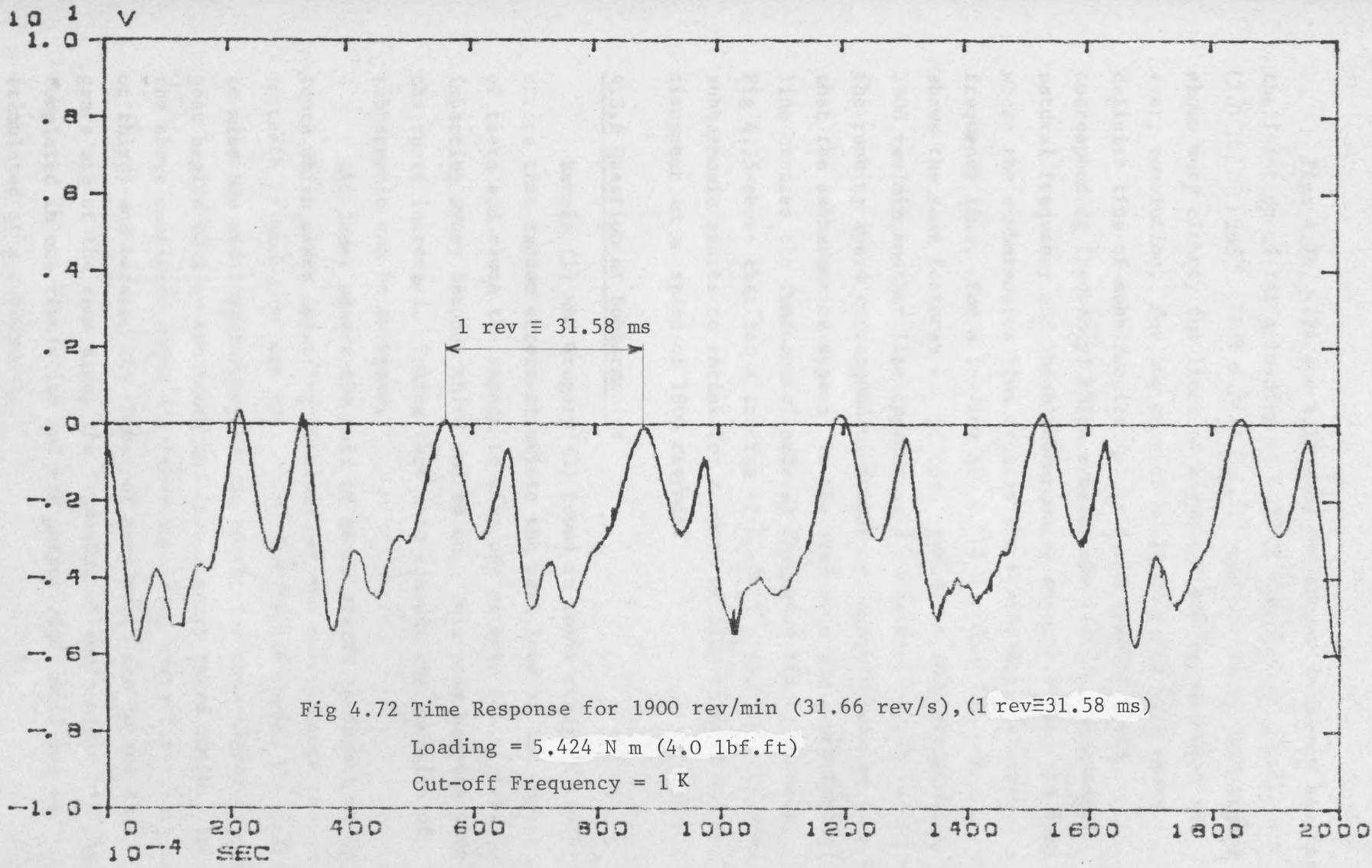
Figs 4.73, 4.74 and 4.75 show the output frequency against the input speed for a loading of 0.0 N m (0.0 lbf.ft), 2.712 N m (2.0 lbf.ft) and 5.424 N m (4.0 lbf.ft) respectively, each figure shows very clearly the lines of harmonics and subharmonics in every revolution. For the case of no loading Fig 4.73 shows a definite line of subharmonics (at half the running speed corresponding frequency) which crosses the line of fundamental natural frequency and these subharmonics appears around the area where the subharmonics line crosses the fundamental natural frequency line. For a loading of 2.712 N m (2.0 lbf.ft), Fig. 4.74 shows the same features except for speeds of 1000 rev/min and 1900 rev/min another line appears at a subharmonic which is 1/3 of the running speed corresponding frequency. Again it can be seen that the subharmonics appear in the area when the subharmonics line crosses the fundamental natural frequency line. Finally, Fig 4.75 shows that for a loading of 5.424 N m (4.0 lbf.ft) the subharmonic starts to shrink for a speed of 1700 rev/min and to disappear at a speed of 1900 rev/min.

4.3.6 Question of Subharmonic:

Harris (1) and Gregory (3) found in their study of tooth errors that random errors stimulate the peak load of the impact of teeth and cause the impact to miss one or more teeth; i.e. impacting every second, third and so on. This only happens when the speed increases. Taking that into account the question of subharmonic can be answered.

At lower speeds the pair of gears starts to impact every tooth which means impacting 30 times per one rev.(because the number of teeth in each gear are 30).   For higher speeds the gear begins to miss one and impact every second tooth, for even higher speeds the gear begins to miss two teeth and impact every third tooth. In all the above mentioned cases (the gear impacting every first, second, or third) and because the number of gear teeth are 30 and the gears are of the same size, the impacting of tooth cycle will be completed in one revolution and the output shaft will not be stimulated at a subharmonic.
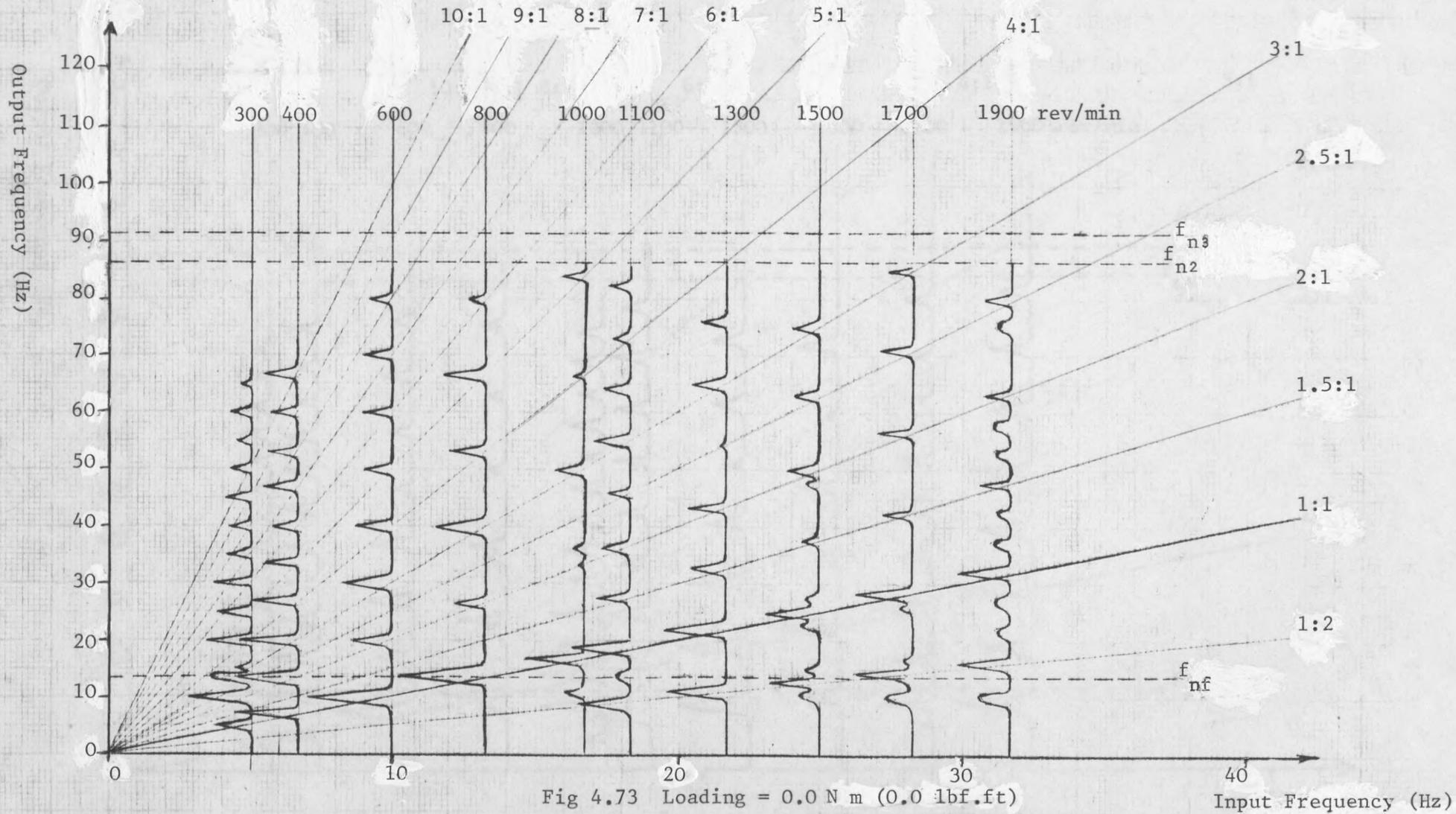
Fig 4.73 Loading = 0.0 N m (0.0 lbf.ft)

-137-
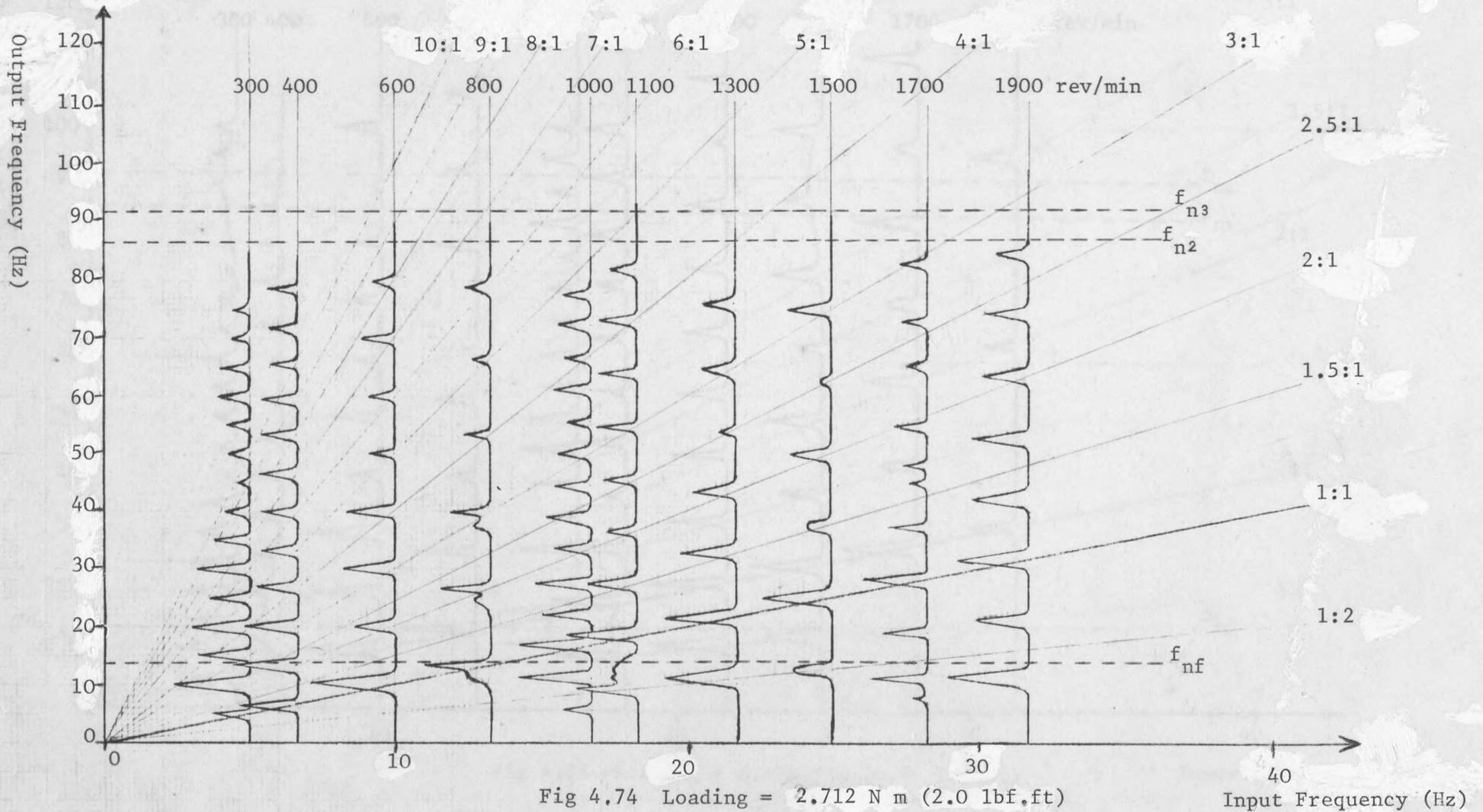
Fig 4.74   Loading = 2.712 N m (2.0 lbf.ft)

Output Frequency (Hz)

Input Frequency (Hz)

10:1 9:1 8:1 7:1   6:1   5:1   4:1   3:1

2.5:1

2:1

1.5:1

1:1

1:2

300 400   600   800 1000 1100   1300   1500   1700   1900 rev/min

f_{n3}

f_{n2}

f_{nf}

-138-

Fig 4.75   Loading = 5.424 N m. (4.0 lbf.ft)

Input Frequency (Hz)
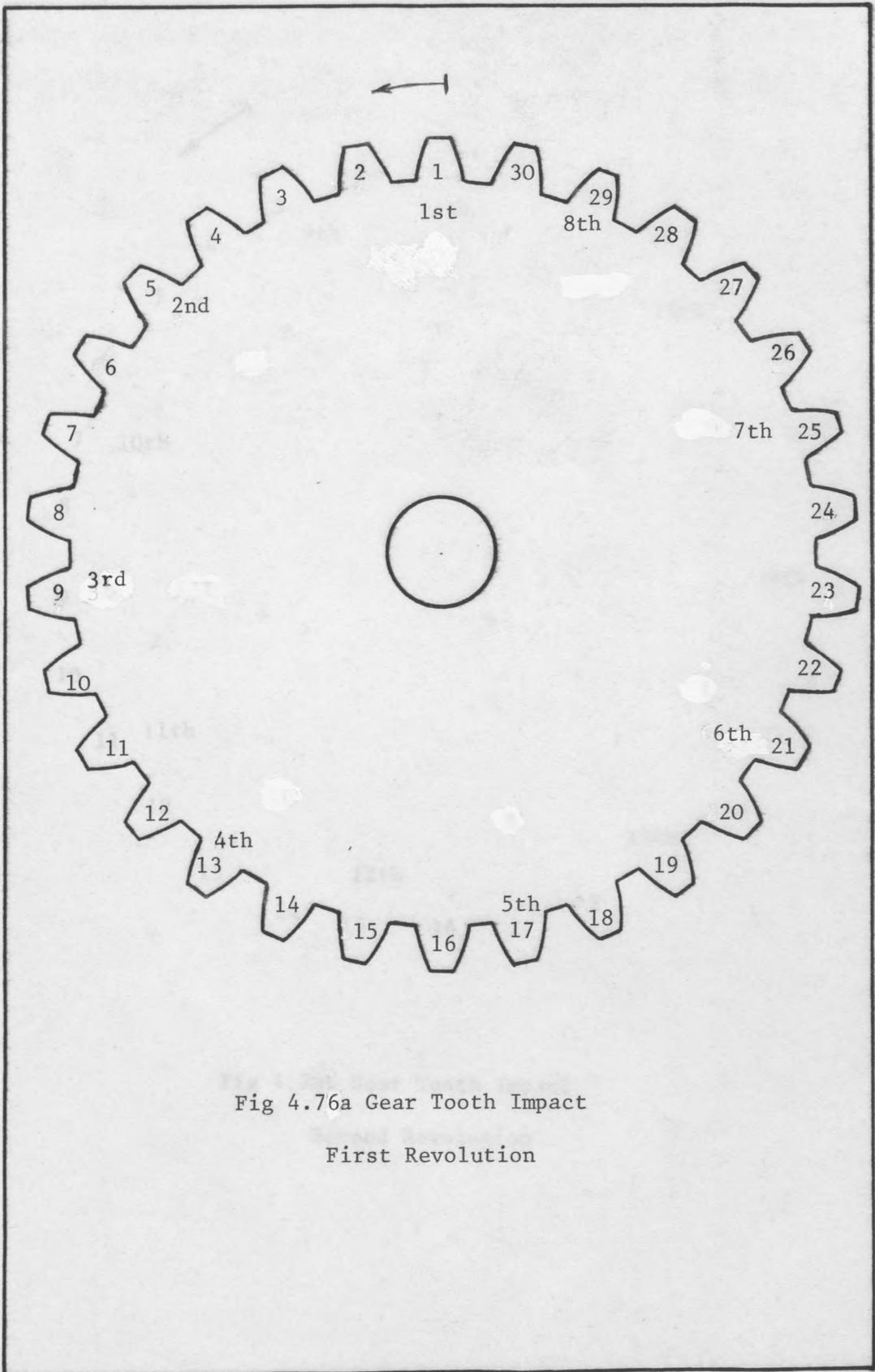
Fig 4.76a Gear Tooth Impact

First Revolution
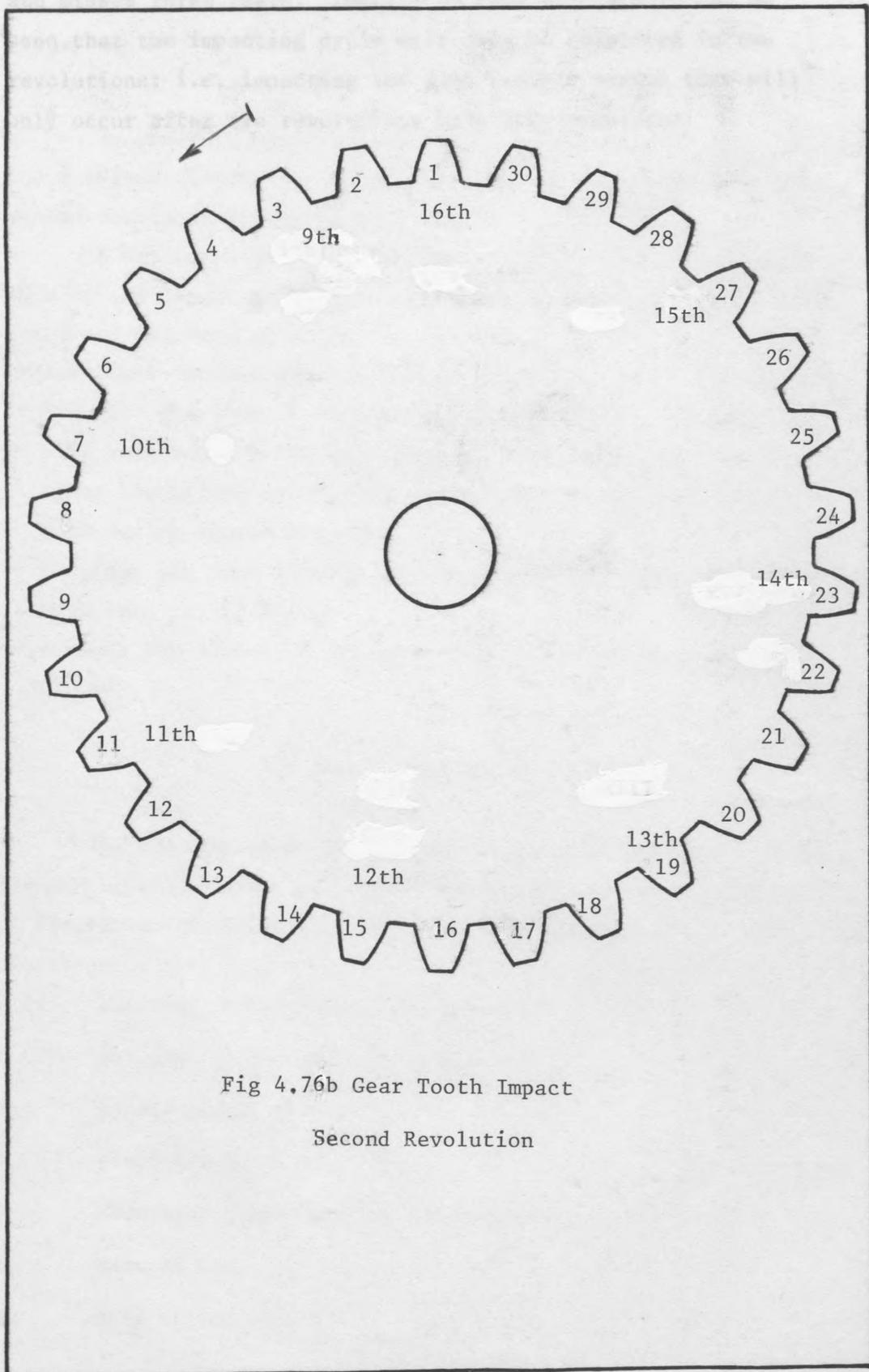
Fig 4.76b Gear Tooth Impact

Second Revolution

At even higher speed the gear impacts every fourth tooth and misses three teeth. Looking at Figs 4.76 a,b it can be seen that the impacting cycle will only be completed in two revolutions; i.e. impacting the same tooth a second time will only occur after two revolutions have been completed.

V. THEORETICAL ANALYSIS AND SYSTEM MODELLING

5.1 Introduction

In order to reproduce the experimental results described in the previous chapter a simulation study was worked out for the geared torsional system in hand.

A mathematical model was developed to take into account some of the important factors affecting the system in this study. The model was developed to:

1- Take into account the inertias and stiffnesses of the system.

2- Simulate the loss of contact and the impact phenomenon.

3- Take into account the effect of backlash variation or some times the effect of stiffness variation of the gear teeth in mesh during system rotation.

4- Consider the load (steady or variable) at the gear pair or at both ends of the drive.

5- Include the effect of friction (i.e. damping) throughout the system.

5.2 Impact Pair Model

The discussion in chapter (I) shows that Dubowsky (28,29) has developed an impact pair model to investigate the dynamic effect of clearances on mechanical system. This model is shown in Fig 5.1, where:

$F_2(t)$ external force applied to mass M_2.

$F_3(t)$ external force applied to mass M_3.

X_2 displacement of mass M_2.

X_3 displacement of mass M_3

B   clearance (backlash for gears model).

M_2 mass of body 2.

M_3 mass of body 3.
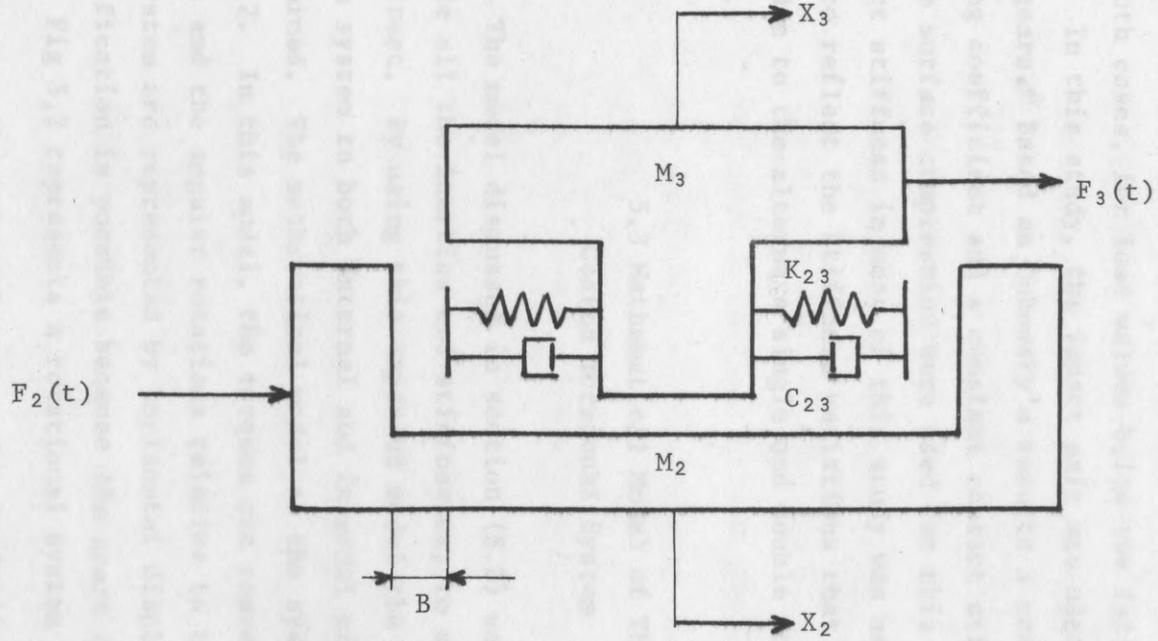
Fig 5.1 Impact Pair Model

C_{23} contact viscous damping.

K_{23} Contact stiffness.

Dubowsky has shown that the impact pair model yields a unique solution while exhibiting nonlinear behaviour common to complex mechanical systems with clearances. He has investigated the Hertzian contact characteristics of the ball joint and pin joint and has found that a linear approximation for the contact stiffness results in an adequate representation of the impact phenomenon for both cases, for load values below the fatigue limit.

In this study, the impact pair was used to represent the spur gears. Based on Dubowsky's results a constant viscous damping coefficient and a constant contact stiffness with respect to the surface compression were used for this study. However, the contact stiffness in most of this study was assumed to vary with time to reflect the stiffness variations that occur in the gear mesh due to the alternate single and double contact of the gear teeth.

5.3 Mathematical Model of The
Geared Torsional System

The model discussed in section (5.2) was expanded to include all the inertias and stiffnesses, to simulate the system under test. By using this expanded model the response of the entire system to both external and internal effects can be determined. The mathematical model of the system is shown in Fig 5.2. In this model, the torques are represented by horizontal forces and the angular rotations relative to the mean rotation of the system are represented by horizontal displacements. A further simplification is possible because the gears are equal in size.

Fig 5.2 represents a rotational system where:

$F_1(t)$ the external torque due to driving motor.

$F_2(t), F_3(t)$ the torque effects of the driving and driven gears

                   due to gear teeth errors.

$F_5(t)$ the load torque representing the Eddy Current Brake.

M_1 the moment of inertia of the driving motor.

M_2 the moment of inertia of the fixed mass and the driving gear.

M_3 the moment of inertia of the driven gear.

M_4 the moment of inertia of the movable mass (to shift the natural frequency when needed).

M_5 the moment of inertia of the Eddy Current Brake.

X_1 the displacement of the mass M_1.

X_2 the displacement of the mass M_2.

X_3 the displacement of the mass M_3.

X_4 the displacement of the mass M_4.

X_5 the displacement of the mass M_5.

$2B$ the angular backlash between the gears in mesh.

C_{12} the equivalent viscous damping coefficient of the input shaft.

C_{23} the equivalent viscous damping coefficent of the gear teeth.

C_{34} the equivalent viscous damping coefficent of the shaft between the driven gear (M_3) and the movable mass (M_4).

C_{45} the equivalent viscous damping coefficent of the shaft between the movable mass (M_4) and the Eddy Current Brake (M_5).

K_{12} the stiffness of the input shaft.

$K_{23}(t)$ time-varying stiffness of the gear teeth.

K_{34} the stiffness of the shaft between M_3 and M_4.

K_{45} the stiffness of the shaft between M_4 and M_5.

F_{XT} the torque transmitted through the gears.
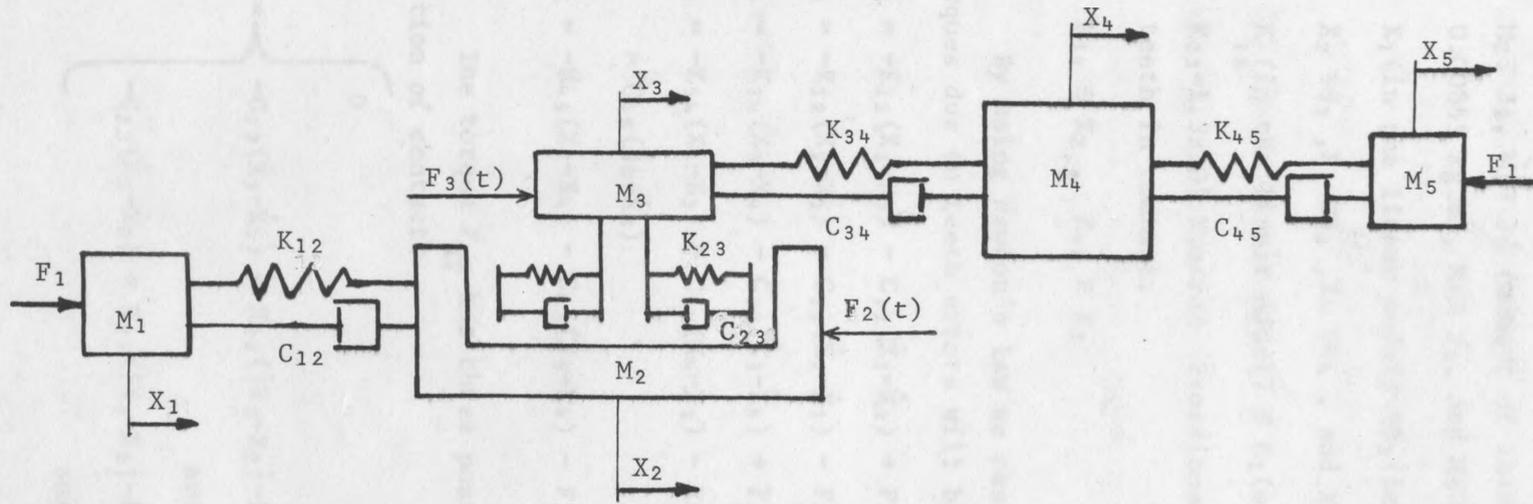
Fig 5.2 Model of Torsional Geared System

Bearing in mind that:

1)- M_1 (in the linear model) $\equiv J_1$ (in the torsional system),

   $M_2 \equiv J_2$, $M_3 \equiv J_2'$ (moment of inertia of the driven gear)= 0.00865 kg.m^2, $M_4 \equiv J_3$, and $M_5 \equiv J_4$.

2)- X_1 (in the linear model) $\equiv \theta_1$ (in the torsional system),

   $X_2 \equiv \theta_2$, $X_3 \equiv \theta_3$, $X_4 \equiv \theta_4$, and $X_5 \equiv \theta_5$.

3)- $\underset{12}{K}$ (in the linear model) $\equiv K_1$ (stiffness of the input shaft)

   $K_{23} = 1.3 \times 10^6$ N.m/rad $\equiv$ torsional stiffness of a pair of teeth in contact.

   $K_{34} \equiv K_2$, $K_{45} \equiv K_3$

   By using Newton's law we can write the equations of motion, (torques due to teeth errors will be neglected).

$$M_1 \ddot{X}_1 = -K_{12}(X_1-X_2) - C_{12}(\dot{X}_1-\dot{X}_2) + F_1 \tag{5.1}$$

$$M_2 \ddot{X}_2 = -K_{12}(X_2-X_1) - C_{12}(\dot{X}_2-\dot{X}_1) - F_{XT} \tag{5.2}$$

$$M_3 \ddot{X}_3 = -K_{34}(X_3-X_4) - C_{34}(\dot{X}_3-\dot{X}_4) + F_{XT} \tag{5.3}$$

$$M_4 \ddot{X}_4 = -K_{34}(X_4-X_3) - C_{34}(\dot{X}_4-\dot{X}_3) - K_{45}(X_4-X_5)$$
$$- C_{45}(\dot{X}_4-\dot{X}_5) \tag{5.4}$$

$$M_5 \ddot{X}_5 = -K_{45}(X_5-X_4) - C_{45}(\dot{X}_5-\dot{X}_4) - F_1 \tag{5.5}$$

   The torque F_{XT} has three possible values depending on the position of contact.

$$F_{XT} = \begin{cases} 0 & |X_3-X_2| < B \\[2ex] -C_{23}(\dot{X}_3-\dot{X}_2) - K_{23}(|X_3-X_2|-B) \; ; & |X_3-X_2| \geqslant B \\ & \text{and} \quad X_3-X_2 > 0 \\[2ex] -C_{23}(\dot{X}_3-\dot{X}_2) + K_{23}(|X_3-X_2|-B) \; ; & |X_3-X_2| \geqslant B \\ & \text{and} \quad X_3-X_2 < 0 \end{cases} \tag{5.6}$$

Dividing each equation by its mass to find the accelerations, we get:

$$\ddot{X}_1 = -\omega_1^2 (X_1 - X_2) - 2\zeta_1\omega_1 (\dot{X}_1 - \dot{X}_2) + \frac{F_1}{M_1} \tag{5.7}$$

$$\ddot{X}_2 = -\omega_2'^2 (X_2 - X_1) - 2\zeta_2'\omega_2' (\dot{X}_2 - \dot{X}_1) - \frac{F_{XT}}{M_2} \tag{5.8}$$

$$\ddot{X}_3 = -\omega_3^2 (X_3 - X_4) - 2\zeta_3\omega_3 (\dot{X}_3 - \dot{X}_4) + \frac{F_{XT}}{M_3} \tag{5.9}$$

$$\ddot{X}_4 = -\omega_4'^2 (X_4 - X_3) - 2\zeta_4'\omega_4' (\dot{X}_4 - \dot{X}_3) - \omega_4^2 (X_4 - X_5)$$

$$\quad -2\zeta_4\omega_4 (\dot{X}_4 - \dot{X}_5) \tag{5.10}$$

$$\ddot{X}_5 = -\omega_5^2 (X_5 - X_4) - 2\zeta_5\omega_5 (\dot{X}_5 - \dot{X}_4) - \frac{F_1}{M_5} \tag{5.11}$$

Where;

$$\omega_1^2 = \frac{K_{12}}{M_1} \tag{5.12}$$

$$\omega_2'^2 = \frac{K_{12}}{M_2} \tag{5.13}$$

$$\omega_2^2 = \frac{K_{23}}{M_2} \tag{5.14}$$

$$\omega_3^2 = \frac{K_{34}}{M_3} \tag{5.15}$$

$$\omega_3'^2 = \frac{K_{23}}{M_3} \tag{5.16}$$

$$\omega_4'^2 = \frac{K_{34}}{M_4} \tag{5.17}$$

$$\omega_4^2 = \frac{K_{45}}{M_4} \tag{5.18}$$

$$\omega_5^2 = \frac{K_{45}}{M_5} \tag{5.19}$$

$$\zeta_1 = \frac{C_{12}}{2M_1\omega_1} = \frac{C_{12}\omega_1}{2M_2\omega_2'^2} = \zeta_2'\sqrt{\frac{M_2}{M_1}} = 0.008 \tag{5.20}$$

$$\zeta_2 = \zeta_3'\sqrt{\frac{M_3}{M_2}} = 0.1 \tag{5.21}$$

$$\zeta_3 = \zeta_4'\sqrt{\frac{M_4}{M_3}} = 0.01 \tag{5.22}$$

$$\zeta_4 = \zeta_5\sqrt{\frac{M_5}{M_4}} = 0.0018 \tag{5.23}$$

Where $\zeta_1, \zeta_2, \zeta_3$ and ζ_4 represent convenient ratios (as described above) related to the system damping

5.4.1 Introduction:

The mathematical model obtained in the previous section as a set of equations (5.7 - 5.11) will form a set of coupled, second order, nonlinear differential equations with time-varying coefficients.

The exact solution obtained by Dubowsky (28) for a linearized two mass model, is clearly not possible.

5.4.2 Subroutines:

Fig 5.3 shows the three possible positions of the gear (M_3) with respect to the gear (M_2) when the gears start to oscillate. These positions are as follow :

1- The tooth floating between the R.H.S. and L.H.S.

2- The tooth touching the right hand side.

3- The tooth touching the left hand side.

The five equations of motion (5.7 - 5.11), according to the three possible positions, will become three sets of equations. Each set includes five equations of motion. These equations of motion will be used in the main computer programme as subroutines. After small mathematical operations each set of equations will became a sub-routine and will be called as: FCN1, FCN2, FCN3. A detailed description of how this subroutine will be used in the main programme is shown in section (5.4.3).

The three sets of equations (or subroutines) are:

1) FCN1 : (F_{XT} =0)

$$\ddot{X}_1 = -\omega_1^2 (X_1-X_2) - 2\zeta_1\omega_1 (\dot{X}_1-\dot{X}_2) + \frac{F_1}{M_1} \qquad (5.24)$$

$$\ddot{X}_2 = -\omega_2^2 (X_2-X_1) - 2\zeta_2'\omega_2' (\dot{X}_2-\dot{X}_1) \qquad (5.25)$$

$$\ddot{X}_3 = -\omega_3^2 (X_3-X_4) - 2\zeta_3\omega_3 (\dot{X}_3-\dot{X}_4) \qquad (5.26)$$

$$\ddot{X}_4 = -\omega_4'^2 (X_4-X_3) - 2\zeta_4'\omega_4' (\dot{X}_4-\dot{X}_3) - \omega_4^2 (X_4-X_5)$$

$$\qquad - 2\zeta_4\omega_4 (\dot{X}_4-\dot{X}_5) \qquad (5.27)$$

$$\ddot{X}_5 = -\omega_5^2 (X_5-X_4) - 2\zeta_5\omega_5 (\dot{X}_5-\dot{X}_4) - \frac{F_1}{M_5} \qquad (5.28)$$
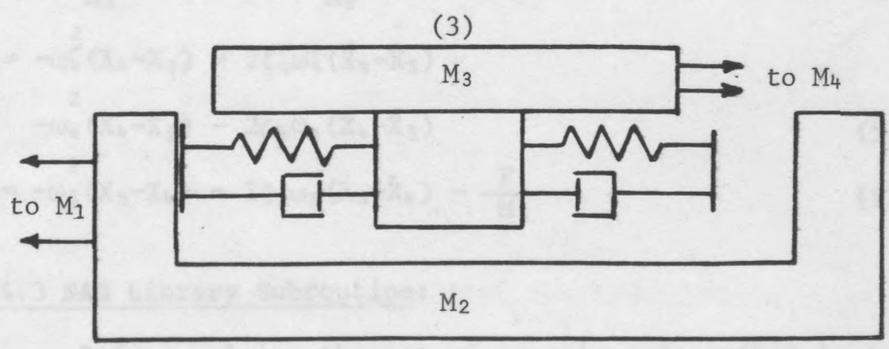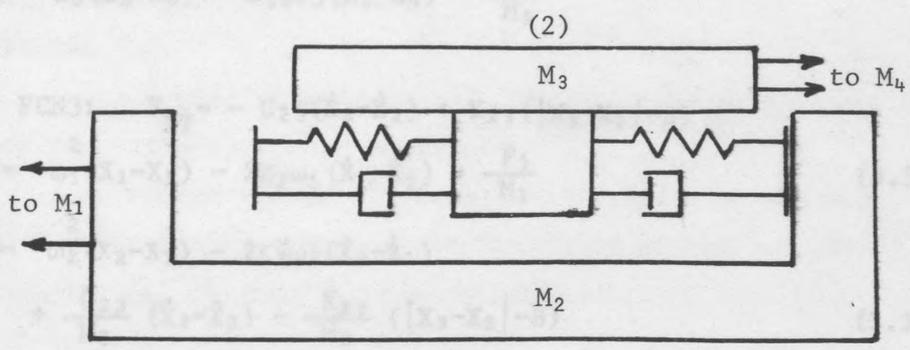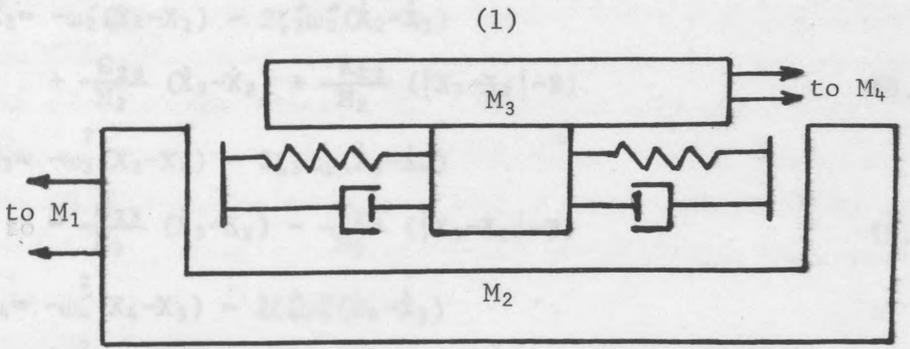
Fig 5.3 Positions of Tooth on M_3 Relative to M_2

2) FCN2: $F_{XT} = -C_{23}(\dot{X}_3 - \dot{X}_2) - K_{23}(|X_3 - X_2| - B)$

$$\ddot{X}_1 = -\omega_1^2(X_1 - X_2) - 2\zeta_1\omega_1(\dot{X}_1 - \dot{X}_2) + \frac{F_1}{M_1} \qquad (5.29)$$

$$\ddot{X}_2 = -\omega_2^2(X_2 - X_1) - 2\zeta_2\omega_2(\dot{X}_2 - \dot{X}_1)$$
$$+ \frac{C_{23}}{M_2}(\dot{X}_3 - \dot{X}_2) + \frac{K_{23}}{M_2}(|X_3 - X_2| - B) \qquad (5.30)$$

$$\ddot{X}_3 = -\omega_3^2(X_3 - X_4) - 2\zeta_3\omega_3(\dot{X}_3 - \dot{X}_4)$$
$$- \frac{C_{23}}{M_3}(\dot{X}_3 - \dot{X}_2) - \frac{K_{23}}{M_3}(|X_3 - X_2| - B) \qquad (5.31)$$

$$\ddot{X}_4 = -\omega_4^2(X_4 - X_3) - 2\zeta_4\omega_4(\dot{X}_4 - \dot{X}_3)$$
$$-\omega_4^2(X_4 - X_5) - 2\zeta_4\omega_4(\dot{X}_4 - \dot{X}_5) \qquad (5.32)$$

$$\ddot{X}_5 = -\omega_5^2(X_5 - X_4) - 2\zeta_5\omega_5(\dot{X}_5 - \dot{X}_4) - \frac{F_1}{M_5}$$

3) FCN3: $F_{XT} = -C_{23}(\dot{X}_3 - \dot{X}_2) + K_{23}(|X_3 - X_2| - B)$

$$\ddot{X}_1 = -\omega_1^2(X_1 - X_2) - 2\zeta_1\omega_1(\dot{X}_1 - \dot{X}_2) + \frac{F_1}{M_1} \qquad (5.34)$$

$$\ddot{X}_2 = -\omega_2^2(X_2 - X_1) - 2\zeta_2\omega_2(\dot{X}_2 - \dot{X}_1)$$
$$+ \frac{C_{23}}{M_2}(\dot{X}_3 - \dot{X}_2) - \frac{K_{23}}{M_2}(|X_3 - X_2| - B) \qquad (5.35)$$

$$\ddot{X}_3 = -\omega_3^2(X_3 - X_4) - 2\zeta_3\omega_3(\dot{X}_3 - \dot{X}_4)$$
$$- \frac{C_{23}}{M_3}(\dot{X}_3 - \dot{X}_2) + \frac{K_{23}}{M_3}(|X_3 - X_2| - B) \qquad (5.36)$$

$$\ddot{X}_4 = -\omega_4^2(X_4 - X_3) - 2\zeta_4\omega_4(\dot{X}_4 - \dot{X}_3)$$
$$-\omega_4^2(X_4 - X_5) - 2\zeta_4\omega_4(\dot{X}_4 - \dot{X}_5) \qquad (5.37)$$

$$\ddot{X}_5 = -\omega_5^2(X_5 - X_4) - 2\zeta_5\omega_5(\dot{X}_5 - \dot{X}_4) - \frac{F_1}{M_5} \qquad (5.38)$$

5.4.3 NAG Library Subroutine:

Before solving the set of equations described in section
5.4.2 one has to classify the equations. The equations of motion
(5.7-5,11)are; second order, nonlinear differential equations.
But after deriving the three sets of equations from the position
of the mass M_2 relative to M_3 each set will become a set of second order
linear differential equations; this means that the sets of equations
(5.24-5.28), (5.29-5.33), and (5.34-5.38) will be considered as

second order linear differential equations.

The solution of these equations becomes easier, by finding
a way of solving the differential equations. There are many
available subroutines in the computer library which is known as the
NAG Library. More than one routine was tried before deciding on
the present subroutine; the subroutine used was DO2EAF. The
purpose of this routine is to integrate a stiff system of first
order differential equations over a range with suitable initial
conditions using a variable-order variable-step Gear method. The
subroutine was of the form:

SUBROUTINE DO2EAF (T,TEND,N,X,TOL,FCN,W,IW,IFAIL)

INTEGER N, IW,IFAIL

REAL TOL,T,TEND,X(N),W(N,IW)

EXTERNAL FCN

App.F will show in detail how this subroutine was used and
what the parameters used represent.

To reduce the second order differential equation to first
order differential equation the following change in variables will
be used: (as required by the subroutine).

$$F_1 = \dot{X}_1 = X_6$$
$$F_2 = \dot{X}_2 = X_7$$
$$F_3 = \dot{X}_3 = X_8$$
$$F_4 = \dot{X}_4 = X_9$$
$$F_5 = \dot{X}_5 = X_{10}$$

And to avoid using the same index for two different variables the
second first derivative will take a new sequence which is:

$$F_6 = \ddot{X}_1$$
$$F_7 = \ddot{X}_2$$
$$F_8 = \ddot{X}_3 \qquad \text{(By taking the first five indices for } \dot{X}_1, \dot{X}_2 \text{...\& so on)}$$
$$F_9 = \ddot{X}_4$$
$$F_{10} = \ddot{X}_5$$

This means each set of equations (5.24-5.28), (5.29-5.33), and
(5.34-5.38) will become a set consisting of (10) equations of
motion of first order, for example, the set of equations
(5.24-5.28) will be written as:

$$F_1 = X_6 \hspace{6cm} (5.39)$$

$$F_2 = X_7 \tag{5.40}$$

$$F_3 = X_8 \tag{5.41}$$

$$F_4 = X_9 \tag{5.42}$$

$$F_5 = X_{10} \tag{5.43}$$

$$F_6 = -\omega_1^2(X_1-X_2) - 2\zeta_1\omega_1(X_6-X_7) + \frac{F_1}{M_1} \tag{5.44}$$

$$F_7 = -\omega_2^2(X_2-X_1) - 2\zeta_2\omega_2(X_7-X_6) \tag{5.45}$$

$$F_8 = -\omega_3^2(X_3-X_4) - 2\zeta_3\omega_3(X_8-X_9) \tag{5.46}$$

$$F_9 = -\omega_4^2(X_4-X_3) - 2\zeta_4\omega_4(X_9-X_8) - \omega_4^2(X_4-X_5)$$
$$\qquad -2\zeta_4\omega_4(X_9-X_{10}) \tag{5.47}$$

$$F_{10} = -\omega_5^2(X_5-X_4) - 2\zeta_5\omega_5(X_{10}-X_9) - \frac{F_1}{M_5} \tag{5.48}$$

Taking the values of inertias and stiffnesses to obtain the ratios $\omega_1, \omega_2^2, \omega_2, \omega_3, \omega_3^2, \omega_4^2, \omega_4,$ & ω_5 & taking the values of the ratios $\zeta_1, \zeta_2, \zeta_3$ & ζ_4, then substituting these values into the three sets of equations (5.24-5.38) the following sets of equations were obtained:

FCN1: $(F_{XT}=0)$

$F(1) = X(6)$

$F(2) = X(7)$

$F(3) = X(8)$

$F(4) = X(9)$

$F(5) = X(10)$

$F(6) = -318784.45 * (X(1)-X(2)) - 9.03376 * (X(6)-X(7)) + \frac{F_1}{M_1}$

$F(7) = -14636.16 * (X(2)-X(1)) - 0.4162 * (X(7)-X(6))$

$F(8) = -300358.8 * (X(3)-X(4)) - 10.961 * (X(8)-X(9))$

$F(9) = -5772.96 * (X(4)-X(3)) - 0.2097 * (X(9)-X(8))$
$\qquad\quad -9621.648 * (X(4)-X(5)) - 0.3531 * (X(9)-X(10))$

$F(10) = -288680.54 * (X(5)-X(4)) - 10.5954 * (X(10)-X(9)) - \frac{F_1}{M_5}$

FCN2:

$F(1) = X(6)$

$F(2) = X(7)$

$F(3) = X(8)$

$F(4) = X(9)$

$F(5) = X(10)$

$F(6) = -318784.45 * (X(1)-X(2)) - 9.03376 * (X(6)-X(7)) + \dfrac{F_1}{M_5}$

$F(7) = -14636.16 * (X(2)-X(1)) - 0.4162 * (X(7)-X(6))$

$\qquad + 366197.98\ E1 * ((X(3)-X(2))-B) + 382.726 * (X(8)-X(7))$

$F(8) = -300358.8 * (X(3)-X(4)) - 10.961 * (X(8)-X(9))$

$\qquad - 150288.00\ E3 * ((X(3)-X(2))-B) - 15691.827 * (X(8)-X(7))$

$F(9) = -5772.96 * (X(4)-X(3)) - 0.2097 * (X(9)-X(8))$

$\qquad - 9621.648 * (X(4)-X(5)) - 0.3531 * (X(9)-X(10))$

$F(10) = -288680.54 * (X(5)-X(4)) - 10.5954 * (X(10)-X(9)) - \dfrac{F_1}{M_5}$

and finally:

FCN3:

$F(1) = X(6)$

$F(2) = X(7)$

$F(3) = X(8)$

$F(4) = X(9)$

$F(5) = X(10)$

$F(6) = -318784.45 * (X(1)-X(2)) - 9.03376 * (X(6)-X(7)) + \dfrac{F_1}{M_5}$

$F(7) = -14636.16 * (X(2)-X(1)) - 0.4162 * (X(7)-X(6))$

$\qquad - 366197.97\ E1 * ((X(2)-X(3))-B) + 382.726 * (X(8)-X(7))$

$F(8) = -300358.8 * (X(3)-X(4)) - 10.951 * (X(8)-X(9))$

$\qquad + 150288.00\ E3 * ((X(2)-X(3))-B) - 15691.827 * (X(8)-X(7))$

$F(9) = -5772.96 * (X(4)-X(3)) - 0.2097 * (X(9)-X(8))$

$\qquad - 9621.648 * (X(4)-X(5)) - 0.3531 * (X(9)-X(10))$

$F(10) = -288680.54 * (X(5)-X(4)) - 10.5954 * (X(10)-X(9)) - \dfrac{F_1}{M_5}$

Note that the values of inertias and stiffnesses are shown in
App.C and the value of tooth stiffness was taken from the graph in
ref.(40).

5.4.4 Programme Description:

The source programme is stored in a specially created user
file in the university Honeywell computer system. This programme
can be called   and executed using a remote control VDU terminal.

The principal feature of the source programme is a NAG
Library Subroutine for solving first order ordinary differential
equations using a variable order variable step Gear method.

A complete listing of the source programme used in this
study is shown in Fig 5.4. Statements numbered 40 through 120 define
the constants and parameters whose values are read in as input data.
Statements numbered 170 through 270 give the values of the input
data. Statements 290 through 380 represent the initial condition
for displacements and speeds. Statements 460 through 700 evaluate
the amount of shifting in each tooth depending on which side is the
contact. Statements 940 through 1670 define the three external
subroutines for which the solution should be found.

5.4.5 Numerical Tooth Shifting:

The main idea of shifting was to create an internal input
rather than external one which is the case for gears in mesh.

The tooth shifting was done assuming that contact was
established between one tooth from each gear; i.e. the contact
ratio is 1.0.

Assuming that the change which takes place is the change in
displacements X_2 and X_3 ; there are two cases:
1) When X_3 (on gear M_3) travels to the right hand side a distance
   bigger than the distance covered by X_2 (on gear M_2) and to
   consume all the backlash B_1 (i.e. $|X_3-X_2|>B_1$; $X_3-X_2>0$), and
   assuming that the tooth equivalent spring deflects an amount
   DX, then each spring ($K_{23}/2$) of the tooth on M_3 and of the tooth
   on M_2 will deflect an amount equals to $\frac{DX}{2}$, this only applies
   for the pair of teeth when they are in contact (see Fig 5.5).

   The next pair of teeth will begin contact as soon as
   the first pair leaves the area of contact and will not be
   deflected which means that the next pair of teeth will have the
   new displacements changed by an amount of $\frac{DX}{2}$:

$$X_{3_{new}} = X_{3_{old}} - \frac{DX}{2} \qquad \text{and} \qquad X_{2_{new}} = X_{2_{old}} + \frac{DX}{2}$$

2) When X_3 (on gear M_3) travels to the left hand side a distance
bigger than the distance covered by X_2 (on gear M_2) and to
consume all the backlash B_1 (i.e. $|X_3-X_2|>B_1$; $X_3-X_2<0$), and
assuming that the tooth equivalent spring deflects an amount
DX, then each spring ($K_{23}/2$) of the tooth on M_3 and of the
tooth on M_2 will deflect an amount equal to $\frac{DX}{2}$; this only
applies for the pair of teeth when they are in contact (see
Fig 5.6).

The next pair of teeth will begin contact as soon as the
first pair leaves the area of contact and will not be deflected
which means that the next pair of teeth will have the new
displacements changed by an amount of $\frac{DX}{2}$:

$$X_{3_{new}} = X_{3_{old}} + \frac{DX}{2} \qquad \text{and} \qquad X_{2_{new}} = X_{2_{old}} - \frac{DX}{2} \,.$$

Fig 5.5 Schematic Representation of Numerical Tooth Shift
when the First Tooth Contacts on the Right.
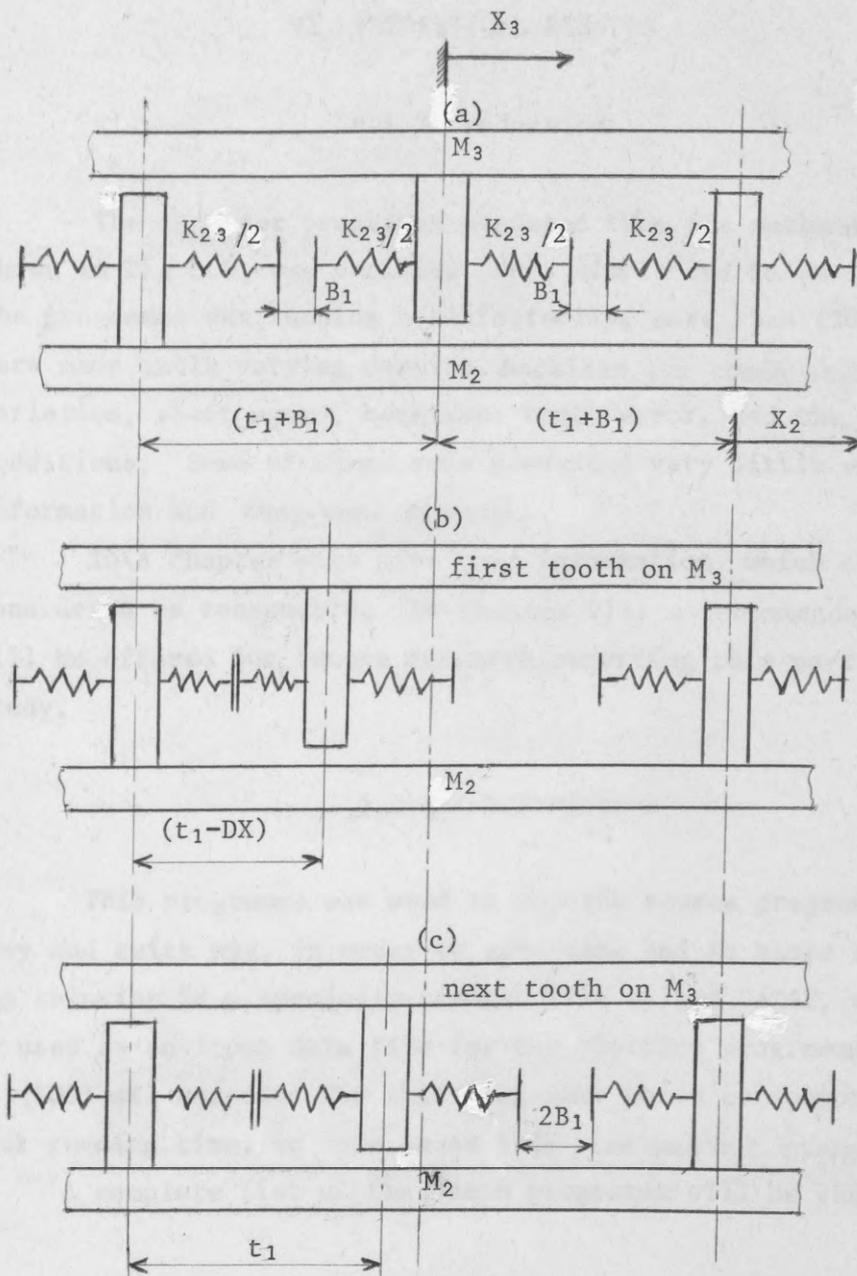
Fig 5.6 Schematic Representation of Numerical Tooth Shift
        when the First Tooth Contacts on the Left.

VI. THEORETICAL RESULTS

6.1 Introduction

The computer programme produced from the mathematical model shown in Fig 5.2, was verified for a simple and known input. When the programme was running satisfactorily, more than (200) runs were made while varying damping, backlash (or tooth stiffness) variation, shaft speed, backlash, tooth error, and the initial conditions. Some of these runs presented very little valuable information and they were ignored.

This chapter will give some information which could be considered as reasonable. In Chapter VIII a recommendation will be offered for future research regarding this part of the study.

6.2 Batch Programme

This programme was used to run the source programme in an easy and quick way, in order to save time and to store the resulting solution in a specially created file called DATAF, which will be used as an input data file for the plotting programme. A limit of (100) mil was used for this programme which corresponds to one hour running time, in some cases this time was not enough.

A complete list of the batch programme will be shown in App.G.

6.3 Plotting Programmes

6.3.1 Introduction:

Each time the source programme was run, the output which corresponds to certain input conditions was then stored in a specially created file to plot it and compare it with the experimental results obtained before as explained in chapter IV. Special programmes were used for plotting and observing the resulting data which was obtained by running the source programme.

6.3.2 Plotting on IMLAC:

This programme will read and plot the data from the DATAF file which stores the output of the source programme, then if required a plot can be obtained by pressing a special key required for transferring the graph on the screen to the printing machine. A list of this programme will be shown in App.H.

6.3.3. Plotting on Tektronix:

For quick plotting and observing the time signal obtained by solving the source programme, another programme was used to plot the results from the DATAF. This programme will be shown in App.I.

6.3.4 Plotting Direct from Computer:

A third plotting programme was also used to plot the solution of equations (5.24 - 5.38) on a bigger roll paper (size 1.0x3.0m app.) for better and clearer observation of the resulting graph. The programme list is in App.J.

6.4 Paper Tape Programme

For future analysis a paper tape programme can be used to record the source programme results on a standard 9 holes ASCII tape. This programme which is called "Punch" will be shown in App.H.

6.5 Computer Programme Results

6.5.1 Introduction:

The computer results which are presented in this part of the study are not complete and a recommendation is offered in chapter VII to continue the progress being made by the present method and to modify the idea of tooth shifting (which simulates the tooth meshing).

When the method of solving the differential equations representing the mathematical model used in chapter V was decided,

many subroutines were available and it was decided to use DO2EAF subroutine because this subroutine was the most suitable one in the author's opinion. There is a possibility that a more advanced method could be used to solve this numerically stiff system.

In this programme many factors and parameters could be varied, these include; damping, backlash, backlash variation, loading and speed.

There are two ways of including the effect of time variation during gear rotation; one is the stiffness variation and the other is the backlash variation. After trying both it was decided to use the backlash variation because the results obtained from this variation were more realistic. The function used to represent this variation is:

$$B(1-C_1 \cos \omega t) \; ; \; C_1 = 0.38$$

Another function was added to gears M_2 and M_3 to represent the forces due to errors which could exist in the gears, this function is:

$$F_2(t) = F_3(t) = -C_2 \cos \omega t - C_3 \cos 2\omega t$$

where ω represents the rotational speed frequency.

6.5.2 Time Response Results:

The first results (Figs 6.1 through 6.4) show that the mathematical model was working and could be applied to represent the system shown in Fig 5.2.

Fig 6.1 shows the system running at a speed of 200 rev/min, no damping, a circular backlash of 1.46 mm and a loading of 0.05 N m Fig 6.2 shows a time response plot without numerical tooth shift, no backlash and a loading of 0.05 N m. It can be seen that the system is running at a frequency equal to the calculated natural frequency of 17.84 Hz (or $T = \dfrac{1}{f} = 56$ ms). Also Fig 6.3 shows the same conditions as in Fig 6.2 but with numerical tooth shift every 2 ms. Fig 6.4 shows the time response for a speed of 1200 rev/min, backlash of 1.46mm and a loading of 5.0 N m. A subharmonic is clearly seen in this figure but the backlash is twice the value used in chapter IV (Experimental Results).

Figs 6.5 through 6.14 will have the same value of backlash as used in experimental study in Chapter IV, this backlash = 0.73 mm (or $\Delta C = 1.0$ mm)

Figs 6.5 and 6.6 show the time response for a speed of 200 rev/min and a loading of 1.0 N m and 2.0 N m respectively. A tooth shift of 2 ms has been used. It can be seen that a period of 300 ms (equivalent to 1 revolution for that speed) is apparent and no subharmonic was obtained for this low speed. Figs 6.7 and 6.8 show the time response for a speed of 1600 rev/min and a loading of 1.0 N m and 2.0 N m respectively. A shift of 2 ms has been used. It can be seen that for both loadings the system oscillates at a subharmonic of that speed. Figs 6.9 and 6.10 show the time response for a speed of 1200 rev/min and a loading of 1.5 N m and 5.0 N m respectively. A shift of 2 ms has been used. It is seen that for the lower loading the system oscillates at a subharmonic (half the running speed) while for the higher loading the system oscillates at a harmonic corresponding to the running speed, this is shown in Fig 6.10 where a period of $T = \dfrac{1}{f} = 50$ ms (corresponding to 1 revolution for that speed) is clearly marked which verifies the point made in Fig 4.75, that the subharmonic has disappeared for higher loading. Fig 6.11 shows the time response for a loading of 4.0 N m and a speed of 200 rev/min. A shift of 10 ms related to the speed and the number of teeth has been used. It can be seen that the system oscillates with a period of 300 ms corresponding to 1 revolution of the running speed. The shift related to the number of teeth (which equals 30 teeth) can be calculated as follows:

$$\text{Shift} = \frac{300 \text{ (period of 1 rev)}}{30 \text{ (number of teeth)}} = 10 \text{ ms}$$

Also Fig 6.12 shows the time response for a loading of 4.0 N m and a speed of 333.33 rev/min. A shift of 6 ms related to the speed and the number of teeth has been used. It can be seen that the system settled down to a period of 180 ms (corresponding to 1 revolution of that speed).

Finally, Figs 6.13 and 6.14 show the time response for speeds of 200 rev/min and 1000 rev/min respectively and constant loading of 1.7 N m. Each figure has a related shift of 10 ms (for 200 rev/min) and 2 ms (for 1000 rev/min). These results were

obtained by a slightly different approach from the previous ones and it is clearly seen that the relevant response was produced with no subharmonic for a lower speed and with subharmonic for a higher speed for these loading conditions.

Because of some numerical difficulties the results obtained were limited. One of the main difficulties in the present method is the time step used for the integration inside the subroutines which solves the set of differential equations. A smaller time step was needed to overcome this problem and this was sometimes not possible because the small time step could cause instability in the system.
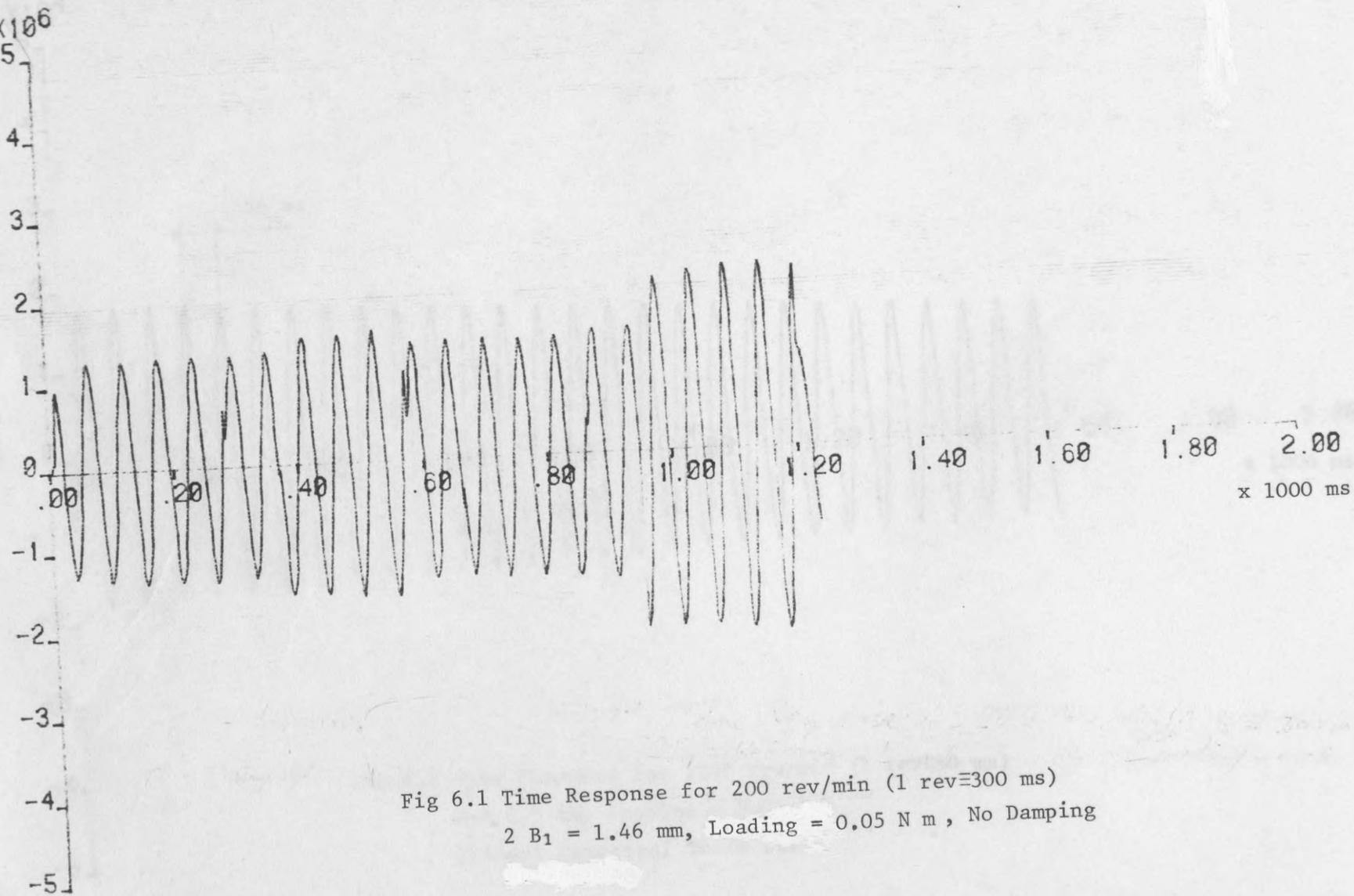
Fig 6.1 Time Response for 200 rev/min (1 rev≡300 ms)

2 B_1 = 1.46 mm, Loading = 0.05 N m , No Damping
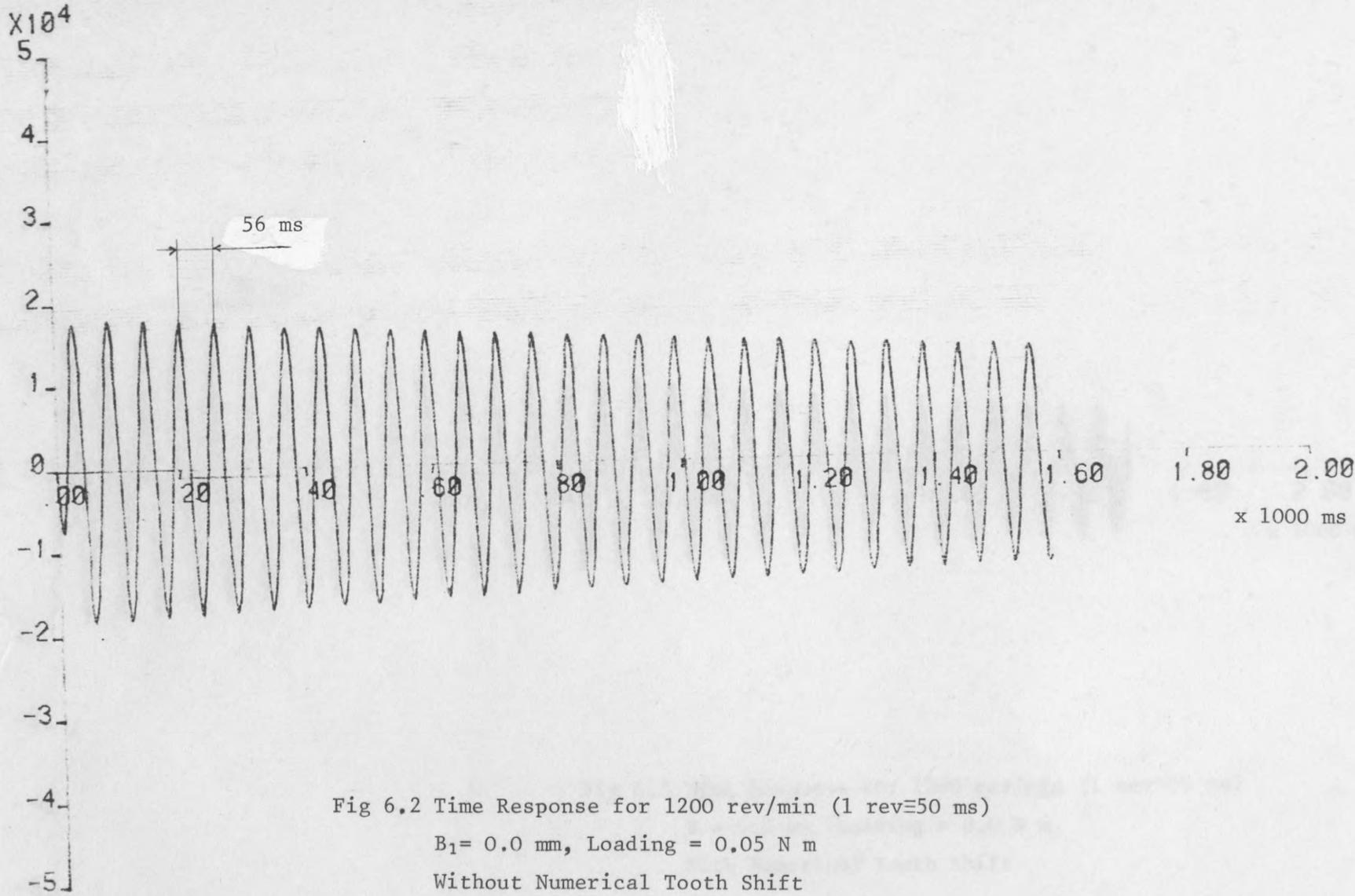
Fig 6.2 Time Response for 1200 rev/min (1 rev≡50 ms)
B_1= 0.0 mm, Loading = 0.05 N m
Without Numerical Tooth Shift
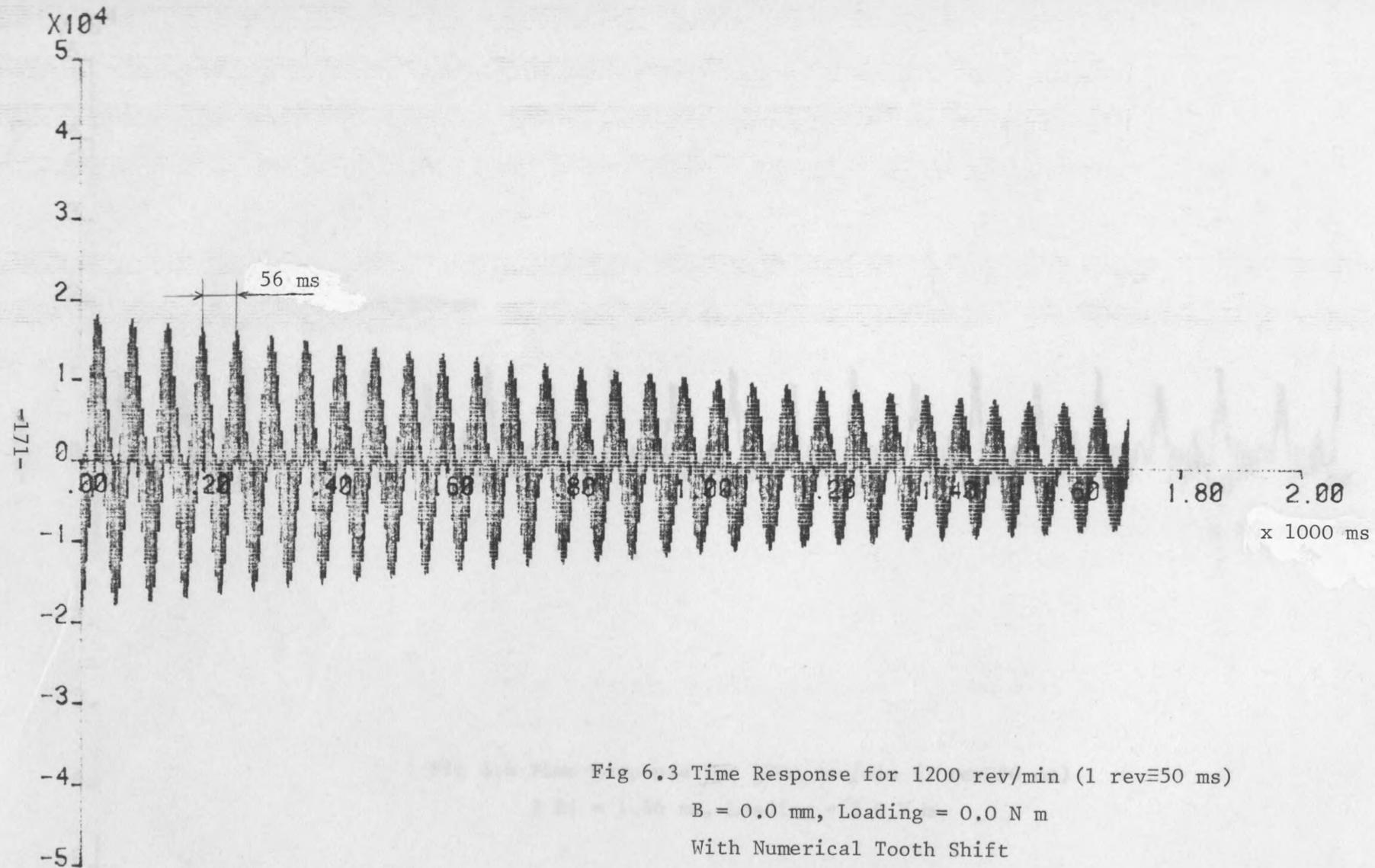
Fig 6.3 Time Response for 1200 rev/min (1 rev≡50 ms)

B = 0.0 mm, Loading = 0.0 N m

With Numerical Tooth Shift
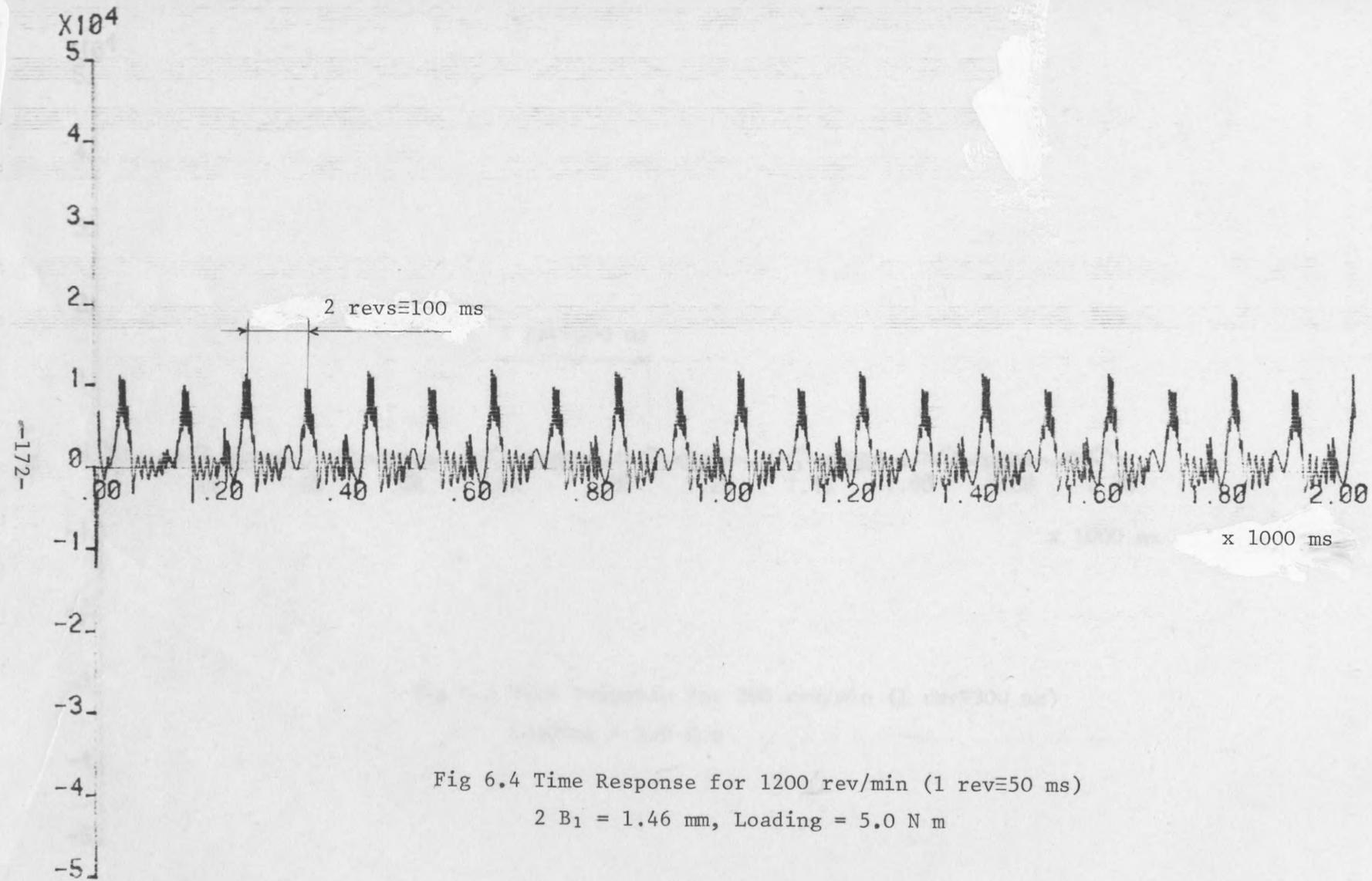
Fig 6.4 Time Response for 1200 rev/min (1 rev≡50 ms)
2 B₁ = 1.46 mm, Loading = 5.0 N m

X10^4

1 rev≡300 ms

x 1000 ms
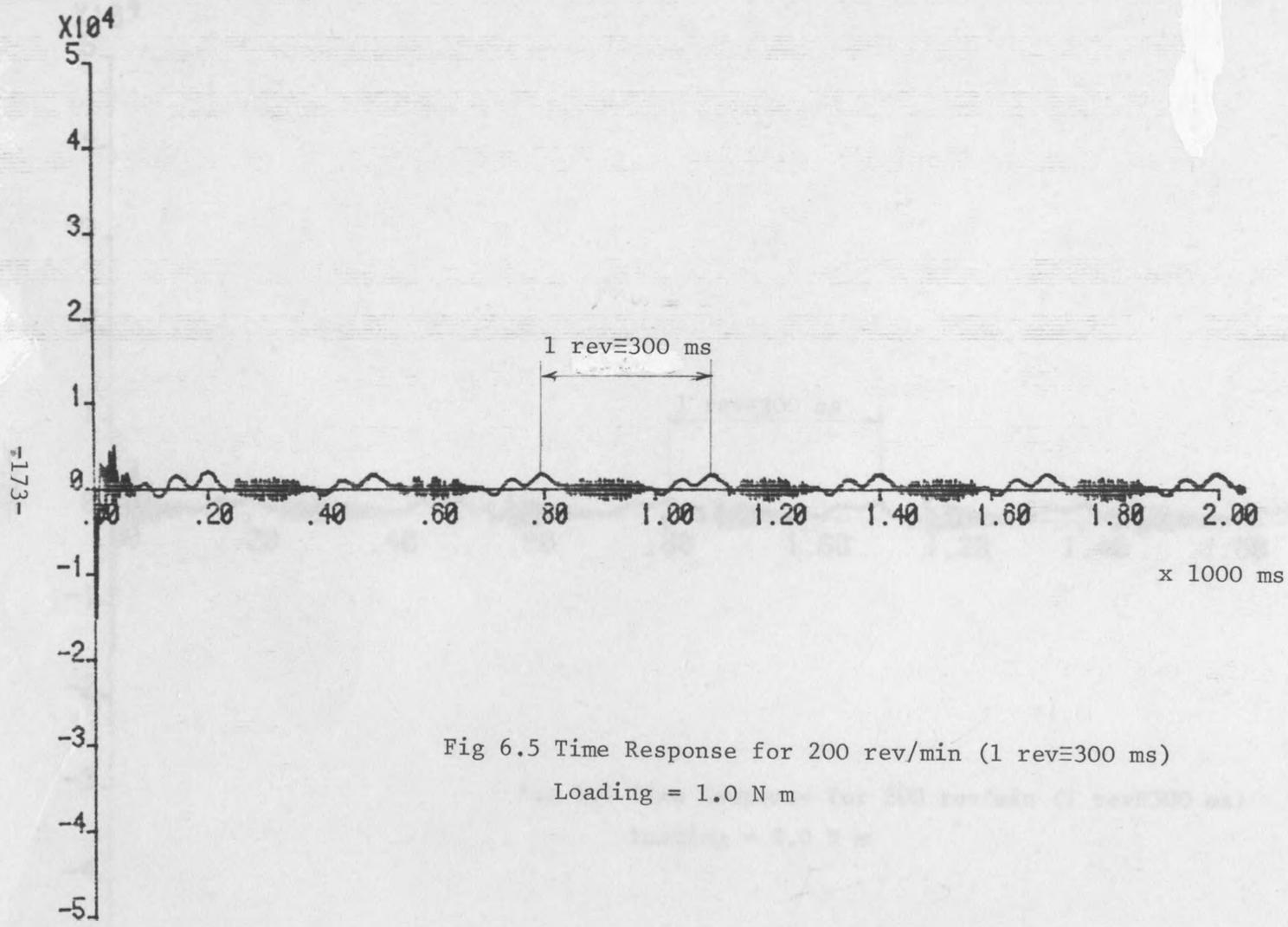
Fig 6.5 Time Response for 200 rev/min (1 rev≡300 ms)

Loading = 1.0 N m
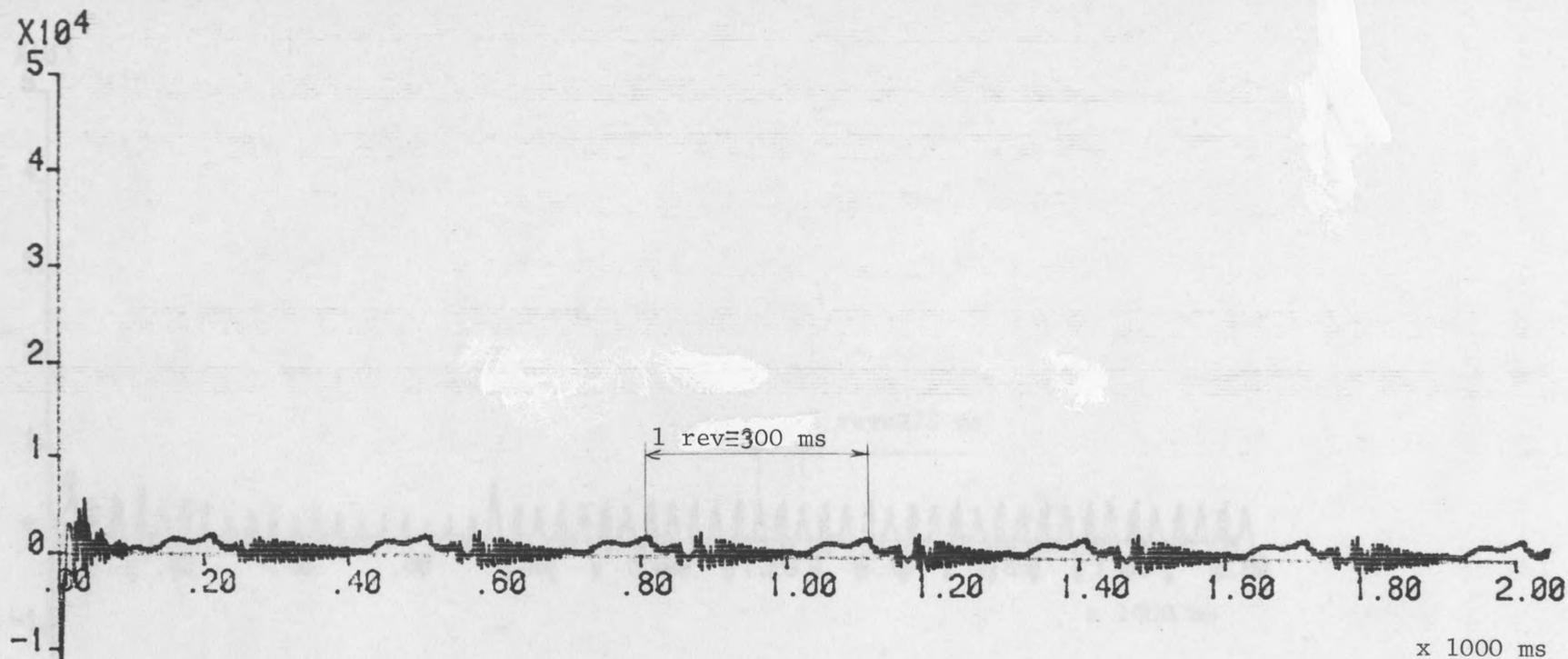
Fig 6.6 Time Response for 200 rev/min (1 rev≡300 ms)

Loading = 2.0 N m
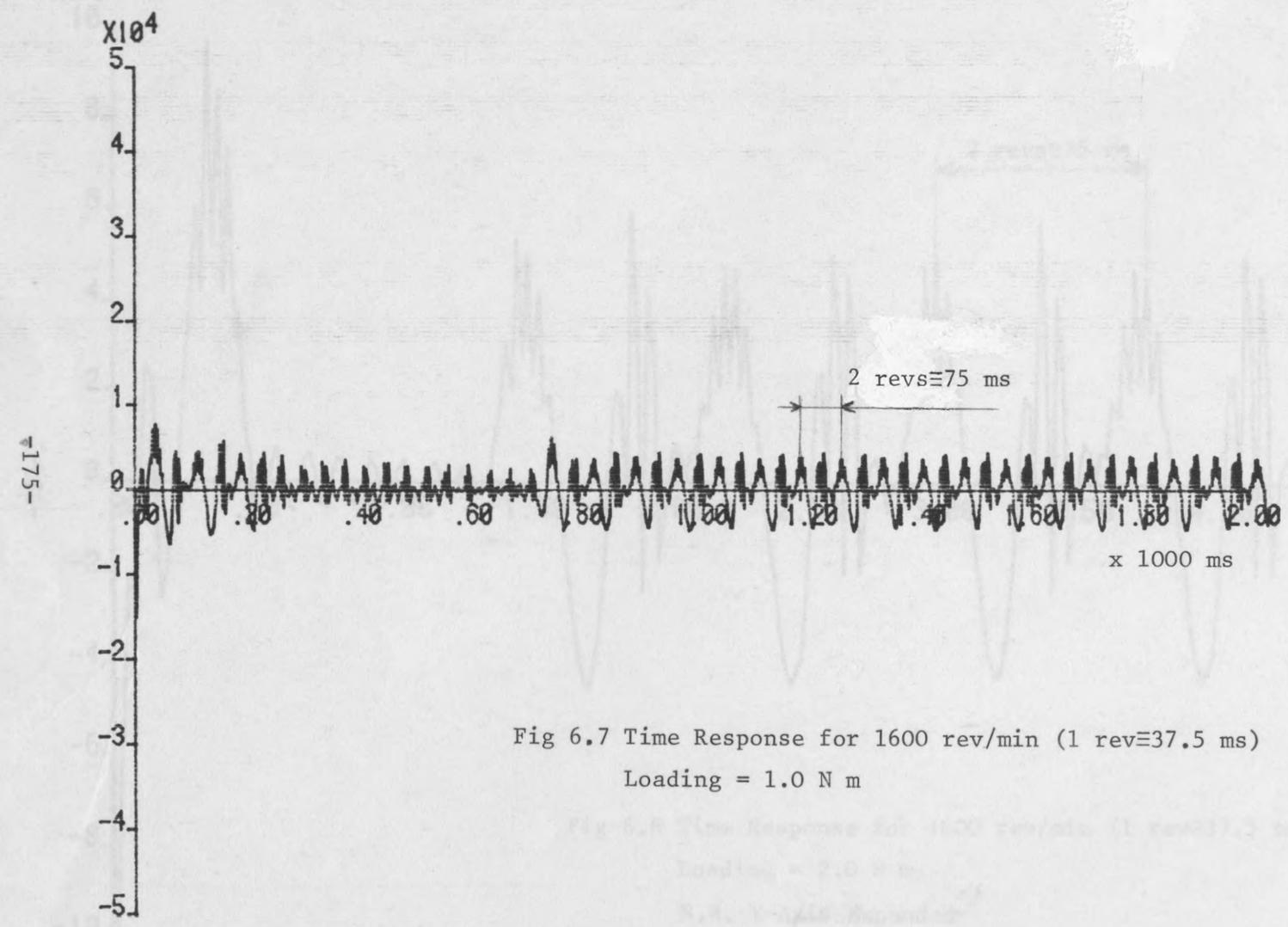
Fig 6.7 Time Response for 1600 rev/min (1 rev≡37.5 ms)
Loading = 1.0 N m

Fig 6.8 Time Response for 1600 rev/min (1 rev≡37.5 ms)

Loading = 2.0 N m

N.B. Y-Axis Expanded
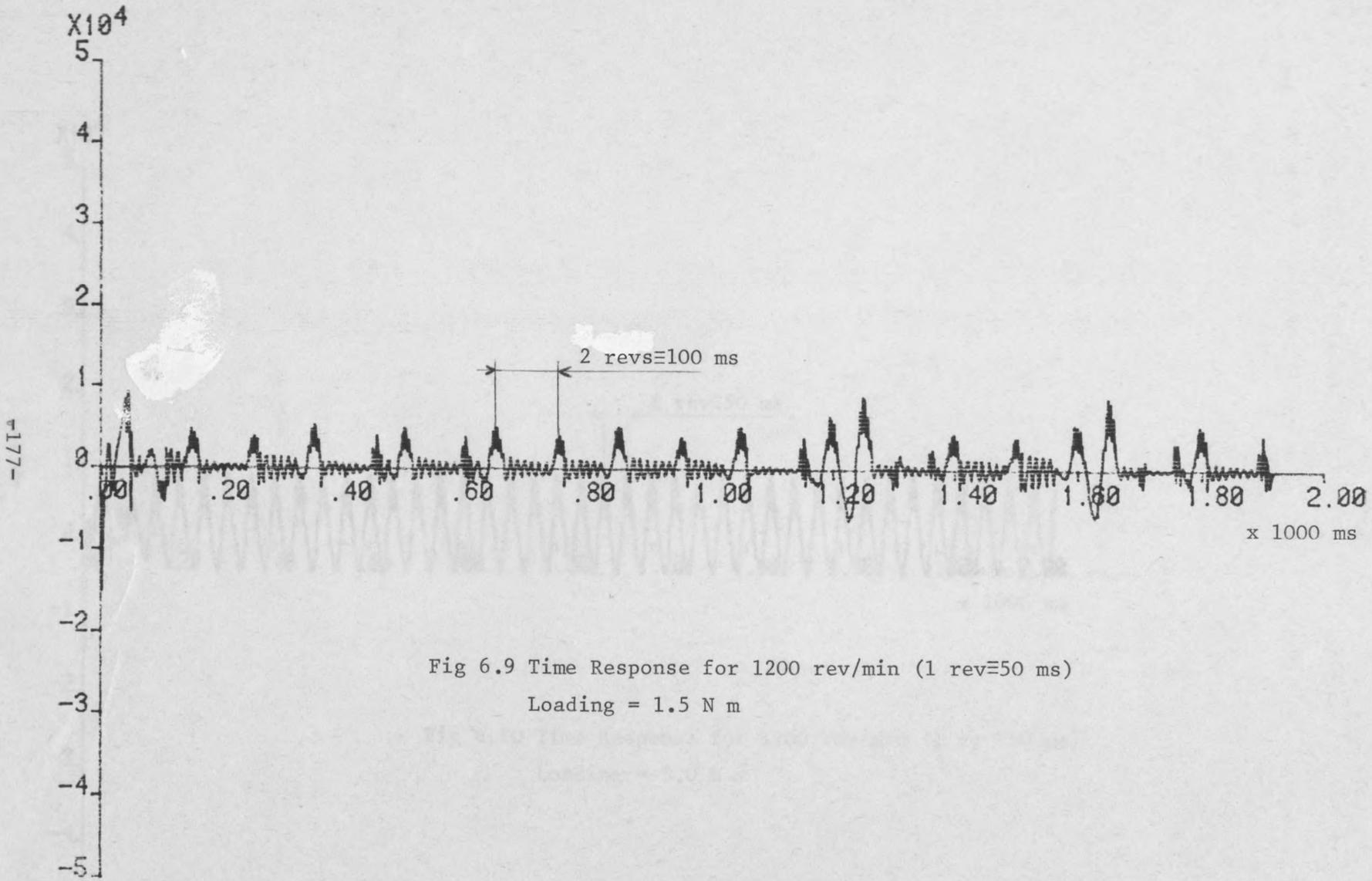
Fig 6.9 Time Response for 1200 rev/min (1 rev≡50 ms)

Loading = 1.5 N m
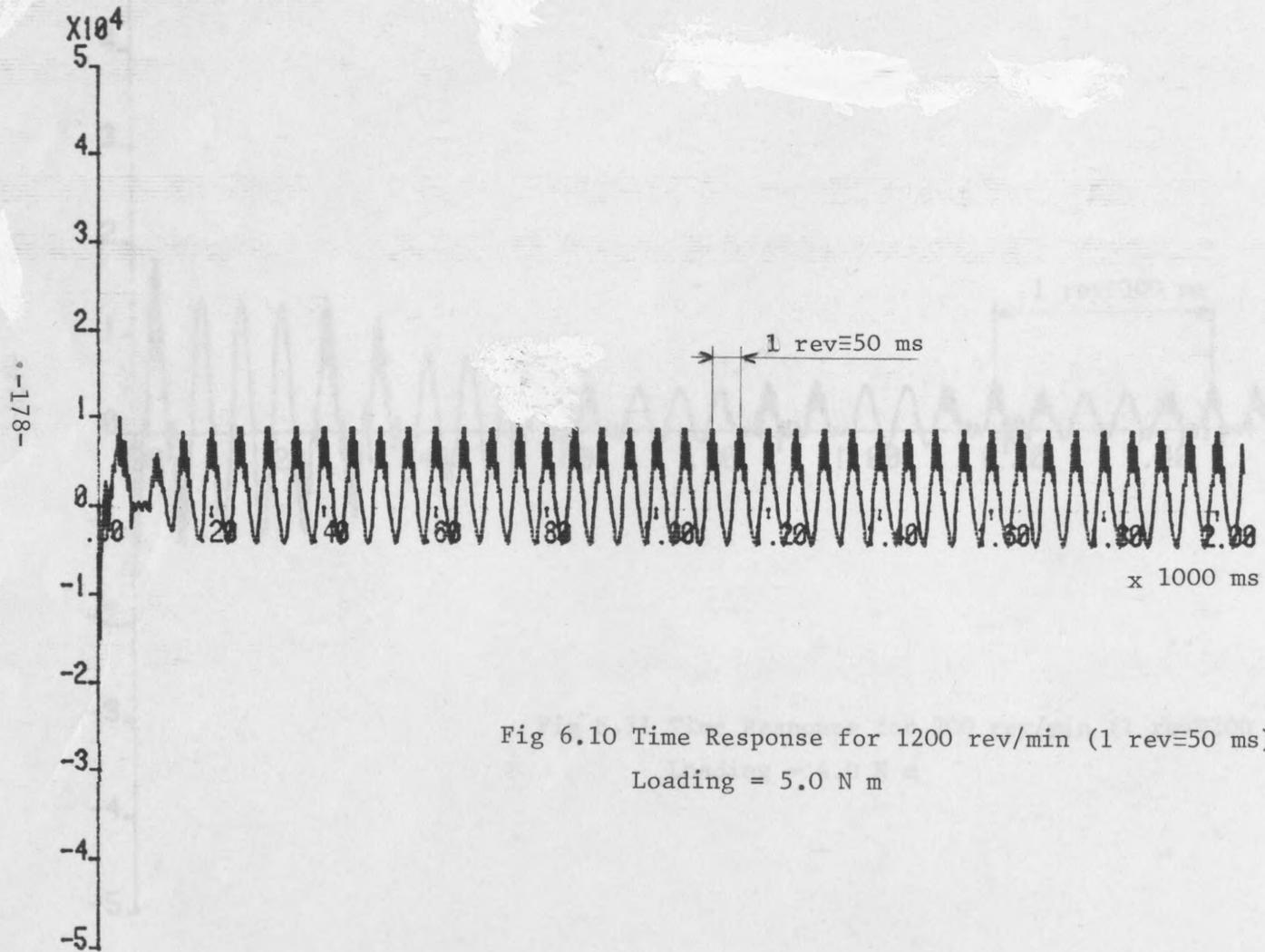
Fig 6.10 Time Response for 1200 rev/min (1 rev≡50 ms)
Loading = 5.0 N m
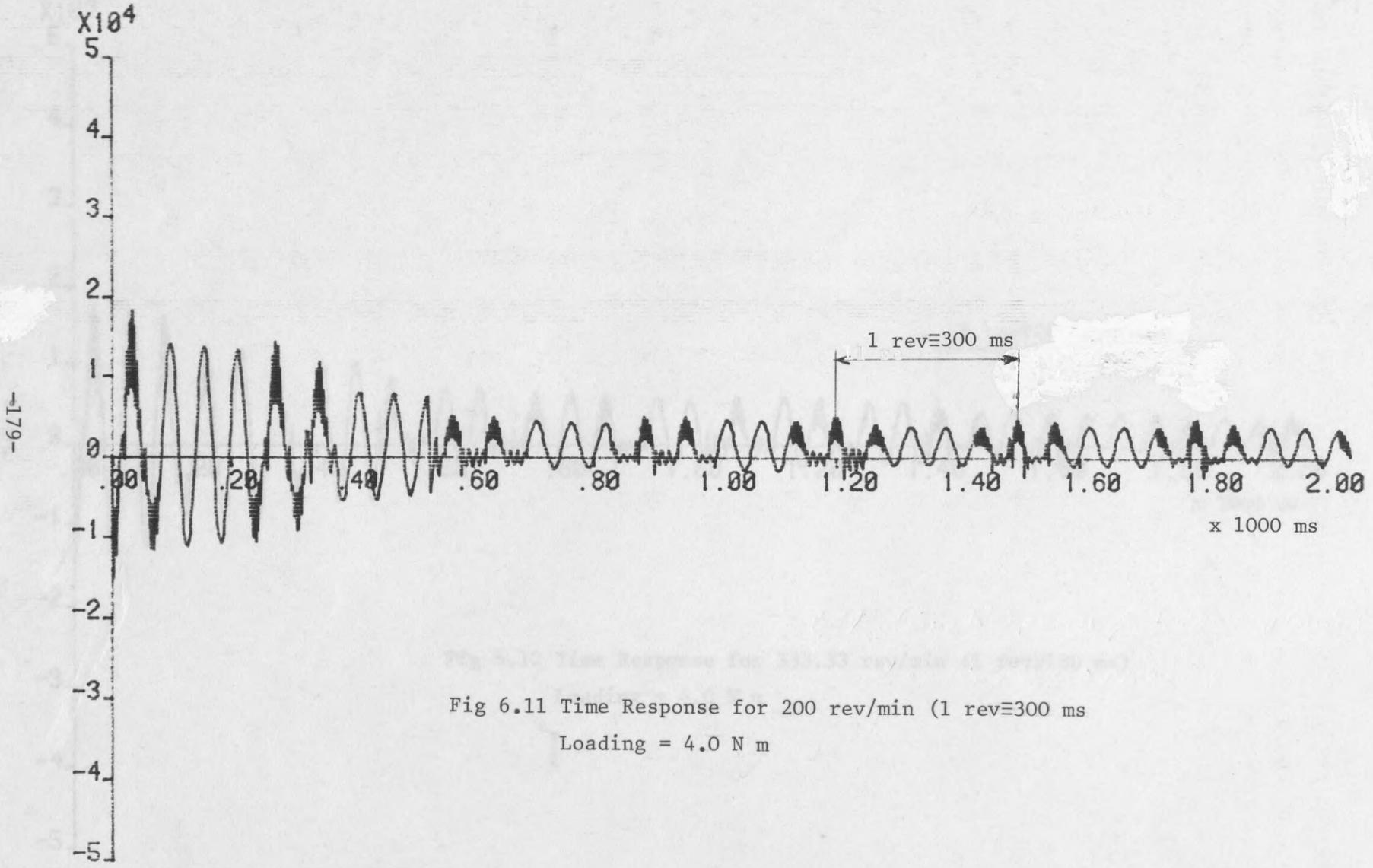
Fig 6.11 Time Response for 200 rev/min (1 rev≡300 ms

Loading = 4.0 N m
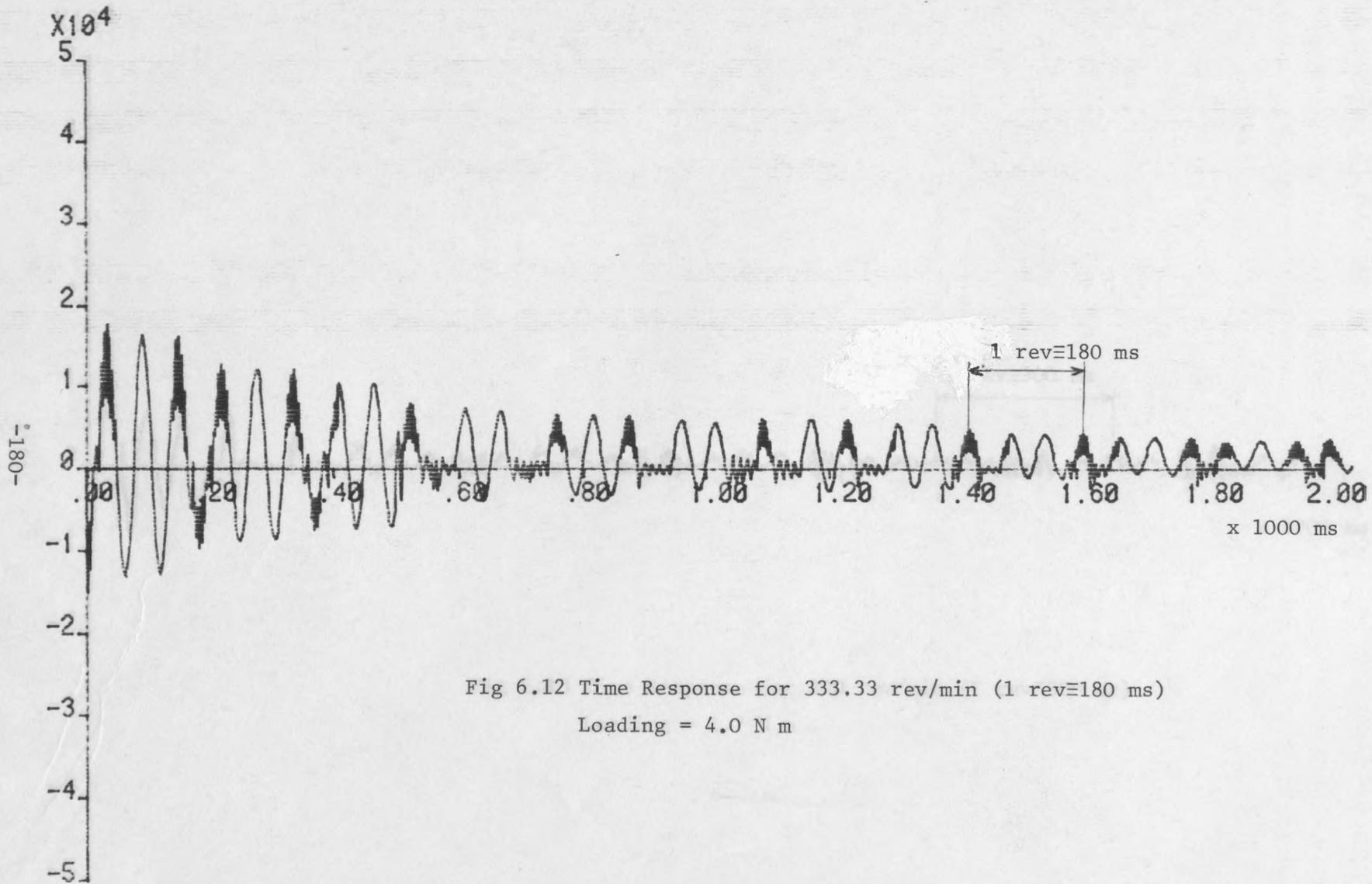
Fig 6.12 Time Response for 333.33 rev/min (1 rev≡180 ms)

Loading = 4.0 N m
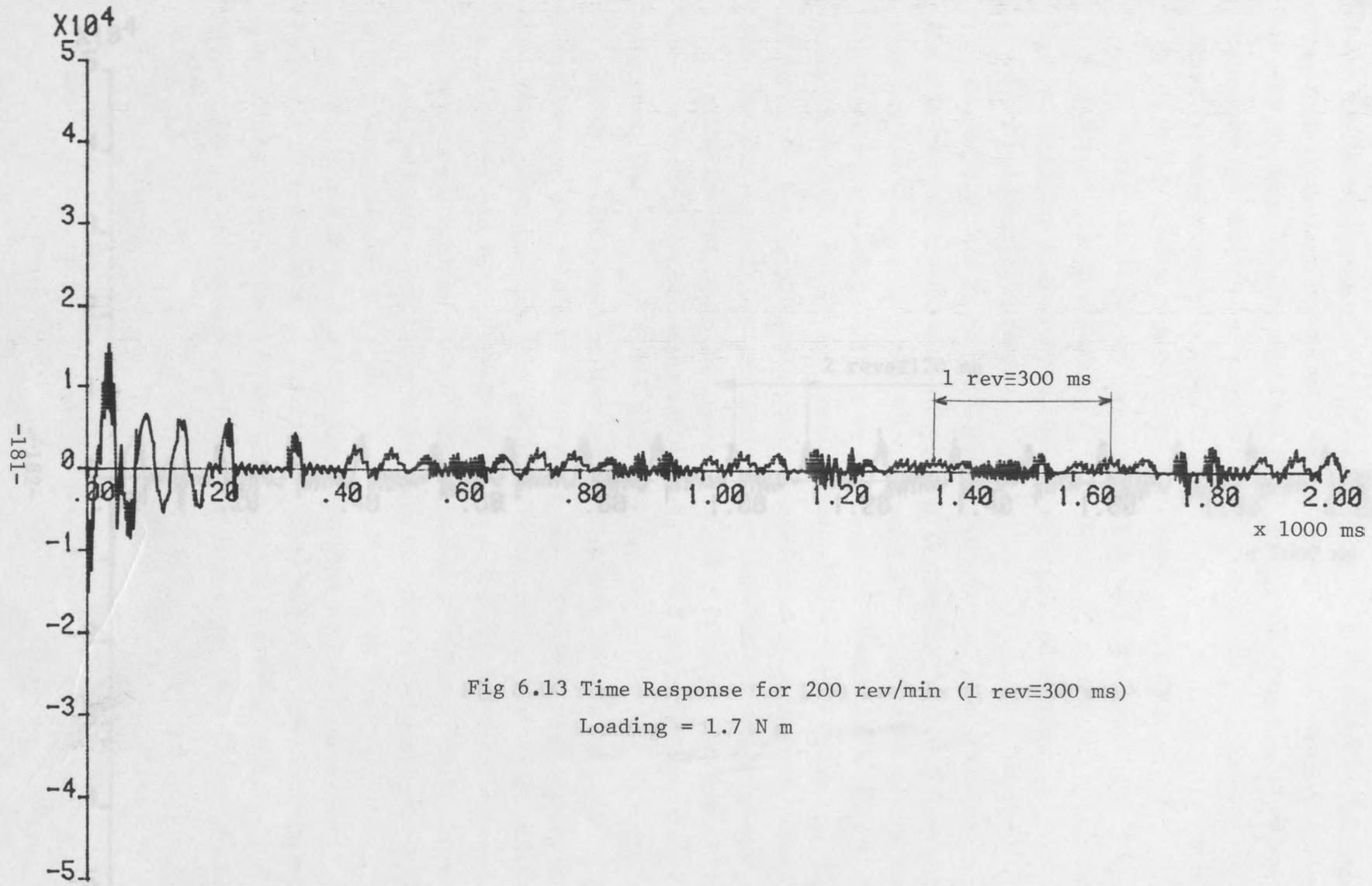
Fig 6.13 Time Response for 200 rev/min (1 rev≡300 ms)

Loading = 1.7 N m

X10^4

Fig 6.14 Time Response for 1000 rev/min (1 rev≡60 ms)

Loading = 1.7 N m
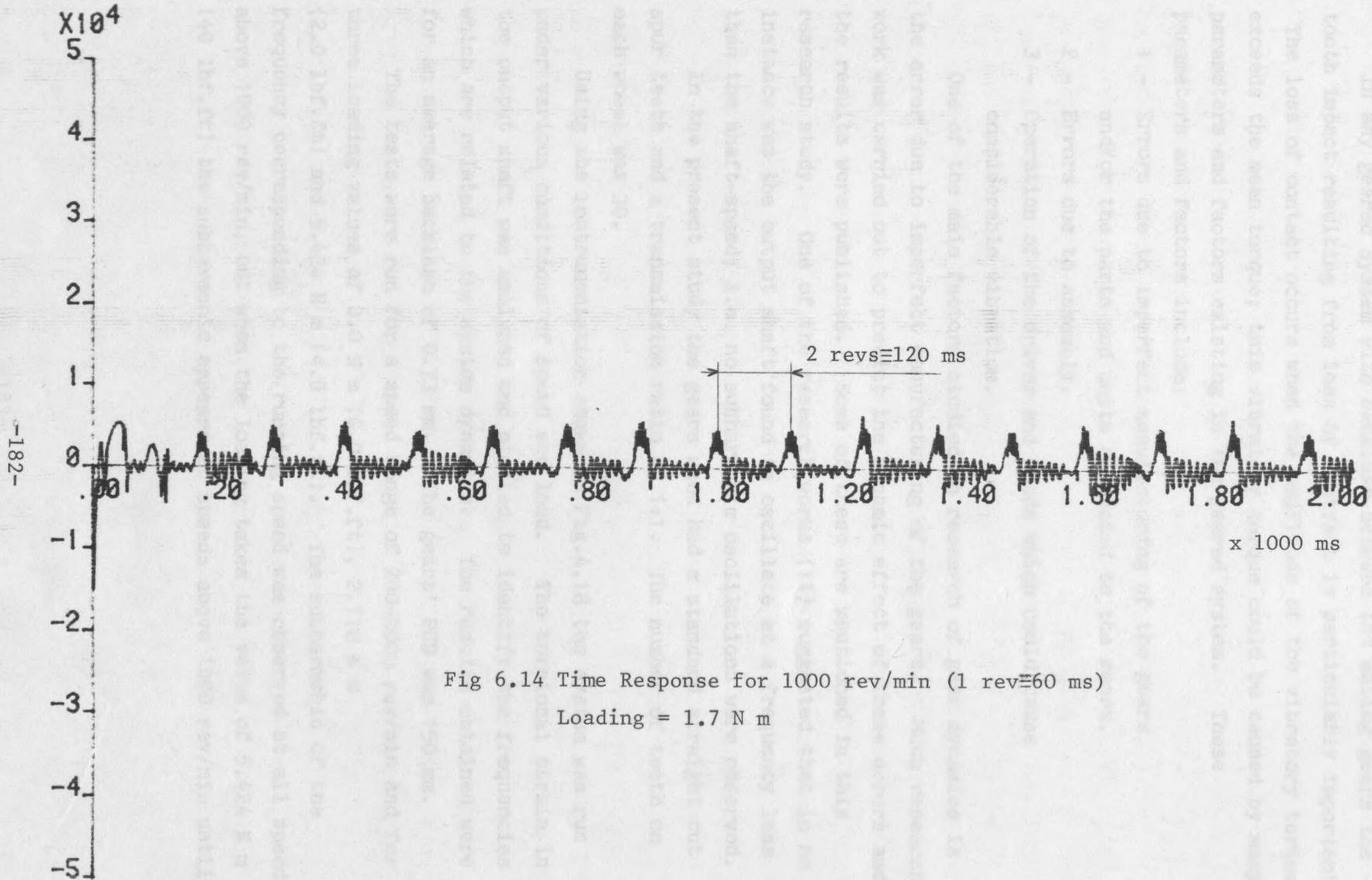
VII. DISCUSSION

In any geared system with backlash between the mating gears the tooth impact resulting from loss of contract is particularly important. The loss of contact occurs when the amplitude of the vibratory torque exceeds the mean torque; this vibratory torque could be caused by many parameters and factors existing in the geared system. These parameters and factors include:

1 - Errors due to imperfect manufacturing of the gears and/or the parts and units connected to the gears.

2 - Errors due to assembly.

3 - Operation of the drives and loads which could cause considerable vibration.

One of the main factors studied in research of gear dynamics is the error due to imperfect manufacturing of the gears. Much research work was carried out to predict the dynamic effect of these errors and the results were published. Some of these are mentioned in this research study. One of the research works (11) suggested that in no instance was the output shaft found to oscillate at a frequency less than the shaft-speed; i.e. no subharmonic oscillations were observed.

In the present study the gears used had a standard straight cut spur teeth and a transmission ratio of 1:1. The number of teeth on each wheel was 30.

Using the instrumentation shown in Fig.4.18 the system was run under various conditions of speed and load. The torsional strain in the output shaft was analysed and plotted to identify the frequencies which are related to the system dynamics. The results obtained were for an average backlash of 0.73 mm. The gears' PCD was 150 mm.

The tests were run for a speed range of 200-2000 rev/min and for three loading values of 0.0 N m (0.0 lbf.ft), 2.712 N m (2.0 lbf.ft) and 5.424 N m (4.0 lbf.ft). The subharmonic of the frequency corresponding to the running speed was observed at all speeds above 1000 rev/min, but when the loading takes the value of 5.424 N m (40 lbf.ft) the subharmonic appears at speeds above 1000 rev/min until

the speed reaches 1700 rev/min; at this speed the subharmonic starts
to weaken and disappear. It is also observed that the subharmonic did
not appear at any speed between 200-1000 rev/min inclusive for all the
load values of 0.0 N m (0.0 lbf.ft), 2.712 N m (2.0 lbf.ft) and 5.424
N m (4.0 lbf.ft).

A possible explanation for the presence of a subharmonic in this
geared system is that the subharmonic of the tooth engaging frequency
(i.e. impacting of teeth every second tooth or third tooth and so on)
may cause the subharmonic of the geared system to appear at speeds
above the first natural frequency (the term 'first natural frequency'
is used as a reference point). For the case of 30 teeth on each wheel
the explanation of the subharmonic of the geared system can be given as
follows. When the running speed is between 200-1000 rev/min, the
gears impact on every tooth, second tooth or third tooth and the
impacting of tooth cycle will be completed in one revolution, in which
case the output shaft will not be stimulated at a subharmonic. If the
speed of the gears is higher than the speed corresponding to the first
natural frequency and also above 1000 rev/min, the gears may impact
every fourth tooth, thus the impacting cycle will be completed in two
revolutions. This is because the number of teeth on the gear is
thirty, the factors of which are 1,2,3,5,6,10 and 15. From this
sequence of factors it is possible to see that impacting every tooth,
second tooth and third tooth will not stimulate a subharmonic while
impacting every fourth tooth will stimulate a subharmonic of the second
order (i.e. subharmonic at half the speed (since the number 4 is a
factor of 2 x 30). For the factors 5 and 6 (which means impacting
every fifth tooth and sixth tooth) the impacting of teeth will not
stimulate a subharmonic. But for the case of impacting, every seventh
tooth will stimulate a subharmonic of the seventh order, because the
number 7 is a factor of 7 x 30 and this is very unlikely to occur.
This is why the number 4 is important in this study.

If the number of teeth is changed to any other number (which could
be itself a prime number or have a different set of factors), then
depending on the new number of teeth and speed range the position of

the subharmonic may be shifted from the position found in the present study, for example, if the number of teeth on each wheel is 31 (which is a prime number) and if the pair of gears impact every second tooth (which may occur at a lower speed), then the tooth impacting cycle will be completed in two revolutions and a subharmonic of the second order may appear at a lower speed (the number 2 is a factor of 2 x 31). In the two previous cases the transmission ratio was 1:1. If the transmission ratio is changed, then there are two cases: one case when the number of teeth of the driven gear is 30 and the driving is not 30 the subharmonic of the driven gear speed may appear at the same speed as suggested in this study (when impacting of teeth takes place every fourth tooth). The second case when the number of teeth of the driving gear has any number not equal to the driven gear and the number of teeth of the driven gear is not 30, then depending on the new number of teeth on the driven gear the subharmonic of the geared system may appear when the tooth impacting cycle will be completed in more than one revolution.

The maximum speed available in this test rig was 2000 rev/min. Up to this speed the tooth subharmonic of engaging frequency (in particular impacting every fourth tooth) may have caused the subharmonic of the geared system to appear for the conditions of load and speed mentioned before. If the speed is high enough to cause the gear teeth to impact every fifth tooth, which means that the tooth impacting frequency will be completed in one revolution (because 5 is a factor of 30), then the subharmonic will disappear again.

For the test rig in hand the maximum torque which is applied to the subharmonic test results was 5.424 N m (4.0 lbf.ft). If this torque is increased to a higher value than the present maximum value, then the subharmonic will start to disappear at a lower speed than 1700 rev/min. At even higher torque the subharmonic may not appear at all, this is because the higher torque tends to prevent separation.

To discuss the effect of changing backlash on the existence of a subharmonic one has to think about the time available for the free flight of the tooth on the driving gear. If the backlash is reduced, then the time available for free flight is also reduced. As a result the tooth on the driving gear has less time to separate and impact again, and depending on the amplitude of torque variation, the tooth may even impact on the rear side. this means that the subharmonic may appear at a speed much higher than 1100 rev/min and it could completely disappear (in the speed range of 1100-2000 rev/min) for certain backlash values. If the backlash takes a value bigger than the present amount, then, depending on the amplitude of the torque variation, it can be deduced whether the backlash will have any effect on the presence of a subharmonic, for if the amplitude of torque variation is big enough to produce an impact on the rear side, then a bigger backlash will cause the subharmonic to appear at an earlier speed. However, if the amplitude is not great enough to produce an impact on the rear side, then a bigger backlash will have no effect on shifting the subharmonic from the suggested speed range.

Finally, the damping may have the effect of either shifting the position or reducing the effect of the subharmonic in the present geared system. The effect of damping depends greatly on whether it is negative damping or positive damping.

In this experimental study it was mentioned many times that the subharmonic of tooth engaging frequency may cause the subharmonic of the geared system. A possible explanation for the subharmonic of tooth engaging frequency was offered by Harris (1) and Gregory (3). They found in their study of tooth errors that random errors tend to stimulate the peak load of the tooth impact and when the speed gets higher these errors cause the impact to miss one or more tooth; i.e. impacting every second tooth, third tooth and so on, which is called 'subharmonic of the tooth engaging frequency'.

An expansion of the model previously used by Azar (11), which is based on an impact pair model produced by Dubowsky (28,29), was used to develop a simulation model for the geared torsional system in hand.

This model was simple and easy to solve numerically. The model represents a vibrating rear system and can be transferred to represent a torsionally vibrating system by introducing the assumptions that the parameters in the linear model contain the actual values of the parameters in the torsional model as it is described in section 5.3; then the solution of this model can be dealt with relatively easier.

The conditions that determine on which side the contact is established (by the use of the interaction force F_{XT} between the mating teeth) was useful for transferring the equations of motion from the non-linear situation to the linear one.

Two functions were added to the model, one of which was to include the effect of vibrations of backlash during gear rotation and the second was added to represent the forces due to other errors (which could exist in the gears) such as eccentricity and ovality. These forces are only applied to the driving and driven gears. A stiffness variation during gear rotation was also tried but the results obtained from this variation did not give an output which could be related to the geared torsional system from the point of view of amplitude or frequency content. The function used to represent the backlash variation each time the backlash came into action was

$$B \Rightarrow B(1 - C_1 \cos \omega t); \quad C_1 = 0.38$$

This variation comes into action only when the teeth are in contact either on the left side or on the right side of the tooth flank.

The principal novel feature of the mathematical model is the numerical tooth shifting. This was based on the fact that when a pair of teeth move out of contact they are deflected and when the next pair of teeth approach the area of contact they are undeflected. This means that the deflection has to be taken out by subtracting the amount of deflection DX from the next pair and this is done by changing the displacements on the gears at the moment of shift from one pair to the next by an amount $\frac{DX}{2}$ (because the driving gear tooth and the driven

gear tooth have the same stiffness).   This is only applied when the teeth are in contact.   The time between the engagement of each pair can be determined when the speed is known, because this time is related to the speed and the number of teeth and can be calculated as follows:

$$\text{Shift} = \frac{\text{Period of one revolution(ms)}}{\text{Number of gear teeth (30)}}$$

Looking at the results obtained, it can be seen that the programme derived from the mathematical model produced reasonably good results which represent the general behaviour of the present geared torsional system.   This shows that the model is a good representation of the real system and reproduced some of the results which were obtained experimentally.   With a shorter calculation time step it would be possible to reproduce most of the experimental results for the present system.

VIII CONCLUSIONS AND RECOMMENDATIONS

8.1 Conclusions

The main direction in the present study is to investigate the effect of backlash on dynamic behaviour of torsional systems, taking that into account one can conclude:

1. If there is no subharmonic of the tooth impacting frequency, then no subharmonic of the gear speed corresponding frequency will be stimulated for any number of teeth.

2. For a similar test set-up, if the driven gear has a prime tooth number, then any subharmonic of the tooth impacting frequency of order N will produce a subharmonic of the gear speed corresponding frequency of the same order.   If the driven gear does <u>not</u> have a prime number of teeth and if the subharmonic of the tooth impacting frequency of order N is a factor of this tooth number, then there is no possibility of a subharmonic of the running speed being produced for this number of teeth.   The subharmonic of the tooth impacting frequency can only stimulate a subharmonic of the running speed if the tooth impacting cycle is completed after "k" number of revolutions.   The subharmonic of the running speed will then be of order "k".

3. The presence of a subharmonic in any vibrating system could make a significant contribution to the study of the dynamics of gears and may explain many problems existing in similar geared systems.

4. If a geared torsional system is running at a speed high enough to produce a subharmonic of this speed then not only the frequency of the running speed will exist but also the frequency of half of the running speed will occur.   This may cause a new and unexpected regime of dynamic operation of gears through backlash.

5. Any loading which is high enough to stop tooth separation will
    prevent the occurrence of subharmonic response.

6. The speed range of the subharmonic and the backlash value are
    related to each other.   The presence of a subharmonic of the
    running speed means that a change in backlash value will produce a
    subharmonic of the running speed in a different speed range.

7. One of the main advantages of the computer program used in this
    study is the development of the idea of tooth shifting numerically
    without the need to add any type of function to represent certain
    criteria; i.e. to create an internal input rather than the assumed
    external input.

8.2 Recommendations

An investigation of dynamics of gears due to impact through
backlash, especially from the point of view of subharmonics, should
include the following:

1. Extensive experimental work is strongly recommended to be carried
    out on the presence of subharmonics in a similar torsional system.

2. Separation of the system's natural frequencies would be helpful
    for easy identification of all sources of input frequencies.

3. An extensive study needs to be done for similar conditions with
    the strain guage fixed near the teeth to confirm the number of
    tooth impacts during one revolution.

4. Tooth shifting, as described in section 5.4.5 should be studied
    more to include the shifting of two or more teeth as real gear
    systems have a contact (meshing) ratio always greater than unity.

5. More advanced theoretical work needs to be done for the
   mathematical model presented in Chapter V, Fig. 5.2 to overcome
   the problem of time shift related to the number of teeth which
   limited the number of results obtained in Chapter VI.

6. The theoretical work has to be extended to include a suitable
   transformation of the time response into a frequency spectrum for
   more accurate analysis of the theoretical results.

REFERENCES

1- Harris, S.L.   "Dynamic Loads on the Teeth of Spur Gears,"
                         Proceedings of the Institution of Mechanical
                         Engineers, London, Vol. 172, 1958. PP. 87-112.

2- Attia, A.Y.   "Dynamic Loading of Spur Gear Teeth," Journal
                         of Engineering for Industry, Trans. ASME,
                         Series B, Vol. 81, February, 1958. PP. 1-7.

3- Gregory, R.W.,   "Dynamic Behaviour of Spur Gears," Proceedings
   Harris, S.L.,   of the Institution of Mechanical Engineers,
   Munro, R.G.   London, Vol. 178, Part 1, No. 8, 1963-64.
                         PP. 207-218.

4- Gregory, R.W.,   "Torsional Motions of a Pair of Spur Gears,"
   Harris, S.L.,   Institution of Mechanical Engineers, Applied
   Munro, R.G.   Mechanics Convention, London, paper 6, 1964.

5- Houser, D.R.,   "An Experimental Investigation of Dynamic
   Seireg, A.   Factors in Spur and Helical Gears," Journal
                         of Engineering for Industry, Trans. ASME,
                         Series B, Vol. 92, May, 1970. PP. 495-503.

6- Seireg, A.,   "Evaluation of Dynamic Factors for Spur and
   Houser, D.R.   Helical Gears, "Journal of Engineering for
                         Industry, Trans. ASME, Series B, Vol. 92,
                         May, 1970. PP. 504-515.

7- Baronet, C.N.,   "Exact Stress Distribution in Standard Gear
   Tordion, G.V.   Teeth and Geometry Factors," Journal of
                         Engineering for Industry, Trans. ASME,
                         November, 1973. PP. 1159-1163.

8- Brickner, T.S.,   "Dynamics of Gear train with Backlash,"
   Olerich, R.J.   Southeast Symp. on System Theory, 6th Annual
                         Proceedings, 1974.

9- Chabert, G.,   "An Evaluation of Stresses and Deflection of
    Dang Tran, T.,   Spur Gear Teeth Under Strain," Journal of
    Mathis, R.   Engineering for Industry, Trans. ASME,
                     February, 1974. PP. 85-93

10- Ichimaru, K.,   "Dynamic Behaviour of Heavy-loaded Spur Gears,"
    Hirano, F.   Journal of Engineering for Industry, Trans.
                     ASME, May, 1974. PP. 373-381.

11- Azar, R.C.,   "An Experimental Investigation of Impact
    Crossley, F.R.E. Phenomenon in Spur Gear System," Institution
                     of Mechanical Engineers, 1975. PP. 157-161.

12- Seireg, A.,   "Dynamic Stresses in Gear Teeth Under
    Shah, S.C.,   conditions of Sustained Oscillations through
    Khazekhan, K.   the Backlash," Institution of Mechanical
                     Engineers, 1975. PP. 205-208.

13- Tobe, T.,   "Statistical Analysis of Dynamic Loads on
    Sato, K.   Spur Gear Teeth," Bull. of JSME, Vol. 20,
                     No. 145, July, 1977. PP. 882-889.

14- Tobe, T.,   "Statistical Analysis of Dynamic Loads on
    Sato, K.   Spur Gear Teeth," Bull. of JSME, Vol. 20,
                     No. 148, October, 1977. PP. 1315-1320.

15- Johnson, D.C.   "Modes and Frequencies of Shafts Coupled by
                     Straight Spur Gears," Journal of Mechanical
                     Engineering Science, Vol. 4, No. 3, 1962.
                     PP. 241-250.

16- Wang,S.M.,   "Torsional Response of a gear Train System,"
    Morse, Jr., I.E. Journal of Engineering for Industry, Trans.
                     ASME, Series B, Vol. 94, No. 2, 1972.
                     PP. 583-594.

17- Wallace, D.B.,   "Computer Simulation of Dynamic Stress,
    Seireg, A.   Deformation, and Fracture of Gear Teeth,"
                     Journal of Engineering for Industry, Trans.
                     ASME, Nov., 1973. PP. 1108-1114.

18- Conry, T.F.,   "A mathematical Programming Technique for
    Seireg, A.   the evaluation of load Distribution and
                     Optimal Modifications for Gear Systems,"
                     Journal of Engineering for Industry, Trans.
                     ASME, November, 1973. PP. 1115-1122.

19- Wilcox, L.,   "Application of Finite Elements to the
    Coleman, W.   Analysis of Gear Tooth Stresses," Journal
                     of Engineering for Industry, Trans. ASME,
                     November, 1973. PP. 1139-1148.

20- Wang, S.M.   "Analysis of Nonlinear Transient Motion of a
                     Geared Torsional," Journal of Engineering for
                     Industry, Trans. ASME, February, 1974.
                     PP. 51-59.

21- Randall, R.B.   "Gear Box Fault Diagnosis Using Cepstrum
                     Analysis," Proceedings of Institution of
                     Mechanical Engineers, 1975. PP. 169-174.

22- Mitchell, L.D.   "A New Branching Technique for the Static and
                     Dynamic Analysis of Geared Systems,"
                     Institution of Mechanical Engineers, 1980.
                     PP. 37-42.

23- Lees, A.W.,   "Vibration Spectra from Gear Drives,"
    Pandey, P.C.   Institution of Mechanical Engineers, 1980.
                     PP. 103-108.

24- Taylor, J.I.   "Fault Diagnosis of Gears Using Spectrum
                     Analysis, Institution of Mechanical Engineers,
                     1980. PP. 163-168.

25- Randall, R.B.   "Advances in the Application of cepstrum
                     analysis to Gear Box Diagnosis," Institution
                     of Mechanical Engineers, 1980. PP. 169-174.

26- Kobrinskii,A.E.,   "Dynamics of Mechanisms with Elastic
connections and Impact System," Iliffe
Books Ltd., London,1969, Chapters 7-9.

27- Sikarskie,D.L.,   "Periodic Motions of a two-Body System
Paul, B.   Subjected to Repetitive Impact," Journal of
Engineering for Industry, Trans. ASME,
November, 1969. PP. 931-938.

28- Dubowsky, S.,   "Dynamic Analysis of Mechanical Systems with
Freudenstein,F.   Clearances, Part 1: Formation of Dynamic
Model," and Part 2: "Dynamic Response,"
Journal of Engineering for Industry, Trans.
ASME, Vol. 93, Series B, No.1, February, 1971.
PP. 305-316.

29- Dubowsky, S.   "On predicting the Dynamic Effects of
Clearances in One-Dimensional Closed Loop
Systems," Journal of Engineering for Industry,
Trans. ASME, February, 1974. PP. 324-329.

30- Veluswami, M.A.,   "Multiple Impacts of a Ball Between Two Plates,
Crossley, F.R.E.   Part 1: Some Experimental Observations,"
Journal of Engineering for Industry, Trans.
ASME, August, 1975. PP. 820-827.

31- Veluswami, M.A.,   "Multiple Impacts of a Ball Between Two Plates,
Crossly, F.R.E.,   Part 2: Mathematical Modelling," Journal of
Horvay, G.   Engineering for Industry, Trans. ASME,
August, 1975. PP. 828-835.

32- Nayfeh, A.H.,   "Nonlinear Oscillations," Wiley-Interscience,
Mook, D.T.   1979.

33- Doebelin, E.O.   "System Modelling and Response, Theoretical
and Experimental Approaches," Wiley-
Interscience, 1980.

34- Steidel, Jr.,R.F. "An Introduction to Mechanical Vibrations,"
                       Wiley-Interscience, 1971.

35- Wilson, W.K.   "Practical Solution of Torsional Vibration
                       Problems," Volume Five, Chapman and Hall Ltd.
                       1969.

36- Tuplin, W.A.   "Torsional Vibration," Pitman, 1966.

37- Daniel, J.W.,   "Computation and Theory in Ordinary
    Moore, R.E.   Differential Equations," W.H. Freeman and
                       Company, San Francisco, 1970.

38- Lambert, J.D.   "Computational Methods in Ordinary
                       Differential Equations,"Wiley -Interscience,
                       1973.

39- Timoshenko, S.,   "Strength of Gear Teeth," Mechanical
    Baud, R.V.   Engineering, Vol. 48, November, 1926.
                       PP. 1105-1109.

40- Reason, B.R.   "Gear Design", MSc. Notes, Part II, Cranfield
                       Institute of Technology, 1975-76.

41- Movnin, M.,   "Machine Design," MIR Publishers, Moscow,
    Goltziker, D.   1971.

42- Bannister, R.H.   "Vibration Instrumentation," MSc.Notes, Part
                       II, Cranfield Institute of Technology,
                       1975-76.

43- The City   NAG Library, User's Manual, London, 1981.
    University,
    Computer center.

Inside | Outside the dynamo

VR$_1$=100 KΩ
C$_2$=10 μF

A

FG

VR$_1$

L$_1$

V

TR$_2$

R$_2$=1 Ω

TR$_1$

CRO
Display

R$_1$=470 Ω

C$_1$=3000 μF

L$_2$

Rec

TR$_1$ Type: 2N3773

TR$_2$ Type: 2N3053

FG- Function Generator
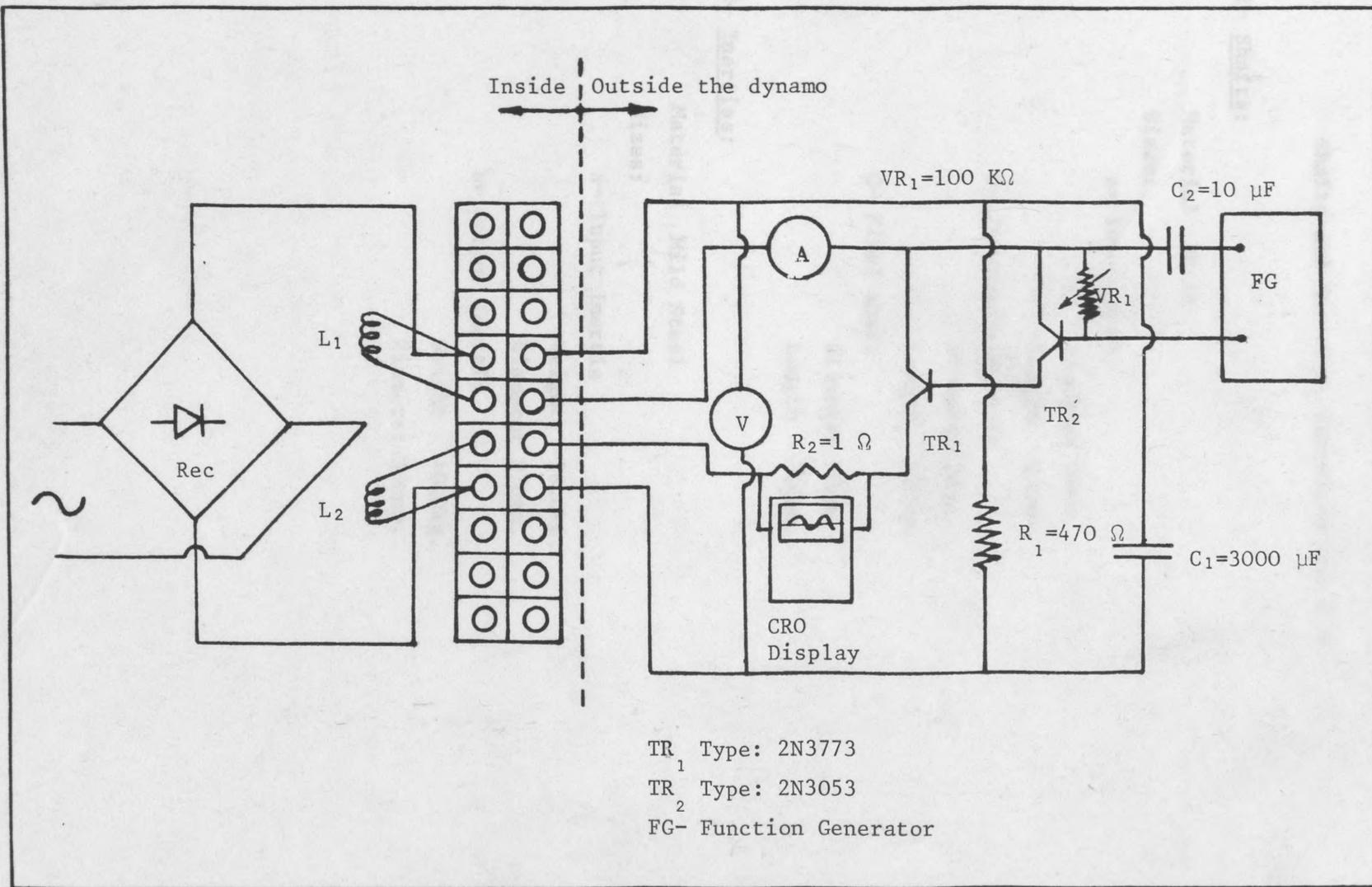
APPENDIX B

Shafts and Inertias, Materials and Sizes

1- Shafts:

Material   EN 1A
Sizes:
a- Input shaft
Diameter 20mm.
Length   250mm.
b- Intermediate shaft
Diameter 20mm.
Length   500mm.
C- Final shaft
Diameter 20mm.
Length   300mm.

2- Inertias:

Material Mild Steel
Sizes:
a- Input Inertia
Weight   38.0kg.
Diameter 270mm.
b- Output Inertia
Weight   40.0kg.
Diameter 300mm.

Natural Frequencies of the System and Subsystems

a) - Natural Frequencies of the Whole System.
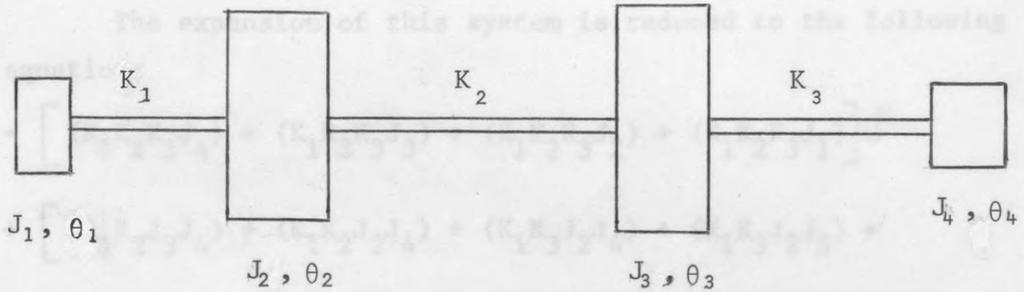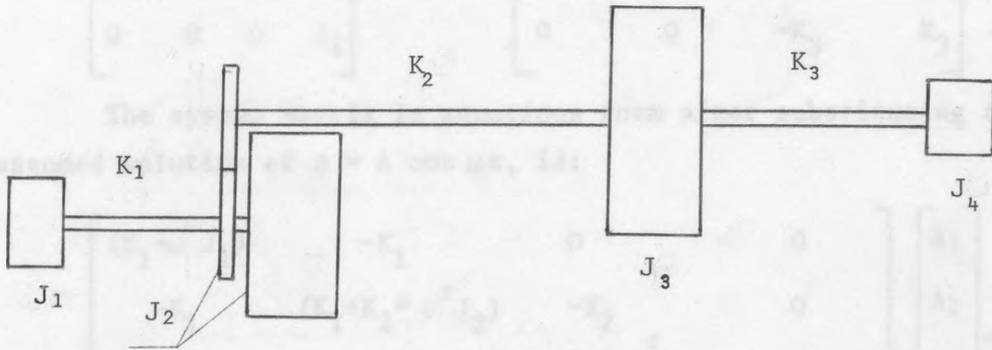
The first figure represents the vibrating system, but the
second represents the equivalent system after being transfered
through gears with transmission ratio of 1:1. The equations
of motion are:

$$J_1 \ddot{\theta}_1 + K_1 (\theta_1 - \theta_2) = 0$$

$$J_2 \ddot{\theta}_2 + K_1 (\theta_2 - \theta_1) + K_2 (\theta_2 - \theta_3) = 0$$

$$J_3 \ddot{\theta}_3 + K_2 (\theta_3 - \theta_2) + K_3 (\theta_3 - \theta_4) = 0$$

$$J_4 \ddot{\theta}_4 + K_3 (\theta_4 - \theta_3) = 0$$

From these equations of motion we can find the mass matrix and stiffness matrix which are:

$$
\begin{bmatrix}
J_1 & 0 & 0 & 0 \\
0 & J_2 & 0 & 0 \\
0 & 0 & J_3 & 0 \\
0 & 0 & 0 & J_4
\end{bmatrix}
\quad \text{and} \quad
\begin{bmatrix}
K_1 & -K_1 & 0 & 0 \\
-K_1 & K_1+K_2 & -K_2 & 0 \\
0 & -K_2 & K_2+K_3 & -K_3 \\
0 & 0 & -K_3 & K_3
\end{bmatrix}
$$

The system matrix in equations form after substituting the assumed solution of $\theta = A \cos \omega t$, is:

$$
\begin{bmatrix}
(K_1-\omega^2 J_1) & -K_1 & 0 & 0 \\
-K_1 & (K_1+K_2-\omega^2 J_2) & -K_2 & 0 \\
0 & -K_2 & (K_2+K_3-\omega^2 J_3) & -K_3 \\
0 & 0 & -K_3 & (K_3-\omega^2 J_4)
\end{bmatrix}
\begin{bmatrix}
A_1 \\ A_2 \\ A_3 \\ A_4
\end{bmatrix} = 0
$$

To calculate the natural frequencies of the system, the expansion of the determinant of system matrix has to be found.

The expansion of this system is reduced to the following equation:

$$
-\left[(K_1K_2K_3J_4) + (K_1K_2K_3J_3) + (K_1K_2K_3J_2) + (K_1K_2K_3J_1) \right]\omega^2
$$

$$
+\left[(K_1K_2J_3J_4) + (K_1K_2J_2J_4) + (K_1K_3J_2J_4) + (K_1K_3J_2J_3) + \right.
$$

$$
(K_1K_2J_1J_4) + (K_1K_3J_1J_4) + (K_1K_3J_1J_3) + (K_2K_3J_1J_4) +
$$

$$
\left. (K_2K_3J_1J_3) + (K_2K_3J_1J_2) \right]\omega^4 - \left[(K_1J_2J_3J_4) + (K_1J_1J_3J_4) + \right.
$$

$$
\left. (K_2J_1J_3J_4) + (K_2J_1J_2J_4) + (K_3J_1J_2J_4) + (K_3J_1J_2J_3) \right]\omega^6
$$

$$
+\left[J_1J_2J_3J_4 \right]\omega^8 = 0
$$

Or: $A\omega^6 - B\omega^4 + C\omega^2 - D = 0$

Where;

$A = 1$

$B = (\dfrac{K_1}{J_1} + \dfrac{K_1}{J_2} + \dfrac{k_2}{J_2} + \dfrac{k_2}{J_3} + \dfrac{k_3}{J_3} + \dfrac{k_3}{J_4})$

$C = (\dfrac{K_1K_2}{J_1J_2} + \dfrac{K_1K_2 + K_1K_3}{J_1J_3} + \dfrac{K_1K_2 + K_1K_3 + K_2K_3}{J_2J_3}$

$+ \dfrac{K_1K_3 + K_2K_3}{J_2J_4} + \dfrac{K_1K_3}{J_1J_4} + \dfrac{K_2K_3}{J_3J_4})$

$D = (\dfrac{J_1 + J_2 + J_3 + J_4}{J_1\,J_2\,J_3\,J_4})\,K_1K_2K_3$

The values of the inertias and stiffnesses are as follows,

(Bearing in mind that $K_t = \dfrac{GI_p}{\ell} = G\,\dfrac{\pi\,d^4}{32\,\ell}$)

$K_1 = 5196.2$ N m/rad.

$K_2 = 2598.1$ N m/rad.

$K_3 = 4330.2$ N m/rad.

$J_1 = 0.0163$ kg.m^2

$J_2 = 0.355$ kg.m^2

$J_3 = 0.45$ kg.m^2

$J_4 = 0.015$ kg.m^2

$\therefore$ $A = 1$

$B = 644817.27$

$C = 10.756876\ 10^{10}$

$D = 1.2516763\ 10^{15}$

Solving the equation of frequencies, by finding the roots ω_1^2, ω_2^2, and ω_3^2, the natural frequencies of the whole system are:

$\omega_{n1} = 112.088$ rad/s.

$f_1 = 17.839$ Hz.

$\omega_{n2} = 546.347$ rad/s.

$f_2 = 86.954$ Hz.

$\omega_{n3} = 577.718$ rad/s.

$f_3 = 91.947$ Hz.

b)- Natural frequencies of the separated systems.

1- Natural frequency of the input system
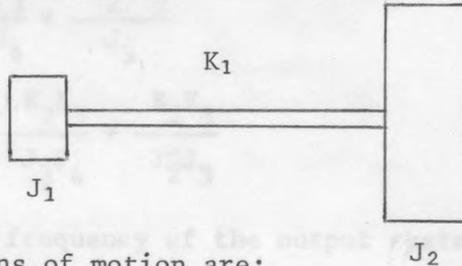
The equations of motion are:

$J_1 \ddot{\theta}_1 + K_1(\theta_1 - \theta_2) = 0$

$J_2 \ddot{\theta}_2 + K_1(\theta_2 - \theta_1) = 0$

∴ The natural frequency of input system (motor side) is:

$$\omega_{nm} = \sqrt{\frac{K_1(J_1 + J_2)}{J_1 J_2}}$$

$= 577.427$ rad/s.

$f_m = 91.900$ Hz.

2- Natural frequency of the output system:
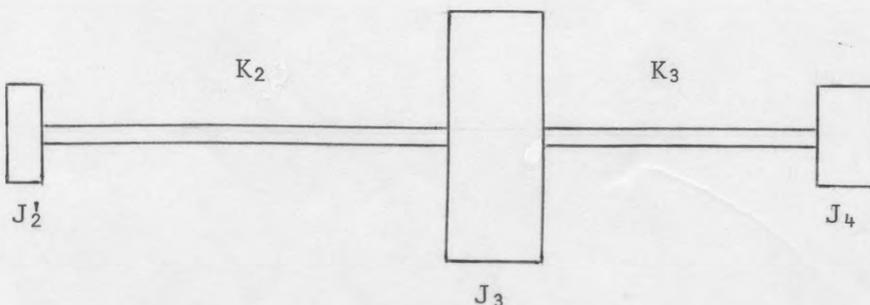
The equations of motion are:

$$J_2' \ddot{\theta}_2 + K_2(\theta_2 - \theta_3) = 0$$

$$J_3 \ddot{\theta}_3 + K_2(\theta_3 - \theta_2) + K_3(\theta_3 - \theta_4) = 0$$

$$J_4 \ddot{\theta}_4 + K_3(\theta_4 - \theta_3) = 0$$

Where

J_2' is the moment of inertia of the driven gear

$$J_2' = 0.00865 \ Kg.m^2$$

The equation for which the roots have to be found is:

$$A\omega^4 - B\omega^2 + C = 0$$

$$A = 1$$

$$B = \frac{K_2}{J_2'} + \frac{K_3}{J_4} + \frac{K_2 + K_3}{J_3}$$

$$C = \frac{K_2 K_3}{J_2' J_4} + \frac{K_2 K_3}{J_3 J_4} + \frac{K_2 K_3}{J_2' J_3}$$

∴ The natural frequency of the output system (brake side) is:

$$\omega_{nb} = 542.140 \ rad/s.$$

$$f_b = 86.284 \ Hz.$$

$$\omega_{nb2} = 557.13 \ rad/s.$$

$$f_{b2} = 88.67 \ Hz.$$

APPENDIX D

Strain Gauge Bridge Calculation
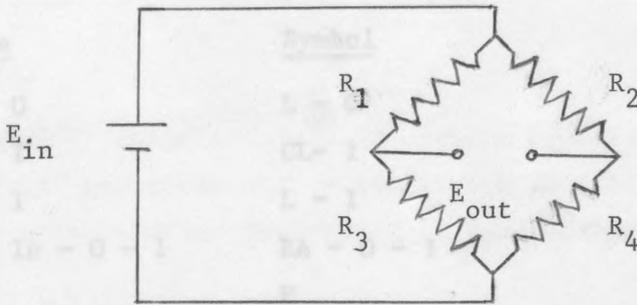
The relationship between the input and output voltages of the strain gauge bridge shown in the figure is:

$$E_{out} = E_{in}\left(\frac{R_1}{R_1+R_3} - \frac{R_2}{R_2+R_4}\right)$$

When $R_1/R_3 = R_2/R_4$ the bridge is balanced.

Letting $R_1=R_2=R_3=R_4=R$ be the resistance of each strain gauge and $\Delta R_1=-\Delta R_2=\Delta R_4=-\Delta R_3=\Delta R$ be the change in resistance of each strain gauge then the voltage equation can be written as

$$E_{out} = \frac{\Delta R}{R} E_{in}$$

For a strain gauge:

$$\frac{\Delta R}{R} = GF \cdot \varepsilon$$

where GF is the gauge factor and ε is the strain. After substitution the output voltage is defined by:

$$E_{out} = GF\, E_{in}\, \varepsilon$$

APPENDIX E

Programme List of Fourier Analyser Operation

Key name	Symbol
Label - 0	L - 0
Clear - 1	CL- 1
Label - 1	L - 1
Analog In - 0 - 1	RA - 0 - 1
Fourier	F
Power Spectrum	SP
Count - 0 - 10	# - 0 - 10 - 0
Divide - 1 - 10	: - 1 - 10
Display - 1	D - 1
Take Log	TL
Display - 1	D - 1
End	.

Special commands were used to plot the graph from the screen onto a white paper placed on the plotter.

Description of NAG Library Subroutine

1.Purpose:

DO2EAF integrates a stiff system of first-order ordinary
differential equations over a range with suitable initial conditions,
using a variable-order variable-step Gear method.

2.Specification: (FORTRAN)

```
      SUBROUTINE DO2EAF (T,TEND,N,X,TOL,FCN,W,IW,IFAIL)
C     INTEGER N,IW,IFAIL
C     real T,TEND,X(N),TOL,W (N,IW)
C     EXTERNAL FCN
```

3.Description:

The routine integrates a system of ordinary differential
equations

$$X_i' = F_i(T,X_1,X_2,\ldots,X_N), \quad i = 1,2,\ldots,N,$$

From Z=T to Z=TEND using a variable-order variable-step Gear method.

The system is defined by a subroutine FCN supplied by the
user, which evaluates F_i in terms of Z and $X_1,X_2,\ldots X_N$ (see Section 5),
and the values of $X_1,X_2,\ldots,X_N$ must be given at Z=T. The accuracy
of the integration is controlled by the parameter TOL. This routine
is primarily intended for integrating stiff systems of differential
equations, that is systems with widely differing time constants,
but should integrate all systems satisfactorily. For a description
of Gear's method and its practical implementation see (1).

4.References:

(1) Hall, G.   Modern Numerical Methods for Ordinary
Watt; J.M. (eds.)   Differential Equations. Clarendon Press,
                      Oxford, 1976.

5.Parameters:

T- real

Before entry, T must be set to the initial value of the independent variable Z. On exit, it contains TEND, unless an error has occurred, when it contains the value of Z at the error.

TEND- real

On entry, TEND specifies the final value of the independent variable. If TEND $<$ T on entry, integration will proceed in the negative direction. Unchanged on exit.

N- INTEGER

On entry, N specifies the number of differential equations. Unchanged on exit.

X- real array of DIMENSION at least (N).

Before entry, X(1), X(2),..., X(N) must contain the initial values of the solution $X_1, X_2,..., X_N$. On exit, X(1), X(2),... X(N) contain the computed values of the solution at the final value of Z.

TOL- real

Before entry, TOL must be set to a positive tolerance for controlling the error in the integration. The routine DO2EAF has been designed so that for most problems a reduction in TOL leads to an approximately proportional reduction in the error in the solution at TEND. However, the actual relation between TOL and the accuracy achieved cannot be guaranteed. The user is strongly recommended to call DO2EAF with more than one value for TOL and to compare the results obtained to estimate their accuracy. In the absence of any prior knowledge, the user might compare the results obtained by calling DO2EAF with TOL = $10.0^{**(-P)}$ and TOL = $10.0^{**(-P-1)}$ if he requires P correct decimal digits in the solution. TOL is normally unchanged on exit. However if the range T to TEND is so short that a small change in TOL is unlikely to make any change in the computed solution, then, on return, TOL has its sign changed. This should be treated as a warning that the computed solution is likely to

-207-

be more accurate than would be produced by using the same
value of TOL on a longer range.

FCN-SUBROUTINE, supplied by the user. FCN must evaluate the
functions F_i (i.e. the derivatives X_i') for given values of
its arguments $Z, X_1, \ldots, X_N$. Its specification is:

      SUBROUTINE FCN (Z,X,F)

      real Z,X(n),F(n)

Where n is the actual value of N in the call of DO2EAF.

      Z-real

          On entry, Z specifies the value of the argument
          Z. Its value must not be changed.

      X-real array of DIMENSION (n).

          On entry, X(I) contains the value of the argument
          X_I, for I=1,...,n. These values must not be
          changed.

      F-real array of DIMENSION (n).

          On exit, F(I) must contain the value of F_I, for
          I=1,...,n.

FCN must be declared as EXTERNAL in the (sub) program from
which DO2EAF is called.

W- Real array of DIMENSION (N,IW). used as a working space.

IW-INTEGER.

On entry, IW must specify the second dimension of the array W
as declared in the calling (sub) program. IW $\geqslant$ 18 + N.
Unchanged on exit.

IFAIL-INTEGER.

Before entry, IFALL must be set to 0 or 1. Unless the routine
detects an error (see Section 6), IFAIL contains 0 on exit.

6. <u>Error Indicators</u>:

Errors detected by the routine:

IFAIL=1 On entry, TOL $\leqslant$ 0.0 or IW< 18+N or N$\leqslant$ 0. The latter
        error will cause a program breakdown with some
        compilers.

IFAIL=2 With the given value of TOL, no further progress can be
        made across the integration range from the current

point Z=T, or the dependence of the error on TOL would
be lost if further progress across the integration range
were attempted (see Section 11 for a discussion of this
error exit). The components $X(1),X(2),...,X(N)$ contain
the computed values of the solution at the current point
Z=T.

IFAIL=3 TOL is too small for the routine to start the integration
(see Section 11). T and $X(1),X(2),...,X(N)$ retain their
initial values.

IFAIL=4 A serious error has occurred in an internal call to
DO2QBF. Check all subroutine calls and array dimensions.

7.Auxiliary Routines:

This routine calls the NAG Library routines DO2QBF and
PO1AAF.

8.Timing:

This depends on the complexity and mathematical properties
of differential equations defined by FCN, on the length of the
range, and on the tolerance. There is also a small overhead of
the form A+B*N, where A and B are machine-dependent computing
times.

9.Storage:

The storage required by internally declared arrays is 33
real elements.

10.Accuracy:

The accuracy depends on TOL, on the mathematical
properties of the differential system, on the length of the range
of integration and on the method. It can be controlled by
varying TOL but the approximate proportionality of the error to
TOL holds only for a restricted range of values of TOL. If TOL is
too large, the underlying theory may break down and the result of
varying TOL may be unpredictable. If TOL is too small, the rounding
error may affect the solution significantly and an error exit
with IFAIL=2 or IFAIL=3 is possible. If the user requires a
more reliable estimate of the accuracy achieved than can be
obtained by varying TOL, he is recommended to call the routine

DO2BDF where both the solution and a global error estimate are computed.

11.Further Comments:

If the routine fails with IFAIL=3 then it could be called again with a larger value of TOL if this had not already been tried. If the accuracy requested is really needed and cannot be obtained with this routine, then the system may be very stiff or so badly scaled that it cannot be solved to the required accuracy.

If the routine fails with IFAIL=2, it is probable that it has been called with a value of TOL so small that a solution cannot be obtained on the range T to TEND. This can happen for well-behaved systems and very small values of TOL. The user should, however, consider whether there is a more fundamental difficulty. For example, in the region of a singularity (infinite value) of the solution, the routine will usually stop with IFAIL=2, unless overflow occurs first.

If overflow occurs using DO2EAF, routine DO2QBF can be used instead to trap the increasing solution before overflow occurs. In any case, numerical integration cannot be continued through a singularity, and analytical treatment should be considered.